DESIGN AND DEVELOPMENT OF A DYNAMIC LED LUMINAIRE FOR EFFICIENT LIGHTING DESIGN CONSIDERING MESOPIC PHOTOMETRY

A THESIS

SUBMITTED IN PARTIAL FULFILLMENT OF

THE REQUIREMENT FOR A DEGREE OF

MASTER OF ENGINEERING

IN

ILLUMINATION ENGINEERING

SUBMITTED BY

PRASANJIT GHOSH PRANTA

EXAMINATION ROLL NO: M4ILN24018

REGISTRATION NO: 136035 of 2016-17

UNDER THE SUPERVISION OF

SANGITA SAHANA

Assistant Professor

ELECTRICAL ENGINEERING DEPARTMENT

FACULTY OF ENGINEERING AND TECHNOLOGY

JADAVPUR UNIVERSITY

KOLKATA- 700032

August, 2024

JADAVPUR UNIVERSITY

FACULTY OF ENGINEERING AND TECHNOLOGY

ELECTRICAL ENGINEERING DEPARTMENT

RECOMMENDATION CERTIFICATE

This is to verify that the thesis entitled **"DESIGN AND DEVELOPMENT OF A DYNAMIC LED LUMINAIRE FOR EFFICIENT LIGHTING DESIGN CONSIDERING MESOPIC PHOTOMETRY"** submitted by **PRASANJIT GHOSH PRANTA**, (Examination Roll No. **M4ILN24018**, Registration No. **136035 of 2016-17**) of this University in partial fulfilment of requirements for the award of the degree of Master of Engineering in Illumination Engineering, Department of Electrical Engineering, is a bonafide record of the work carried out by him under my guidance and supervision.

_____

(*Thesis supervisor*)

SANGITA SAHANA

Assistant Professor

Electrical Engineering Department,

Jadavpur University,

Dr. BISWANATH ROY	Prof. DIPAK LAHA
Head of the Department	Dean
Electrical Engineering Department,	Faculty of Engineering and Technology
Jadavpur University	Jadavpur University
Kolkata- 700032	Kolkata- 700032

JADAVPUR UNIVERSITY

FACULTY OF ENGINEERING AND TECHNOLOGY

ELECTRICAL ENGINEERING DEPARTMENT

CERTIFICATE OF APPROVAL

This foregoing thesis is hereby approved as a creditable study in the area of Illumination Engineering, carried out and presented by **PRASANJIT GHOSH PRANTA**, in a manner of satisfactory warrant its acceptance as a pre-requisite to the degree for which it has been submitted. It is notified to understood that by this approval, the undersigned does not necessarily endorse or approved the thesis only for the purpose for which it has been submitted.

FINAL EXAMINATION FOR EVALUATION OF THESIS

BOARD OF EXAMINERS

……

……

(Signature of Examiners)

JADAVUR UNIVERSITY

DECLARATION OF ORIGINALITY AND COMPLIANCE OF

ACADEMIC ETHICS

I hereby declare that this thesis contains a literature survey and original research work by the undersigned candidate, as part of my Master of Engineering in Illumination Engineering studies.

All information in this document has been obtained and presented in accordance with academic rules and ethical conduct.

I also declare that, as required by thesis rules and conduct, I have fully cited and referenced all material and results which are not original to this work.

NAME	**:**	**PRASANJIT GHOSH PRANTA**
EXAMINATION ROLL NO.	**:**	**M4ILN24018**
REGISTRATION NO.	**:**	**136035 of 2016-17**
THESIS TITLE	**:**	**"DESIGN AND DEVELOPMENT OF A DYNAMIC LED LUMINAIRE FOR EFFICIENT LIGHTING DESIGN CONSIDERING MESOPIC PHOTOMETRY"**
SIGNATURE WITH DATE	**:**	

ACKNOWLEDGEMENT

I would like to express my profound gratitude to my thesis supervisor, Sangita Sahana, Assistant Professor, Department of Electrical Engineering, Jadavpur University, Kolkata. Her visionary guidance and steadfast support were pivotal to the successful completion of this thesis.

I am equally grateful to Prof. (Dr.) Biswanath Roy, Head of the Department of Electrical Engineering, Jadavpur University, for his academic guidance and for providing me with the opportunity to conduct my research in the Illumination Engineering Laboratory.

My sincere thanks extend to Prof. (Dr.) Saswati Mazumdar, Department of Electrical Engineering, Jadavpur University, and Prof. (Dr.) Suddhasatwa Chakraborty, Associate Professor, Department of Electrical Engineering, Jadavpur University, for their continuous academic support and valuable insights throughout this journey.

I would also like to acknowledge my batchmates Shaheen Wasif, Sreemanti Basu, Roni Jana and others for their cooperation and companionship during our thesis work throughout the academic year.

Finally, I wish to express my heartfelt appreciation to my parents, friends, and seniors for their constant encouragement and support, without which this endeavor would not have been possible.

Place: Jadavpur University

Kolkata, 700032

Date:

PRASANJIT GHOSH PRANTA

Table of Contents

	Page no.
Abstract	1
Chapter 1: Introduction	2-11
1.1: Literature Survey	4
1.2: Problem Definition	9
1.3: Objective	10
1.4: Methodology	10
1.5: Outline of Dissertation	11
Chapter 2: Mesopic Photometry & Lighting Design Standards	12-28
2.1: Mesopic Photometry	13
2.1.1: Spectral eye sensitivity	13
2.1.2: Human eye and photometric quantities	15
2.1.3: Contribution of Rods and Cones to Human vision	16
2.1.4: Photometry & Human visual Response to light	17
2.1.5: Photometric vision	17
2.2: Lighting design and standards	20
2.2.1: Sequential steps to successful lighting	23
2.2.2: Application of Lighting Design	23
2.2.3: Mesopic Vision and Lighting Design	24
2.2.4: Mesopic Photometry Standards and Recommendations	25
2.2.5: Application of mesopic system	26
2.2.6: Limitation of mesopic photometry	26
2.2.7: Calculation of Mesopic Luminance	27
2.2.8: Comparison of Light Sources	27
Chapter 3: Area Lighting Design	29-84
3.1: Introduction	30
3.2: Methodology	31
3.3: Lighting Design in Photopic Region	32
3.3.1: Lighting Design using HPSV luminaire	34
3.3.2: Lighting Design using HPSV luminaire with surrounded CFL	36
3.3.3: Lighting Design using MH luminaire	38
3.3.4: Lighting Design using MH luminaire with surrounded CFL	40
3.1.5: Lighting Design using LED luminaire	42
3.1.6: Lighting Design using LED luminaire with surrounded CFL	44
3.1.7: An overview of the luminaires' designs in Photopic region	46
3.2: Lighting Design in Mesopic Region	47
3.2.1: Conversion process for photopic data to corresponding mesopic data	47
3.2.2: Modified Photometric file creation through LDT Editor software and implementation in DIALux Design	50
3.2.3: Lighting Design using modified HPSV luminaire	53
3.2.4: Lighting Design using modified HPSV luminaire with surrounded CFL	55

3.2.5: Lighting Design using modified MH luminaire 57
3.2.6: Lighting Design using modified M H luminaire with surrounded CFL 59
3.2.7: Lighting Design using modified LED luminaire 61
3.2.8: Lighting Design using modified LED luminaire with surrounded CFL 63
3.2.9: An overview of the luminaires' designs in Mesopic region 65
3.3: Data analysis 66

Chapter 4: Street Lighting Design 85-125
4.1: Introduction 86
4.2: Methodology 87
4.3: Lighting Design in Photopic Region 88
4.3.1: Lighting Design using HPSV luminaire 89
4.3.2: Lighting Design using MH luminaire 91
4.3.3: Lighting Design using MH luminaire 93
4.3.4: An overview of the luminaires' designs in Photopic region 95
4.2: Lighting Design in Mesopic Region 96
4.2.1: Conversion process for photopic data to corresponding mesopic data 96
4.2.2: Modified Photometric file creation through LDT Editor software and implementation in DIALux design 99
4.2.3: Lighting Design using modified HPSV luminaire 102
4.2.4: Lighting Design using modified MH luminaire 104
4.2.5: Lighting Design using modified LED luminaire 106
4.2.6: An overview of the luminaires designs in Mesopic region 108
4.3: Data analysis 109

Chapter 5: Design & development of low wattage tunable LED luminaire 126-139
5.1: Prototype LED luminaire 127
5.2: Instrument used for measurement 129
5.3: Detailed of cool white LED array at 100% duty cycle 131
5.4: Detailed of warm white LED array at 100% duty cycle 134
5.5: Detailed of combined cool & warm white LED array at 100% duty cycle 136

Chapter 6: Manually directed LED controller for a tunable LED 139-164
6.1: Introduction 140
6.2: Dimmer controller circuit 141
6.3: Components used for making LED dimmer circuit 142
6.4: Design & development of proposed LED controller 148
6.5: Experimental set up for tuning LED with controller 153
6.6: Details Circuit Diagram of the proposed controller 159
6.7: Data Analysis 160

Chapter 7: Result Analysis 165-169
Chapter 8: Conclusion & future scopes 170-173
References 174-178

ABSTRACT

This thesis investigates the enhancement of lighting design efficiency by exploring the transition from photopic to mesopic vision in outdoor and transitional lighting contexts. The study converts photopic luminous flux provided by luminaire manufacturers into its mesopic equivalent and simulates average mesopic luminance values using DIALux software. It compares these simulated values with photopic luminance, mesopic luminance across different luminaires, including High Pressure Sodium Vapor, Metal Halide, and Light Emitting Diode. Additionally, the research evaluates the impact of isolines diagrams, luminance surfaces, and light distribution curves in both photopic and mesopic regions, concluding how these differences support the use of mesopic photometry over photopic photometry in outdoor lighting design. It highlights how the characteristics of luminaires, such as luminous flux, luminous efficacy, and optical efficiency, affect performance in the mesopic region. To address the lack of effective techniques for estimating visual efficacy in the mesopic range, this study utilizes a corrected photopic luminance table from previous research, allowing designers to optimize their designs within existing frameworks. The findings indicate potential energy and cost savings when using white light sources, which are more effective in the mesopic range. The study also supports Light Emitting Diode (LED) technology in modern lighting by introducing and validating a cost-effective pulse-width modulation (PWM) dimming technique for LEDs, which enables tunable and dynamic lighting. Tested through a prototype luminaire with cool and warm white LED arrays, this technique demonstrates effectiveness and durability under low wattage conditions. This research provides valuable insights for improving outdoor lighting designs, such as area and street lighting, focusing on energy efficiency, visual effectiveness, and the advantages of modern LED technology, particularly its prominence in lighting design.

CHAPTER 1: INTRODUCTION

INTRODUCTION

Lighting technology has evolved significantly over the past century, transitioning from simple incandescent bulbs to highly efficient systems like Light Emitting Diodes (LEDs). This advancement is not merely technological but is intricately linked to the understanding of human vision, particularly in the context of mesopic vision. Mesopic vision, which occurs in low to moderate lighting conditions, represents the transition between photopic and scotopic vision. This transition is characterized by dynamic changes in the sensitivity of the human eye, as cone cells (responsible for color vision in bright light) become less active and rod cells (which are more sensitive to light but not color) begin to take over. Understanding this transition is crucial for the development of lighting systems that are both efficient and effective in varying lighting conditions. The sensitivity of the human eye varies across the visible spectrum, making it challenging to describe all forms of vision with a single spectral luminous efficiency function. Traditionally, the photopic luminous efficiency function, $V(\lambda)$ has been used to measure the sensitivity of the human eye to different wavelengths of light in brighter environments. However, this function is not sufficient for accurately evaluating light in mesopic conditions, where both rod and cone cells contribute to vision. This limitation has led to significant errors in the measurement of light under intermediate lighting conditions, underscoring the need for a more accurate approach to mesopic photometry [1-6].

The Commission Internationale de l'Eclairage (CIE) has developed a mesopic table, which provides values of mesopic luminance for different lamp Scotopic/Photopic (S/P) ratios corresponding to various photopic luminance levels. This table represents a substantial advancement in our understanding of mesopic vision and offers a foundation for determining appropriate illumination levels in fluctuating lighting environments such as dawn, dusk, or urban areas. Despite its importance, the CIE has not provided comprehensive guidelines for the practical implementation of this table, limiting its usefulness for both academics and practitioners [6-8].

With the rapid advancements in lighting technology, particularly the widespread adoption of LEDs, there is a growing need to revisit and update the standards for measuring luminous efficacy. LEDs are known for their extended lifespan, superior light output, and exceptional energy efficiency, making them an essential technology in the context of global warming and rising energy costs. However, the pursuit of higher light output in LEDs has also led to challenges, particularly in managing the significant amount of heat generated during operation. Effective thermal management is crucial to maintain the performance and longevity of LEDs, which are increasingly being integrated into diverse lighting applications [9-12]. The increasing global energy demand, with lighting accounting for about 20% of total power consumption, highlights the need for high-efficiency lighting systems like LEDs. LEDs operate based on the principle of electroluminescence, where they emit light when an electrical current passes through a semiconductor material. However, the drive to enhance LED light output by increasing the

electric current also raises a significant challenge: while LEDs convert only 20% of input energy into visible light, the remaining 80% is dissipated as heat. This heat generation becomes a critical issue as higher power LEDs are used to achieve greater luminous efficacy. Therefore, managing heat in LEDs is crucial for optimizing their efficiency and performance in lighting applications. [13-15]

In addition to their efficiency and longevity, LEDs offer the advantage of rapid response to variations in electrical characteristics, allowing for precise control over light levels. Among the various methods available for regulating LED light output, Pulse Width Modulation (PWM) dimming has emerged as the most effective. PWM dimming operates by delivering a pulsed direct current to the LED, adjusting the duty cycle of this signal to control light output without causing a significant rise in junction temperature. This method not only extends the lifespan of LEDs but also enhances energy efficiency, making it a preferred choice for many lighting applications [16-20].

This thesis aims to explore the transition from photopic to mesopic vision and the implications for modern lighting design. By leveraging the CIE mesopic table and advanced simulation tools, the research seeks to provide lighting designers with more accurate and efficient methods for optimizing lighting in environments where mesopic vision predominates. Additionally, the study introduces and validates an economical PWM dimming technique for LEDs, demonstrating its potential to enhance the performance and adaptability of LED-based lighting systems. Through this comprehensive investigation, the thesis contributes to the ongoing development of lighting standards and technologies that meet the demands of contemporary lighting applications, with a focus on energy efficiency, visual effectiveness, and sustainability.

1.1 LITERATURE REVIEW

- "Adjustment of Lighting Parameters from Photopic to Mesopic Values in Outdoor Lighting Installations Strategy and Associated Evaluation of Variation in Energy Needs" by Enrique Navarrete-de Galvez, Alfonso Gago-Calderon, Luz Garcia-Ceballos, Miguel Angle Contreras-Lopez and Jose Ramon Andres-Diaz [21]

This study examines the emission spectra of common light sources used in public street lighting installations, focusing on an urban configuration (ME6). Through extensive simulations, the research identifies the optimal configuration of light points, considering variables such as luminance, light point height, and pole distance ratio. The findings suggest that by selecting the appropriate light source and adjusting regulatory values to better align with human vision under artificial street lighting conditions, it is possible to achieve an average energy savings of 15% and reduce the number of light points required by 8%. Additionally, the study offers a statistical

range of energy requirements for lighting installations, enabling the generation of accurate electrical designs or estimates with 77.5% less variability compared to conventional design criteria.

- "Simplified field measurement methods for the CIE mesopic photometry system" by T Uchida and Y Ohno PhD [22]

This paper implements a mesopic photometry system for outdoor lighting using the CIE 191:2010 framework, comparing two methods: Adaptation SPD and Source SPD. The Adaptation SPD method assumes reflected light matches the road surface's SPD, while the Source SPD method aligns with the light source's SPD. The study validates the Source SPD method as effective for measuring mesopic quantities without specialized meters, though it shows limited sensitivity with multiple light sources. An error simulation with real road surface reflectance data is included, and a correction method is proposed to improve accuracy and applicability across various conditions.

- "Driver decision making in response to peripheral moving targets under mesopic light levels" by Yukio Akashi PhD, MS Rea PhD and JD Bullough PhD [23]

This paper reports a field study examining visual performance under mesopic lighting in driving scenarios. Participants drove on a well-lit street and made high-level decisions to respond to an off-center target by braking or accelerating. The study compared ceramic metal halide and high-pressure sodium lights, with daylight conditions serving as a control. Results showed that increasing unified luminance levels consistently reduced response times for braking and acceleration. These findings suggest that unified luminance is an effective parameter for assessing light levels for complex visual tasks in driving, regardless of the light source used.

- "Defining the visual adaptation field for mesopic photometry Does surrounding luminance affect peripheral adaptation?" By T Uchida and Y Ohno [24]

This study addresses the need to define an adaptation field for assessing adaptation state. Vision experiments were conducted to investigate the impact of surrounding luminance on the adaptation state at a peripheral task point. The findings indicate that the adaptation state is predominantly influenced by the local luminance at the task point, with a minor effect from surrounding luminance. Although the surrounding luminance effect exceeds the veiling luminance predicted by existing foveal models, it remains insignificant for mesopic luminance under uniform luminance distributions.

- "A modified CIE mesopic table and the effectiveness of white light sources" by MB Kostic and LS Djokic [25]

This paper addresses the practical challenges associated with the implementation of the recently developed CIE mesopic system, which necessitates new measurement devices, recommendations, and software for road lighting design. To bridge this gap, a corrected photopic luminance table is introduced, allowing lighting designers to continue using existing design procedures and measurement methods until these new tools are available. The study also highlights the importance of the CIE mesopic system, even though on-axis object recognition primarily involves photopic vision. Using the corrected photopic luminance table, the paper analyzes potential electricity and cost savings associated with the use of white light sources, which offer greater visual effectiveness in the mesopic range.

- "Energy Efficiency Consequences of Scotopic Sensitivity" by S.M. Berman [26]

Recent research from Lawrence Berkeley Laboratory (LBL) has expanded the understanding of rod receptors, traditionally linked to night vision, showing their active role under typical office lighting conditions. Studies indicate that rod activity affects pupil size and brightness perception, suggesting that light sources with higher scotopic content require less photopic luminance for comparable visual performance and clarity. This challenges previous studies that relied solely on photopic luminance to explain visual performance variations. Re-analysis of past research and evaluation of current lamps reveal significant potential for improving lighting energy efficiency by optimizing lamp spectra. Historically, lighting evaluations focused on photopic lumen output, disregarding spectral distribution. This approach, based on the V(X) function, overlooks the rods' contribution to vision, which peaks at 508 nm compared to the photopic response peak at 555 nm. Considering scotopic responses in lighting design could enhance overall visual quality and efficiency.

- "Light-emitting diodes in street and roadway lighting – a case study involving mesopic effects" by AM Kostic MArcha, MM Kremic, LS Djokic and MB Kostic [27]

Recent evaluations of light-emitting diode (LED) technology for urban lighting highlight both its advantages and limitations. LED luminaires are praised for their architectural applications, offering benefits such as compact size, controlled light distribution, and vibrant color options. They are particularly effective in ambient lighting, enhancing spaces like parks and monuments with pleasant color and high color rendering. However, their suitability for street and roadway lighting remains debated. Studies indicate that while LEDs can offer 19–26% energy savings

over high-pressure sodium (HPS) lamps, they are 1.36 to 6.44 times more expensive, even when accounting for mesopic effects. Additionally, practical issues such as color rendering challenges and potential distractions from dynamic lighting warrant careful consideration. Comparisons of LED and metal halide (MH) lamps for pedestrian paths show mixed results in energy savings, suggesting that LED performance is context-dependent and may not always meet efficiency expectations.

- "A High-Efficiency Dimmable LED Driver for Low-Power Lighting Applications" by Huang-Jen Chiu, Yu-Kang Lo, Jun-Ting Chen, Shih-Jen Cheng, Chung-Yi Lin, and Shann-Chyi Mou [28]

In recent studies, a novel dimmable LED driver has been proposed for low-power lighting applications, utilizing an adaptive feedback control mechanism. This driver employs a coupled inductor single-ended primary inductance converter (SEPIC) with a transition-mode power factor correction (PFC) circuit to achieve high efficiency and power factor across a universal input voltage range. The research focuses on enhancing pulse width modulation (PWM) dimming techniques to regulate LED current and brightness more effectively than traditional linear current-regulator or simple PWM methods. Notably, the improved PWM approach addresses the limitations of current amplitude control and reduces potential LED lifetime issues. Previous works have highlighted the importance of minimizing input current ripple and meeting harmonic regulations, which this study addresses by using a commercial low-cost PFC control IC. The feasibility of the proposed design was validated through laboratory testing, confirming the effectiveness of the improved dimming technique and adaptive control design.

- "A cost-effective PWM dimming method for LED lighting applications" by Huang-Jen Chiu, Yu-Kang Lo, Yu-Liang Lin and Gwan-Chi Jane [29]

Recent research presents a cost-effective pulse-width modulation (PWM) dimming method for LED lighting using a Flyback power factor correction (PFC) converter, which combines high efficiency and simplicity. LEDs are replacing incandescent and fluorescent lights due to their compact size, high efficacy, and environmental benefits. Compliance with IEC 61000-3-2 Class-C regulations require effective PFC, with Flyback converters being preferred for their low cost and high input power factors. The paper compares traditional dimming methods such as analog dimming, with its limited range and color shift, and PWM dimming, which offers a wider range and less color shift. The proposed method improves efficiency, dynamic response, and reduces current stress.

- "Comparative Analysis of Power LEDs Dimming Methods" by W.A. Rodrigues, L.M.F. Morais, P.F. Donoso-Garcia, P.C. Cortizo, S.I. Seleme JR [30]

Light-emitting diodes (LEDs) are valued for their compact size, high efficiency, long lifespan, and durability, making them ideal for applications like traffic signals, vehicle interiors, and architectural lighting. Initially used as indicators, LEDs have evolved to match the performance of traditional lighting sources, achieving efficiencies around 100 lm/W. LEDs also offer dimming control through methods like continuous current variation and pulse-width modulation (PWM), which enable precise light output management. This study explores these dimming techniques using a DC-DC Buck converter and digital controller, focusing on their effects on LED performance and energy efficiency in various lighting applications.

- "Dimming Techniques Focusing on the Improvement in Luminous Efficiency for High-Brightness LEDs" by Kun-Che Ho, Shun-Chung Wang and Yi-Hua Liu [31]

Pulse-width modulation (PWM) dimming is commonly used for high-brightness LEDs (HBLEDs) to adjust brightness by modulating the duty cycle. However, conventional PWM dimming can limit luminous efficiency due to the nonlinear current-illuminance relationship. Recent research introduces two multilevel current dimming methods—varying dimming signal voltage and current sensing resistance—that enhance luminous flux without increasing power consumption. Experimental results show these methods improve luminous efficacy by 16.37% to 21.36% and reduce average power output by 13.17% to 17.08% compared to traditional PWM dimming. This research highlights the need for efficient LED drivers and advanced dimming controls as LEDs become more prevalent in public lighting.

- "A Study on the Working Performance of Dimming Methods for Single- and Multichip Power LEDs" by Ismail Kıyak [32]

Light-emitting diodes (LEDs) are popular for their long lifespan, low power consumption, and high luminous efficacy, making them suitable for energy-saving applications. The demand for efficient lighting solutions has accelerated LED adoption, particularly in general lighting. Research into dimming techniques like pulse-width modulation (PWM) and current variation (CV) aims to optimize LED performance, affecting current, temperature, and luminous output. Effective thermal management is crucial, as high operating currents and heat can reduce LED performance and lifespan. Studies show that advanced cooling strategies and AlN-based ceramics enhance heat dissipation, with experiments indicating that thermal management significantly impacts LED efficiency and illuminance.

- "Lumen Effectiveness Multipliers for Outdoor Lighting Design" by Ian Lewin [33]

The paper investigates lumen effectiveness multipliers for outdoor lighting design, focusing on how different environments and technologies affect visual performance and energy efficiency. It highlights the need to account for both photopic and mesopic conditions, as traditional metrics may not reflect effectiveness in low light. The paper introduces new multipliers considering the spectral power distribution (SPD) of light sources, especially LEDs, which differ from high-pressure sodium (HPS) lamps. These multipliers aim to optimize lighting system design for better energy efficiency and visual comfort. The study underscores the importance of integrating these multipliers into design standards for more effective and sustainable outdoor lighting.

1.2 PROBLEM DEFINITION

The primary challenge in lighting design lies in optimizing the balance between energy efficiency and visual performance, especially in outdoor lighting installations such as an area or street. Traditional systems often fail to adjust to the varying lighting needs of different environments and times of day, leading to unnecessary energy consumption. The transition from photopic to mesopic lighting conditions is crucial for enhancing impact of efficiency, energy consumption or human visual performance in public spaces, yet the complexity of implementing mesopic photometry and the limitations of current measurement systems create significant barriers to consistent and accurate lighting designs. The shift from traditional high-pressure sodium (HPS) lamps to modern light sources like LEDs and metal halide lamps has introduced new challenges, particularly in terms of luminance accuracy and energy efficiency in lighting design. Moreover, integrating LED dimming technologies presents unique challenges in achieving high luminous efficacy while ensuring the long-term reliability of LEDs. Conventional dimming methods, such as pulse width modulation (PWM) and current variation (CV), often fail to optimize luminous output and thermal management, leading to reduced efficiency and potential degradation of LED components. The non-linear current-illuminance relationship in LEDs further complicates effective dimming, necessitating the development of advanced techniques to enhance both energy efficiency and luminous efficacy. As LEDs dominate lighting research, particularly in applications requiring precise light output control, the need for improved dimming solutions is critical.

1.3 OBJECTIVES

- To explore the application of mesopic photometry in optimizing energy efficiency and comparison among luminaires in outdoor lighting, particularly in area and street lighting.
- To identify and address the limitations of current measurement systems in implementing mesopic photometry, with the goal of improving consistency and accuracy in lighting designs and study the behavior of different lamps under mesopic conditions.
- To compare simulated photopic luminance, simulated mesopic luminance and the mesopic luminance calculated from CIE 191:2010 Table for different lamps.
- To develop advanced lighting strategies that effectively manage energy consumption while maintaining high visual standards in public spaces using LED luminaires.
- To assess the effectiveness and efficiency of various light sources such as LEDs, metal halide lamps, and high-pressure sodium lamps, under mesopic conditions in area lighting.
- To identify the factors that contribute to and distinguish the internal characteristics of luminaires.
- To develop a comprehensive approach to road lighting design and a prototype tunable LED that prioritizes both energy efficiency and visual performance based on mesopic photometry.

1.4 Methodology

This research involves a multi-step approach to evaluating and optimizing road lighting designs under both photopic and mesopic conditions. First, photopic luminance is simulated using DIALux software. The S/P ratios are then determined, followed by the calculation of mesopic luminance based on the CIE 191:2010 standard. The M/P (mesopic/photopic) ratio is established, and the original photopic luminance values are adjusted by multiplying them with the appropriate M/P ratio. Subsequently, mesopic luminance is simulated using DIALux for comparison with both the calculated mesopic luminance and the simulated photopic luminance across different lamp types. Additionally, the research proposes the creation of a low-wattage LED luminaire using cool and warm white arrays, alongside a PWM dimming controller circuit designed to control the arrays individually or in combination. The duty cycle of the arrays is adjusted via rotating encoders, and detailed measurements of each array, both individually and in combination, are recorded using a CL70F meter.

1.5 Outline of Dissertation

Chapter 1: This chapter provides an introduction to the thesis, outlining the objectives of the research and the methodology employed throughout the project.

Chapter 2: This chapter explores lighting design standards and the concepts of mesopic Photometry.

Chapter 3: This chapter examines area lighting, focusing on the conversion from photopic to mesopic conditions and its implementation, while comparing area luminaires based on their effectiveness and prominence.

Chapter 4: This chapter explores street lighting, highlighting the significance of mesopic implementation, comparing luminaires, and emphasizing the superiority of LEDs for roadway illumination.

Chapter 5: This chapter details the design and development process of a low-wattage LED luminaire, focusing on creating a tunable LED luminaire that can be manually adjusted by the user.

Chapter 6: This chapter presents the design and development of a proposed LED dimming controller, aimed at enhancing the functionality and energy efficiency of LED systems.

Chapter 7: This chapter analyzes the results of the research, comparing the performance of various lighting designs and technologies under study.

Chapter 8: This chapter concludes the thesis, summarizing the key findings, comparing the outcomes with the objectives, and discussing potential future research directions in the field.

CHAPTER 2: MESOPIC PHOTOMETRY AND LIGHTING DESIGN STANDARDS

2.1 Mesopic Photometry

Photometry is the scientific study of light measurement, aimed at quantifying light under various conditions of stimulus and observation. Vision can be categorized into three types: scotopic, mesopic, and photopic, each involving different levels of activity between the two types of light-sensitive cells in the retina, rods and cones. In scotopic vision, which occurs at very low adaptation levels below 0.005 cd/m², only rods are active. As adaptation levels increase to between 0.005 and 5 cd/m², both rods and cones contribute to vision, resulting in mesopic vision [35]. At adaptation levels above 5 cd/m², cones are predominantly active, leading to photopic vision [36,37]. Most road lighting conditions fall within the mesopic range, where the spectral sensitivity of the visual system shifts towards shorter wavelengths as rod activity increases. Consequently, peripheral task performance and subjective brightness perception improve with light sources that have a higher proportion of short-wavelength light. This shift in effectiveness is not reflected in traditional photometric units, which are based on photopic vision [25]. To address this discrepancy, correction factors have been developed based on the spectrum of the light source, characterized by its S/P (scotopic-to-photopic) ratio, and the lighting level of the installation.

2.1.1 Spectral eye sensitivity

In the mechanism of vision, the retina houses two distinct types of light-sensitive cells: rods and cones, which function differently depending on the lighting conditions to which the eyes are adapted. Under high luminance levels, greater than approximately 5 cd/m², cones are the primary active photoreceptors, facilitating photopic vision. This type of vision supports color perception through three types of cones—red, green, and blue—each sensitive to specific wavelengths of light. The spectral sensitivity of photopic vision is described by the V(λ) curve, peaking around 555 nm, corresponding to green-yellow light. Photometric units such as luminous flux, luminous intensity, illuminance, and luminance are based on this V(λ) function. Conversely, at very low luminance levels, below approximately 0.005 cd/m², rods are the sole active photoreceptors, resulting in scotopic vision. Rods, which are highly sensitive to low light, have a luminous efficacy of about 1700 lumens per watt, compared to the cones' 683 lumens per watt. Scotopic vision, characterized by the V′(λ) curve, peaks at around 505 nm, which corresponds to blue-green light. The V′(λ) curve demonstrates a shift towards shorter wavelengths compared to the V(λ) curve.

In intermediate luminance levels, between 0.005 and 5 cd/m², both rods and cones contribute to vision, termed mesopic vision. In this range, the visual sensitivity gradually shifts from the photopic to the scotopic curve, moving towards shorter wavelengths and increasing sensitivity to blue-green light. This shift in spectral sensitivity reflects the increasing influence of rod activity as luminance decreases. The effectiveness of light sources for road lighting and other mesopic conditions is enhanced by those emitting more green-blue light (cool-white) rather than yellow-

red light (warm-white), although such claims are generally applicable to peripheral vision rather than direct line-of-sight vision [38].

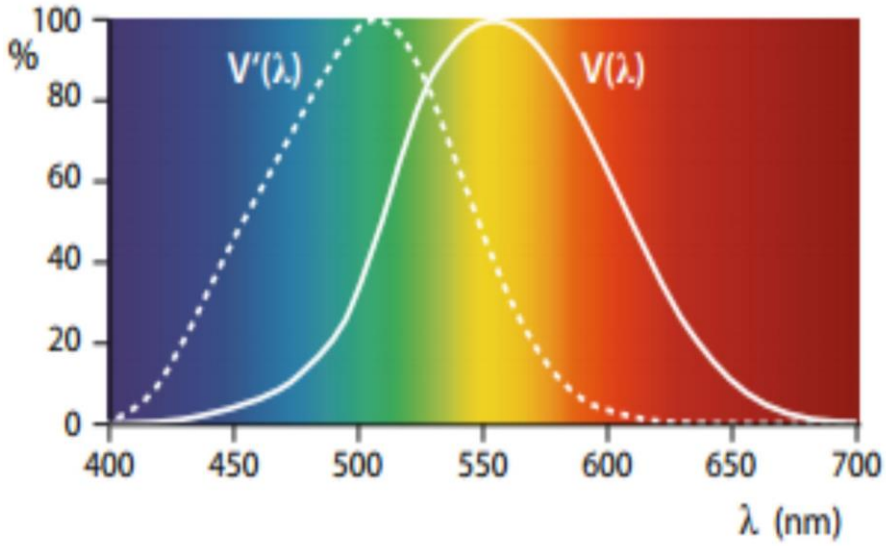

Figure 2.1: **Spectral eye sensitivity curves for photopic vision (CIE 1926) and scotopic vision (CIE 1951) [6]**

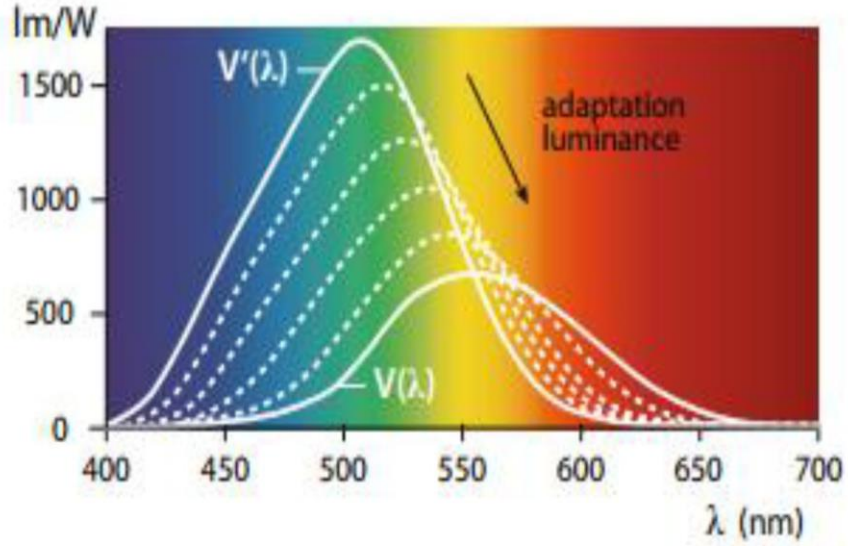

Figure 2.2: **Spectral luminous efficacy curves for scotopic V(λ), photopic V(λ) and mesopic vision $V_{mes}(\lambda)$ (broken lines) [6]**

2.1.2 Human eye and photometric quantities

The retina, located in the innermost layer of the eye, plays a crucial role in light detection and visual processing. It houses two types of photoreceptor cells: rods and cones. These cells are distributed non-uniformly across the retina, with significant implications for visual acuity and color perception. The fovea, situated at the center of the macula lutea, is a specialized region of the retina that contains a high concentration of cone cells and lacks rods. This area is essential for high-resolution vision and color discrimination, as it provides the sharpest visual acuity. Surrounding the fovea is the macula, which also contains cone cells but with decreasing density as one moves away from the center. In contrast, rod cells are predominantly located in the peripheral regions of the retina. These cells are highly sensitive to low light levels and are responsible for night vision, also known as scotopic vision. The distribution of rods ensures that peripheral vision remains functional even under dim lighting conditions. When light enters the eye, it is absorbed by the visual pigments within the rods and cones. The primary pigments involved are rhodopsin in rods and iodopsin in cones. Exposure to light causes these pigments to undergo a photochemical change, breaking down into their constituent parts and generating nerve impulses. These impulses are transmitted through the optic nerve to the brain, where they are interpreted as visual images. In darkness, the visual pigments are resynthesized to restore their light-sensitive properties, a process known as the photochemical cycle. The retina's structure is thus intricately designed to support both high-resolution color vision in bright light and sensitive low-light vision. The central region, with its dense concentration of cones, provides detailed and color-rich vision, while the peripheral regions, rich in rods, support vision in low-light conditions. This distribution and functionality of rods and cones are fundamental to the visual process and are critical in understanding how different lighting conditions affect visual perception [39].

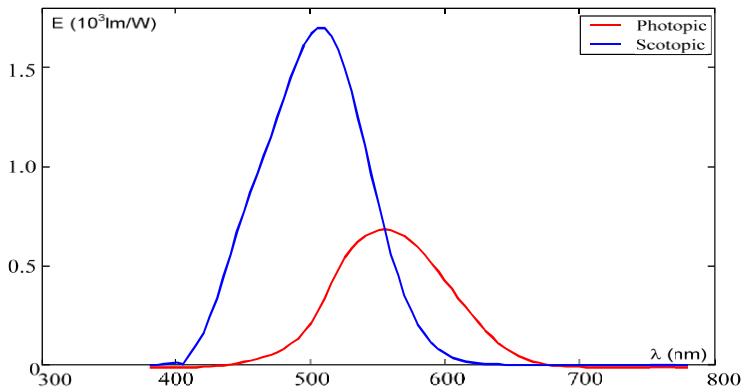

Figure 2.3: **Relative spectral sensitivity curves of the human eye, for photopic and scotopic conditions [40]**

2.1.3 Contribution of Rods and Cones to Human vision

Within the human retina, there are two primary types of photoreceptor cells: rods and cones. Rods, which are distributed throughout the retina with a higher concentration in the peripheral regions, are highly sensitive to low light conditions. They are essential for night vision, or scotopic vision, allowing the detection of faint light levels and contributing to vision in dimly lit environments. Cones, conversely, are predominantly located in the central part of the retina, particularly in the fovea, and are responsible for color vision and high-acuity tasks in bright light. There are three types of cones red, green, and blue each sensitive to different wavelengths of light, facilitating color discrimination and detailed vision, known as photopic vision. In addition to these, there is a third visual phenomenon called mesopic vision, which occurs under intermediate light levels where both rods and cones are active. This type of vision bridges the gap between scotopic and photopic vision, enabling visual perception in conditions that are neither too dark nor too bright.

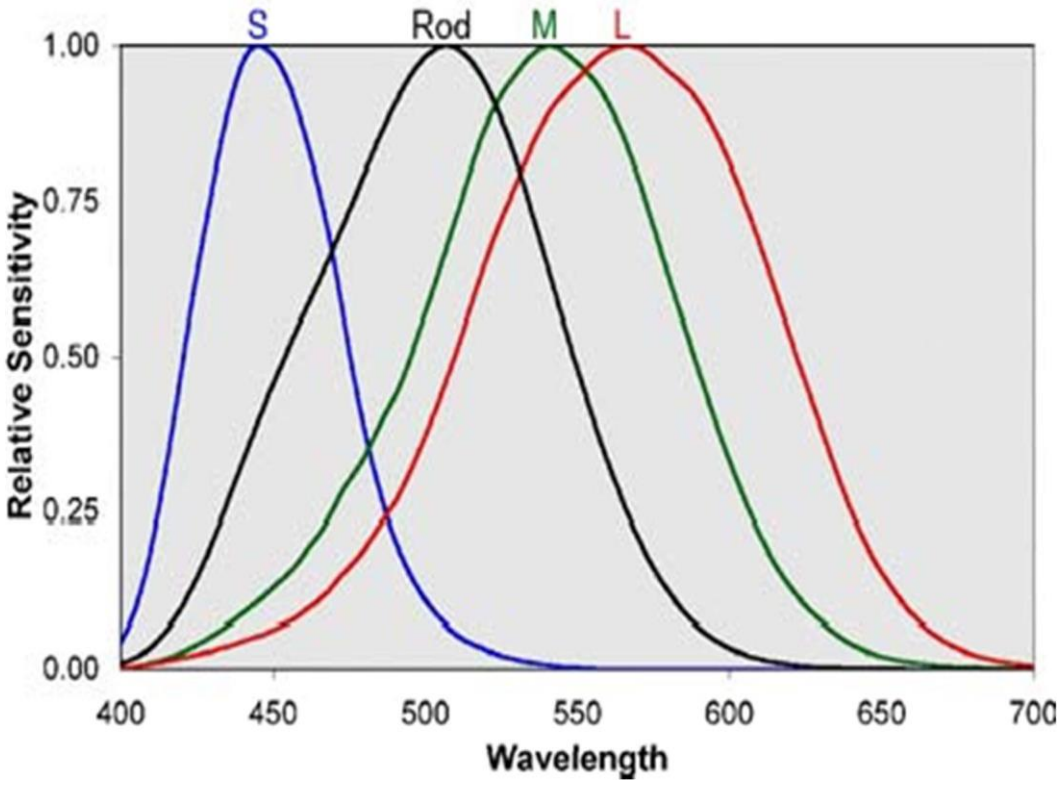

Figure 2.4: **The spectral sensitivity functions of the cones and rods [41]**

2.1.4 Photometry & Human visual Response to light

Photometry is a specialized branch of optics focused on the precise measurement of light. The term "photometry" derives from "photo," meaning light, and "metry," meaning measurement. The primary goal of photometry is to quantify visible radiation in a manner that accurately reflects human visual perception. To achieve this, photometric measurements utilize spectral luminous efficiency functions, which describe the eye's sensitivity to light across various wavelengths. Specifically, two key functions are used: V(λ) for photopic vision and V′(λ) for scotopic vision. **V(λ)** function is applied in photopic conditions, where light levels are sufficient for daylight vision. It represents the eye's sensitivity to different wavelengths under well-lit conditions and is crucial for evaluating light's impact on color perception and fine detail resolution. **V′(λ)** function is used in scotopic conditions, typical of low light environments where night vision predominates. It characterizes the eye's sensitivity to light at low luminance levels, reflecting the rod-mediated vision that is effective in dimly lit settings. These spectral luminous efficiency functions allow for a comprehensive assessment of how light affects human vision, ensuring that photometric data is aligned with the actual visual experiences of standard human observers. By incorporating these functions, photometry provides accurate and relevant measurements that reflect the human visual system's response to various lighting conditions. [42].

2.1.5 Photometric vision

Rod vision, also known as scotopic vision, involves the use of rod photoreceptors in low-light conditions. Cone vision, or photopic vision, relies on cone photoreceptors and is effective under bright light conditions. The mesopic vision, situated between these two extremes, involves the combined contribution of both rods and cones and occurs in intermediate lighting conditions.
Light is quantified in lumens, representing radiant power measured in watts and weighted according to its wavelength by a spectral luminous efficiency function. This function reflects the eye’s sensitivity to light at various wavelengths. The luminous value of a light source is calculated using either the photopic response function (V(λ)) for bright light conditions or the scotopic response function (V′(λ)) for low-light conditions.

In the mesopic range, where light levels transition from photopic to scotopic, the spectral response shifts gradually between the photopic and scotopic curves. This results in a spectrum of mesopic curves that vary in shape and sensitivity based on the light level and distribution within the visual field. Due to these variations and associated challenges, a standardized approach for computing lumens in the mesopic region is necessary. This standardization addresses issues related to accurate measurement and provides a framework for evaluating mesopic vision. For a comprehensive review of these issues and methods, refer to the section on Mesopic Photometry.

Photopic vision

Photopic vision occurs at luminance levels greater than 5 cd/m², predominantly involving cone photoreceptors in the retina. This type of vision supports color perception and is responsible for chromatic vision, making it effective in well-lit conditions such as daylight. The maximum luminous efficacy for photopic vision is 683 lumens per watt, occurring at a wavelength of 555 nm, which corresponds to green light. At this wavelength, photopic vision achieves its peak photosensitivity of 100%. Under photopic conditions, the human eye is capable of perceiving fine details due to the high spatial resolution provided by cone cells. This form of vision is also characterized by rapid adaptation to changes in light levels, making it efficient for tasks requiring detailed visual acuity. The sensitivity of photopic vision varies with different wavelengths of visible light, affecting color perception and overall visual performance. Adaptation to light changes in photopic vision is faster compared to other types of vision, facilitating quick adjustments to varying lighting conditions. [44]

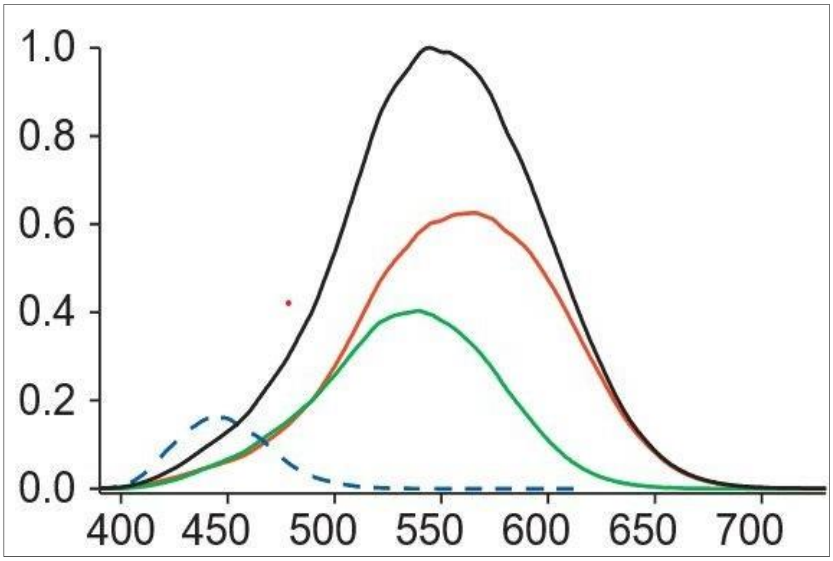

Figure 2.5: **Spectral sensitivities in photopic (cone) vision [43]**

Scotopic Vision

Scotopic vision, also known as dark-adapted or night vision, is facilitated exclusively by rod cells in the retina. These rod cells are most sensitive to light at approximately 498 nm, which is in the blue-green part of the spectrum. Scotopic vision operates effectively at luminance levels ranging from 0.000001 cd/m² to 0.005 cd/m², which are much lower than those required for photopic vision. In scotopic conditions, visual acuity is reduced due to the distribution of rod

cells primarily in the peripheral regions of the retina. This distribution contributes to lower spatial resolution and detail perception compared to photopic vision. The primary advantage of scotopic vision is its heightened sensitivity to low light levels, allowing for visual perception in near-darkness. However, the trade-off is a lack of color discrimination and decreased ability to resolve fine details, which are limitations inherent to the rod-mediated visual system. [45]

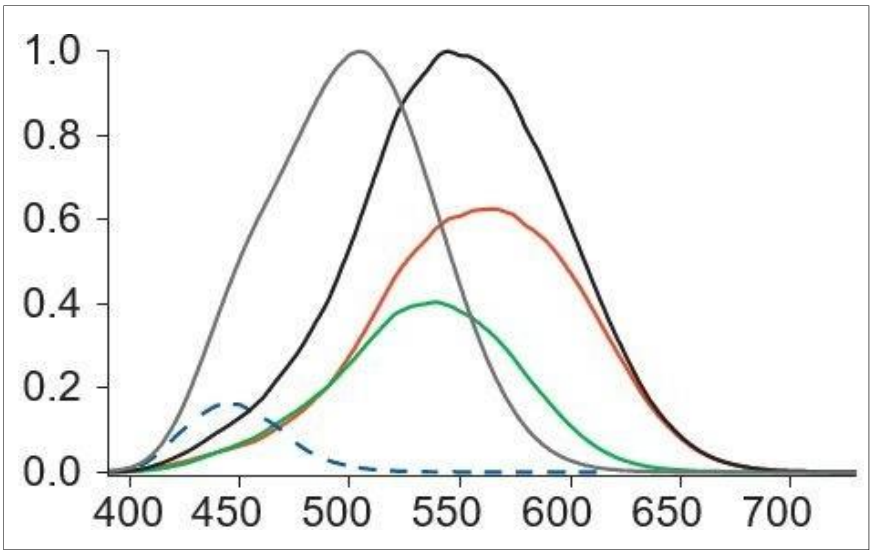

Figure 2.6: **Spectral sensitivities in Mesopic (rod-cone) vision [43]**

Mesopic vision

Mesopic vision represents a transitional visual state that arises from the simultaneous involvement of both rod and cone photoreceptors in the human eye. This type of vision occurs in an intermediate luminance range, specifically between the higher light levels of photopic vision (daytime) and the very low light levels of scotopic vision (nighttime). The luminance range for mesopic vision spans from approximately 0.005 cd/m² to 5 cd/m², making it particularly significant for evaluating outdoor lighting conditions and nighttime traffic scenarios. In the mesopic range, the spectral sensitivity of the visual system is variable and depends on the prevailing light level. Unlike in photopic or scotopic conditions, where the spectral sensitivity functions are well-defined ($V(\lambda)$ for photopic and $V'(\lambda)$ for scotopic), mesopic vision does not adhere to a fixed spectral response. Instead, the sensitivity shifts gradually between the photopic and scotopic curves as the light level changes. To address the challenges associated with measuring and assessing mesopic vision, the Commission Internationale de l'Eclairage (CIE) introduced the standard CIE 191:2010. This system provides a standardized method for mesopic photometry by utilizing a linear combination of the photopic and scotopic efficiency functions.

LED light sources are frequently employed in mesopic photometry due to their adaptability in varying light conditions. As luminance decreases from photopic to mesopic levels, the absolute sensitivity of the visual system diminishes, although spectral sensitivity remains relatively stable until it transitions to scotopic vision. During mesopic conditions, rod photoreceptors become more dominant, leading to diminished color vision and a shift in sensitivity towards shorter wavelengths. This transition is described by the Purkinje effect, which accounts for changes in color perception between well-lit and low-light environments [42,46].

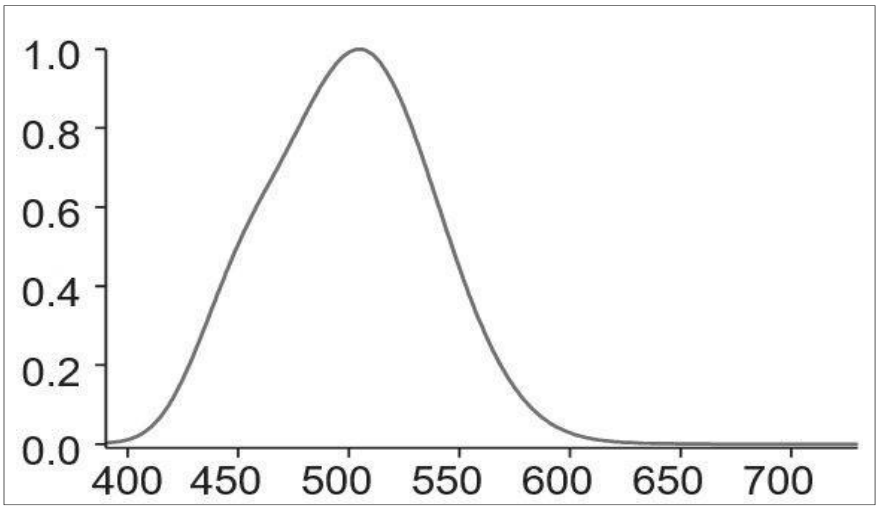

Figure 2.7: **Spectral sensitivities Scotopic (rod) vision [43]**

2.2 LIGHITING DESIGN AND STANDARDS

Lighting design is a fundamental aspect of creating spaces that are not only visually appealing but also functional, comfortable, and efficient. Whether applied in residential, commercial, industrial, or outdoor settings, effective lighting design enhances both the aesthetic quality and usability of an environment. It involves a delicate balance between technical precision and artistic expression, ensuring that illumination meets the specific needs of the space while also contributing to the overall ambiance and mood. A well-executed lighting design begins with a thorough understanding of the space's intended function and the activities that will take place within it. For example, the lighting requirements for a residential living room, where comfort and relaxation are prioritized, will differ significantly from those of a commercial office, which demands high levels of brightness for productivity. In industrial environments, safety and visibility are paramount, necessitating robust and durable lighting solutions that can withstand harsh conditions. Outdoor lighting, on the other hand, must consider factors such as security, aesthetics, and the interaction with natural light sources like the sun and moon. To achieve these

varied goals, lighting designers must consider a range of parameters, each contributing to the overall effectiveness of the design. These include Correlated Color Temperature (CCT), which affects the perceived warmth or coolness of the light and is critical in setting the mood of a space. For instance, warmer light (lower CCT) is typically used in residential and hospitality settings to create a cozy, inviting atmosphere, while cooler light (higher CCT) is preferred in workspaces for its clarity and focus-enhancing properties [47,48].

Correlated Color Temperature (CCT): CCT, measured in Kelvin (K), determines the "warmth" or "coolness" of the light emitted by a source. Lower CCT values (around 2700K to 3000K) produce a warm, yellowish light that evokes the familiar glow of incandescent bulbs, making them ideal for creating cozy and intimate environments in settings like bedrooms and restaurants. In contrast, higher CCT values (5000K to 6500K) emit a cooler, bluish light, akin to daylight, which is more suited to spaces such as offices and retail stores where clarity and focus are paramount. The selection of CCT is essential as it significantly impacts the mood and ambiance of a space, shaping the experience of those who occupy it.

Color Rendering Index (CRI): CRI is a metric that evaluates how accurately a light source renders colors compared to natural light, with a scale ranging from 0 to 100. A higher CRI value indicates better color accuracy, which is crucial in environments where true color representation is vital, such as art galleries, retail spaces, and hospitals. In these settings, high CRI lighting ensures that colors appear vibrant and true to life, enhancing the visual experience and maintaining the integrity of the displayed items or work being done.

Distribution of Light (Direct/Indirect): Light distribution refers to how light is spread within a space, impacting both the quality of illumination and the atmosphere. Proper light distribution ensures even lighting across a room, avoiding harsh shadows or bright spots that can cause discomfort or reduce functionality. Different lighting fixtures, such as floodlights, spotlights, wall sconces, and pendant lights, provide varied distribution patterns. The choice and placement of these fixtures are guided by the specific needs of the space, whether the goal is to highlight certain features, provide task lighting, or create a general ambient light.

Lighting Uniformity: Achieving uniform lighting is crucial for creating a balanced and visually comfortable environment. This involves careful planning of light source placement and fixture selection to avoid dark spots and overly bright areas, ensuring that the entire space is evenly illuminated. Uniform lighting is particularly important in workspaces and public areas where consistent visibility is required.

Glare and Unified Glare Rating (UGR): Glare is an issue that can significantly affect visual comfort, arising from excessive brightness either directly from the light source or from reflections off surfaces. To minimize glare, lighting designers employ techniques such as selecting appropriate fixtures, using shields, and controlling the angles of light. The UGR is a numerical measure used to quantify the level of glare in indoor environments, with lower UGR

values indicating less glare and a more comfortable visual experience. Effective glare management is essential in spaces where visual tasks are critical, ensuring both comfort and safety for occupants.

Dimming and Control: The ability to adjust lighting levels through dimming and control systems offers dynamic lighting scenarios, energy savings, and the ability to tailor lighting to user preferences. Advanced control systems can also integrate with other building management systems, allowing for automated adjustments based on time of day, occupancy, or ambient light levels, further enhancing energy efficiency and comfort.

Energy Efficiency: In modern lighting design, energy efficiency is a top priority, driven by the need to reduce energy consumption and minimize environmental impact. LED technology stands out as the most energy-efficient option, offering significant benefits such as longer lifespans, lower energy use, and reduced maintenance costs compared to traditional lighting solutions like incandescent or fluorescent bulbs. Energy-efficient lighting not only contributes to sustainability goals but also reduces operational costs.

Safety and Emergency Lighting: Ensuring safety in lighting design involves incorporating emergency lighting systems that provide reliable illumination during power outages or emergencies. This includes strategically placed exit signs, escape route lighting, and backup power sources, which are critical for safe evacuation and overall safety compliance.

Flicker and Strobe Effects: Flicker and strobe effects can be more than just a nuisance; they can cause discomfort, eyestrain, and even health issues such as headaches or visual disturbances. High-quality light sources and advanced dimming systems are key to minimizing these effects, ensuring a stable and comfortable lighting experience for users.

Daylight Integration: Integrating natural daylight into lighting design is an effective way to reduce reliance on artificial lighting during daylight hours. By maximizing the use of available daylight, designers can create more energy-efficient spaces that are also more pleasant to occupy, as natural light is generally preferred for its positive effects on mood and well-being.

Architectural Integration: Lighting fixtures should complement the architecture and design of a space, enhancing its visual appeal while providing the necessary illumination. Seamless integration of lighting with the architectural elements can elevate the overall aesthetic and contribute to the design's success.

Maintenance and Serviceability: The long-term success of a lighting design also depends on the ease of maintenance and serviceability of the fixtures. Choosing fixtures that are easy to maintain and replace ensures the lighting system remains functional and cost-effective over time, reducing downtime and maintenance costs.

These lighting design parameters are essential for creating environments that are not only visually appealing but also functional, comfortable, and sustainable. By carefully considering each parameter, lighting designers can tailor solutions to meet the specific needs of any space, enhancing both the experience of the occupants and the efficiency of the lighting system.

2.2.1 Sequential steps to successful lighting design solution

Successful lighting design begins with clearly establishing the design criteria, which encompass both the quantity and quality of illumination. Designers must assess the specific needs of the project, adjusting light levels based on factors such as the age of workers, the size and contrast of tasks, and regulatory standards. Quality considerations include the overall appearance of the space and luminaires, color quality, and the integration of daylighting. Additionally, designers must control direct and reflected glare, minimize flicker, ensure uniform light distribution, and strategically position lighting to enhance visual comfort and aesthetic appeal. Flexibility and control over lighting, including the ability to highlight points of interest and manage shadowing, are also crucial to achieving a successful design [48].

2.2.2 Application of Lighting Design

Lighting design is tailored to the unique requirements of various settings, each demanding a specific approach to achieve optimal results. In residential environments, the emphasis is on creating cozy and inviting spaces that are also functional, typically achieved through the use of warm color temperatures and versatile dimming options that allow for personalized ambiance. Commercial lighting, on the other hand, must strike a balance between functionality and aesthetics, ensuring that workspaces are well-lit to enhance productivity while also incorporating energy-efficient solutions that align with modern sustainability goals. In hospitality settings, the focus shifts to creating memorable experiences through carefully crafted ambiance and mood, often achieved by using accent lighting, decorative fixtures, and dynamic control systems that can adapt to different occasions or times of day. Retail lighting plays a crucial role in driving consumer behavior by strategically highlighting products, creating visually appealing displays, and guiding customers through the store in a way that enhances the shopping experience. Industrial lighting demands robust solutions that prioritize safety, efficiency, and durability, with fixtures designed to withstand challenging conditions such as dust, moisture, and vibrations, thereby ensuring a safe and productive work environment. Finally, outdoor lighting serves a dual purpose of providing safety and security while also enhancing the aesthetic appeal of architecture, landscapes, and public spaces. Properly designed outdoor lighting not only ensures visibility and safety but also contributes to the overall visual experience, making spaces more inviting and accessible during nighttime hours.

2.2.3 Mesopic Vision and Lighting Design

Understanding mesopic vision is essential for lighting designers, particularly because many common outdoor lighting scenarios, such as street lighting, roadways, and public spaces, often operate within the mesopic range. Mesopic vision occurs at intermediate lighting levels, typically between the fully illuminated photopic (daylight) and the dim scotopic (night) vision. Traditional lighting design has primarily focused on photopic vision, where cone cells in the retina are most active, and bright, daylight-like conditions are assumed. However, this approach can lead to suboptimal lighting performance and unnecessary energy consumption when applied to environments that actually fall within the mesopic range. In mesopic conditions, the visual system behaves differently due to the combined activity of both rod and cone cells in the retina. Rod cells, which are more sensitive to lower light levels and predominantly responsible for scotopic vision, become more active, while cone cells, which are responsible for color perception in brighter conditions, still contribute to vision but to a lesser extent. This dual contribution leads to several unique characteristics in visual perception and performance that lighting designers must consider [49]. One key characteristic is the **Purkinje shift**, a phenomenon where the eyes' sensitivity to blue light increases under mesopic conditions. This shift occurs because rod cells, which are more sensitive to shorter wavelengths (blue light), contribute more to visual perception as ambient light levels decrease. As a result, colors may appear different under mesopic lighting compared to photopic lighting. For instance, red objects, which are typically more visible under photopic conditions, may seem less prominent, while blue or green objects may appear more vivid. This altered color perception can affect how well objects are seen and recognized in outdoor environments, such as on roads or in public spaces [50].

Another important aspect of mesopic vision is the reduction in **contrast sensitivity** and **spatial resolution** compared to photopic conditions. In mesopic environments, the ability to detect differences in luminance (contrast) between objects and their backgrounds diminishes, making it more challenging to discern fine details or subtle differences in brightness. This reduction in visual acuity can have significant implications for safety and performance in outdoor lighting applications, such as roadways, where the ability to quickly and accurately perceive potential hazards is critical. Given these factors, lighting designers need to consider the unique characteristics of mesopic vision when designing lighting systems for environments that operate within this range. This may involve selecting light sources with a spectral power distribution (SPD) that enhances visual performance under mesopic conditions, such as those with higher blue light content to account for the Purkinje shift. Additionally, optimizing light levels and distribution to maintain sufficient contrast and visibility in mesopic environments can improve safety and comfort for users while reducing energy consumption. By accounting for mesopic vision in their designs, lighting professionals can create more effective and efficient lighting solutions that better align with real-world conditions, ultimately leading to improved visual performance, safety, and energy efficiency in outdoor and transitional lighting environments.

2.2.4. Mesopic Photometry Standards and Recommendations

To address the complexities inherent in mesopic lighting environments, various organizations and researchers have established standards and recommendations that specifically cater to the unique characteristics of mesopic vision. These guidelines are designed to enhance visibility, safety, and overall visual comfort in conditions where traditional photopic-focused approaches may fall short. A key contribution in this domain is the International Commission on Illumination (CIE) technical Report CIE 191:2010, titled "Recommended System for Mesopic Photometry Based on Visual Performance." This seminal report outlines a comprehensive methodology for mesopic photometry, which is critical for accurately assessing lighting performance in mesopic environments. The report introduces a hybrid approach that combines the scotopic and photopic luminous efficiency functions, enabling a more accurate calculation of mesopic luminous efficiency. Central to this methodology is the concept of mesopic luminance level, a pivotal parameter in mesopic photometry that integrates the contributions of both rod and cone cells. By adopting these standards, lighting designers can more effectively tailor their solutions to real-world conditions, ultimately improving the quality and effectiveness of lighting in mesopic settings.

Recommended System for Performance Based Mesopic Photometry

The recommended system for visual performance-based mesopic photometry defines spectral luminous efficiency, $V_{mes}(\lambda)$, in the mesopic region as a linear combination of the photopic $V(\lambda)$ and scotopic $V'(\lambda)$ spectral luminous efficiency functions. This system establishes a gradual transition between these functions across the mesopic region, with specific parameters for photopic and scotopic luminance and the S/P-ratio (scotopic-to-photopic luminous output). The system is designed for evaluating lighting for peripheral visual tasks in mesopic conditions, while on-axis tasks, where foveal vision dominates, should use the photopic function. The system maintains additivity, aligns with human visual psychophysics, and correlates with visual performance under varying conditions, offering a practical and effective solution for mesopic photometry. This approach bridges the gap between photopic and scotopic functions and is based on extensive visual psychophysical research and photometric principles [51].

System for mesopic photometry based on visual task performance

The foundation of any photometric system is grounded in empirical visual performance data derived from human subjects, acknowledging that current photometry accurately reflects human spectral sensitivity only for a limited range of visual tasks. Mesopic vision, which lies between

photopic and scotopic vision, is not adequately represented by the existing spectral luminous efficiency functions $V(\lambda)$ and $V'(\lambda)$. The complexity of vision, influenced by various factors such as stimulus size, location, ambient light, and contrast, makes it impossible for any single system to predict visual performance under all conditions.

To address mesopic conditions, the emphasis has been on developing a practical photometric system rather than a precise one. Key constraints for this system include additivity and a gradual transition between the photopic $V(\lambda)$ at the upper end of the mesopic region and scotopic $V'(\lambda)$ at the lower end. A linear combination of these functions satisfies these requirements, making the mesopic spectral sensitivity functions $V_{mea}(\lambda)$ additive, though only within a specific adaptation level.

Recent systems, such as the USP and MOVE systems, follow this approach, bridging the photopic and scotopic domains while preserving additivity. Differences between these systems arise from the transition points between mesopic and photopic regions and the adaptation coefficients used, leading to varying predictions of mesopic values. An Intermediate system also exists, combining elements of both USP and MOVE, with adjusted luminance limits for the mesopic region.

2.2.5 Application of mesopic system

Mesopic photometry provides a standardized framework for evaluating light sources under low-light conditions, offering a unified criterion for comparison and assessment. Its adoption is anticipated to be significant within the lighting community due to its validity and practical benefits. Implementing mesopic photometry will facilitate the optimization of outdoor lighting by aligning it more closely with human visual performance needs while also considering energy consumption. This approach allows for the development of lighting products specifically designed for low-light scenarios, which can enhance both visual effectiveness and energy efficiency. Consequently, the adoption of mesopic photometry is poised to advance the creation of more efficient and effective lighting solutions, improving overall outdoor lighting quality and performance.

2.2.6 Limitation of mesopic photometry

Despite its advancements, the mesopic photometry system has several limitations. Firstly, it is not applicable to tasks viewed across all angles of the retina, which restricts its generalizability to a wide range of visual tasks. Additionally, the system is unsuitable for scenarios involving high light levels, as the CIE 191 system's experiments predominantly utilized white light, making it less effective in such conditions. Lastly, mesopic photometry is inadequate for light sources with

extremely high Spectral Power (S/P) ratios, as it cannot accurately account for the effects of these high ratios on visual performance. These limitations underscore the need for caution when applying the mesopic photometry system to diverse lighting and viewing conditions.

2.2.7 Calculation of Mesopic Luminance

To accurately calculate mesopic luminance, it is essential to consider the Spectral Power (S/P) ratio of the light source. A higher S/P ratio corresponds to greater luminous efficacy in mesopic conditions. It illustrates the variations in luminance values when computed using the mesopic photometric systems (USP, MOVE, and Intermediate systems, including MES1 and MES2) compared to those calculated using the traditional photopic spectral luminous efficiency function. The table highlights discrepancies greater than 5% in color for emphasis. According to the MES-2 system results, light sources with higher short-wavelength output (S/P ratio > 1) show increased luminance values when measured by the mesopic system, while those with greater long-wavelength output exhibit decreased luminance values. This effect is more pronounced at lower light levels. The table also marks the currently recommended road surface luminance levels, ranging from 0.3 cd/m² to 2 cd/m², with rectangles for reference. Many white light sources used in road lighting applications, such as high-pressure sodium lamps and certain metal halides, have S/P ratios varying from approximately 0.65 to 2.50. This demonstrates the significant impact of the S/P ratio on the perceived luminance under mesopic conditions [52].

2.2.8 Comparison of Light Sources

The application of mesopic dimensioning significantly impacts the luminous output and alters the luminous efficacy rankings of various lamps. Figure 2.8 provides an overview of the scotopic/photopic (S/P) ratios for light sources commonly utilized in outdoor lighting. Light sources with an S/P ratio greater than 1 exhibit a higher proportion of their spectral output in the short-wavelength region, which enhances their efficiency under mesopic conditions. Conversely, light sources with an S/P ratio less than 1 have a lower short-wavelength content and are therefore less efficient in mesopic lighting scenarios. This distinction underscores the importance of considering the S/P ratio when evaluating and optimizing the performance of lighting systems designed for low-light environments.

Light source	R_{sp}
Low pressure sodium	0.23
High pressure sodium	0.4
Mercury vapour lamp	0.8
Incandescent	1.41
Quartz halogen	1.5
Fluorescent	1.5–2.4
Cool white LED	2.3
LED – red (635 nm)	0.06
LED – blue (470 nm)	14.3
LED – royal blue (450 nm)	28
Diode laser – red (650 nm)	0.016
Diode laser – blue (445 nm)	32

Figure 2.8: **Scotopic/photopic (S/P) ratios for light sources commonly utilized in outdoor lighting [7]**

CHAPTER 3: AREA LIGHTING DESIGN

INTRODUCTION

This chapter examines mesopic vision in area lighting, emphasizing the transition between photopic and scotopic vision and its impact on lighting design. The dynamic sensitivity of the human eye across this range complicates accurate visual perception representation. Luminance adaptation is vital, enabling the eye to adjust to varying light intensities, which is crucial in mesopic environments. [36,53]

For area lighting design, luminaires such as HPSV, MH, and LED, commonly used as floodlights, are selected for their specific distribution curves, spectral power density, beam angles, and luminous flux characteristics. The detailed specifications of these floodlights are provided in the table below. Traditionally, these luminaires are designed based on photopic values; however, according to CIE guidelines, manufacturing floodlights with mesopic photometry in mind could enhance both visual performance and energy efficiency. While designing luminaires based on mesopic photometry presents challenges, research indicates that such luminaires can positively impact luminance distribution and outperform those designed for photopic conditions.

The CIE mesopic table, a cornerstone of the CIE mesopic system, significantly advances our understanding of mesopic vision. It includes the S/P ratio of lamps, showing that fluctuations in the S/P ratio impact luminance levels in the photopic region. These changes in photopic luminance subsequently alter the simulated luminance levels in the mesopic region, demonstrating the interconnectedness of these lighting conditions. [42,54]

This chapter investigates the internal characteristics of floodlight luminaires that need adjustment according to mesopic photometry to achieve optimal luminance levels for human vision. It also compares different luminaires, highlighting the superiority of LEDs in outdoor lighting scenarios. The uniformity and simulated luminance values for these lamps are analyzed to assess their impact on outdoor lighting design. Given the significant variation in the spectral output and efficacy of modern lighting systems, updated measurement standards are essential to accurately reflect these advancements.

When evaluating light in mesopic photometry, the $V(\lambda)$ function often leads to inaccuracies, as it fails to account for the contributions of both rod and cone cells under intermediate lighting conditions. This limitation indicates that current techniques cannot precisely estimate effective illuminance in mesopic applications. The inadequacy of the $V(\lambda)$ function in capturing the scotopic and photopic components of mesopic vision underscores the need for improved mesopic photometry technology [55]. Therefore, this study aims to explore the distinctions between photopic and mesopic regions and methods for transitioning between them using the CIE mesopic table. The ultimate goal is to enhance lighting solutions in mesopic environments by advancing the understanding and application of mesopic photometry [42].

METHODOLOGY

The methodology for evaluating area lighting in both photopic and mesopic conditions involves a systematic approach to assess the efficacy of different luminaires. The process begins with calculating photopic design values, followed by their conversion to mesopic values to compare the effectiveness of photopic-to-mesopic conversion.

A. Photopic Design

The research methodology involves two main steps. First, lighting calculations and analysis are conducted using DIALux software to simulate area lighting design in a 30x20 meter space. This includes the evaluation of Metal Halide (MH), High-Pressure Sodium Vapour (HPSV), and LED luminaires individually. Second, CFL luminaires are added to each luminaire type from the previous design, and the lighting calculations and analysis are repeated. This sequential approach allows for a comparative assessment of the impact of CFL luminaires on the initial design with MH, HPSV, and LED luminaires. The details of the lamps and luminaires used for the design have been given downwards in table 3.2.

B. Photopic to Mesopic Conversion

In the transition to mesopic lighting design, the initial step involves converting photopic luminous flux provided by luminaire manufacturers into mesopic luminous flux. This process follows specific steps. Firstly, Photopic luminance (**L_p**) is calculated, and corresponding Mesopic luminance (**L_m**) is determined using CIE 191:2010 guidelines and the S/P ratio of the light source. S/P ratios for HPSV, MH, and LED sources are measured using a Scotopic/photopic meter. Mesopic luminance values are then interpolated from known photopic luminance values and S/P ratios using CIE 191:2010 standards. Secondly, Mesopic luminance (**L_m**) having been established, the Mesopic vs. Photopic ratio (M/P) was computed. After the computation, with the M/P ratio determined for each light source, adjustments were made to the photopic luminance values provided by the manufacturers. The LDT Editor from DIAL was utilized for this purpose, enabling modification of original photopic luminance values with corresponding mesopic values. This was achieved by multiplying the source luminance values by the appropriate M/P ratio for each case. The revised photometric files of the three chosen luminaires were integrated into the DIALux light simulation software, maintaining identical design parameters as the previous design. Average luminance was then calculated. A comprehensive table detailing measured s/p ratio, calculate mesopic luminance values using CIE 191:2010 and M/P ratios is provided for reference. M/P ratios is provided for reference. M/P ratio is determined as the quotient of Mesopic luminance (**L_m**) divided by Photopic luminance (**Lp**).

3.3 : Lighting Design in Photopic Region

The following methodology involves two main steps. First, lighting calculations and analysis are conducted using DIALux software to simulate area lighting design in a 30x20 meter space. This includes the evaluation of Metal Halide (MH), High-Pressure Sodium Vapour (HPSV), and LED luminaires individually. Second, CFL luminaires are added to each luminaire type from the previous design, and the lighting calculations and analysis are repeated. This sequential approach allows for a comparative assessment of the impact of CFL luminaires on the initial design with MH, HPSV, and LED luminaires. The details of the lamps and luminaires used for the design have been given downwards in table 3.1. In this chapter, the lighting calculations and High-Pressure Sodium Vapour (HPSV), Metal Halide (MH), and Cool white LED lamps in DIALux are presented. The goal of this section is to evaluate the average illuminance using the lamps separately.

Table 3.1: **Design considerations**

	HPSV	**MH**	**LED**
No. of luminaire	2	2	2
Pole height	9 m	9 m	9 m

In this study, DIALux software is utilized to analyze and design lighting systems by comparing photopic and mesopic regions for various luminaires. Key features such as the Luminaires Layout Plan, Coordinates List, Isolines Diagram, and Value Chart are central to this analysis. The Luminaires Layout Plan visually represents the placement and orientation of luminaires, ensuring effective light distribution and design implementation. The Coordinates List provides precise spatial coordinates (X, Y, Z) for accurate luminaire positioning. The Isolines Diagram illustrates equal luminance or illuminance lines, aiding in the assessment of light distribution uniformity. The Value Chart summarizes key metrics like luminance, illuminance, and uniformity ratios, facilitating detailed analysis and optimization of lighting designs.

The study begins by plotting these DIALux parameters for High-Pressure Sodium Vapor (HPSV), Metal Halide (MH), and Light Emitting Diode (LED) luminaires in both photopic and mesopic regions. This comparison reveals the differences between these lighting conditions for each luminaire type. The analysis is then expanded to include Compact Fluorescent Lamp (CFL) luminaires, providing a comprehensive evaluation of lighting performance across different luminaire types under varying conditions. This approach ensures a thorough understanding of how photopic and mesopic lighting affects the design and efficiency of area lighting systems.

Table 3.2: **Luminaires with specifications**

Luminaire	Details of Fixture	Light Distribution Curve
PHILIPS SWF 101/150W [SYMMETRIC], CLOSED	Luminous flux (Luminaire): 9856 lm Luminous flux (Lamps): 9856 lm Luminaire Wattage: 170.0 W Luminaire classification according to CIE: 100 CIE flux code: 62 91 99 100 100 Fitting: 1 x SON T 150W (Correction Factor 1.000)	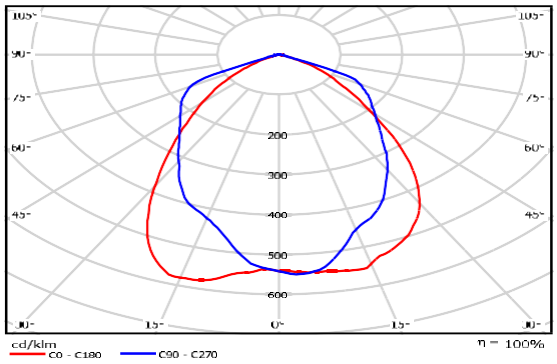
PHILIPS MWF 101/150W [SYMMETRIC], CLOSED	Luminous flux (Luminaire): 8627 lm Luminous flux (Lamps): 8627 lm Luminaire Wattage: 170.0 W Luminaire classification according to CIE: 100 CIE flux code: 71 93 99 100 100 Fitting: 1 x MHN TD 150W (Correction Factor 1.000).	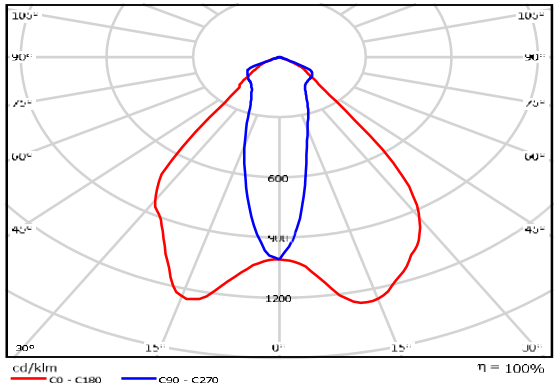
Orbit Industries, Inc.	Luminous flux (Luminaire): 10000 lm Luminous flux (Lamps): 10000 lm Luminaire Wattage: 160.0 W Luminaire classification according to CIE: 100 CIE flux code: 54 89 100 100 100 Fitting: 1 x LFL4-160W (Correction Factor 1.000).	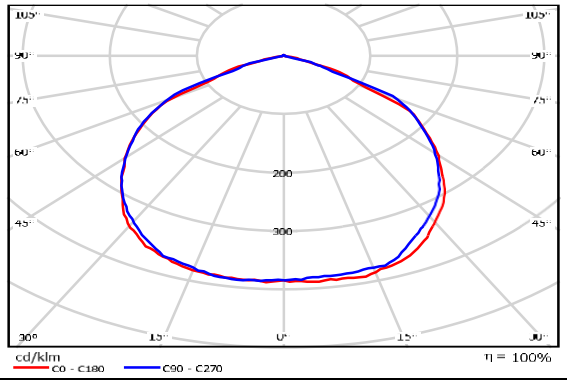
TCS 306 / 136 M1	Luminous flux (Luminaire): 2261 lm Luminous flux (Lamps): 2261 lm Luminaire Wattage: 45.2 W Luminaire classification according to CIE: 100 CIE flux code: 49 87 98 100 100 Fitting: 1 x TL'D'36W/865 (Correction Factor 1.000).	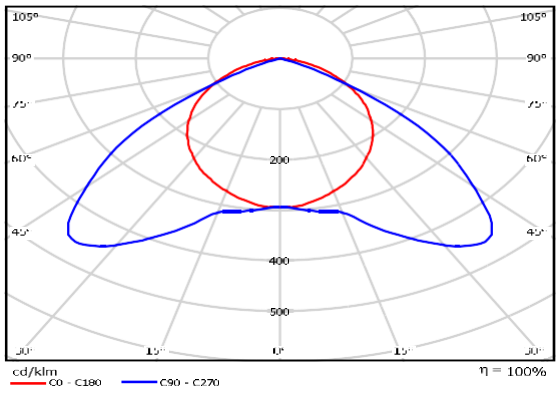

3.3.1 : Lighting Design using HPSV luminaire

Design considerations:

- Area of the space: 30 x 20m
- Luminaire used: 2 x PHILIPS SWF 101/150W [SYMMETRIC]
- Pole height: 9m
- Light loss factor: 0.80

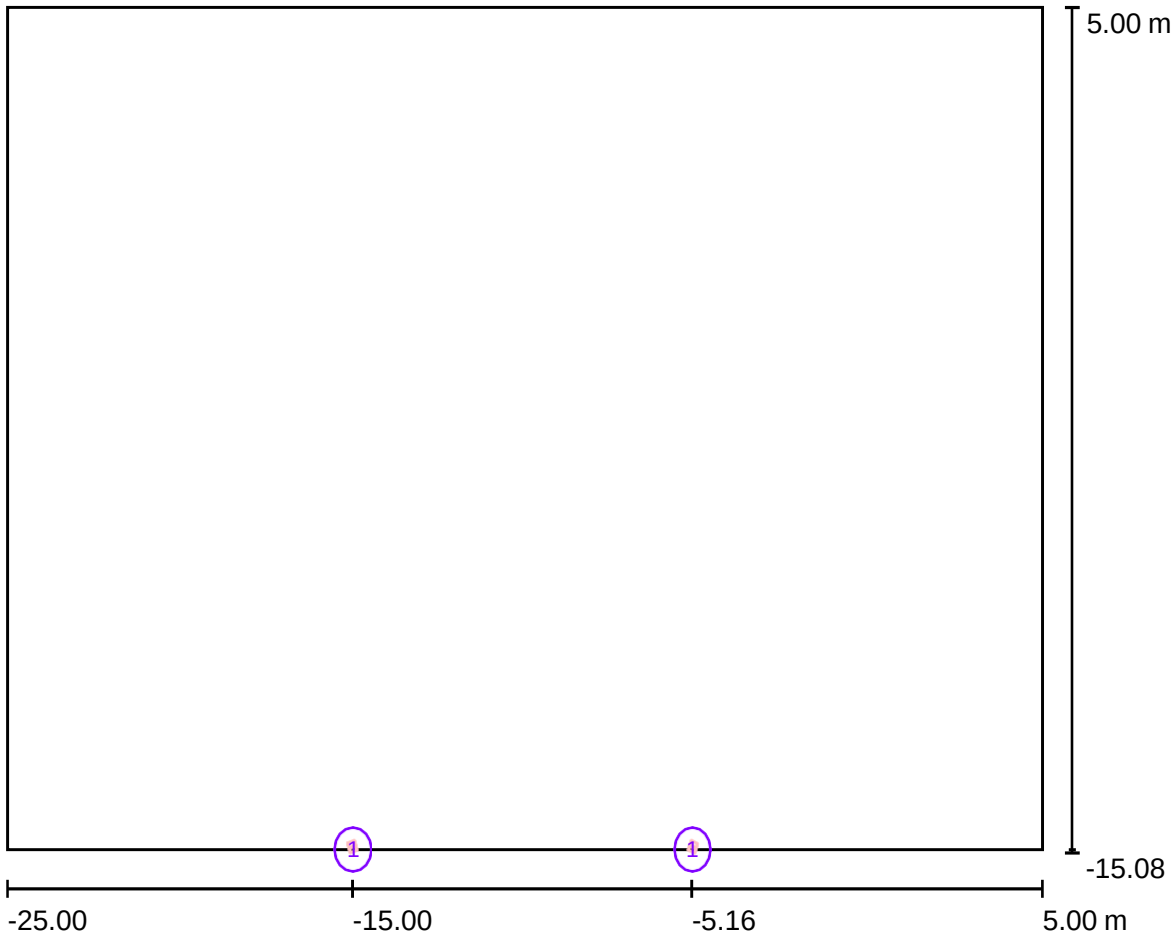

Figure 3.1: **Luminaires layout plan**

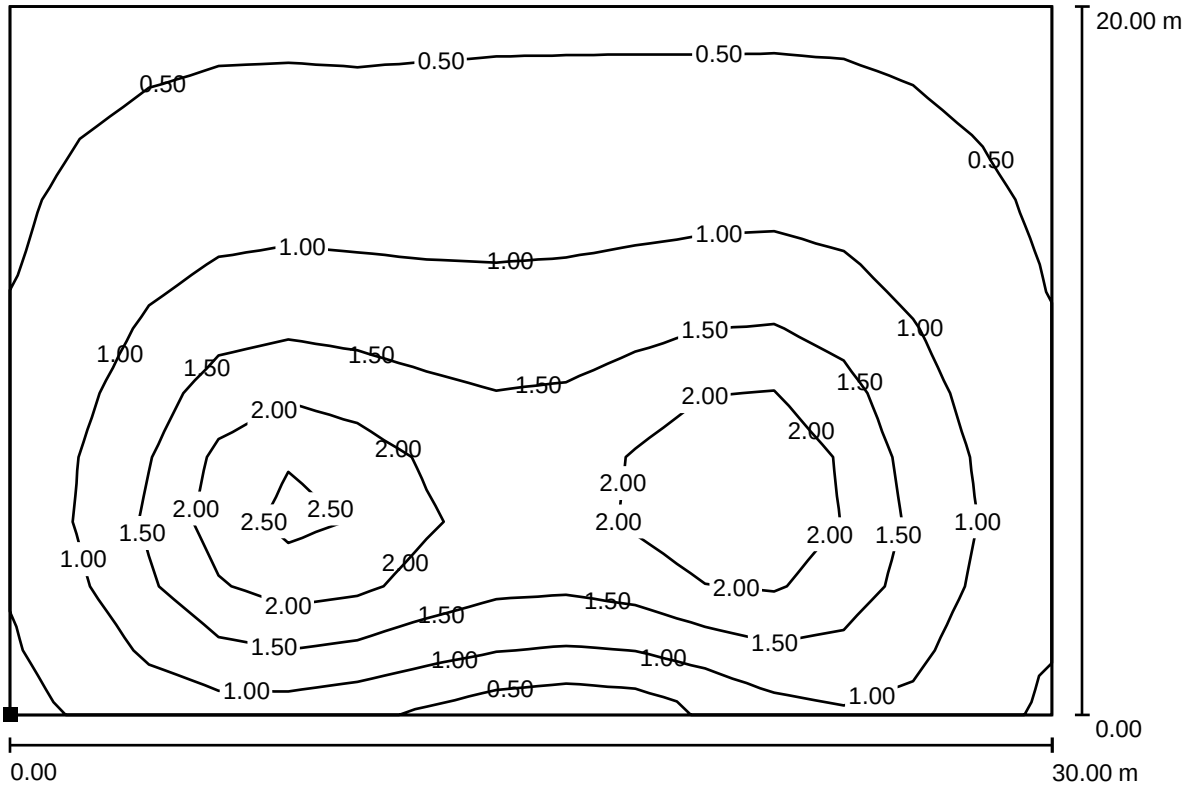

Figure 3.2: **Isolines diagram**

0.35	0.40	0.43	0.46	0.45	0.45	0.47	0.47	0.47	0.47	0.47	0.47	0.45	0.40	0.35
0.41	0.49	0.55	0.58	0.56	0.57	0.58	0.58	0.58	0.58	0.59	0.60	0.55	0.49	0.41
0.48	0.60	0.69	0.74	0.72	0.71	0.72	0.72	0.74	0.75	0.76	0.76	0.69	0.59	0.47
0.54	0.71	0.86	0.93	0.91	0.89	0.89	0.89	0.92	0.94	0.97	0.98	0.85	0.68	0.53
0.61	0.83	1.11	1.21	1.21	1.15	1.13	1.12	1.16	1.24	1.33	1.28	1.07	0.80	0.60
0.71	0.93	1.39	1.61	1.58	1.46	1.39	1.36	1.45	1.60	1.78	1.66	1.31	0.90	0.66
0.79	1.11	1.65	2.23	2.17	1.86	1.70	1.57	1.78	2.08	2.41	2.13	1.50	1.01	0.74
0.84	1.27	1.87	2.65	2.75	2.26	1.92	1.65	1.94	2.39	2.84	2.35	1.63	1.16	0.79
0.81	1.25	1.94	2.50	2.63	2.31	1.85	1.75	1.79	2.23	2.56	2.19	1.68	1.16	0.76
0.66	0.98	1.53	1.86	1.89	1.69	1.47	1.42	1.37	1.49	1.72	1.75	1.44	0.97	0.67
0.53	0.77	1.01	1.12	1.05	0.89	0.66	0.47	0.50	0.64	1.00	1.17	1.13	0.85	0.59

Figure 3.3: **Value chart**

The values obtained throughout the area are as follows:

- Average luminance ($\mathbf{L_{avg}}$) = **1.13 cd/m^2**
- Overall Uniformity ($\mathbf{U_0}$) = **0.311**

3.3.2 : Lighting Design using HPSV luminaire with surrounded CFL

Design Considerations:

- Area of the space: 30 x 20m
- Luminaire used: 2 x PHILIPS SWF 101/150W [SYMMETRIC], and 3 x TCS 306 / 136 M1(surrounding light source)
- Pole height: 9m
- Light loss factor: 0.80

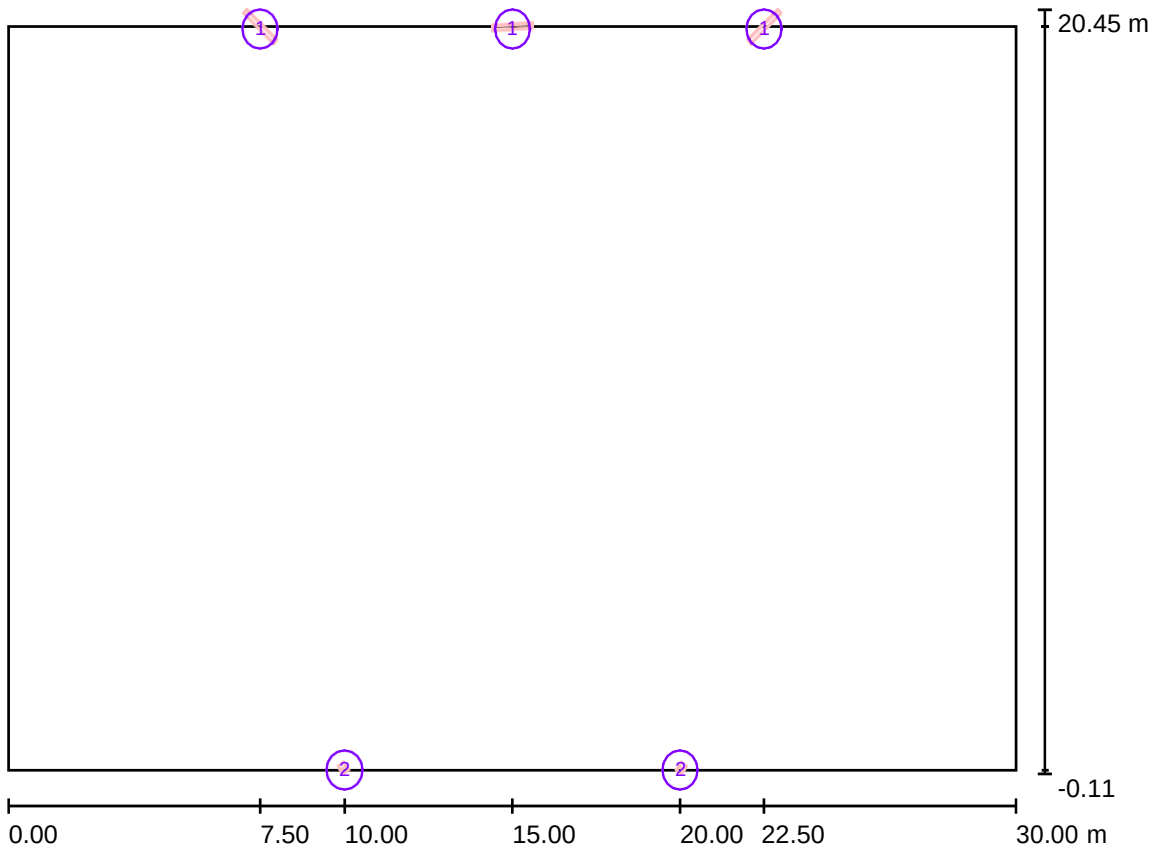

Figure 3.4: **Luminaires Layout Plan**

Here, the HPSV luminaire is denoted as 2 and CFL is denoted as 1.

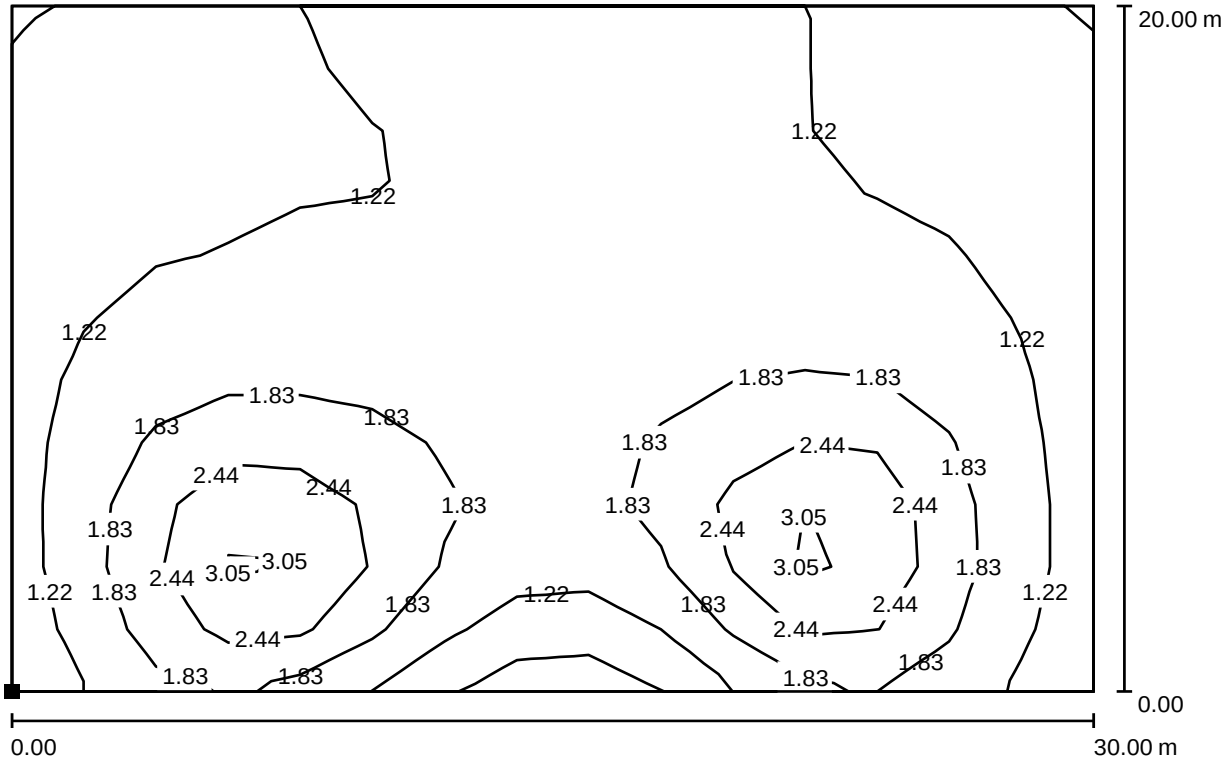

Figure 3.5: **Isoline Diagram**

0.67	0.80	1.01	1.15	1.26	1.35	1.46	1.55	1.47	1.37	1.29	1.17	1.03	0.82	0.69
0.79	0.91	1.03	1.15	1.22	1.26	1.33	1.40	1.35	1.30	1.26	1.20	1.07	0.95	0.82
0.90	1.02	1.08	1.16	1.20	1.21	1.24	1.29	1.28	1.27	1.26	1.21	1.13	1.06	0.93
0.98	1.11	1.14	1.19	1.23	1.22	1.23	1.28	1.29	1.31	1.31	1.26	1.22	1.15	0.99
1.05	1.22	1.28	1.30	1.37	1.31	1.29	1.31	1.35	1.43	1.48	1.37	1.38	1.25	1.04
1.15	1.36	1.51	1.51	1.57	1.50	1.39	1.39	1.46	1.62	1.68	1.64	1.62	1.36	1.11
1.21	1.55	1.87	1.93	1.85	1.79	1.53	1.48	1.63	1.96	2.03	2.17	1.95	1.53	1.13
1.26	1.79	2.44	2.65	2.30	2.14	1.66	1.60	1.73	2.32	2.62	2.99	2.39	1.62	1.17
1.30	1.89	2.94	3.42	2.79	2.18	1.68	1.60	1.68	2.30	3.10	3.48	2.56	1.68	1.20
1.25	1.88	2.73	3.34	2.71	1.94	1.40	1.18	1.28	1.84	2.78	3.14	2.41	1.69	1.16
1.05	1.54	2.16	2.24	1.82	1.32	0.74	0.44	0.63	1.18	1.86	2.25	2.00	1.43	0.98

Figure 3.6: **Value Chart**

The values obtained throughout the area are as follows:

- Average luminance ($\mathbf{L_{avg}}$) = **1.53 cd/m^2**
- Overall Uniformity ($\mathbf{U_o}$) = **0.285**

3.3.3 : Lighting Design using MH luminaire

Design Considerations:

- Area of the space: 30 x 20m
- Luminaire used: 2 x PHILIPS MWF 101/150W [SYMMETRIC], CLOSED
- Pole height: 9m
- Light loss factor: 0.80

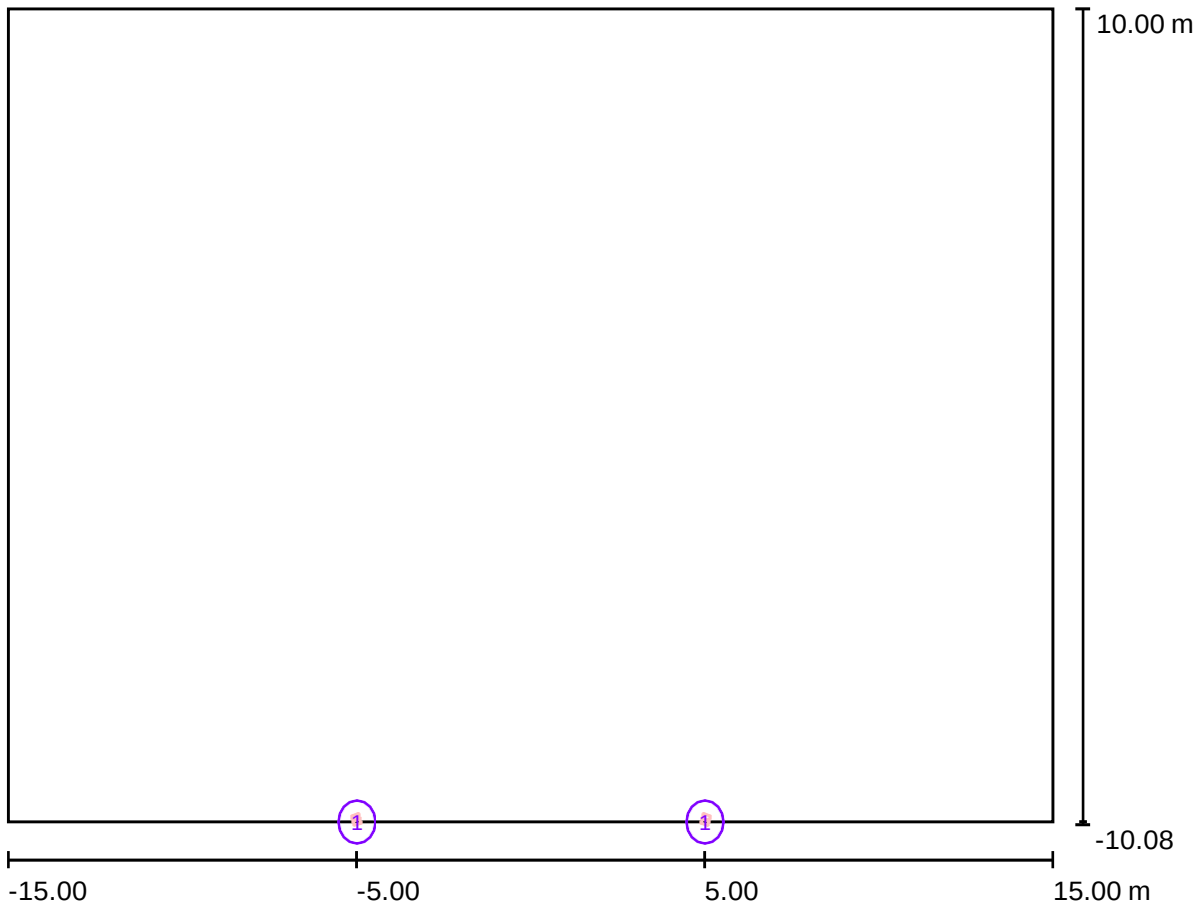

Figure 3.7: **Luminaire Layout Plan**

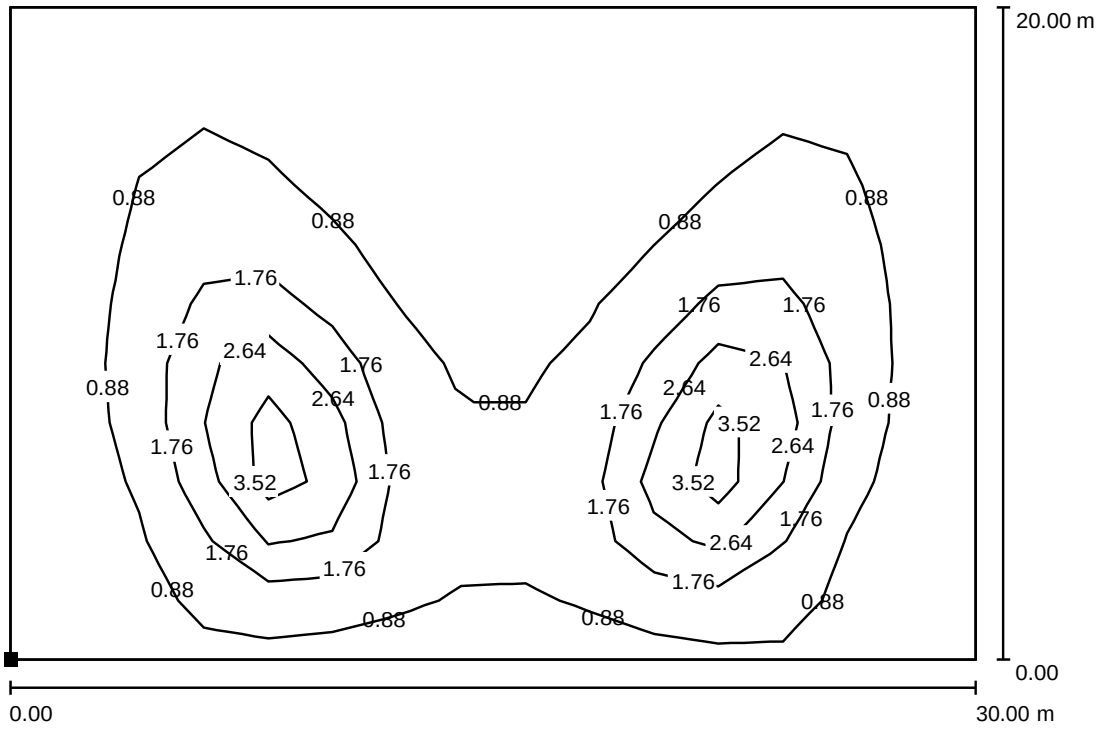

Figure 3.8: **Isoline Diagram**

0.41	0.59	0.66	0.56	0.42	0.31	0.24	0.23	0.25	0.29	0.35	0.51	0.65	0.61	0.45
0.41	0.63	0.82	0.72	0.54	0.39	0.30	0.28	0.30	0.37	0.46	0.67	0.82	0.66	0.47
0.40	0.67	1.02	0.96	0.72	0.52	0.38	0.35	0.38	0.46	0.60	0.91	1.03	0.73	0.49
0.40	0.69	1.20	1.32	0.98	0.67	0.47	0.43	0.48	0.61	0.83	1.25	1.26	0.81	0.49
0.41	0.70	1.42	1.90	1.46	0.92	0.60	0.53	0.61	0.82	1.25	1.85	1.55	0.87	0.48
0.42	0.73	1.64	2.68	2.25	1.28	0.75	0.65	0.75	1.10	2.00	2.69	1.87	0.88	0.45
0.42	0.71	1.80	3.69	3.64	1.73	0.92	0.79	0.92	1.45	3.06	3.97	2.11	0.82	0.42
0.39	0.67	1.47	3.46	4.45	2.06	1.06	0.95	1.06	1.77	3.76	4.12	1.86	0.71	0.41
0.37	0.59	1.20	2.89	4.64	2.23	1.14	1.17	1.18	1.98	4.46	3.28	1.34	0.61	0.40
0.37	0.52	0.85	1.47	1.79	1.47	1.17	0.99	1.11	1.27	1.83	1.71	0.90	0.56	0.40
0.34	0.49	0.77	0.95	0.97	0.82	0.64	0.34	0.63	0.82	1.00	1.05	0.83	0.57	0.37

20.00 m
0.00
0.00
30.00 m

Figure 3.9: **Value Chart**

The values obtained throughout the area are as follows:

- Average luminance ($\mathbf{L_{avg}}$) = **1.09 cd/m^2**
- Overall Uniformity ($\mathbf{U_o}$) = **0.210**

3.3.4. : Lighting Design using MH luminaire with surrounded CFL

Design Considerations:

- Area of the space: 30 x 20m
- Luminaire used: 2 x PHILIPS MWF 101/150W [SYMMETRIC], CLOSED and 3 x TCS 306 / 136 M1 (surrounding light source)
- Pole height: 9m
- Light loss factor: 0.80

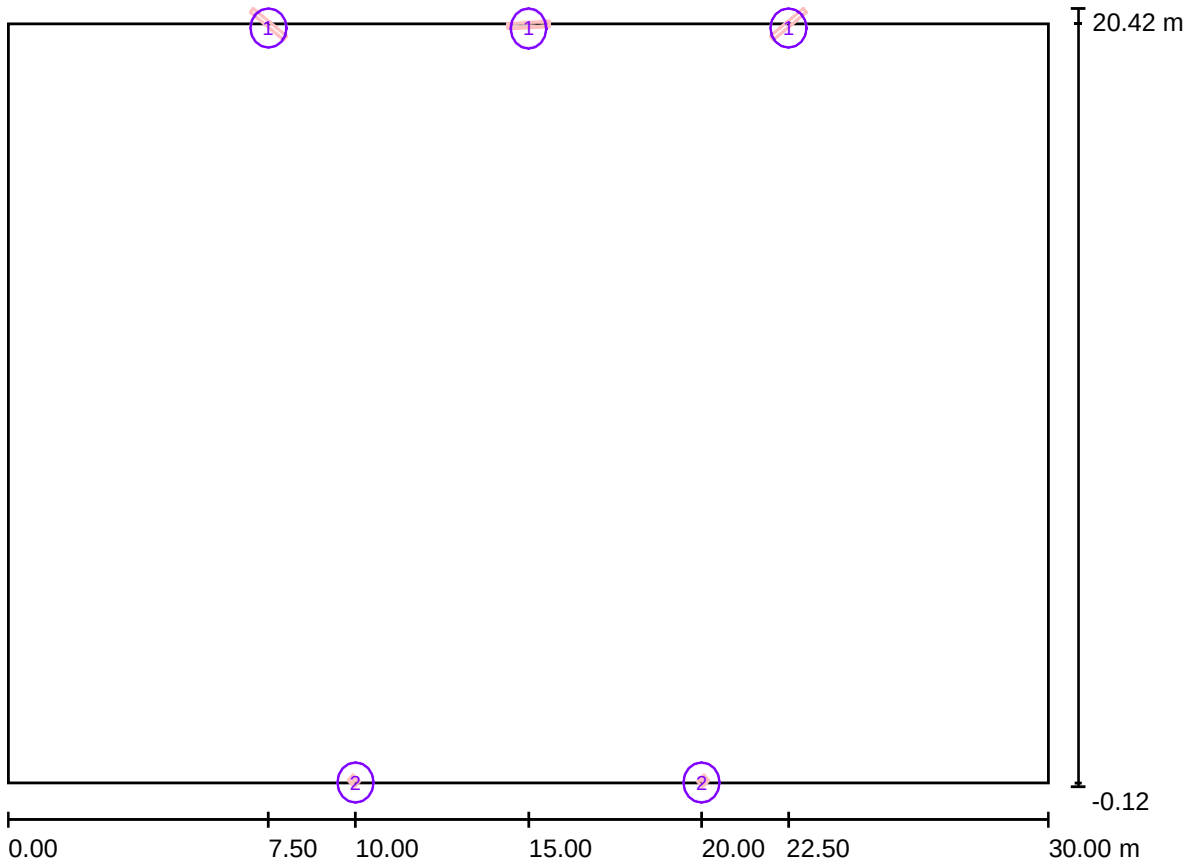

Figure 3.10: **Luminaire Layout Plan**

Here, Metal Halide (MH) luminaires are denoted as 2 and CFL is denoted as 1.

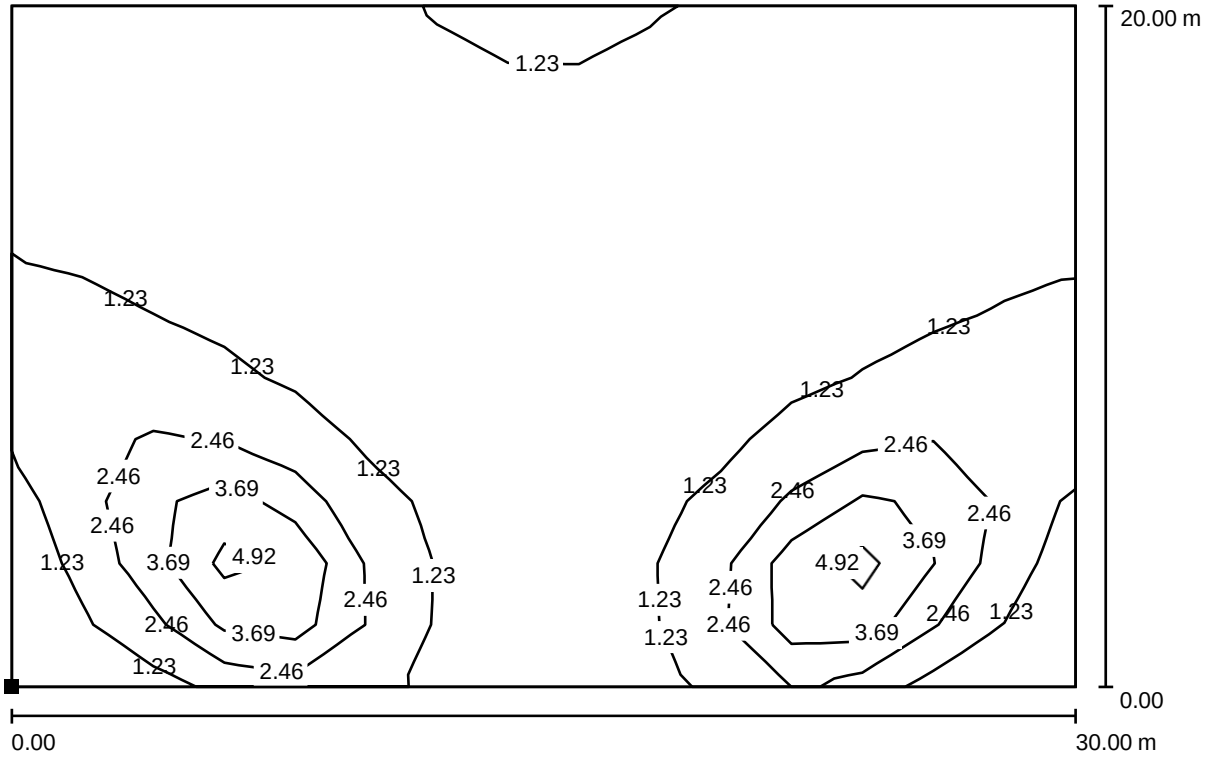

Figure 3.11: **Isoline Diagram**

0.58	0.67	0.82	0.94	1.05	1.15	1.28	1.34	1.28	1.16	1.05	0.94	0.82	0.66	0.55
0.71	0.78	0.85	0.91	0.96	1.04	1.12	1.16	1.13	1.06	0.97	0.91	0.86	0.77	0.65
0.86	0.87	0.88	0.87	0.87	0.93	1.00	1.04	1.02	0.97	0.88	0.87	0.89	0.83	0.75
1.02	0.99	0.90	0.85	0.82	0.85	0.95	0.97	0.97	0.89	0.83	0.87	0.90	0.89	0.87
1.29	1.17	0.98	0.88	0.82	0.82	0.93	0.96	0.93	0.85	0.82	0.88	0.95	1.01	1.19
1.69	1.52	1.25	1.01	0.87	0.83	0.94	0.97	0.94	0.83	0.87	1.00	1.11	1.36	1.64
1.96	2.16	1.93	1.46	1.03	0.87	0.96	0.97	0.96	0.85	1.02	1.31	1.63	2.09	1.98
1.61	2.75	3.41	2.91	1.49	1.00	0.98	0.97	1.01	0.96	1.37	2.41	3.16	2.85	1.78
1.16	2.40	5.08	5.70	2.54	1.19	1.07	0.93	1.06	1.15	2.14	4.75	5.19	2.73	1.45
0.90	1.64	3.91	6.13	4.51	1.43	0.99	0.76	0.90	1.42	3.95	6.40	4.73	2.02	0.97
0.65	1.02	1.85	3.54	2.64	1.36	0.75	0.27	0.76	1.21	2.67	4.02	2.18	1.09	0.66

Figure 3.12: **Value Chart**

The values obtained throughout the area are as follows:

- Average luminance ($\mathbf{L_{avg}}$) = **1.46 cd/m^2**
- Overall Uniformity ($\mathbf{U_o}$) = **0.186**

3.3.5 : Lighting Design using LED luminaire

Design Considerations:

- Area of the space: 30 x 20m
- Luminaire used: 2 x Orbit Industries, Inc.
- Pole height: 9m.
- Light loss factor: 0.80

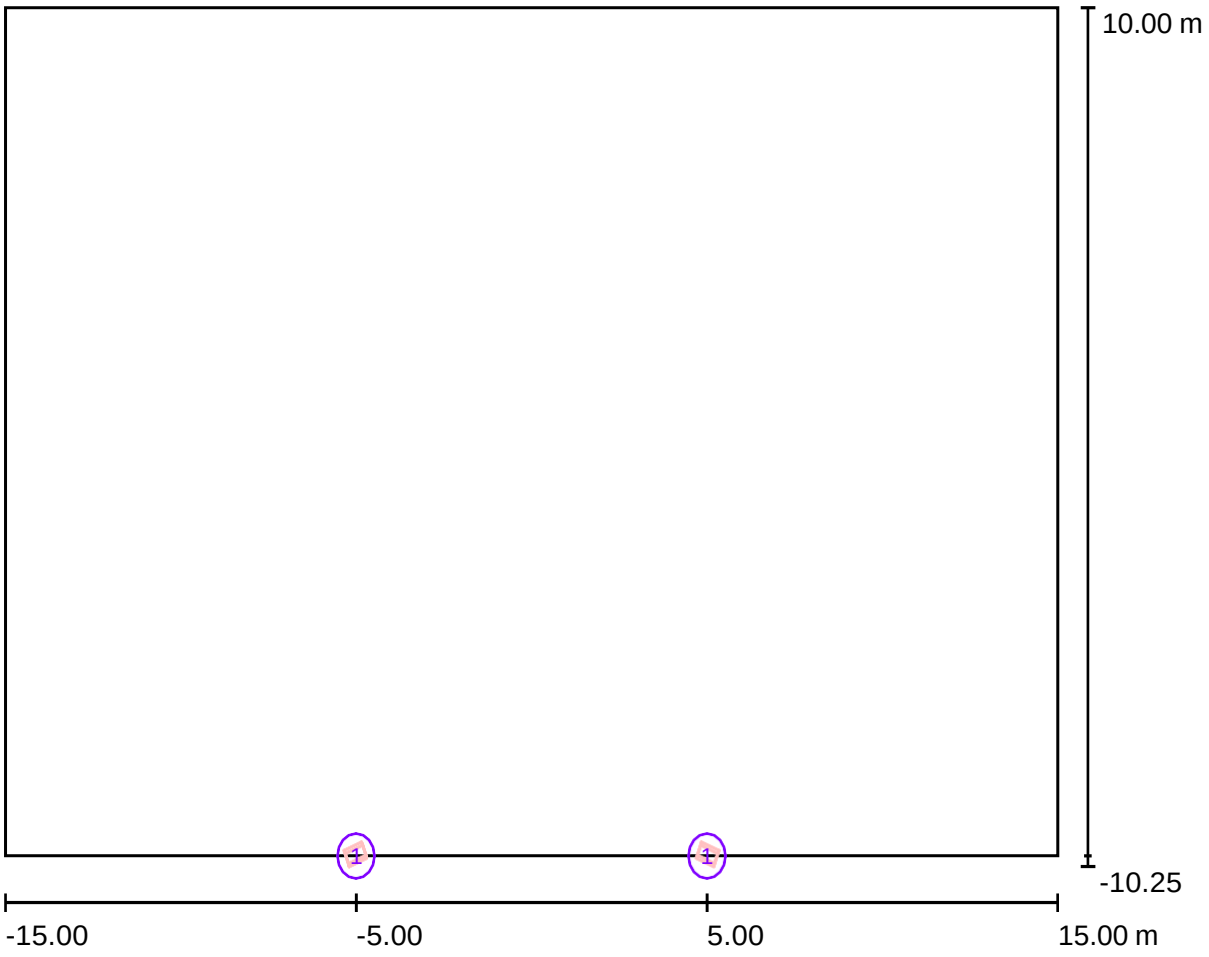

Figure 3.13: **Luminaire Layout Plan**

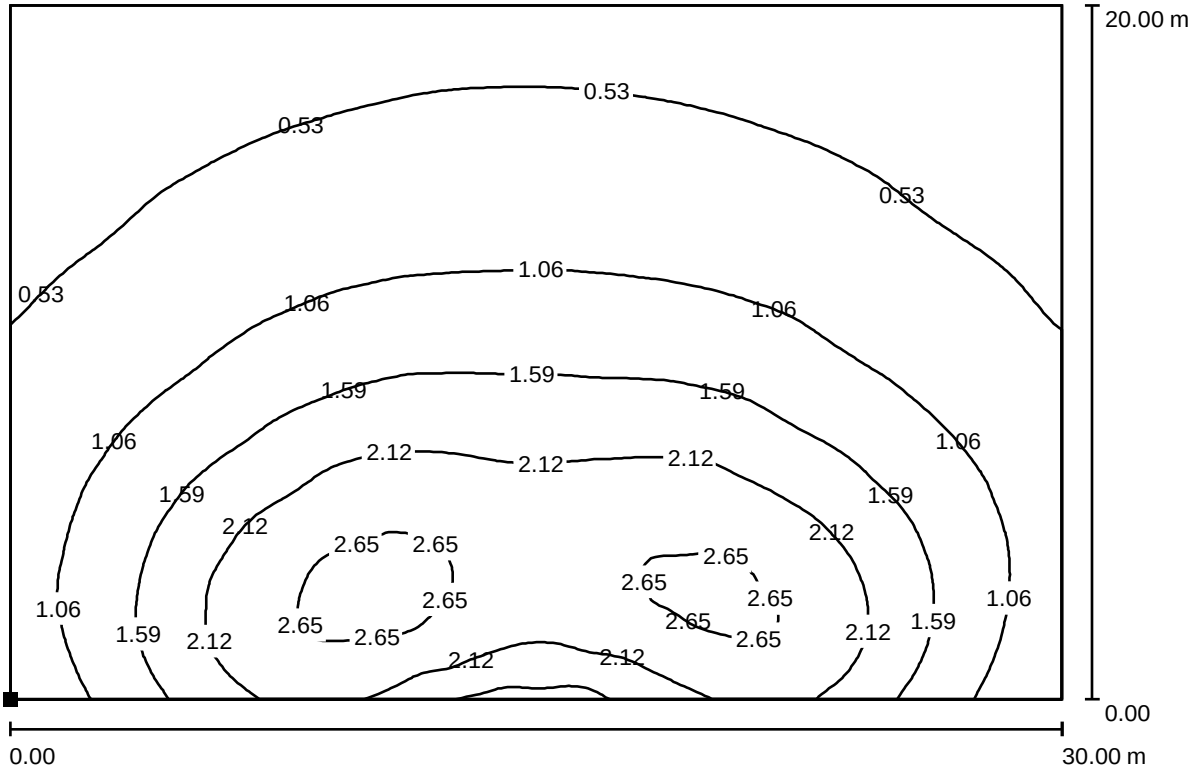

Figure 3.14: **Isoline Diagram**

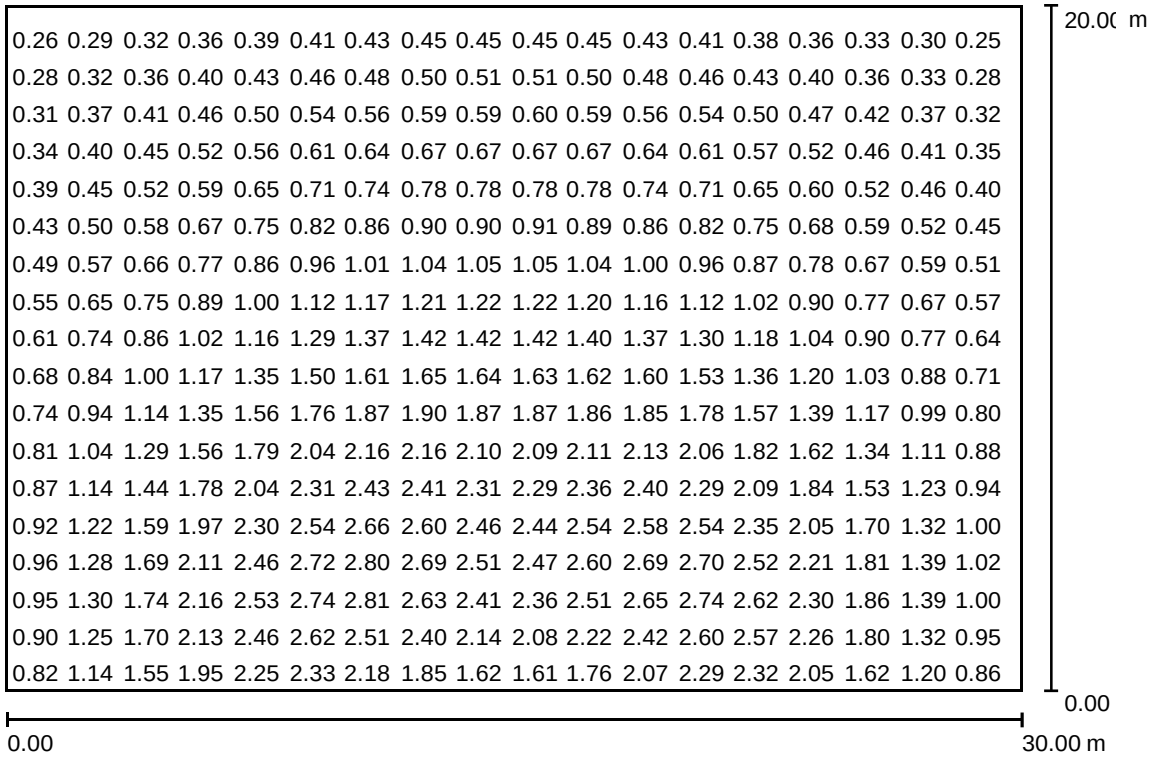

Figure 3.15: **Value Chart**

The values obtained throughout the area are as follows:

- Average luminance ($\mathbf{L_{avg}}$) = **1.21 cd/m^2**
- Overall Uniformity ($\mathbf{U_0}$) = **0.203**

3.3.6 : Lighting Design using LED luminaire with surrounded CFL

Design Considerations:

- Area of the space: 30 x 20m
- Luminaire used: 2 x Orbit Industries, Inc. and 3 x TCS 306 / 136 M1(surrounding light source)
- Pole height: 9m
- Light loss factor: 0.80

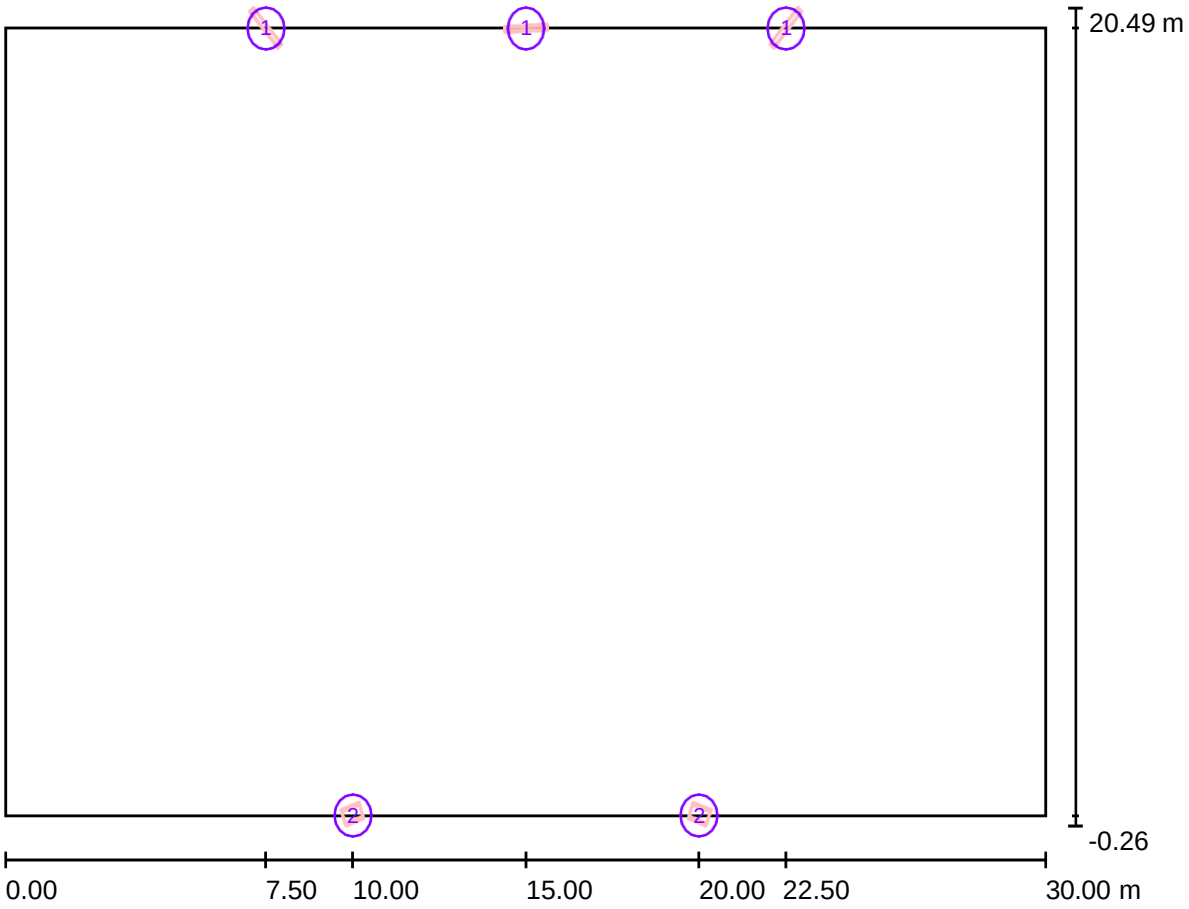

Figure 3.16: **Luminaire Layout Plan**

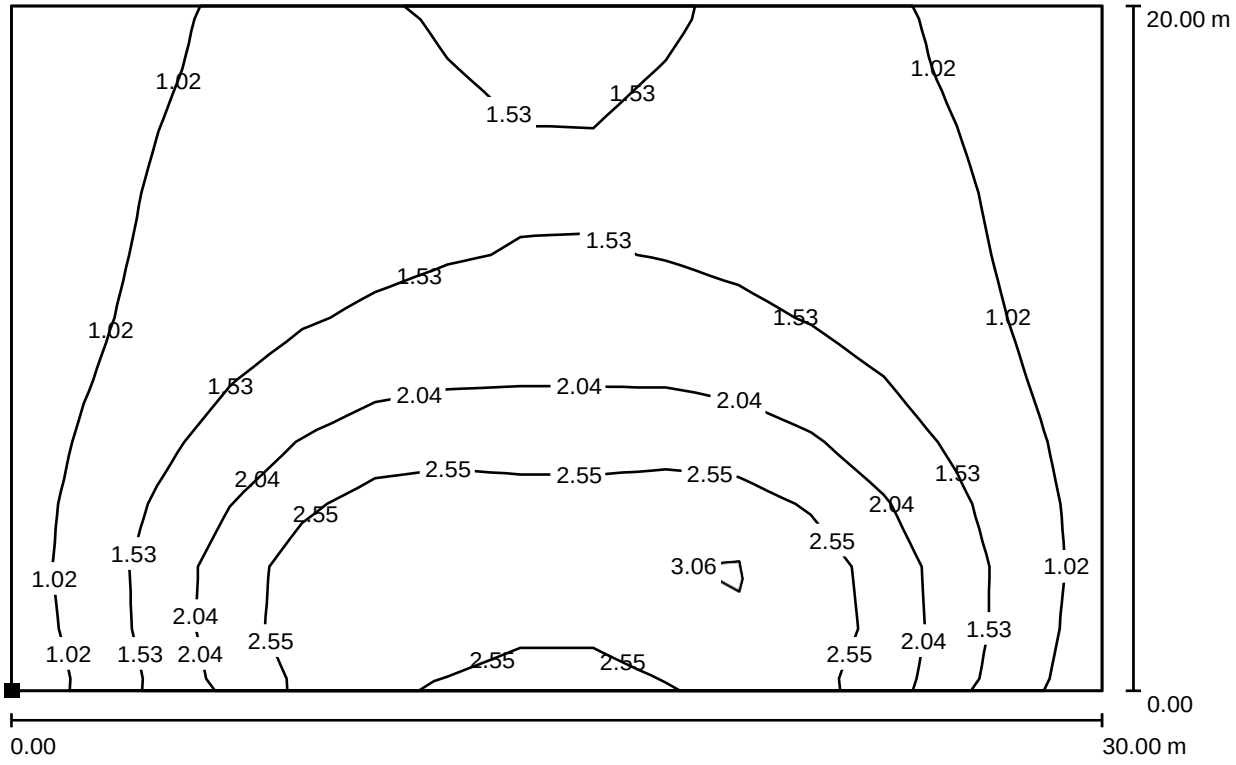

Figure 3.17: **Isoline Diagram**

0.69	0.83	1.03	1.18	1.34	1.49	1.64	1.73	1.64	1.49	1.35	1.18	1.03	0.83	0.70
0.78	0.93	1.05	1.18	1.30	1.40	1.52	1.61	1.53	1.41	1.31	1.18	1.06	0.93	0.79
0.83	0.98	1.09	1.17	1.28	1.36	1.44	1.51	1.46	1.38	1.29	1.18	1.11	0.99	0.84
0.84	1.00	1.13	1.21	1.30	1.40	1.46	1.51	1.47	1.41	1.33	1.22	1.14	1.02	0.86
0.84	1.01	1.19	1.31	1.44	1.54	1.59	1.62	1.60	1.57	1.46	1.33	1.20	1.04	0.85
0.85	1.06	1.29	1.49	1.67	1.77	1.83	1.84	1.83	1.80	1.68	1.51	1.32	1.09	0.87
0.90	1.16	1.45	1.76	2.01	2.14	2.17	2.16	2.17	2.16	2.01	1.78	1.51	1.18	0.93
0.95	1.30	1.69	2.05	2.45	2.61	2.58	2.55	2.58	2.60	2.47	2.12	1.74	1.33	0.99
1.00	1.39	1.94	2.39	2.89	3.02	2.94	2.83	2.91	3.02	2.92	2.44	1.99	1.42	1.03
1.00	1.44	2.10	2.64	3.10	3.25	2.99	2.84	2.99	3.25	3.15	2.71	2.15	1.48	1.03
0.91	1.33	1.97	2.54	2.82	2.77	2.53	2.35	2.53	2.85	2.86	2.61	2.05	1.39	0.95

20.00 m
0.00
0.00
30.00 m

Figure 3.18: **Value Chart**

The values obtained throughout the area are as follows:

- Average luminance ($\mathbf{L_{avg}}$) = **1.65 cd/m^2**
- Overall Uniformity ($\mathbf{U_o}$) = **0.434**

3.1.4: An overview of the luminaires' designs in Photopic region

The summary calculations provided under the tables pertain to designs in the photopic region. These tables present key metrics including the quantity of luminaires used in the designs, the values of average photopic luminance ($\mathbf{L_p}$), and the overall uniformity ($\mathbf{U_0}$). Table 3.3 details the results using the light sources: High-Pressure Sodium Vapor (HPSV), Metal Halide (MH), and Light Emitting Diode (LED) exclusively. In contrast, Table 3.4 presents similar metrics, but incorporates the impact of surrounding light sources in conjunction with HPSV, MH, and LED.

Table 3.3: **Design Summary for All the luminaires in photopic region**

Main Light source	Average photopic luminance ($\mathbf{L_p}$)	Overall Uniformity ($\mathbf{U_0}$)
HPSV	1.13	0.311
MH	1.09	0.210
LED	1.21	0.203

Table 3.4: **Design Summary for All the luminaires in photopic region with surrounding luminaires**

Main Light source	Average photopic luminance ($\mathbf{L_p}$)	Overall Uniformity ($\mathbf{U_0}$)
HPSV+CFL	1.53	0.285
MH+CFL	1.46	0.186
LED+CFL	1.65	0.434

3.4 : Lighting Design in Mesopic Region

3.4.1. Conversion process for photopic data to corresponding mesopic data

Accurately converting photopic luminous flux, as provided by luminaire manufacturers, into mesopic luminous flux is a fundamental and necessary step in making the transition to mesopic lighting design. Since mesopic conditions occur at light levels where both rod and cone photoreceptors in the human eye are active, this approach enables lighting designers to consider and take into consideration the different visual responses under mesopic conditions. There are several detailed phases in the conversion process:

- **Calculation of Mesopic Luminance (L_m):**

The first step in this conversion process is to determine the photopic luminance (**L_p**), which is the amount of light that the human eye perceives in illuminated environments, most often during daylight hours. It is necessary to compute the equivalent mesopic luminance (**L_m**) after determining the photopic luminance. The CIE 191:2010 standards, which offer a uniform procedure for this transformation, serve as the basis for this computation. The light source's scotopic/photopic (S/P) ratio, an important factor which impacts the mesopic intensity, is also needed for the computation. A Scotopic/Photopic meter is used to measure the light sources, with a focus on Metal Halide (MH), Light Emitting Diode (LED), and High-Pressure Sodium Vapour (HPSV) technologies with the goal to acquire the S/P ratio. The connection between the photopic (brightly light vision) and scotopic (low-light vision) responses to a particular light source is represented by the S/P ratio. According to CIE 191:2010 recommendations, mesopic luminance values can be interpolated from known photopic luminance values using these ratios. This is a significant phase as it establishes the foundation for knowing how light sources react in mesopic circumstances which are prevalent in outdoor and transitional lighting circumstances.

- **Calculation of the Mesopic vs. Photopic Ratio (M/P):**

Once the mesopic luminance (**L_m**) has been determined, the Mesopic vs. Photopic ratio (M/P) needs to be calculated. A statistic for comparison that shows how effective a light source is in mesopic vs photopic environments is the M/P ratio. It can be expressed as the ratio of photopic luminance (**L_p**) to mesopic luminance (**L_m**). This ratio is essential as it offers a simple way of altering the photopic data, thereby rendering it applicable to mesopic luminance circumstances. In order to ensure that the lighting design is optimized for the real visual perception in mesopic

circumstances, an appropriate M/P ratio is necessary for translating the photopic data to mesopic equivalents.

- **Adjustment of Photopic Luminance Values:**

The photopic luminance values provided by manufacturers are altered to correspond with the mesopic circumstances once the M/P ratio for each light source has been established. This adjustment procedure is essential for ensuring that, in mesopic lighting circumstances, the lighting design is simultaneously human visual perception-aligned and energy-efficient. To accomplish these modifications, LDT Editor software is used. The original photopic luminance values in the photometric data can be changed to their mesopic equivalents using the LDT Editor. The method for adjusting the values to account for the mesopic response involves multiplying the source luminance values by the matching M/P ratio. The data utilized in lighting simulations is guaranteed to precisely reflect the real performance of the light sources under mesopic circumstances thanks to this comprehensive correction process.

- **Simulation in DIALux:**

The photometric data is imported into the DIALux light simulation software after being modified. DIALux is a prominent lighting design and simulation application that helps designers to accurately simulate and evaluate various lighting configurations. At this point, results may be directly compared since the simulation applies the same design parameters as earlier photopic-based designs. The software determines the average luminance for the lighting scenario under mesopic circumstances by entering the corrected photometric information. This phase is essential for confirming that the conversion process worked as expected while also making sure that the lighting design satisfies the requirements for energy efficiency, safety, and visual comfort. The research includes a comprehensive table that shows the measured S/P ratios, mesopic luminance values computed using CIE 191:2010 criteria, and matching M/P ratios. This data enables the conversion process simpler to reference and compare since it presents the information in a systematic and comprehensible way. It is an essential point of reference for confirming that the modified photometric data is consistent with actual visual circumstances and that the mesopic lighting design is appropriate.

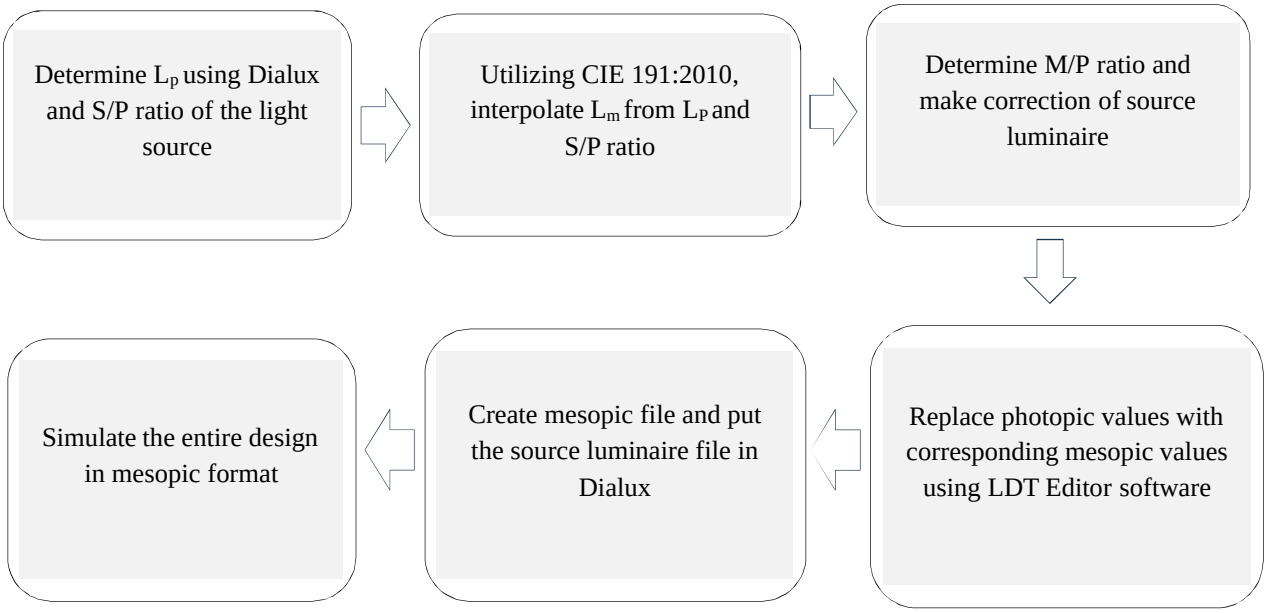

Figure 3.19: **Conceptual flow diagram of the proposed study methodology**

Table 3.5: **Values of L_m of the recommended mesopic system as a function of photopic luminance and s/p ratio [42]**

	Photopic luminance / cd·m^{-2}						
S/P	0,01	0,03	0,1	0,3	1	3	4,5
LPS ~ 0,25	0,002 5	0,014 5	0,070 5	0,246 7	0,913 0	2,926 5	4,478 2
0,35	0,003 5	0,017 4	0,075 0	0,254 5	0,925 3	2,936 7	4,481 2
0,45	0,004 5	0,019 8	0,079 3	0,262 0	0,937 3	2,946 8	4,484 2
HPS ~ 0,55	0,005 7	0,022 0	0,083 4	0,269 3	0,949 2	2,956 8	4,487 2
0,65	0,006 9	0,023 9	0,087 3	0,276 4	0,960 8	2,966 6	4,490 1
0,75	0,007 9	0,025 8	0,091 1	0,283 3	0,972 2	2,976 3	4,492 9
0,85	0,008 8	0,027 5	0,094 7	0,290 1	0,983 5	2,985 9	4,495 8
0,95	0,009 6	0,029 2	0,098 3	0,296 7	0,994 5	2,995 3	4,498 6
1,05	0,010 4	0,030 8	0,101 7	0,303 2	1,005 4	3,004 6	4,501 4
MH warm white ~ 1,15	0,011 1	0,032 3	0,105 1	0,309 6	1,016 1	3,013 9	4,504 1
1,25	0,011 8	0,033 8	0,108 3	0,315 8	1,026 7	3,023 0	4,506 8
1,35	0,012 5	0,035 3	0,111 5	0,322 0	1,037 1	3,031 9	4,509 5
1,45	0,013 2	0,036 7	0,114 7	0,328 0	1,047 3	3,040 8	4,512 2
1,55	0,013 8	0,038 1	0,117 8	0,333 9	1,057 5	3,049 6	4,514 8
1,65	0,014 5	0,039 5	0,120 8	0,339 8	1,067 4	3,058 2	4,517 4
1,75	0,015 1	0,040 8	0,123 8	0,345 5	1,077 3	3,066 8	4,520 0
1,85	0,015 7	0,042 1	0,126 7	0,351 2	1,087 0	3,075 3	4,522 5
1,95	0,016 3	0,043 4	0,129 5	0,356 8	1,096 6	3,083 6	4,525 0
2,05	0,016 9	0,044 6	0,132 4	0,362 3	1,106 0	3,091 9	4,527 5
2,15	0,017 4	0,045 9	0,135 2	0,367 7	1,115 4	3,100 1	4,529 9
2,25	0,018 0	0,047 1	0,137 9	0,373 1	1,124 6	3,108 2	4,532 3
MH day-light ~ 2,35	0,018 5	0,048 3	0,140 6	0,378 4	1,133 8	3,116 2	4,534 7
2,45	0,019 1	0,049 5	0,143 3	0,383 6	1,142 8	3,124 1	4,537 1
2,55	0,019 6	0,050 6	0,145 9	0,388 8	1,151 7	3,131 9	4,539 5
2,65	0,020 1	0,051 8	0,148 5	0,393 9	1,160 5	3,139 6	4,541 8
2,75	0,020 7	0,052 9	0,151 1	0,398 9	1,169 3	3,147 3	4,544 1

All the measured s/p ratio, calculated mesopic luminance value using CIE 191:2010 and m/p ratio are shown table 3.5. Here, M/P ratio=Lm/Lp.

Table 3.6: **Measured and calculated value**

Main Light source	Average photopic luminance ($\mathbf{L_p}$)	Measured S/P ratio	Calculated mesopic luminance ($\mathbf{L_m}$) using CIE 191:2010	Calculated M/P ratio
HPSV	1.13	0.62	1.09	0.97
MH	1.09	1.2	1.11	1.01
LED	1.21	1.6	1.27	1.04

3.4.2 : Modified Photometric file creation through LDT Editor software and implementation in DIALux design

This section outlines the process of using LDT Editor software to convert photopic to mesopic conditions and modify luminaire IES files for mesopic region designs. The procedure begins by uploading the IES file of a selected luminaire into the LDT Editor software, which displays the primary details of the luminaire. To adapt the design for the mesopic region, the luminous intensity data applicable to this region must be replaced via the "Luminous Intensities" option. This replacement automatically adjusts the light distribution and the corresponding luminous flux. Once these changes are made, the file should be saved and renamed to reflect its adaptation for mesopic conditions. The modified luminaire file can then be used to redesign the lighting plan, generating outputs and design values suitable for mesopic lighting conditions.

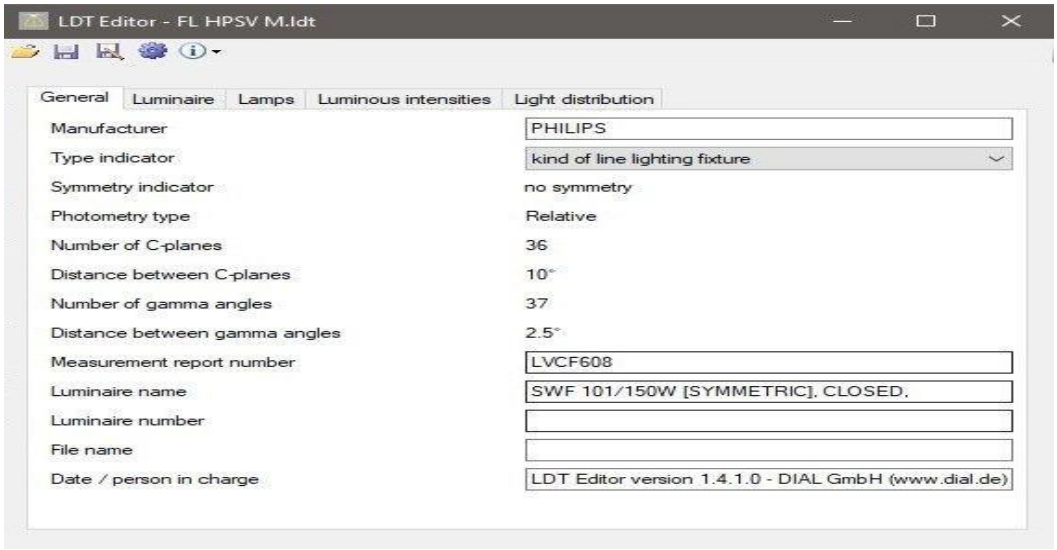

Figure 3.20: **A sample of HPSV luminaire details in LDT Editor software**

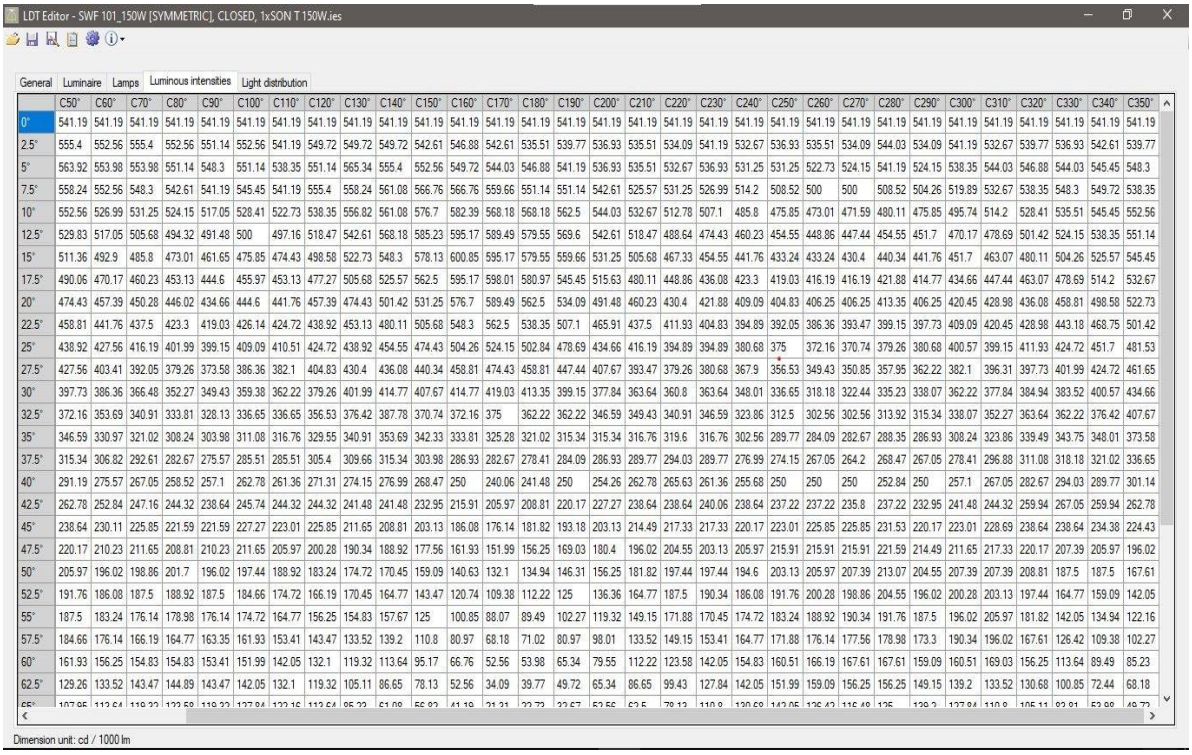

Figure 3.21: **Original intensity data table of HPSV luminaire in photopic region**

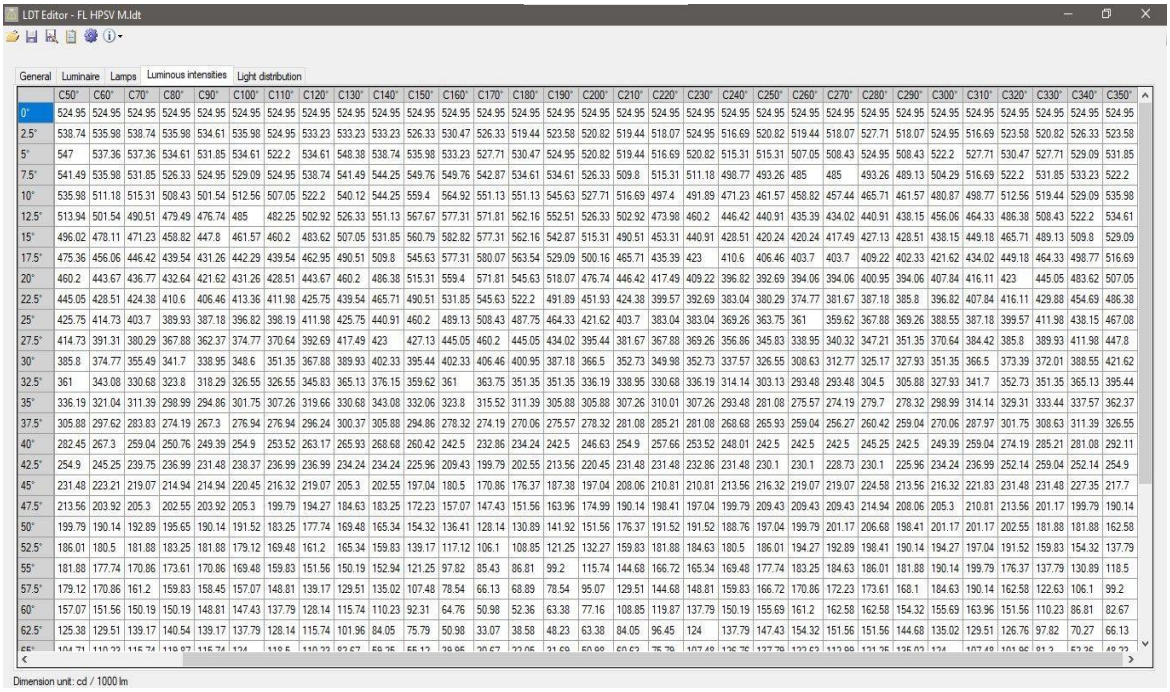

Figure 3.22: **Modified intensity data table of HPSV luminaire in photopic region**

Table 3.7: **Modified Luminaires with Specification**

Name of Luminaire	Details of Fixture	Light Distribution Curve
PHILIPS SWF 101/150W [SYMMETRIC], CLOSED,	Luminous flux (Luminaire): 9560 lm Luminous flux (Lamps): 9856 lm Luminaire Wattage: 170.0 W Luminaire classification according to CIE: 100 CIE flux code: 62 91 99 100 97 Fitting: 1 x SON T 150W (Correction Factor 1.000).	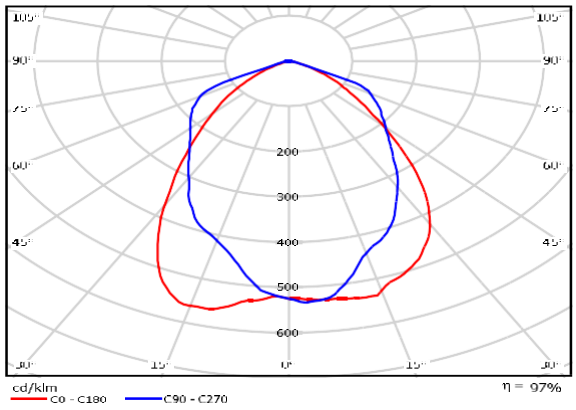
PHILIPS MWF 101/150W [SYMMETRIC], CLOSED,	Luminous flux (Luminaire): 8713 lm Luminous flux (Lamps): 8627 lm Luminaire Wattage: 170.0 W Luminaire classification according to CIE: 100 CIE flux code: 71 93 99 100 101 Fitting: 1 x MHN TD 150W (Correction Factor 1.000)	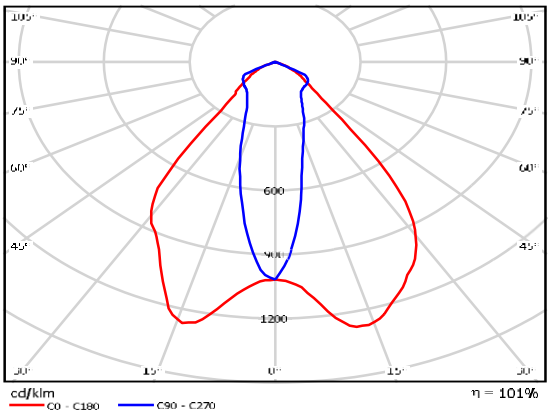
Orbit Inc.	Luminous flux (Luminaire): 10399 lm Luminous flux (Lamps): 10000 lm Luminaire Wattage: 160.0 W Luminaire classification according to CIE: 100 CIE flux code: 54 89 100 100 104 Fitting: 1 x LFL4-160W (Correction Factor 1.000).	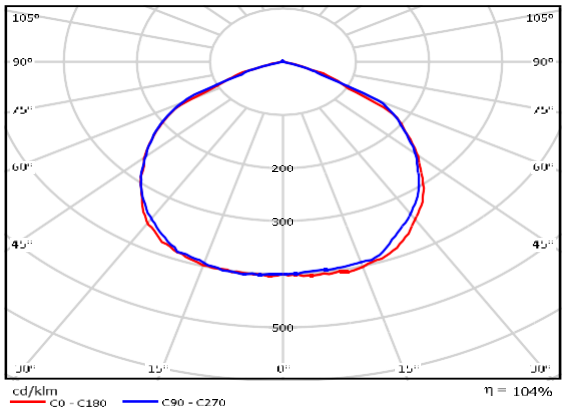

3.4.3 : Lighting Design using modified HPSV luminaire

Design Considerations:

- Area of the space: 30 x 20m
- Luminaire used: 2 x PHILIPS SWF 101/150W [SYMMETRIC]
- Pole height: 9m
- Light loss factor: 0.80

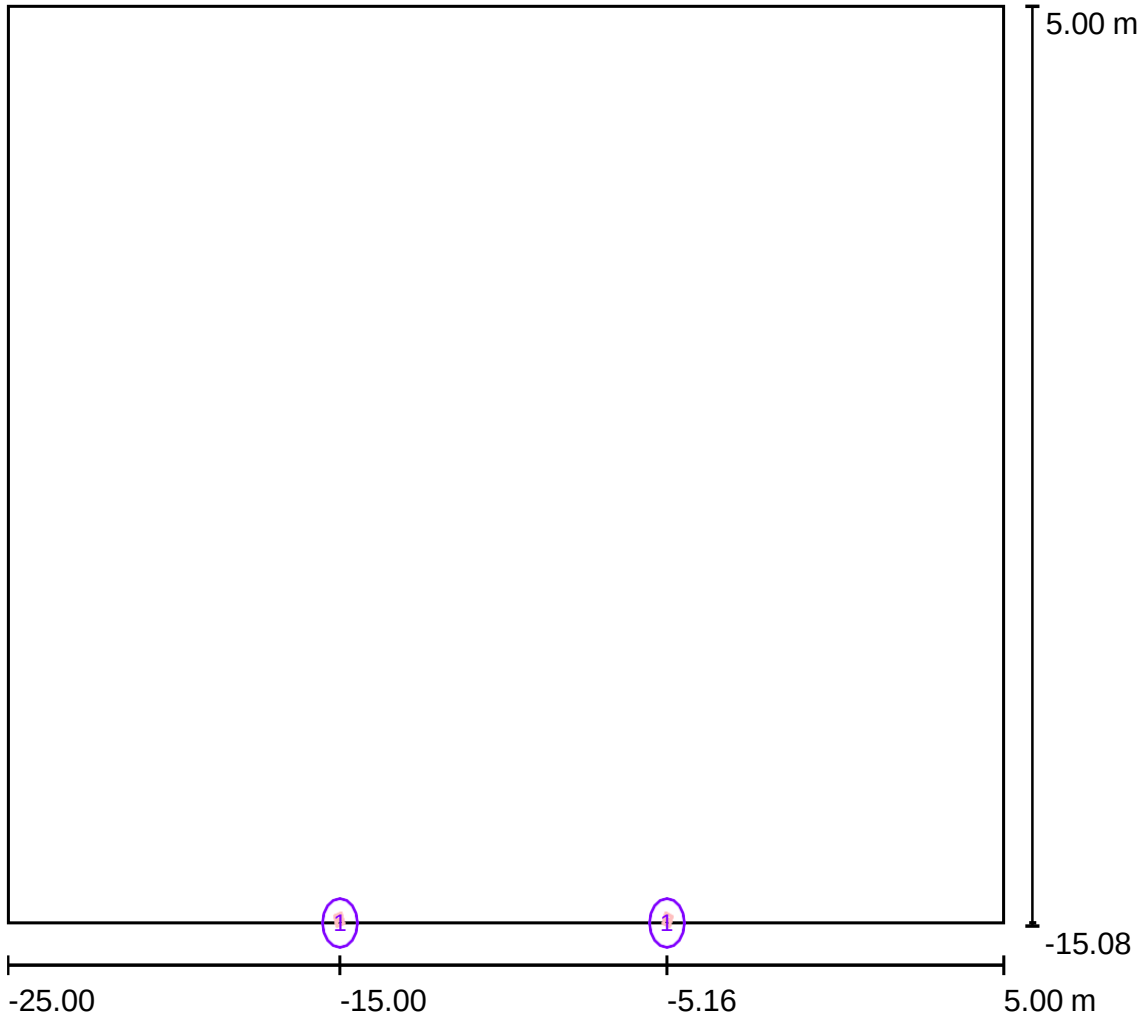

Figure 3.23: **Luminaire Layout Plan**

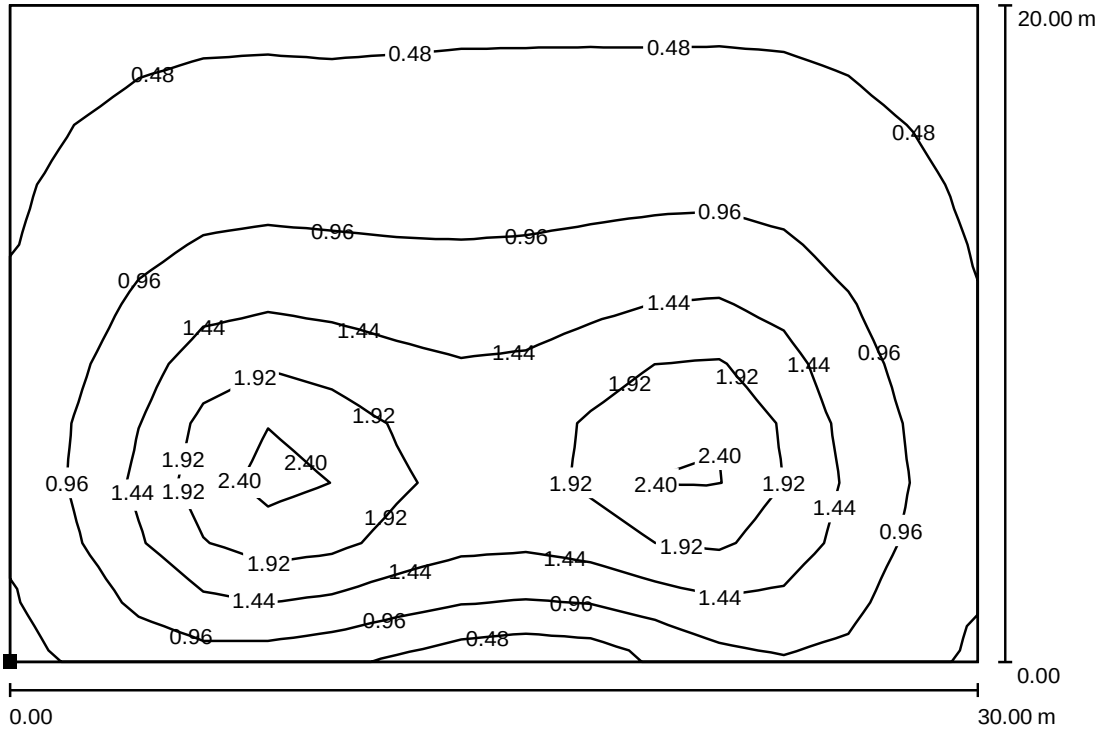

Figure 3.24: **Isoline Diagram**

0.34	0.39	0.42	0.45	0.43	0.43	0.45	0.45	0.46	0.46	0.45	0.45	0.44	0.39	0.34
0.40	0.48	0.53	0.57	0.54	0.55	0.56	0.56	0.57	0.57	0.57	0.58	0.54	0.48	0.39
0.47	0.58	0.67	0.71	0.70	0.69	0.70	0.70	0.72	0.73	0.74	0.74	0.67	0.57	0.45
0.52	0.69	0.83	0.90	0.89	0.87	0.86	0.86	0.89	0.92	0.94	0.95	0.82	0.66	0.52
0.59	0.81	1.07	1.18	1.18	1.11	1.09	1.08	1.13	1.20	1.29	1.24	1.04	0.78	0.58
0.69	0.90	1.35	1.56	1.54	1.42	1.35	1.32	1.41	1.55	1.72	1.61	1.27	0.87	0.64
0.77	1.07	1.60	2.16	2.10	1.80	1.65	1.52	1.72	2.02	2.34	2.07	1.46	0.98	0.72
0.82	1.23	1.81	2.57	2.67	2.19	1.86	1.60	1.88	2.32	2.76	2.28	1.58	1.12	0.77
0.78	1.21	1.88	2.42	2.55	2.24	1.79	1.70	1.74	2.16	2.48	2.12	1.64	1.13	0.73
0.64	0.95	1.48	1.80	1.83	1.64	1.43	1.37	1.33	1.45	1.66	1.70	1.39	0.94	0.65
0.52	0.74	0.98	1.08	1.02	0.86	0.64	0.46	0.48	0.62	0.97	1.14	1.09	0.82	0.57

20.00 m
0.00
0.00
30.00 m

Figure 3.25: **Value Chart**

The values obtained throughout the area are as follows:

- Average luminance ($\mathbf{L_{avg}}$) = **1.10 cd/m^2**
- Overall Uniformity (**Uo**) = **0.311**

3.2.4 : Lighting Design using modified HPSV luminaire with surrounded CFL

Design Considerations:

- Area of the space: 30 x 20m
- Luminaire used: 2 x PHILIPS SWF 101/150W [SYMMETRIC], and 3 x TCS 306 / 136 M1(surrounding light source).
- Pole height: 9m.
- Light loss factor: 0.80

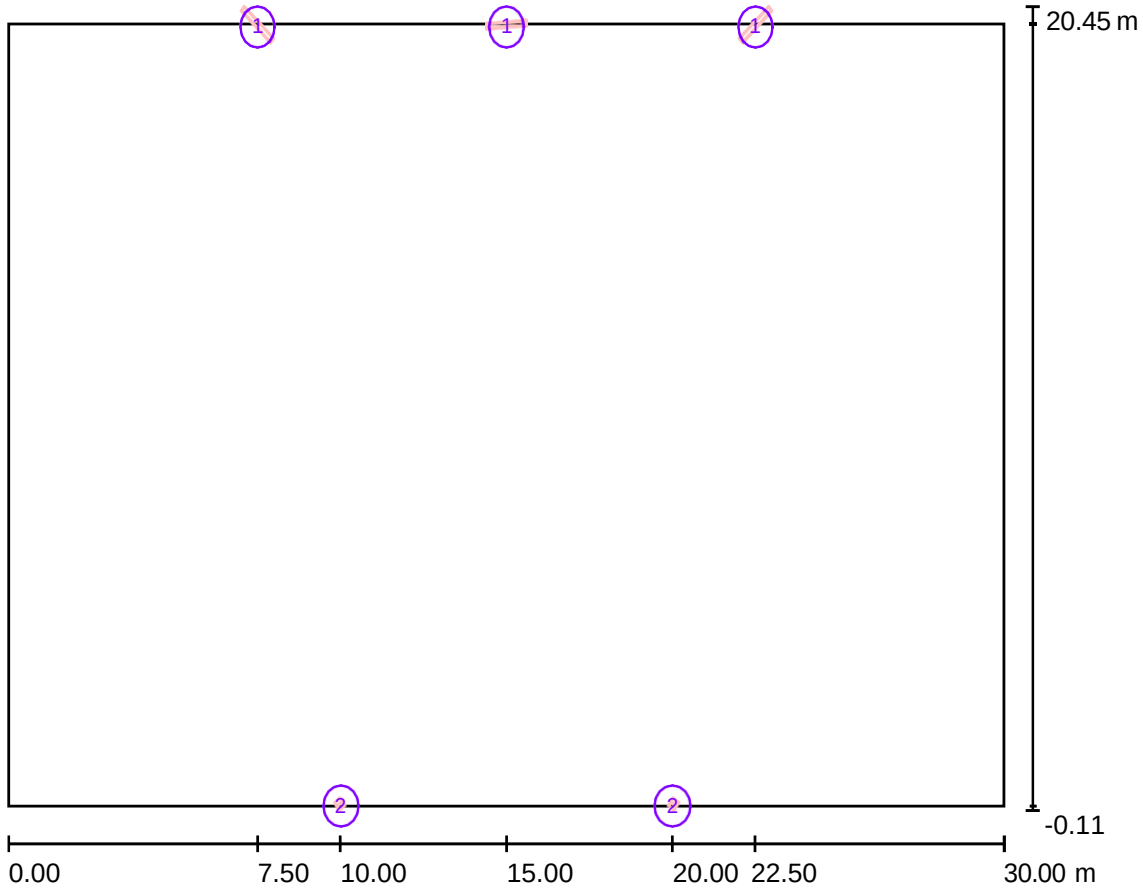

Figure 3.26: **Luminaire Layout Plan**

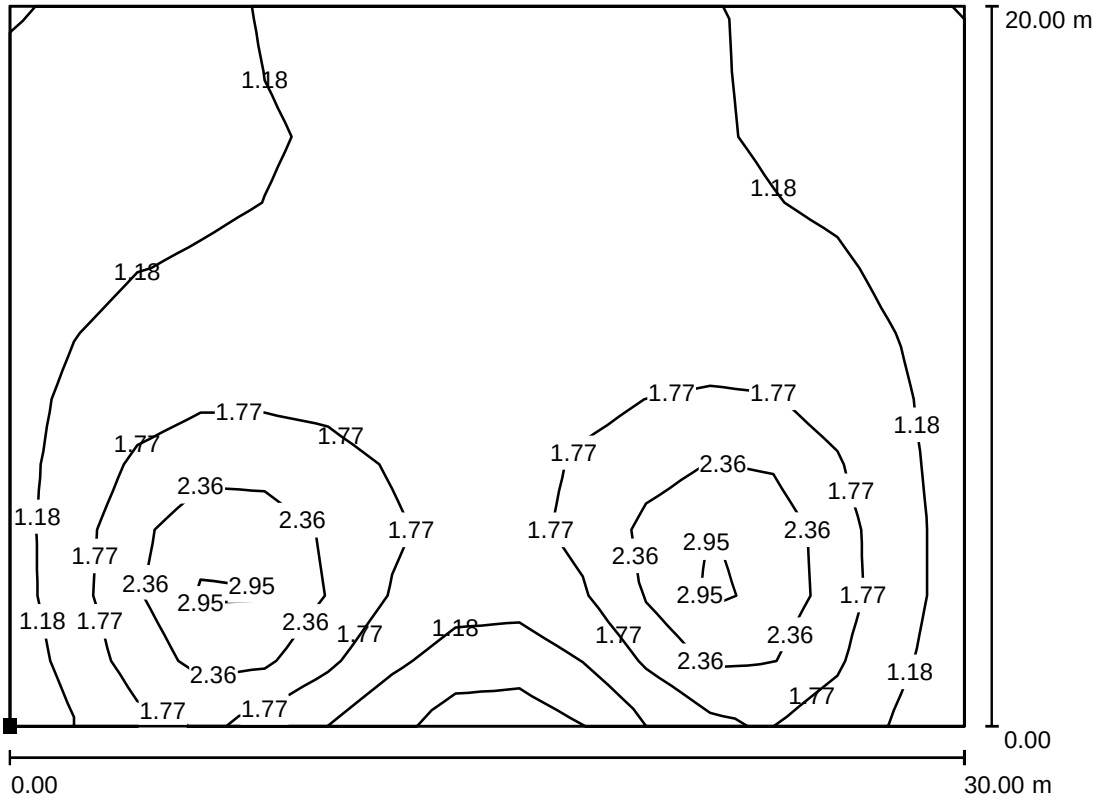

Figure 3.27: **Isoline Diagram**

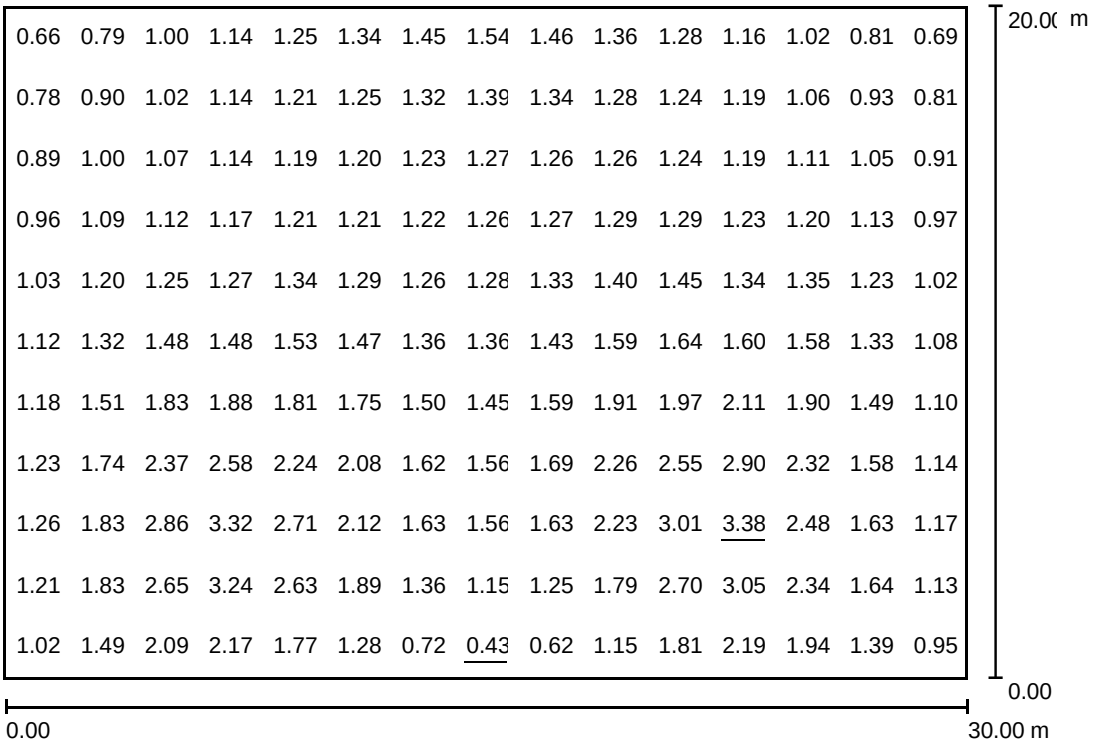

0.66	0.79	1.00	1.14	1.25	1.34	1.45	1.54	1.46	1.36	1.28	1.16	1.02	0.81	0.69
0.78	0.90	1.02	1.14	1.21	1.25	1.32	1.39	1.34	1.28	1.24	1.19	1.06	0.93	0.81
0.89	1.00	1.07	1.14	1.19	1.20	1.23	1.27	1.26	1.26	1.24	1.19	1.11	1.05	0.91
0.96	1.09	1.12	1.17	1.21	1.21	1.22	1.26	1.27	1.29	1.29	1.23	1.20	1.13	0.97
1.03	1.20	1.25	1.27	1.34	1.29	1.26	1.28	1.33	1.40	1.45	1.34	1.35	1.23	1.02
1.12	1.32	1.48	1.48	1.53	1.47	1.36	1.36	1.43	1.59	1.64	1.60	1.58	1.33	1.08
1.18	1.51	1.83	1.88	1.81	1.75	1.50	1.45	1.59	1.91	1.97	2.11	1.90	1.49	1.10
1.23	1.74	2.37	2.58	2.24	2.08	1.62	1.56	1.69	2.26	2.55	2.90	2.32	1.58	1.14
1.26	1.83	2.86	3.32	2.71	2.12	1.63	1.56	1.63	2.23	3.01	3.38	2.48	1.63	1.17
1.21	1.83	2.65	3.24	2.63	1.89	1.36	1.15	1.25	1.79	2.70	3.05	2.34	1.64	1.13
1.02	1.49	2.09	2.17	1.77	1.28	0.72	0.43	0.62	1.15	1.81	2.19	1.94	1.39	0.95

Figure 3.28: **Value Chart**

The values obtained throughout the area are as follows:

- Average luminance ($\mathbf{L_{avg}}$) = **1.50 cd/m^2**
- Overall Uniformity ($\mathbf{U_o}$) = **0.186**

3.2.5 : Lighting Design using modified MH luminaire

Design Considerations:

- Area of the space: 30 x 20m
- Luminaire used: 2 x PHILIPS MWF 101/150W [SYMMETRIC], CLOSED and 3 x TCS 306 / 136 M1(surrounding light source)
- Pole height: 9m
- Light loss factor: 0.80

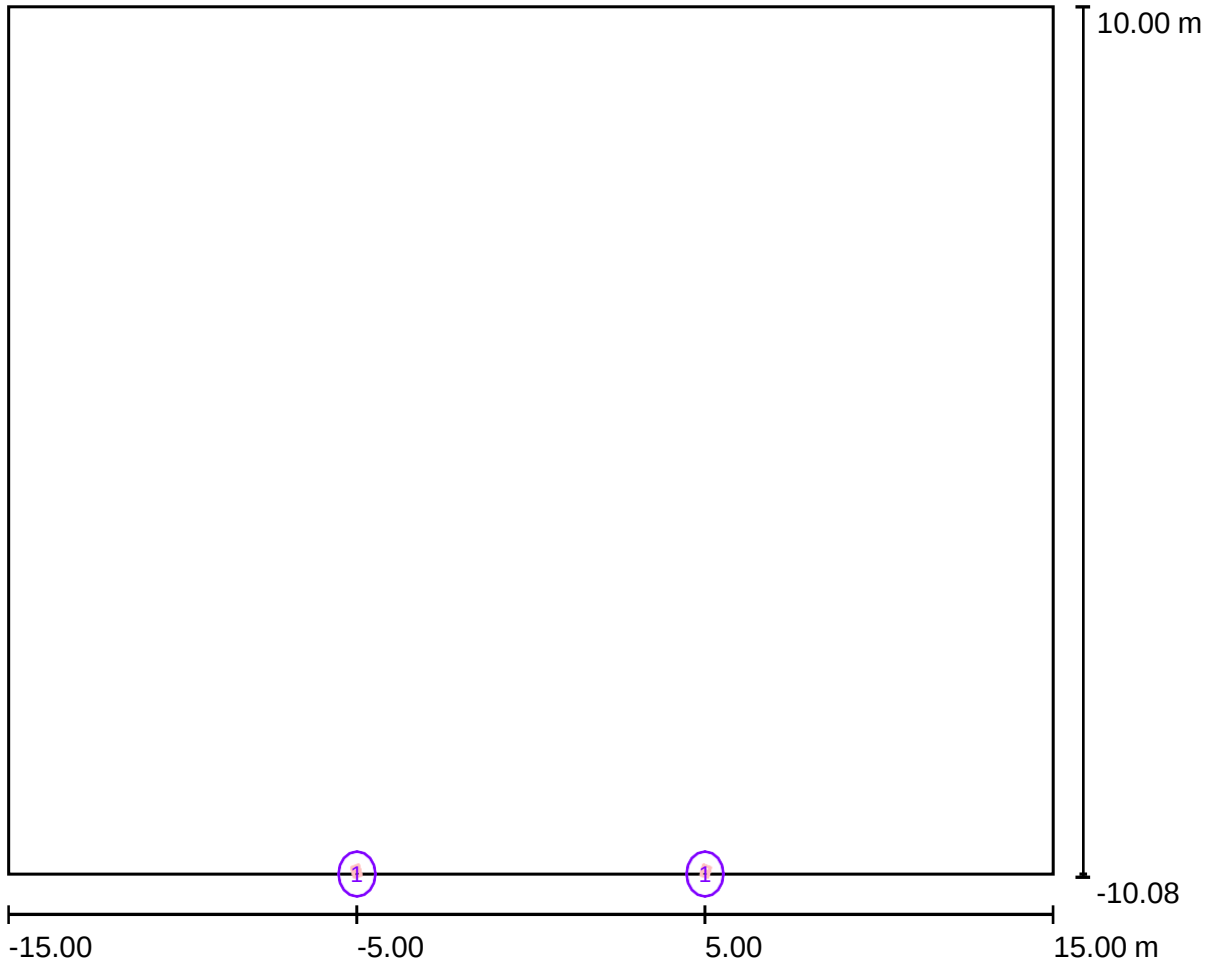

Figure 3.29: **Luminaire Layout Plan**

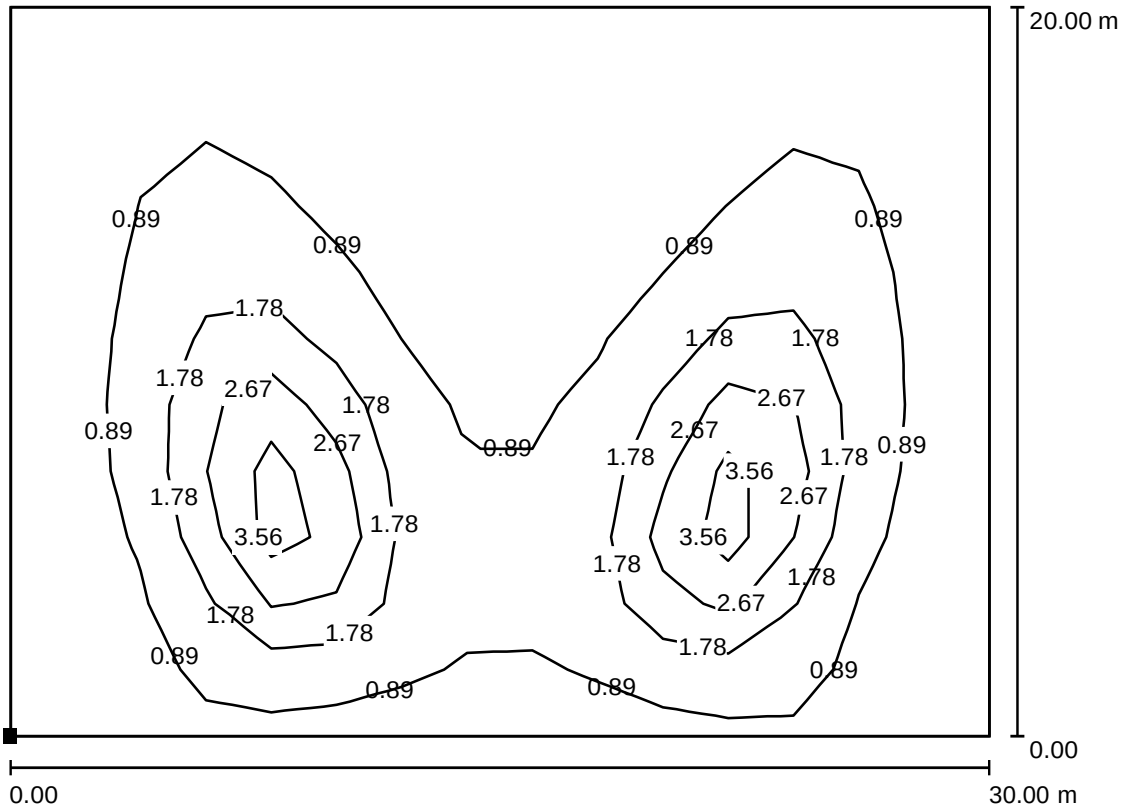

Figure 3.30: **Isoline Diagram**

0.41	0.60	0.67	0.56	0.42	0.31	0.24	0.23	0.25	0.29	0.36	0.52	0.66	0.61	0.45
0.41	0.64	0.83	0.73	0.54	0.40	0.30	0.28	0.31	0.37	0.46	0.67	0.83	0.67	0.48
0.40	0.68	1.03	0.97	0.73	0.52	0.38	0.35	0.39	0.47	0.61	0.92	1.04	0.74	0.49
0.40	0.69	1.21	1.33	0.99	0.68	0.47	0.43	0.49	0.62	0.84	1.26	1.27	0.82	0.49
0.41	0.71	1.43	1.92	1.48	0.93	0.61	0.54	0.61	0.82	1.27	1.87	1.56	0.88	0.48
0.43	0.74	1.66	2.71	2.27	1.29	0.76	0.66	0.75	1.11	2.02	2.71	1.89	0.89	0.45
0.42	0.72	1.82	3.72	3.77	1.75	0.93	0.80	0.93	1.46	3.09	4.01	2.13	0.83	0.43
0.40	0.67	1.49	3.50	4.50	2.08	1.07	0.96	1.07	1.79	3.80	4.16	1.87	0.72	0.41
0.37	0.60	1.21	2.92	4.68	2.25	1.15	1.18	1.20	2.00	4.50	3.31	1.36	0.61	0.40
0.38	0.52	0.86	1.48	1.81	1.49	1.18	1.00	1.12	1.29	1.85	1.73	0.91	0.56	0.40
0.34	0.49	0.77	0.96	0.98	0.82	0.65	0.34	0.64	0.83	1.01	1.06	0.84	0.57	0.37

20.0(m
0.00
0.00
30.00 m

Figure 3.31: **Value Chart**

The values obtained throughout the area are as follows:

- Average luminance ($\mathbf{L_{avg}}$) = **1.11 cd/m^2**
- Overall Uniformity (**Uo**) = **0.210**

3.2.6 : Lighting Design using modified MH luminaire with surrounding luminaire

Design Considerations:

- Area of the space: 30 x 20m
- Luminaire used: 2 x PHILIPS MWF 101/150W [SYMMETRIC], CLOSED and 3 x TCS 306 / 136 M1(surrounding light source)
- Pole height: 9m
- Light loss factor: 0.80

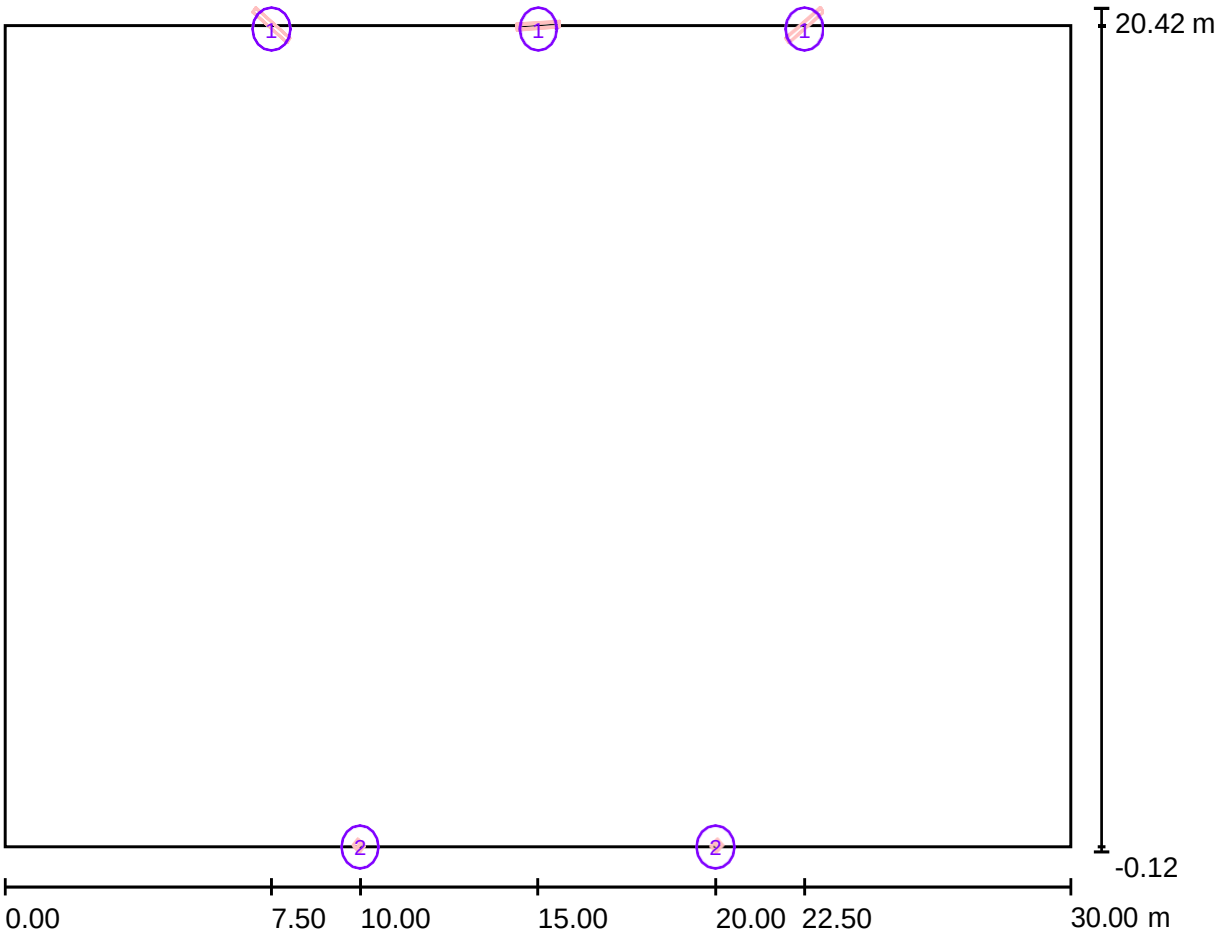

Figure 3.32: **Luminaire Layout Plan**

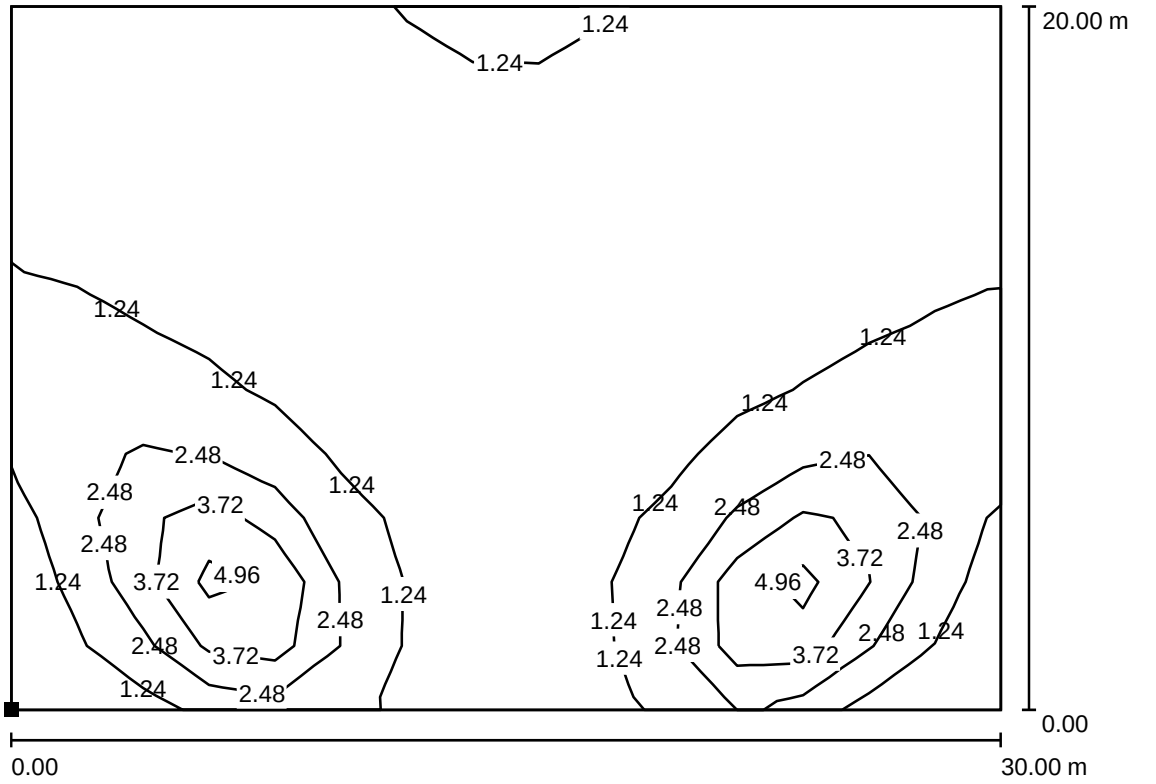

Figure 3.33: **Isoline Diagram**

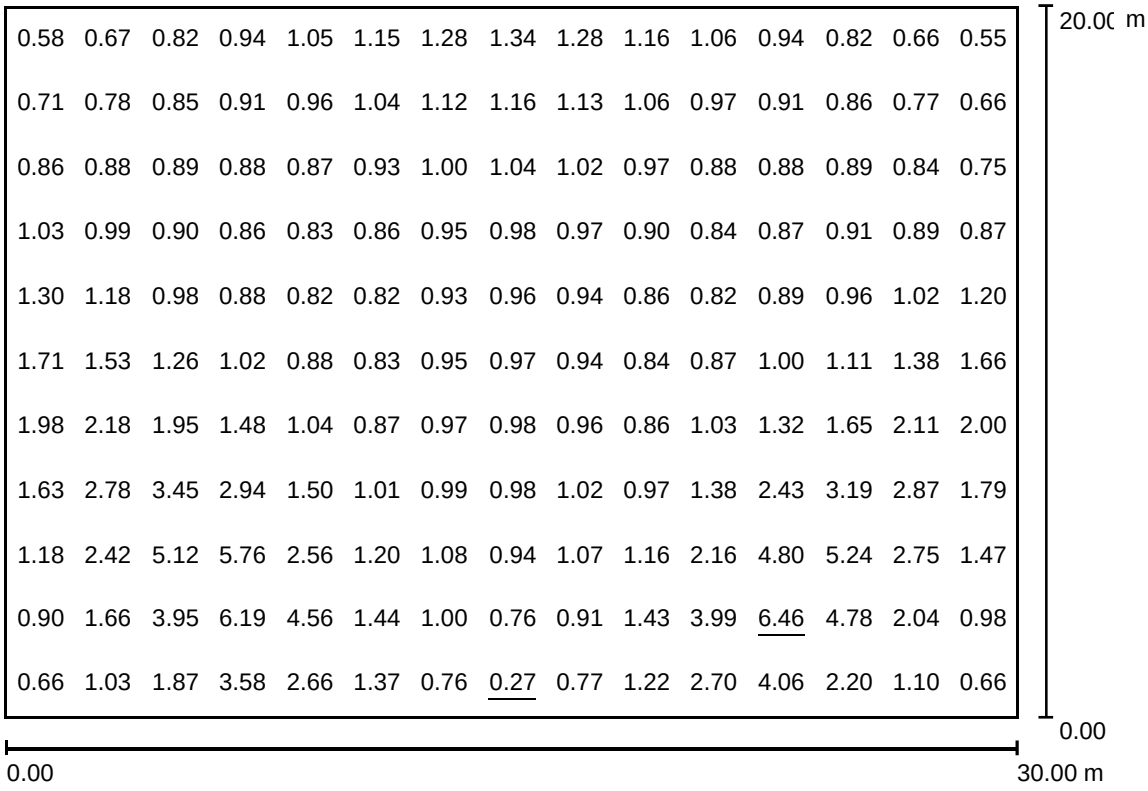

0.58	0.67	0.82	0.94	1.05	1.15	1.28	1.34	1.28	1.16	1.06	0.94	0.82	0.66	0.55
0.71	0.78	0.85	0.91	0.96	1.04	1.12	1.16	1.13	1.06	0.97	0.91	0.86	0.77	0.66
0.86	0.88	0.89	0.88	0.87	0.93	1.00	1.04	1.02	0.97	0.88	0.88	0.89	0.84	0.75
1.03	0.99	0.90	0.86	0.83	0.86	0.95	0.98	0.97	0.90	0.84	0.87	0.91	0.89	0.87
1.30	1.18	0.98	0.88	0.82	0.82	0.93	0.96	0.94	0.86	0.82	0.89	0.96	1.02	1.20
1.71	1.53	1.26	1.02	0.88	0.83	0.95	0.97	0.94	0.84	0.87	1.00	1.11	1.38	1.66
1.98	2.18	1.95	1.48	1.04	0.87	0.97	0.98	0.96	0.86	1.03	1.32	1.65	2.11	2.00
1.63	2.78	3.45	2.94	1.50	1.01	0.99	0.98	1.02	0.97	1.38	2.43	3.19	2.87	1.79
1.18	2.42	5.12	5.76	2.56	1.20	1.08	0.94	1.07	1.16	2.16	4.80	5.24	2.75	1.47
0.90	1.66	3.95	6.19	4.56	1.44	1.00	0.76	0.91	1.43	3.99	6.46	4.78	2.04	0.98
0.66	1.03	1.87	3.58	2.66	1.37	0.76	0.27	0.77	1.22	2.70	4.06	2.20	1.10	0.66

Figure 3.34: **Value Chart**

The values obtained throughout the area are as follows:

- Average luminance ($\mathbf{L_{avg}}$) = **1.47 cd/m^2**
- Overall Uniformity (**Uo**) = **0.186**

3.2.7 : Lighting Design using modified LED luminaire

Design Considerations:

- Area of the space: 30 x 20m
- Luminaire used: 2 x Orbit Industries, Inc
- Pole height: 9m
- Light loss factor: 0.80

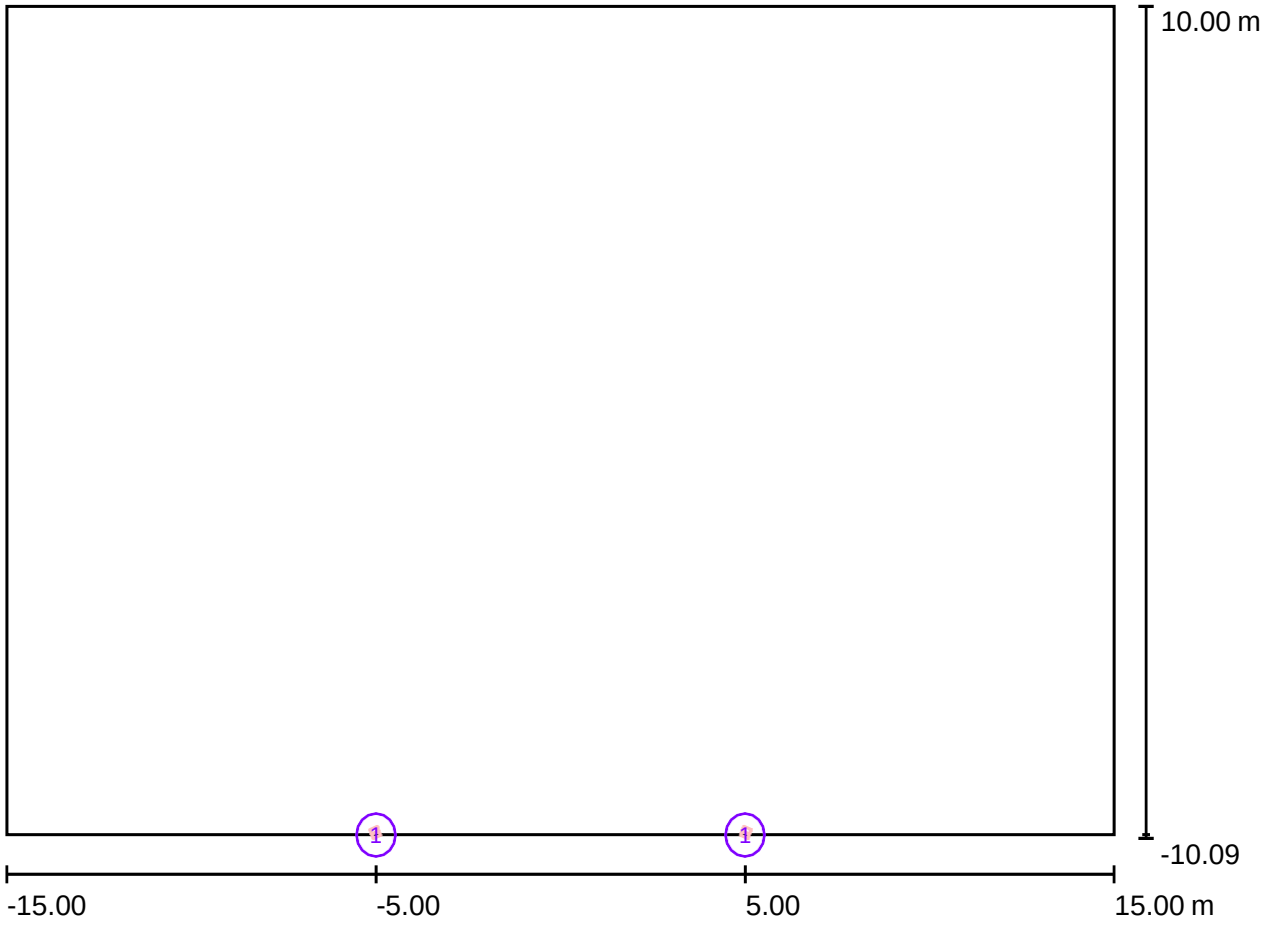

Figure 3.35: **Luminaire Layout Plan**

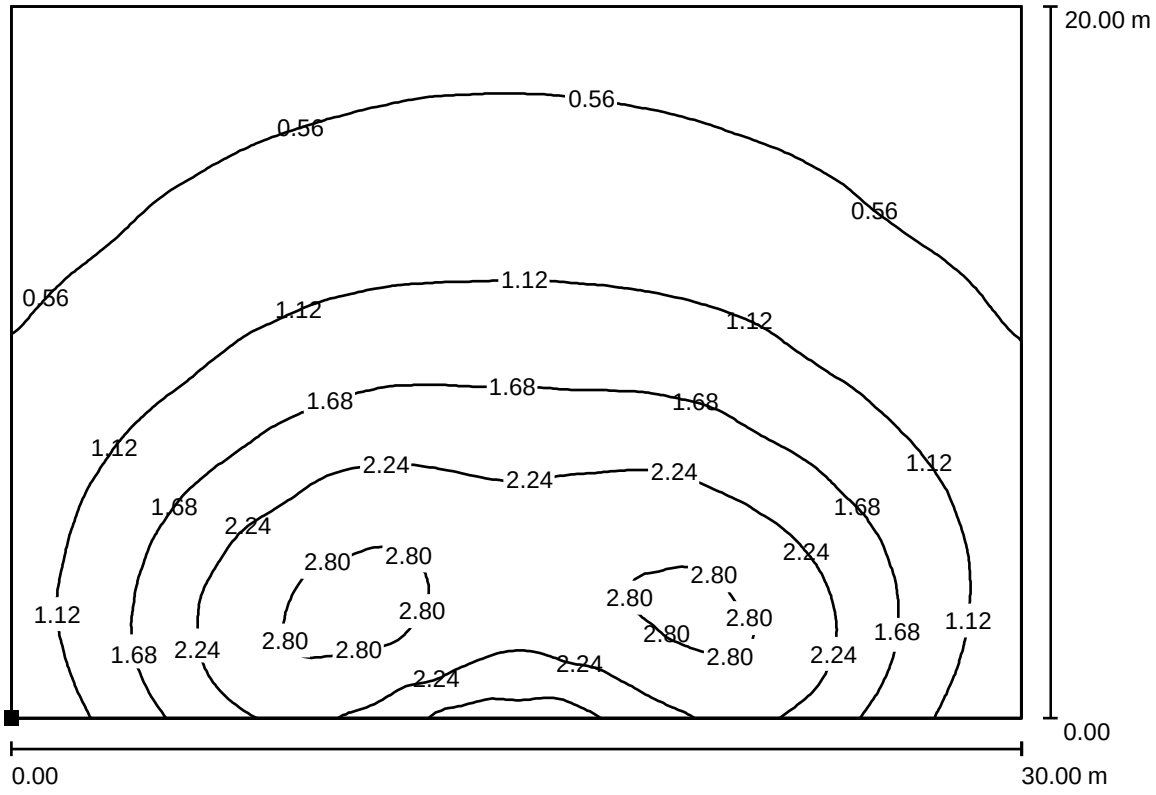

Figure 3.36: **Isoline Diagram**

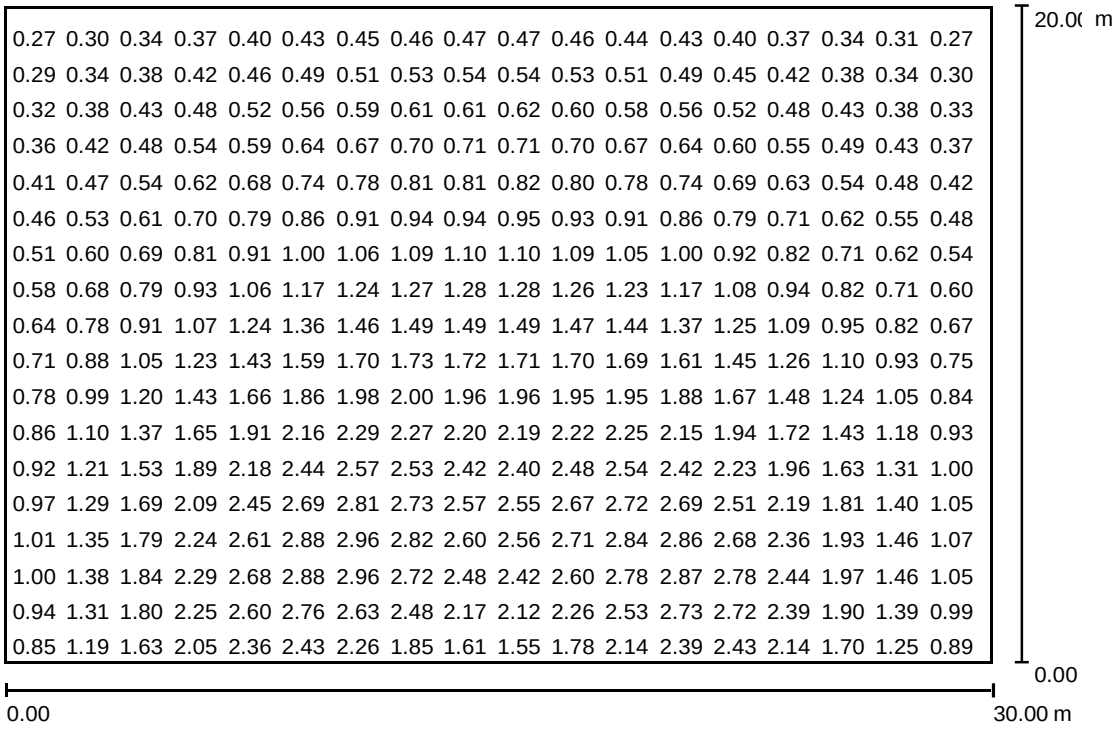

Figure 3.37: **Value Chart**

The values obtained throughout the area are as follows:

- Average luminance ($\mathbf{L_{avg}}$) = **1.27 cd/m^2**
- Overall Uniformity ($\mathbf{U_o}$) = **0.197**

3.2.8 Lighting Design using modified LED luminaire with surrounding CFL

Design Considerations:

- Area of the space: 30 x 20m
- Luminaire used: 2 x Orbit Industries, Inc and 3 x TCS 306 / 136 M1(surrounding light source)
- Pole height: 9m
- Light loss factor: 0.80

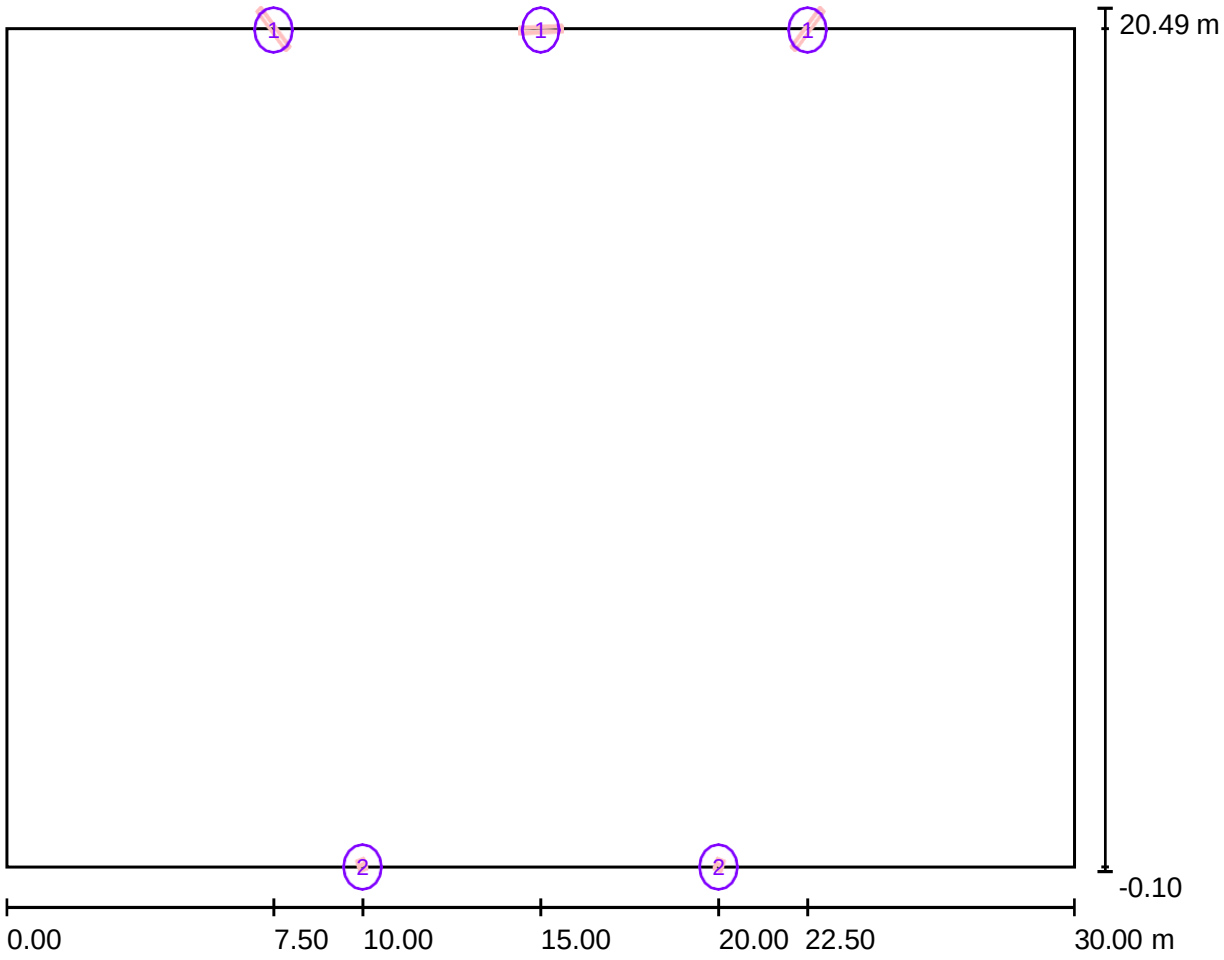

Figure 3.38: **Luminaire Layout Plan**

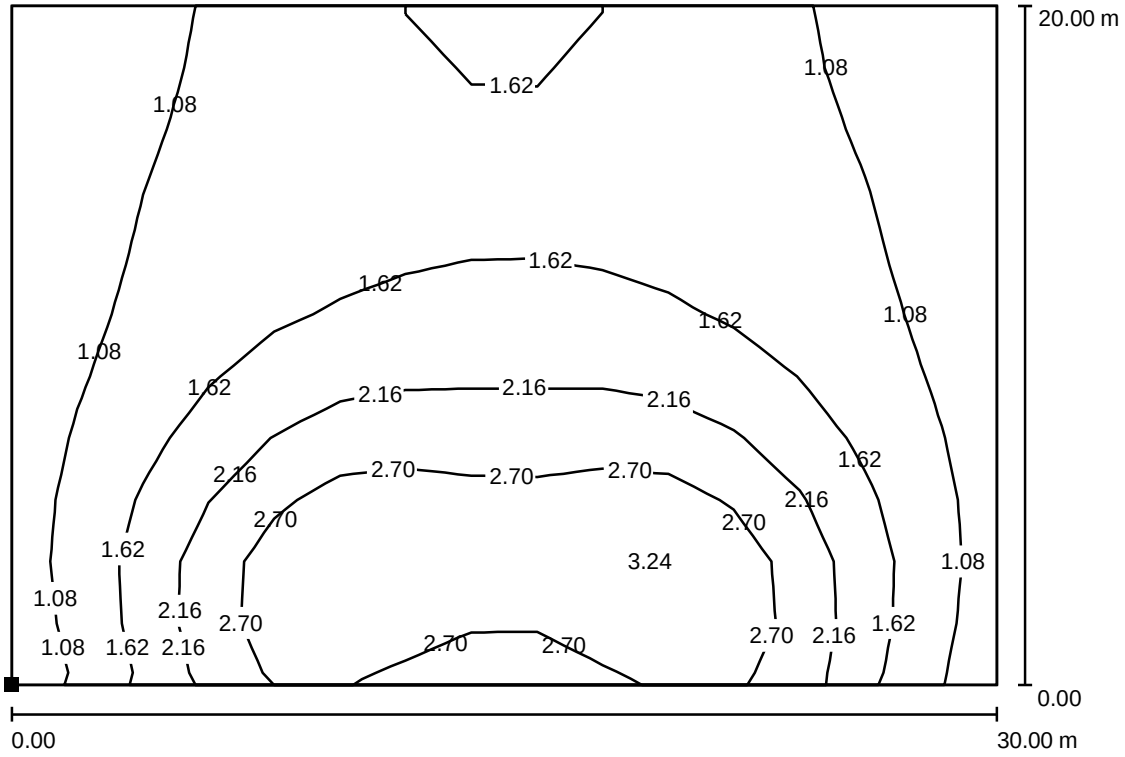

Figure 3.39: **Isoline Diagram**

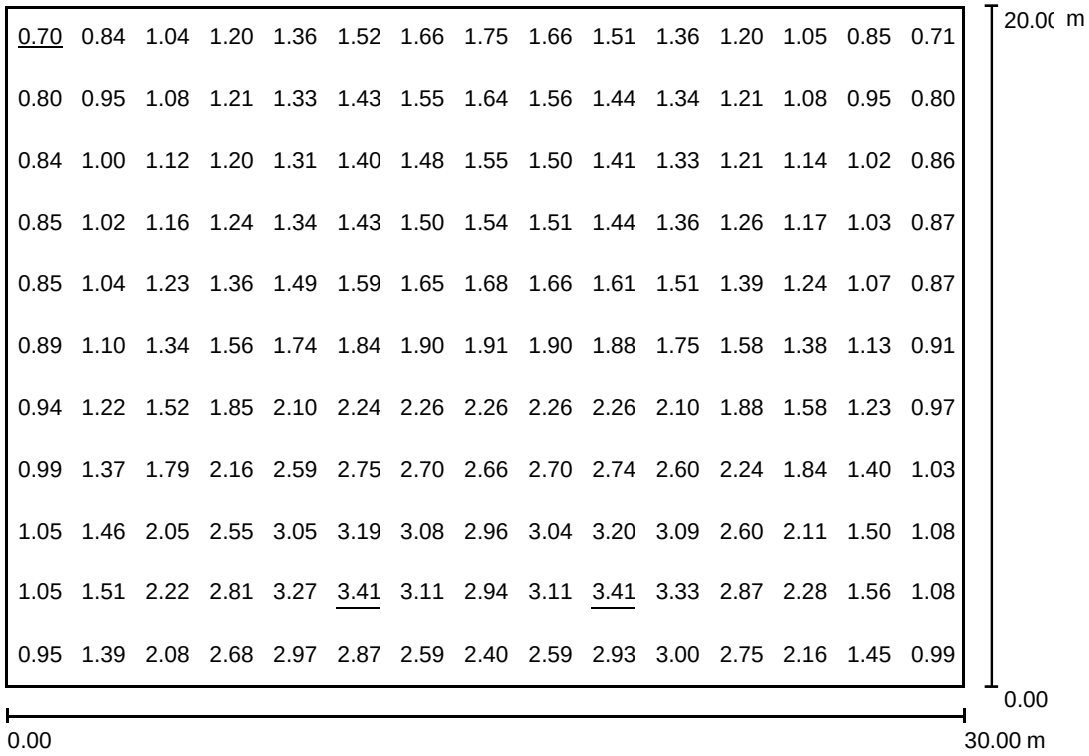

Figure 3.40: **Value Chart**

The values obtained throughout the area are as follows:

- Average luminance ($\mathbf{L_{avg}}$) = **1.27 cd/m^2**
- Overall Uniformity ($\mathbf{U_o}$) = **0.197**

3.2.9 : An overview of the luminaires' designs in Mesopic region

The summary calculations provided under the tables pertain to designs in the mesopic region. These tables present key metrics including the quantity of luminaires used in the designs, the values of average photopic luminance ($\mathbf{L_p}$), and the overall uniformity ($\mathbf{U_o}$). In table 3.8, show the overall data, using HPSV, MH, LED and the other table 3.9, show the overall data for the luminaires with surrounding luminaires.

Table 3.8: **Luminance data for both photopic and mesopic region for HPSV, MH, LED luminaire**

Luminaire	**Average photopic luminance L_{avg} (L_p)**	**Uniformity (U_o)**	**s/p ratio**	**Calculated mesopic luminance (L_m) using CIE 191:2010**	**Calculated m/p ratio**	**Simulated mesopic luminance (L_{ms})**	**Uniformity (U_o)**
HPSV	1.13	0.311	0.62	1.09	0.97	1.10	0.311
MH	1.09	0.210	1.2	1.11	1.01	1.11	0.210
LED	1.21	0.203	1.6	1.27	1.04	1.27	0.177

Table 3.9: **Luminance data for both photopic and mesopic region for HPSV, MH, LED luminaire with surrounding CFL luminaire**

Luminaire	**Average photopic luminance L avg (L_p)**	**Uniformity (U_o)**	**s/p ratio**	**Calculated mesopic luminance (L_m) using CIE 191:2010**	**Calculated m/p ratio**	**Simulated mesopic luminance (L_{ms})**	**Uniformity (U_o)**
HPSV + CFL	1.53	0.285	0.62	1.48	0.97	1.50	0.285
MH + CFL	1.46	0.186	1.2	1.48	1.01	1.47	0.186
LED + CFL	1.65	0.434	1.6	1.71	1.04	1.71	0.411

3.3: Data analysis

In this study, the photopic luminance for a designated area was simulated using various types of lamps, each chosen to represent different lighting technologies and their respective outputs. Following this, the corresponding mesopic luminance values were calculated using the standardized CIE 191:2010 Table, which provides a method for adjusting photopic luminance values to account for mesopic conditions—those intermediate levels of luminance where both rod and cone cells in the human eye are active. To further validate these findings, mesopic luminance for the same area was also simulated using a method previously detailed in the study. This dual approach allowed for a comprehensive comparison between the three key metrics: simulated photopic luminance (**L_p**), calculated mesopic luminance (**L_m**), and simulated mesopic luminance (**L_{ms}**). The results were then systematically compared across different lamp types, highlighting how each light source performs under both photopic and mesopic conditions. This comparison not only provided insights into the accuracy of the simulation methods but also demonstrated the varying effectiveness of different lamps in real-world lighting scenarios, particularly in environments where both photopic and mesopic vision are relevant.

Comparison of Simulated photopic luminance (L_p), Calculated mesopic luminance (L_m) & Simulated mesopic luminance (L_{ms})

High Pressure Sodium Vapour (HPSV) luminaire

For designs utilizing only High-Pressure Sodium Vapor (HPSV) luminaires, the photopic luminance (**L_p**), calculated mesopic luminance (**L_m**), and simulated mesopic luminance (**L_{ms}**) values are presented in Table 3.10. As depicted in Figure 3.41, luminaire with a lower S/P ratio, such as HPSV, exhibit lower **L_m** values compared to **L_p** values within the mesopic zone. This indicates that the effective luminance of the field decreases in mesopic vision relative to photopic luminance when using HPSV lamps. Additionally, there is a slight discrepancy between the calculated mesopic value (**L_m**) and the simulated mesopic value (**L_{ms}**). The uniformity of photopic (**U_o,p**) and mesopic (**U_o,m**) regions is detailed in Table 3.10, while Figure 3.42 illustrates the comparison between simulated photopic and mesopic region uniformity.

Similarly, for designs featuring HPSV luminaires combined with additional Compact Fluorescent Lamp (CFL) luminaires, the photopic luminance (**L_p**), calculated mesopic luminance (**L_m**), and simulated mesopic luminance (**L_{ms}**) values are shown in Table 3.10. As seen in Figure 3.43, the lower S/P ratio of HPSV lamps leads to lower **L_m** values compared to **L_p** values in the mesopic zone, resulting in reduced effective luminance under mesopic vision. Again, a slight difference is observed between the calculated mesopic value (**L_m**) and the simulated mesopic value (**L_{ms}**). The uniformity metrics for photopic (**U_o,p**) and mesopic (**U_o,m**) regions are displayed in Table 3.10, with Figure 3.44 providing a comparison between simulated photopic and mesopic region uniformity.

Table 3.10: **Average luminance values and photopic, mesopic region uniformity of HPSV luminaire**

Main source	Simulated photopic luminance (**L_p**)	Calculated mesopic luminance (**L_m**)	Simulated mesopic luminance (**L_{ms}**)	Photopic region uniformity (**U_o,p**)	Mesopic region uniformity (**U_o,m**)
HPSV	1.13	1.09	1.10	0.311	0.311

Table 3.11: **Average luminance values and photopic, mesopic region uniformity of HPSV with surrounding CFL luminaire**

Main source	Simulated photopic luminance ($\mathbf{L_p}$)	Calculated mesopic luminance ($\mathbf{L_m}$)	Simulated mesopic luminance ($\mathbf{L_{ms}}$)	Photopic region uniformity ($\mathbf{U_o,p}$)	Mesopic region uniformity ($\mathbf{U_om}$)
HPSV	1.53	1.48	1.50	0.285	0.284

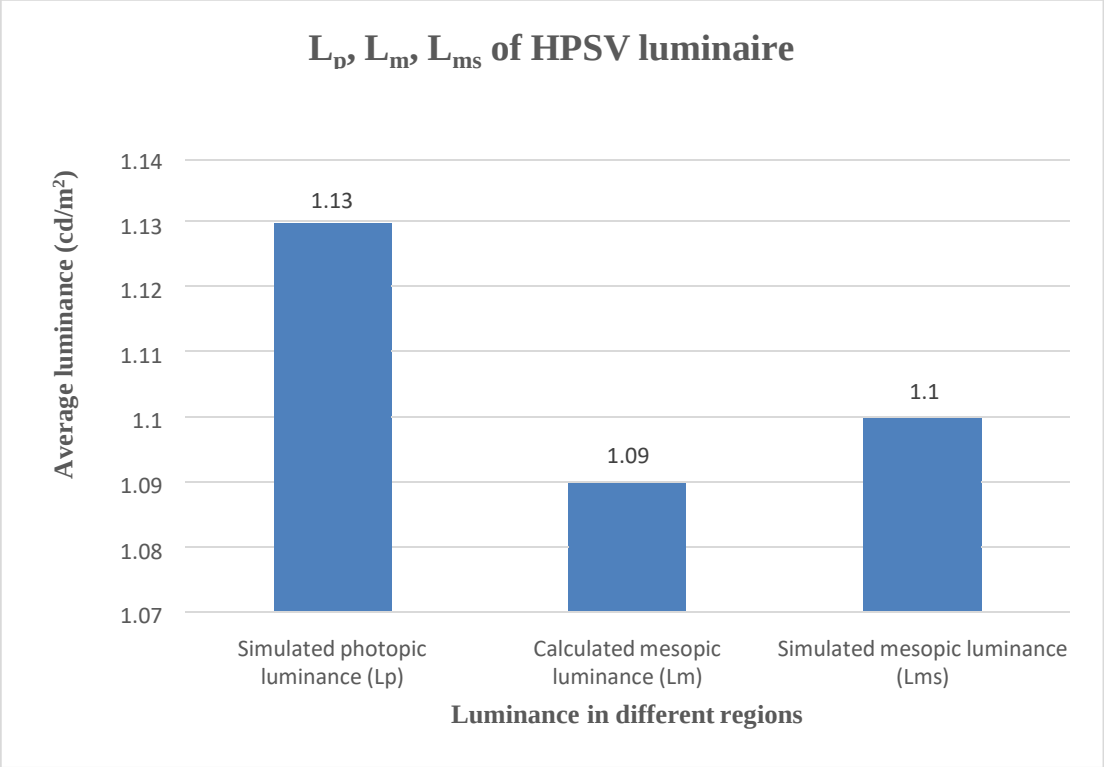

Figure 3.41: **Comparison of L_p, L_m, L_{ms} of HPSV luminaire**

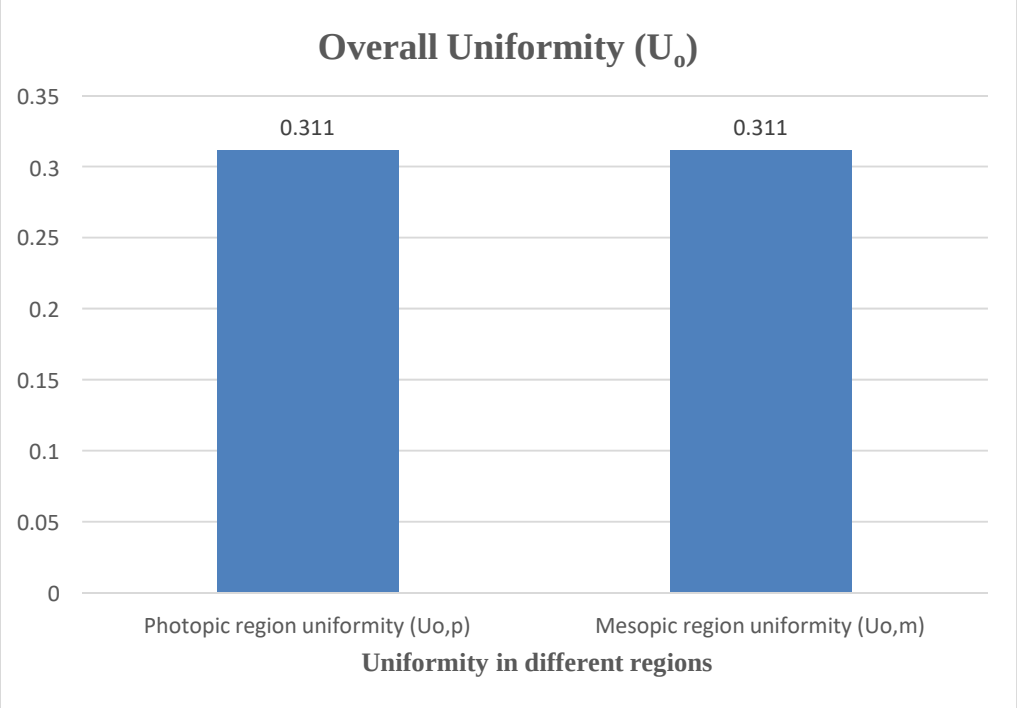

Figure 3.42: **Comparison of photopic and mesopic uniformity of HPSV luminaire**

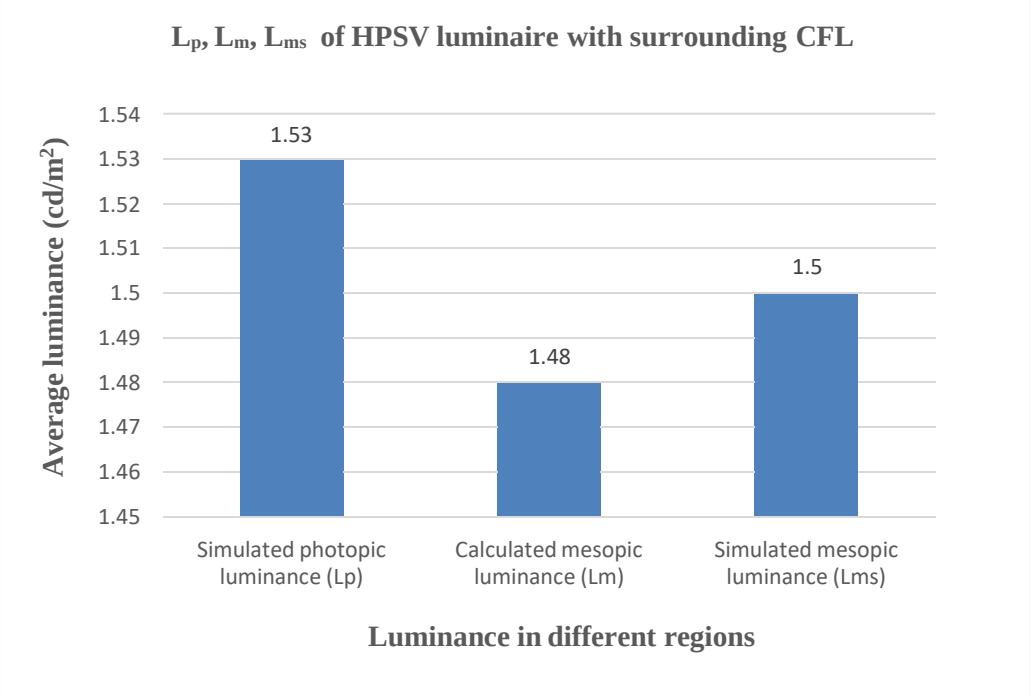

Figure 3.43: **Comparison of L_p, L_m, L_{ms} of HPSV luminaire with surrounding CFL**

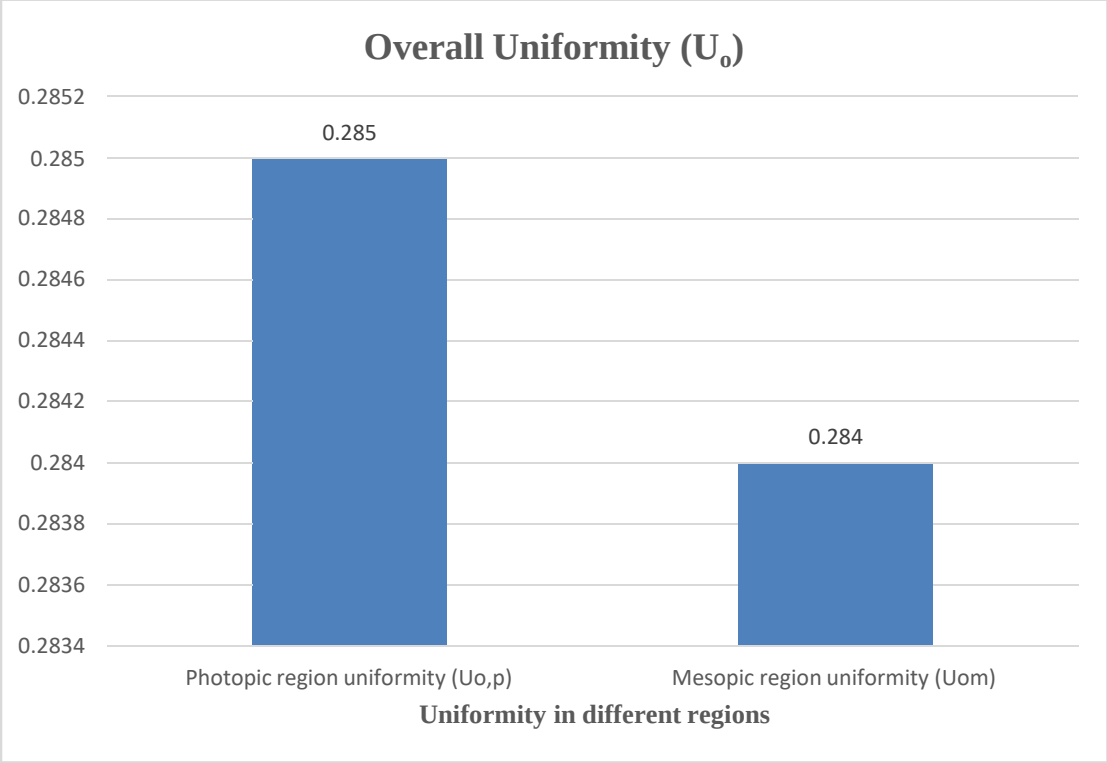

Figure 3.44: **Comparison of photopic and mesopic uniformity with surrounding CFL**

Metal Hallide (MH) luminaire

For designs utilizing only Metal Halide (MH) luminaires, the photopic luminance (L_p), calculated mesopic luminance (L_m), and simulated mesopic luminance (L_{ms}) values are presented in Table 3.12. As depicted in Figure 3.45, MH lamps, which typically have a higher S/P ratio compared to HPSV, exhibit L_m values that are closer to L_p values in the mesopic zone. This suggests that the effective luminance of the field in mesopic vision is relatively well-maintained when using MH lamps, compared to their photopic luminance. However, there is still a slight discrepancy between the calculated mesopic value (L_m) and the simulated mesopic value (L_{ms}), indicating some variations between the theoretical calculations and the simulation results. The uniformity of photopic (**U_o,p**) and mesopic (**U_o,m**) regions is detailed in Table 3.12, and Figure 3.46 illustrates the comparison between simulated photopic and mesopic region uniformity. The results indicate that MH luminaires offer more consistent lighting performance across both photopic and mesopic conditions, which may enhance visual comfort and safety in various lighting scenarios.

Similarly, for designs featuring Metal Halide (MH) luminaires combined with additional Compact Fluorescent Lamp (CFL) luminaires, the photopic luminance (**L_p**), calculated mesopic luminance (**L_m**), and simulated mesopic luminance (**L_{ms}**) values are shown in Table 3.13. As seen in Figure 3.47, the higher S/P ratio of MH lamps results in **L_m** values that remain close to **L_p** values in the mesopic zone, indicating that the effective luminance in mesopic vision is less compromised compared to lower S/P ratio lamps like HPSV. There is again a slight difference between the calculated mesopic value (**L_m**) and the simulated mesopic value (**L_{ms}**), but the discrepancy is minimal. The uniformity metrics for photopic (**U_o,p**) and mesopic (**U_o,m)** regions are displayed in Table 3.13, with Figure 3.48 providing a comparison between simulated photopic and mesopic region uniformity. These findings suggest that adding CFL luminaires to MH lighting designs may improve the overall uniformity and effectiveness of the lighting, particularly in environments where both photopic and mesopic vision are relevant.

Table 3.12: **Average luminance values and photopic, mesopic region uniformity of MH luminaire**

Main source	Simulated photopic luminance (**L_p**)	Calculated mesopic luminance (**L_m**)	Simulated mesopic luminance (**L_{ms}**)	Photopic region uniformity	Mesopic region uniformity
MH	1.09	1.11	1.11	0.210	0.210

Table 3.13: **Average luminance values and photopic, mesopic region uniformity of MH with surrounding CFL luminaire**

Main source	Simulated photopic luminance (**L_p**)	Calculated mesopic luminance (**L_m**)	Simulated mesopic luminance (**L_{ms}**)	Photopic region uniformity	Mesopic region uniformity
MH	1.46	1.48	1.47	0.186	0.186

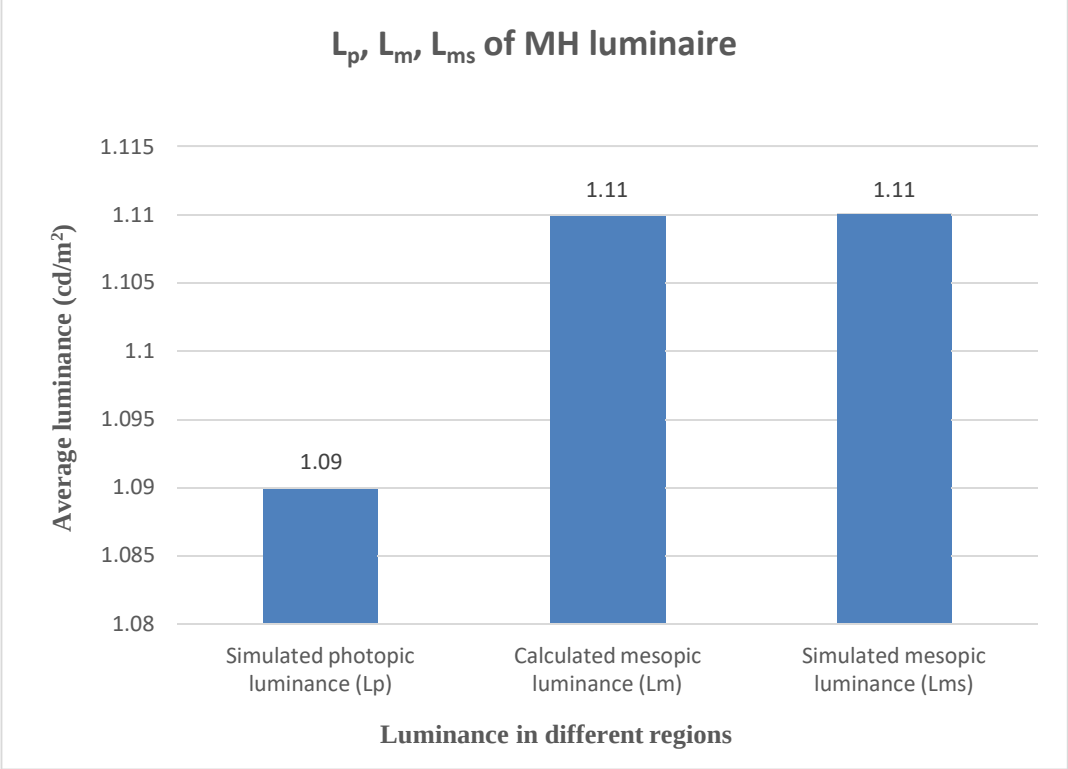

Figure 3.45: **Comparison of L_p, L_m, L_{ms} of MH luminaire**

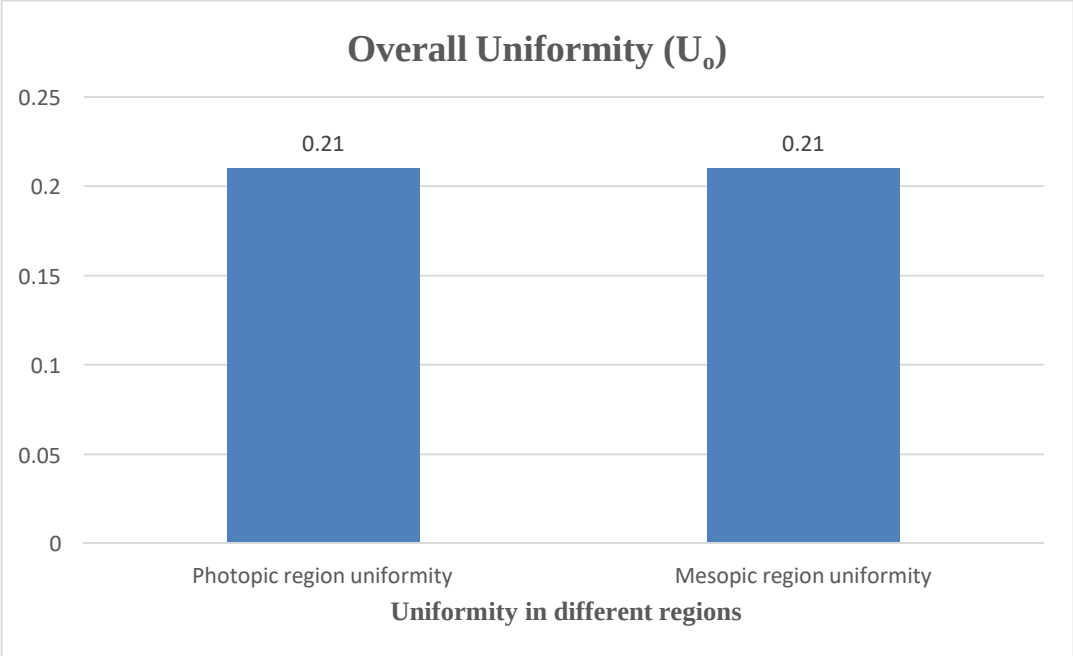

Figure 3.46: **Comparison of photopic and mesopic uniformity of MH luminaire**

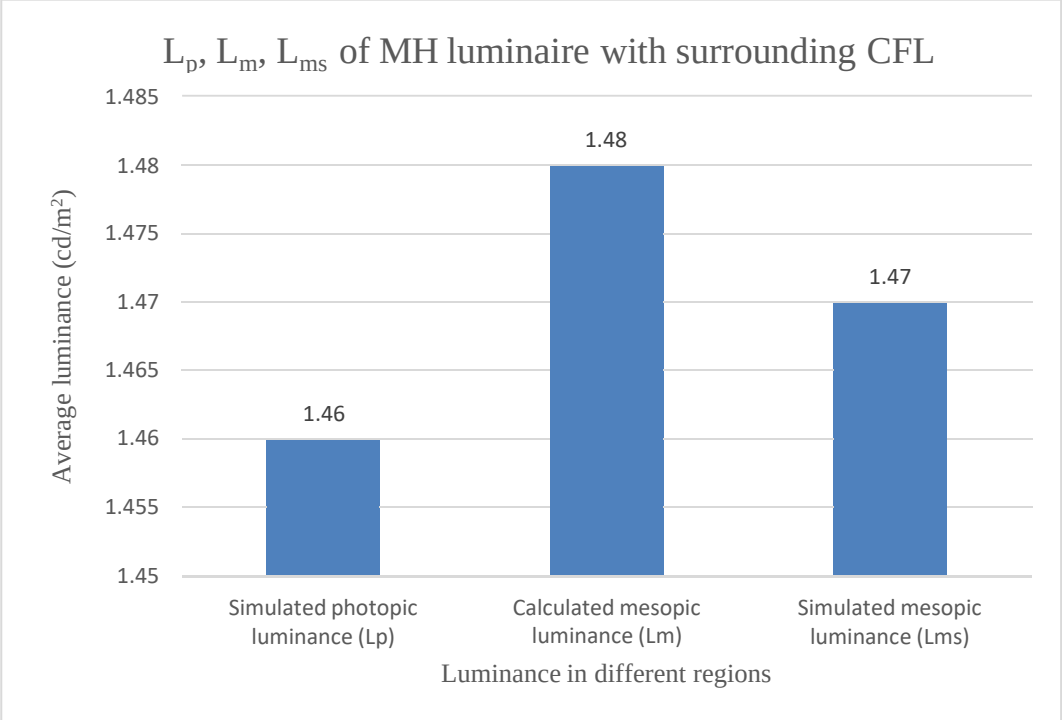

Figure 3.47: Comparison of **L_p, L_m, L_{ms}** of MH luminaire with surrounding CFL

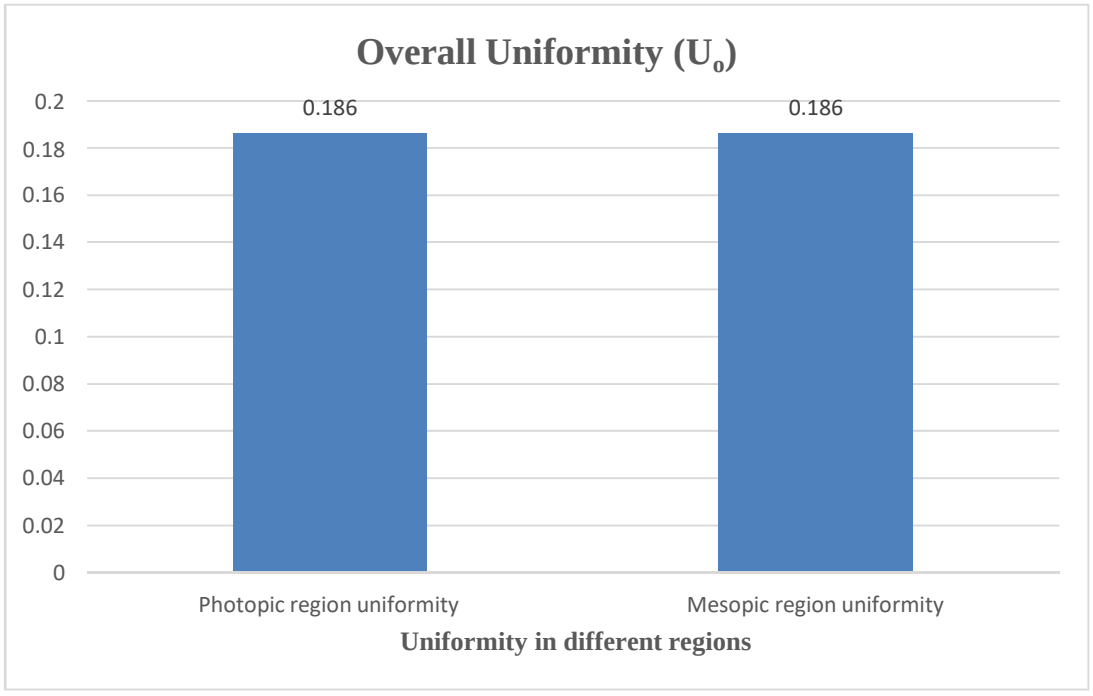

Figure 3.48: **Comparison of photopic and mesopic uniformity with surrounding CFL**

Light Emitting Diode (LED) luminaire

For designs utilizing only LED luminaires, the photopic luminance ($\mathbf{L_p}$), calculated mesopic luminance ($\mathbf{L_m}$), and simulated mesopic luminance ($\mathbf{L_{ms}}$) values are presented in Table 3.17. As depicted in Figure 3.68, LED lamps, known for their high S/P ratio, exhibit $\mathbf{L_m}$ values that are nearly equivalent to $\mathbf{L_p}$ values in the mesopic zone. This indicates that LED luminaires maintain effective luminance in mesopic vision almost as well as in photopic conditions, making them highly suitable for environments where lighting conditions vary. The slight discrepancy between the calculated mesopic value ($\mathbf{L_m}$) and the simulated mesopic value ($\mathbf{L_{ms}}$) is minimal, further demonstrating the accuracy and reliability of LED lighting in both simulation and real-world applications. The uniformity of photopic ($\mathbf{U_o,p}$) and mesopic ($\mathbf{U_o,m}$) regions is detailed in Table 3.18, while Figure 3.69 illustrates the comparison between simulated photopic and mesopic region uniformity. The results confirm that LED luminaires provide consistent and uniform lighting performance across different visual conditions, which is advantageous for both energy efficiency and visual clarity.

Similarly, for designs featuring LED luminaires combined with additional Compact Fluorescent Lamp (CFL) luminaires, the photopic luminance ($\mathbf{L_p}$), calculated mesopic luminance ($\mathbf{L_m}$), and simulated mesopic luminance ($\mathbf{L_{ms}}$) values are shown in Table 3.19. As seen in Figure 3.70, the high S/P ratio of LED lamps ensures that $\mathbf{L_m}$ values closely match $\mathbf{L_p}$ values in the mesopic zone, meaning that the transition from photopic to mesopic vision does not significantly reduce the perceived luminance. A slight difference between the calculated mesopic value ($\mathbf{L_m}$) and the simulated mesopic value ($\mathbf{L_{ms}}$) is noted, but this variation is minor and within acceptable limits. The uniformity metrics for photopic ($\mathbf{U_o,p}$) and mesopic ($\mathbf{U_o,m}$) regions are displayed in Table 3.20, with Figure 3.71 providing a comparison between simulated photopic and mesopic region uniformity. These findings highlight the superior performance of LED luminaires, particularly when supplemented with CFLs, in maintaining uniform and effective lighting across varying visual conditions.

Table 3.14: **Average luminance values and photopic, mesopic region uniformity of LED luminaire**

Main source	Simulated photopic luminance ($\mathbf{L_p}$)	Calculated mesopic luminance ($\mathbf{L_m}$)	Simulated mesopic luminance ($\mathbf{L_{ms}}$)	Photopic region uniformity	Mesopic region uniformity
LED	1.21	1.27	1.27	0.203	0.197

Table 3.15: **Average luminance values and photopic, mesopic region uniformity of LED with surrounding CFL luminaire**

Main source	Simulated photopic luminance (L_p)	Calculated mesopic luminance (L_m)	Simulated mesopic luminance (L_{ms})	Photopic region uniformity	Mesopic region uniformity
LED	1.65	1.71	1.71	0.434	0.411

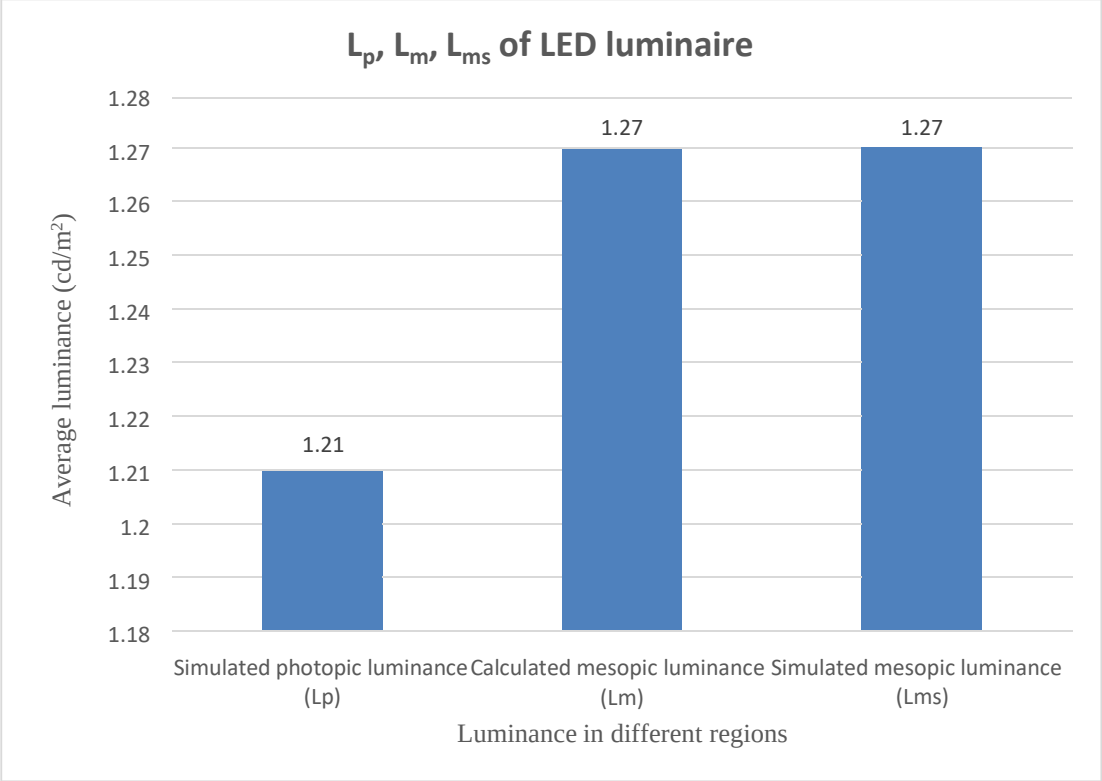

Figure 3.49: **Comparison of L_p, L_m, L_{ms} of LED luminaire**

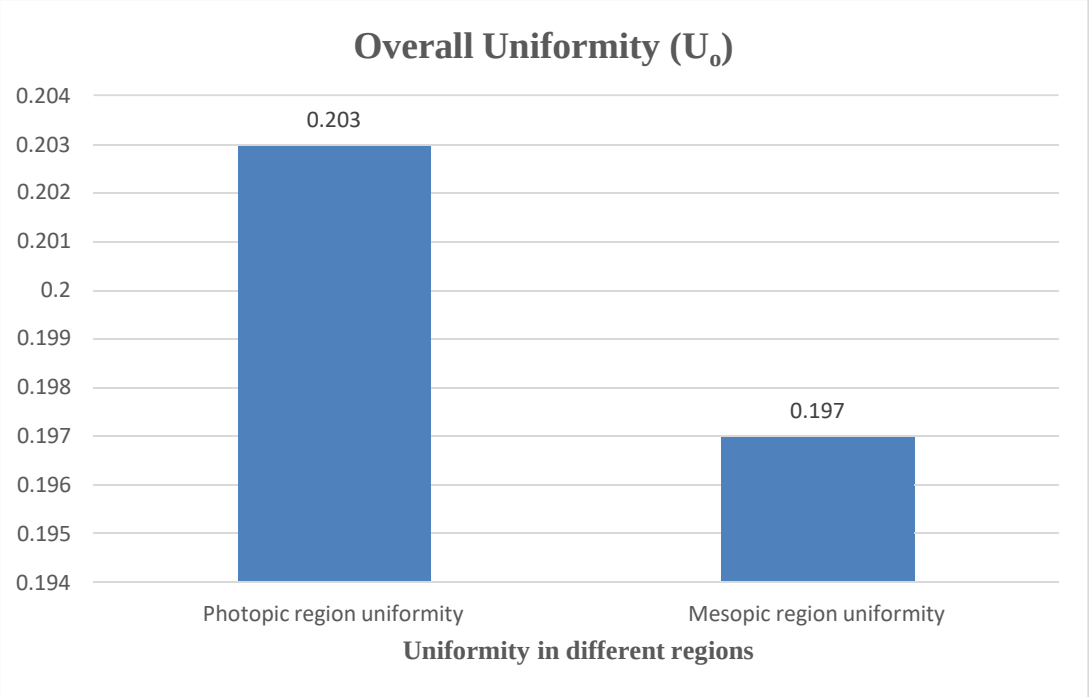

Figure 3.50: **Comparison of photopic and mesopic uniformity of LED luminaire**

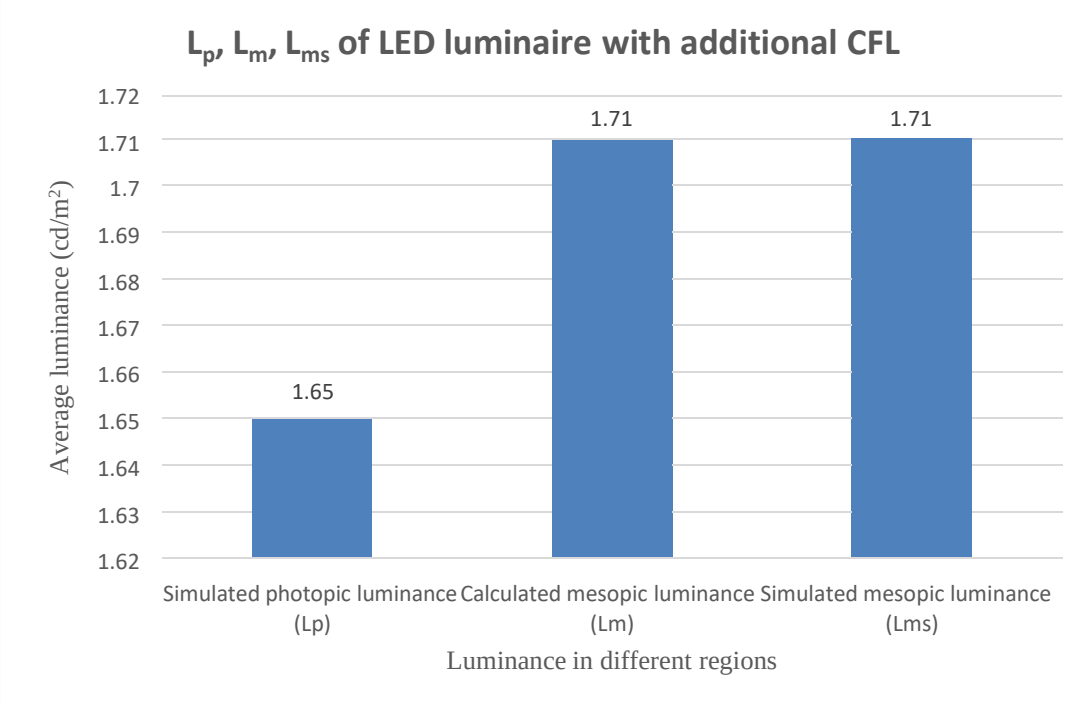

Figure 3.51: **Comparison of L_p, L_m, L_{ms} of LED luminaire with surrounding CFL**

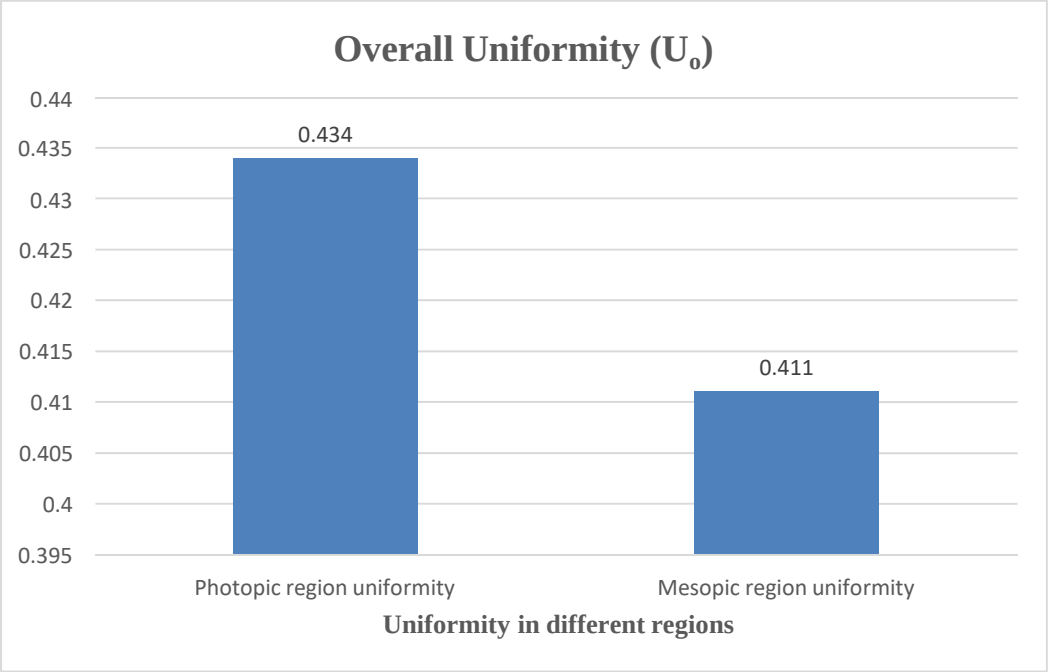

Figure 3.52: **Comparison of photopic and mesopic uniformity of LED with surrounding CFL**

Comparison of average luminance for different luminaires

For HPSV, MH, LED luminaires

Table 3.16 presents the simulated photopic luminance (**L_p**), calculated mesopic luminance (**L_m**), and simulated mesopic luminance (**L_{ms}**) values for HPSV, Metal Halide (MH), and LED lamps. As illustrated in Figure 3.53, High-Pressure Sodium Vapor (HPSV) lamps, which have a lower S/P ratio, exhibit lower mesopic luminance values compared to their photopic luminance values. This results in a dimmer environment under mesopic conditions, necessitating the use of higher wattage lamps for outdoor lighting systems to maintain adequate brightness. In contrast, light sources with a higher S/P ratio, such as Metal Halide (MH) and LED lamps, demonstrate mesopic luminance values that exceed their photopic luminance. This characteristic makes MH and LED lamps more energy-efficient options for outdoor lighting, as they provide greater perceived brightness in mesopic conditions while consuming less power.

Table 3.16: **Average luminance values of HPSV, MH, LED luminaires**

Main source	Simulated photopic luminance (L_p)	Calculated mesopic luminance (L_m)	Simulated mesopic luminance (L_{ms})
HPSV	1.13	1.09	1.10
MH	1.09	1.11	1.11
LED	1.21	1.27	1.27

For HPSV, MH, LED luminaires with surrounding CFL

Table 3.17 presents the simulated photopic luminance (L_p), calculated mesopic luminance (L_m), and simulated mesopic luminance (L_{ms}) values for High-Pressure Sodium Vapor (HPSV), Metal Halide (MH), and LED lamps. These designs also incorporate additional Compact Fluorescent Lamp (CFL) luminaires; however, the primary focus remains on analyzing the behavior of HPSV, MH, and LED lamps. As illustrated in Figure 3.54, HPSV lamps, with their lower S/P ratio, show a significant reduction in mesopic luminance compared to photopic luminance, leading to a dimmer environment under mesopic conditions. This necessitates the use of higher wattage lamps in outdoor lighting to achieve sufficient brightness. Conversely, MH and LED lamps, which have a higher S/P ratio, demonstrate mesopic luminance values that exceed their photopic luminance, making them more energy-efficient by providing greater perceived brightness in mesopic conditions while using less power. The inclusion of CFLs in the designs serves primarily to observe if the transition from photopic to mesopic luminance alters the performance of these main luminaires, with a focus on understanding how HPSV, MH, and LED lamps behave when their photometric files are modified to account for mesopic vision.

Table 3.17: **Average luminance values of HPSV, MH, LED luminaires with surrounding CFL**

Main source	Simulated photopic luminance (L_p)	Calculated mesopic luminance (L_m)	Simulated mesopic luminance (L_{ms})
HPSV	1.53	1.48	1.50
MH	1.46	1.48	1.47
LED	1.65	1.71	1.71

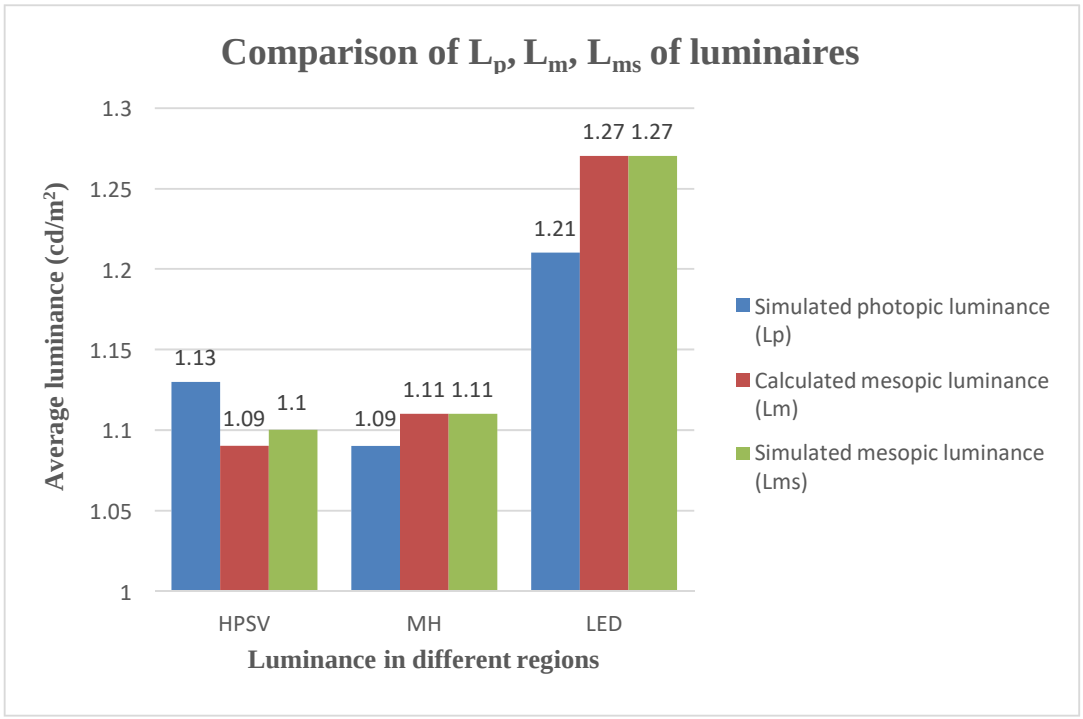

Figure 3.53: **Comparison of L_p, L_m, L_{ms} for HPSV, MH, LED luminaire**

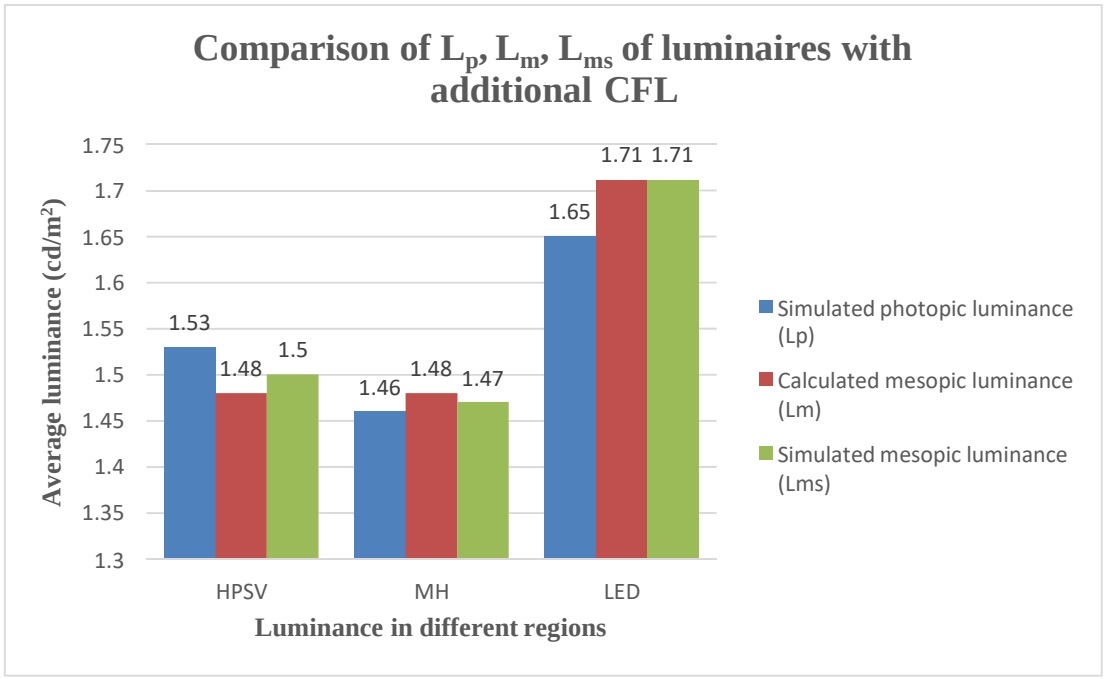

Figure 3.54: **Comparison of L_p, L_m, L_{ms} for different lamps along with surrounding CFL**

Luminous flux comparison

The comparison of luminous flux between photopic and mesopic conditions for HPSV, Metal Halide (MH), and LED luminaires demonstrates that designing lighting systems based on mesopic conditions can lead to reduced electrical consumption. The findings indicate that mesopic design considerations are more energy-efficient, as the luminous flux required for adequate illumination is lower in the mesopic region. To accurately determine the luminous flux values in mesopic conditions, it is essential to calculate key parameters such as the maintenance factor (MF), utilization factor (UF), and the total area. These factors ensure that the lighting design is optimized for both energy efficiency and effective illumination under mesopic vision.

Figures 3.55, 3.56, and 3.57 illustrate the differentiation in luminous flux under both photopic and mesopic conditions for HPSV, Metal Halide (MH), and LED luminaires, respectively. The analysis reveals that in mesopic conditions, HPSV luminaires require more power due to their increased luminous flux, as they perform less efficiently under photopic conditions. Conversely, MH and LED luminaires exhibit a decrease in luminous flux in mesopic conditions, leading to lower power consumption while emitting more light energy compared to HPSV. This trend underscores the energy efficiency of MH and LED luminaires in mesopic settings. Figure 3.58 presents a comparative graph of the luminous flux for all three luminaires, highlighting the overall scenario. The study conclusively demonstrates that lighting designs based on mesopic conditions result in reduced power consumption, making them more energy-efficient, particularly when using MH and LED luminaires.

Table 3.18: **Comparison of luminous flux between photopic and mesopic conditions**

Light source	Luminous flux in Photopic region (lm)	Luminous flux in Mesopic region (lm)
HPSV	9856	9560
MH	8627	8713
LED	10000	10399

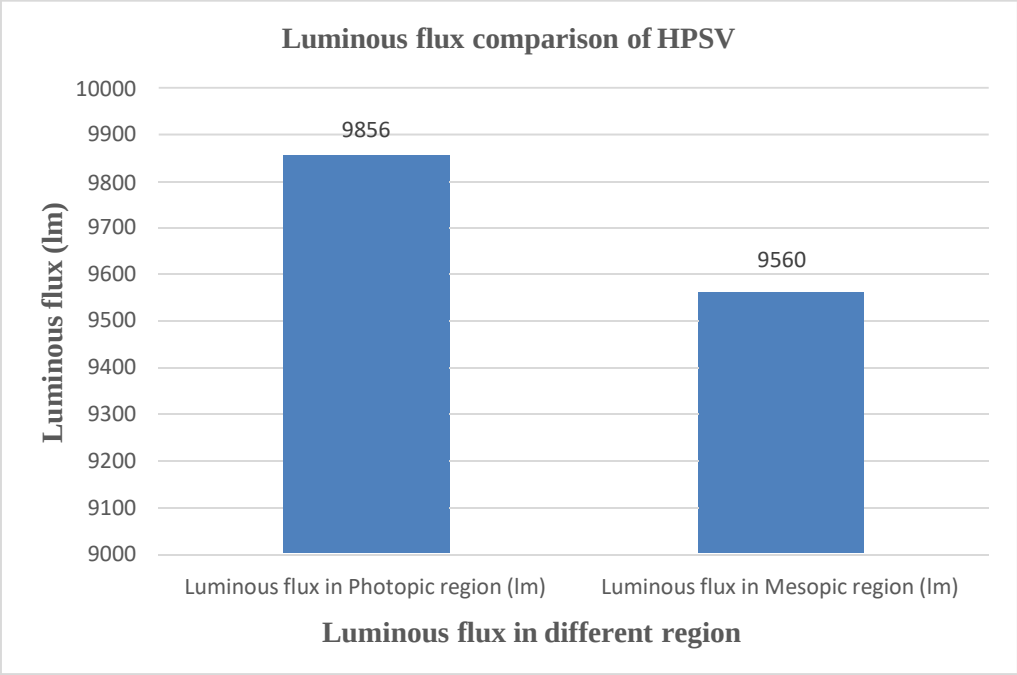

Figure 3.55: **Comparison of luminous flux of HPSV in both photopic and mesopic region**

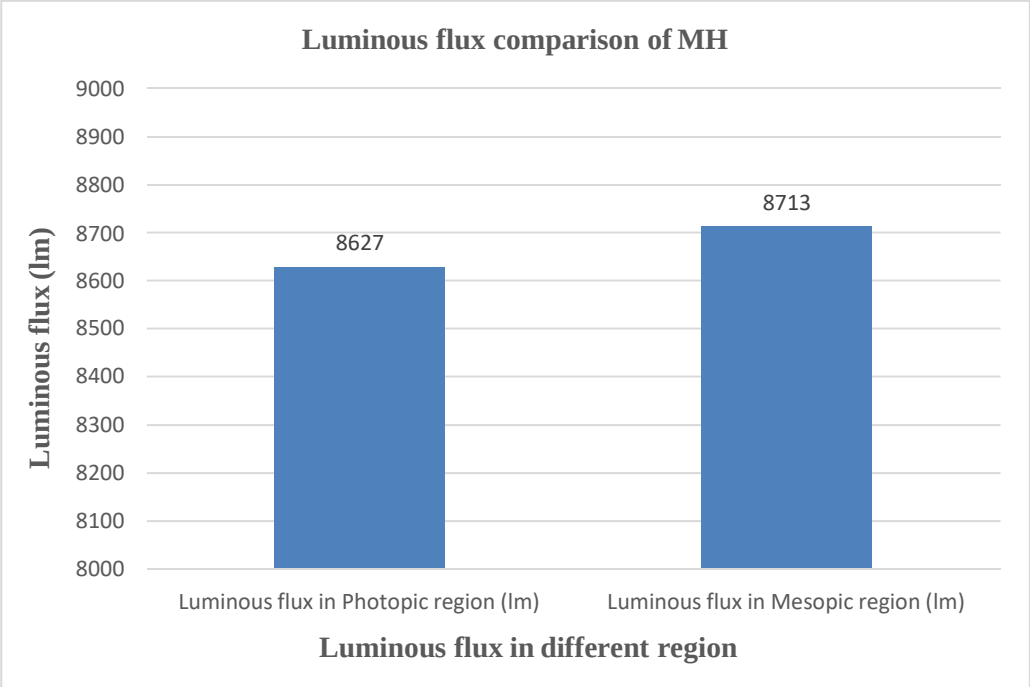

Figure 3.56**: Comparison of luminous flux of MH in both photopic and mesopic region**

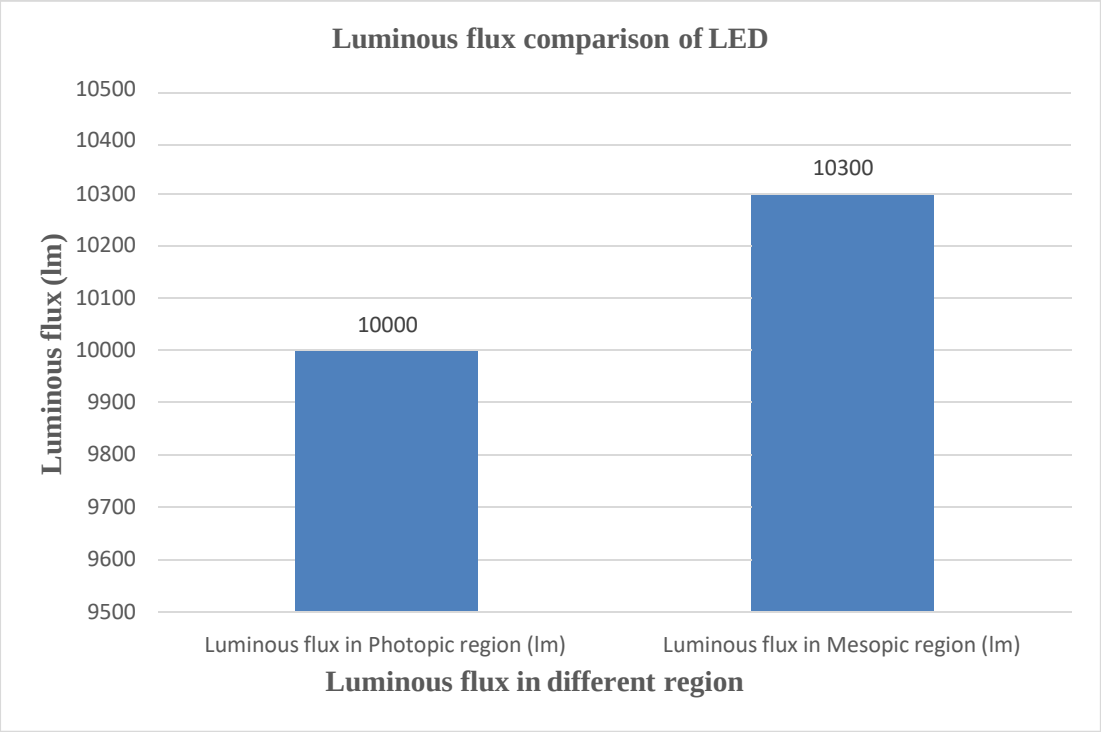

Figure 3.57: **Comparison of luminous flux of LED in both photopic and mesopic region**

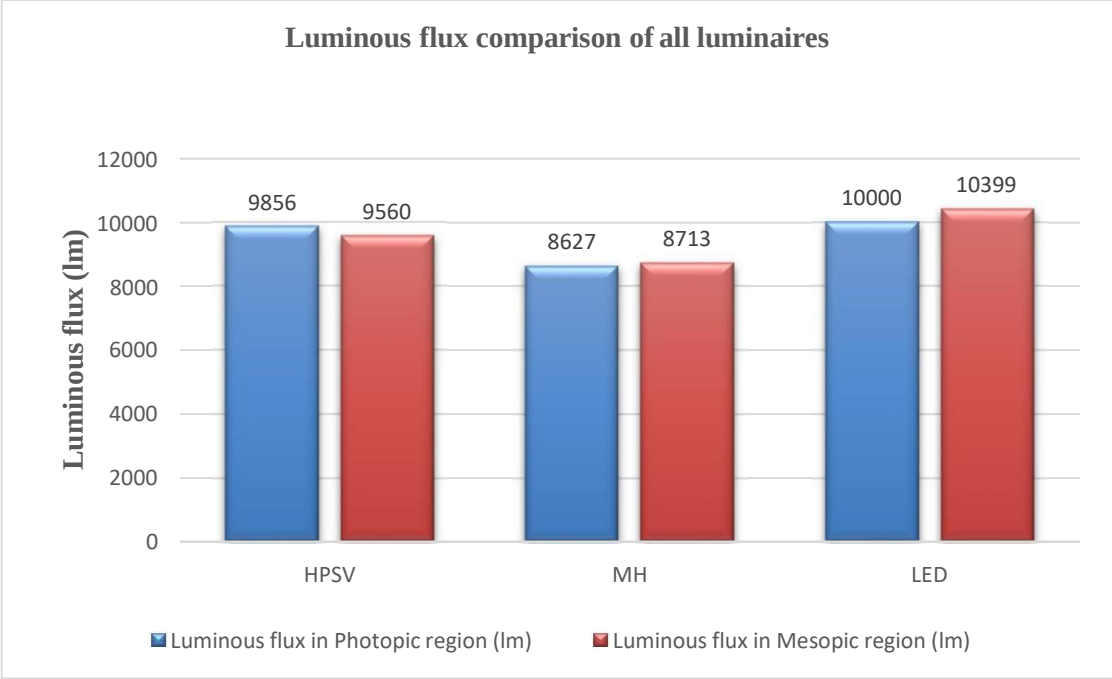

Figure 3.58: **Luminous flux comparison of all luminaires (HPSV, MH, LED) in both regions**

Luminous efficacy

Luminous efficacy measures how efficiently a light source converts electrical power into visible light, expressed in lumens per watt (lm/W). The higher the luminous efficacy, the more light is produced per unit of power consumed, indicating a more efficient light source.

Luminous efficacy plays a crucial role in energy efficiency, as a higher efficacy indicates that a light source can produce lighter while consuming less energy, leading to significant reductions in energy consumption and lower electricity costs. This efficiency is particularly important in large-scale applications where energy savings can be substantial. In lighting design, understanding efficacy is essential for selecting the appropriate light source, ensuring that the chosen lighting solution delivers optimal performance while minimizing energy use. Additionally, more efficient light sources contribute to environmental sustainability by reducing overall energy demand and lowering carbon emissions, thus supporting broader sustainability and climate goals. In the table undermentioned here is the details luminous efficacy of all luminaires (HPSV, MH, LED).

Table 3.19: **luminous efficacy of different luminaires**

Light source	Rated power (W)	Efficacy photopic (lm/w)	LPD for mesopic(lm/w)
HPSV	170	57.97	56.23
MH	170	50.74	51.25
LED	160	62.5	64.99

Comparative Analysis of Luminous Efficacy:

Luminous efficacy, a key metric in evaluating the performance of light sources, quantifies how effectively a luminaire converts electrical power into visible light. It is typically expressed in lumens per watt (lm/W). In lighting design and energy management, understanding and optimizing luminous efficacy is crucial for both energy efficiency and environmental impact. This analysis compares the luminous efficacy of three types of luminaires: High-Pressure Sodium Vapor (HPSV), Metal Halide (MH), and Light-Emitting Diode (LED), based on their performance in both the photopic and mesopic regions.

High-Pressure Sodium Vapor (HPSV)

HPSV lamps, with a rated power of 170 watts, have long been used in street lighting and industrial applications due to their relatively high efficacy compared to older technologies like incandescent bulbs. In the photopic region, which represents typical daylight vision, HPSV

lamps exhibit a luminous efficacy of 57.97 lm/W. In the mesopic region, which corresponds to low-light conditions such as twilight, the efficacy slightly decreases to 56.23 lm/W. While HPSV lamps are efficient, their performance is overshadowed by modern alternatives, particularly LEDs. The moderate energy efficiency of HPSV luminaires, coupled with their monochromatic yellow light output, limits their application in environments where color rendering and energy conservation are priorities.

Metal Halide (MH)

MH lamps, also operating at 170 watts, are commonly used in areas requiring high-intensity lighting, such as sports arenas and large commercial spaces. However, their luminous efficacy is lower than that of HPSV lamps, with values of 50.74 lm/W in the photopic region and 51.25 lm/W in the mesopic region. This lower efficacy indicates that MH lamps are less efficient in converting electrical power into visible light, resulting in higher energy consumption for the same illumination level. Moreover, MH lamps have a shorter lifespan and higher maintenance costs compared to other lighting technologies, further diminishing their appeal in energy-conscious lighting designs.

Light-Emitting Diode (LED)

LEDs, with a rated power of 160 watts, represent the most advanced lighting technology in this comparison. LEDs exhibit the highest luminous efficacy, with 62.5 lm/W in the photopic region and 64.99 lm/W in the mesopic region. This superior efficacy highlights the efficiency of LEDs in producing more light per watt of electricity consumed, making them the most energy-efficient option among the three luminaires. Additionally, LEDs offer numerous advantages, including longer lifespan, lower maintenance costs, and better color rendering capabilities. The higher efficacy of LEDs translates to significant energy savings and reduced environmental impact, aligning with sustainability goals and modern lighting standards.

The comparative analysis clearly demonstrates that LEDs outperform HPSV and MH lamps in terms of luminous efficacy. While HPSV lamps offer moderate efficiency, and MH lamps lag behind both HPSV and LED in efficacy, LEDs stand out as the most efficient and environmentally friendly choice for contemporary lighting applications. This analysis underscores the importance of considering luminous efficacy in the selection of luminaires, particularly in contexts where energy efficiency and sustainability are critical. As lighting technology continues to evolve, the adoption of high-efficacy light sources like LEDs will be integral to reducing energy consumption and minimizing the environmental footprint of lighting systems.

CHAPTER 4: STREET LIGHTING DESIGN

4.1 Introduction

This chapter examines the practical implications of integrating mesopic dimensioning into street lighting design through the simulation and comparison of mesopic luminance values across various lamp types, including High-Pressure Sodium Vapor (HPSV), Metal Halide (MH), and Light Emitting Diodes (LED). Simulations were conducted using DIALux software, following the guidelines outlined in the CIE191:2010 standard [42,54]. A comparative analysis between simulated photopic luminance and calculated mesopic luminance is provided. The performance differences among these lighting technologies are clarified, offering insights into which lamp type provides the most effective balance between visual efficacy and energy efficiency under mesopic conditions, an essential factor for optimizing street lighting design.

The study does not focus on the ideal design of street lights themselves but rather on maintaining a standard road lighting design and analyzing the variations that occur as lighting transitions from the photopic to the mesopic region. In this studies ME4a lighting class has been used as it is designed for roads and areas where minimal lighting is adequate. This class aims to provide basic visibility while prioritizing energy efficiency. It features the lowest luminance levels among the ME classes, emphasizing cost-effectiveness and reducing environmental impact. ME4 is suitable for locations with low traffic and where high levels of illumination are not necessary, thus balancing the need for sufficient visibility with economic and ecological considerations [26]. The S/P ratio for each luminaire has been measured and applied according to the corrected photopic luminance values. This correction is a function of both the relevant photopic luminance and the specific S/P ratio of the lamp. The adjustments assume that current recommendations and design criteria are based on using a luminaire with the particular S/P ratio of the luminaire [28].

The importance of evaluating visual efficacy in the mesopic region has increased in the context of road lighting, particularly given the inadequacy of current methods for accurately assessing this efficacy. As the demand for lighting solutions that are both energy-efficient and visually effective has grown, prompting research into innovative approaches for optimizing street lighting design. The conversion of photopic luminous flux into its mesopic equivalent is addressed in this chapter, representing a critical advancement in enhancing the efficiency of road lighting systems. The shift from traditional reliance on the photopic system to the adoption of the mesopic photometry system by lighting designers is examined in this chapter. The mesopic system offers significant improvements in visual performance and energy efficiency for street lighting, addressing the limitations of photopic lumens, which poorly correlate with visual sensations under mesopic conditions. Research, including He et al., shows that lamp spectrum significantly influences reaction times, particularly for off-axis vision under low light. These findings underscore the importance of incorporating mesopic evaluations in modern street lighting design [56,58].

By evaluating the mesopic dimensioning of surface luminance, a more sophisticated approach to road lighting is contributed to, one that aligns with contemporary goals of energy efficiency and

enhanced visual performance. The findings presented in this chapter are intended to guide lighting designers in selecting the most suitable lighting technologies for outdoor applications, ensuring both functional and aesthetic excellence in street lighting.

4.2 Methodology

The methodology employed in this study systematically evaluates illuminance values under both photopic and mesopic conditions, specifically for road lighting applications. The methodology begins with the calculation of photopic design values in lux, followed by their conversion to mesopic values. The subsequent redesign is based on these mesopic values, enabling a comparative analysis of the effectiveness of the photopic to mesopic conversion. The study primarily focuses on assessing the illuminance provided by High-Pressure Sodium Vapor (HPSV), Metal Halide (MH), and Light Emitting Diode (LED) luminaires, with an additional comparison involving three Compact Fluorescent Lamp (CFL) luminaires. This approach allows for a comprehensive evaluation of how different luminaires impact illuminance levels on roadways.

A. Photopic Design

Initially, lighting calculations and analyses are conducted using DIALux software to simulate road lighting design for a roadway with a width of 20 meters, comprising two lanes, and classified under road lighting class ME4a. The design assumes a mounting height of 9 meters for the luminaires. The analysis includes the evaluation of MH, HPSV, and LED luminaires individually. It is important to note that the designs are not optimized for ideal conditions but rather follow basic road lighting standards to facilitate the distinction between photopic and mesopic regions. The specific details of the lamps and luminaires used in the design are provided in the subsequent sections.

B. Photopic to Mesopic Conversion

The transition from photopic to mesopic lighting design involves converting the photopic luminous flux provided by luminaire manufacturers into mesopic luminous flux. This conversion process includes several key steps. First, photopic luminance ($\mathbf{L_p}$) is calculated, and the corresponding mesopic luminance ($\mathbf{L_m}$) is determined using the CIE 191:2010 guidelines and the S/P ratio of the light source. The S/P ratios for HPSV, MH, and LED sources are measured using a Scotopic/Photopic meter. Mesopic luminance values are then interpolated from the known photopic luminance values and S/P ratios following the CIE 191:2010 standards.

Subsequently, the mesopic to photopic ratio (M/P) is computed. Once the M/P ratio for each light source is determined, adjustments are made to the photopic luminance values provided by the manufacturers. The LDT Editor in DIALux is used for this purpose, allowing the modification of the original photopic luminance values to their corresponding mesopic values by multiplying the source luminance values by the appropriate M/P ratio for each case. The revised photometric files for the three selected luminaires are then integrated into the DIALux light simulation software, ensuring that the design parameters remain consistent with the initial design. The average luminance is calculated based on these adjustments. A detailed table is provided, listing the measured S/P ratios, calculated mesopic luminance values using CIE 191:2010 standards, and the corresponding M/P ratios. The M/P ratio is determined as the quotient of mesopic luminance ($\mathbf{L_m}$) divided by photopic luminance ($\mathbf{L_p}$).

4.3 Lighting Design in Photopic Region

The specifications and characteristics of the lamps and luminaires used in the design process are systematically detailed in Table 4.1. The primary aim of this section is to evaluate and compare the average illuminance provided by each lamp type when applied independently to the road lighting design, thereby establishing a baseline for photopic lighting conditions.

Table 4.1: **Luminaires with specifications**

Luminaire	**Details of Fixture**	**Light Distribution Curve**
PHILIPS SRP501/SONT150W,P1, LT,TOEIN 10 CLOSED, 'N' POT	Luminous flux (Luminaire): 10202 lm Luminous flux (Lamps): 14000 Lm Luminaire Wattage: 170.0 W Luminaire classification according to CIE: 100 CIE flux code: 43 79 97 100 73 Fitting: 1 x SON(T)150W (Correction Factor 1.000).	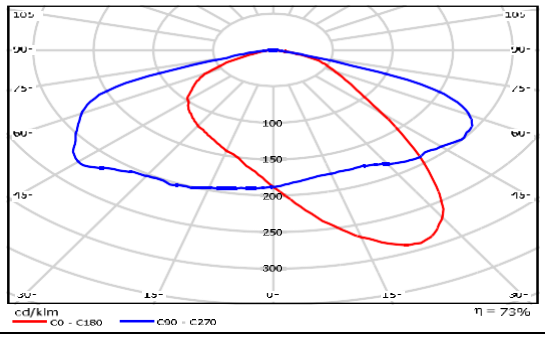

COOPER LIGHTING 175W STREETWORKS LUMINAIRE	Luminous flux (Luminaire): 9527 lm Luminous flux (Lamps): 14000 lm Luminaire Wattage: 175.0 W Luminaire classification according to CIE: 100 CIE flux code: 32 67 95 100 44 Fitting: 1 x 175 WATT MH CLEAR ED17 (Correction Factor 1.000).	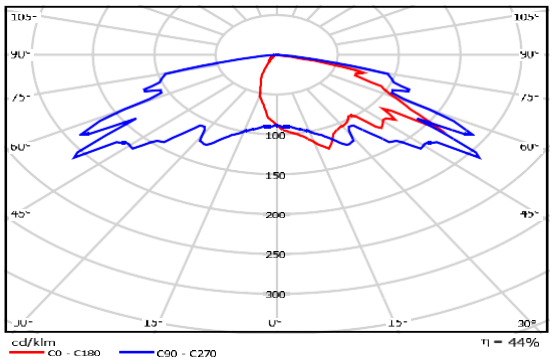
SILVERSUN STHP150NWS Street Light 150W 4000K	Luminous flux (Luminaire): 12000 lm Luminous flux (Lamps): 17442 lm Luminaire Wattage: 145.1 W Luminaire classification according to CIE: 100 CIE flux code: 42 81 98 100 100 Fitting: 0 x User defined (Correction Factor 1.000).	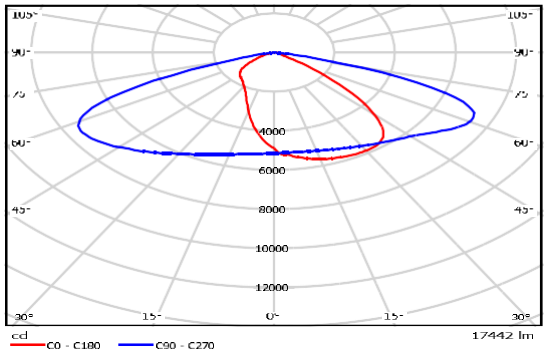

4.3.1 Lighting Design using HPSV luminaire

Design considerations:

- Luminaire used: PHILIPS SRP501/SONT150W,P1,LT,TOEIN 10 CLOSED, 'N' POT
- Area of the road width: 20m
- Number of lanes: 2
- Illuminance class: ME4a
- Luminaire arrangement: double row, opposing
- Luminaire mounting height: 9m
- Distance between two poles: 10m
- Boom length: 0.5m
- Boom angle: 25
- Overhang: 2m
- Distance pole to roadway: -1.5m
- Light loss factor: 0.67

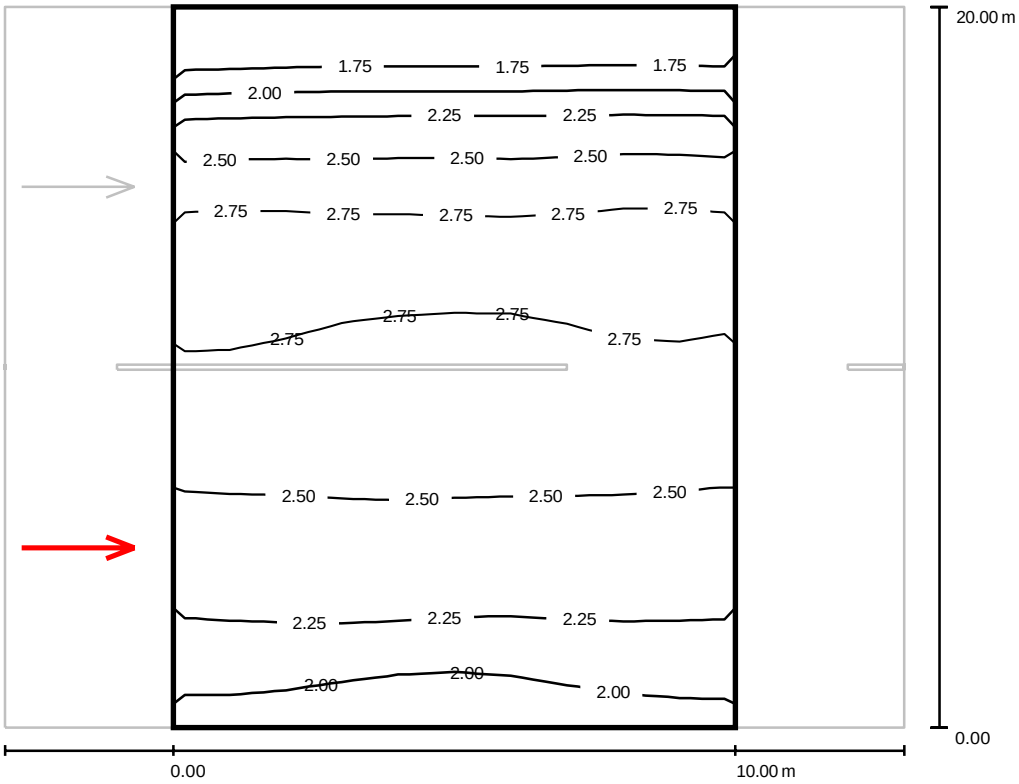

Figure 4.1: **Isolines Diagram of HPSV luminaire in photopic region**

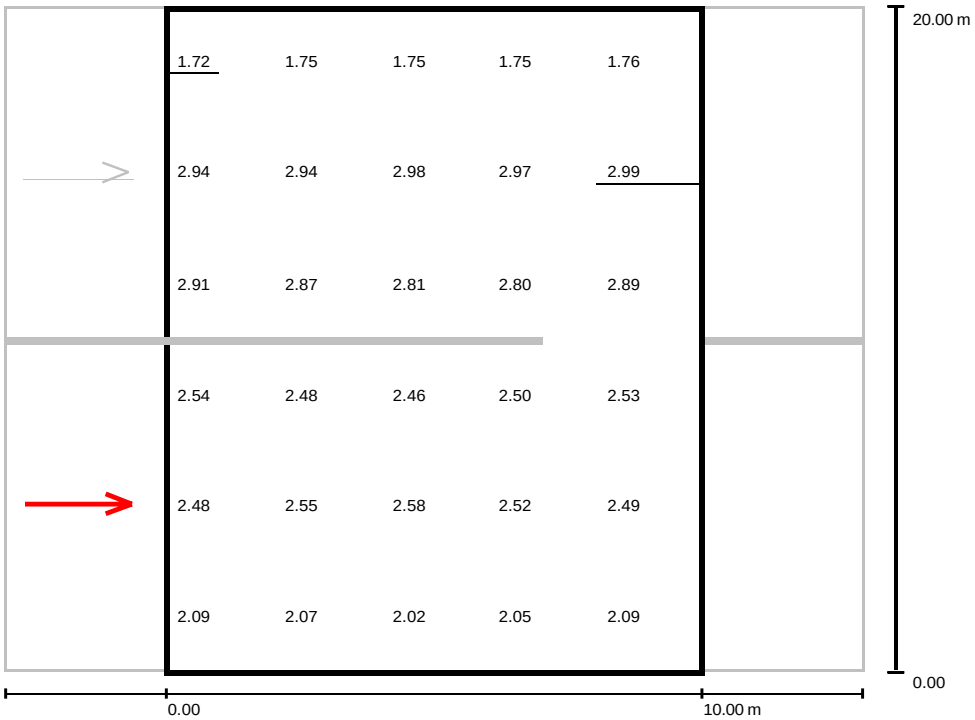

Figure 4.2: **Value chart of HPSV luminaire in photpic region**

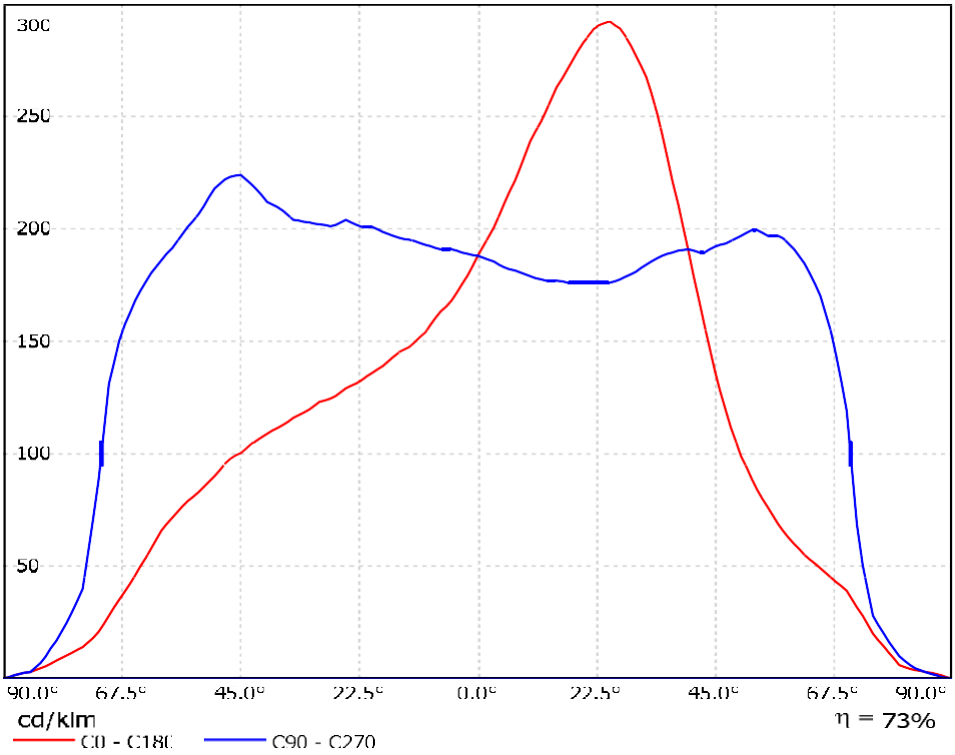

Figure 4.3: **LDC (linear) graph of HPSV luminaire in photpic region**

4.3.2 Lighting Design using MH luminaire

Design considerations:

- Luminaire used: COOPER LIGHTING 175W STREETWORKS LUMINAIRE
- Area of the road width: 20m
- Number of lanes: 2
- Illuminance class: ME4a
- Luminaire arrangement: double row, opposing
- Luminaire mounting height: 9m
- Distance between two poles: 12m
- Boom length: 0.5m
- Boom angle: 25
- Overhang: 2m
- Distance pole to roadway: -1.5m
- Light loss factor: 0.67

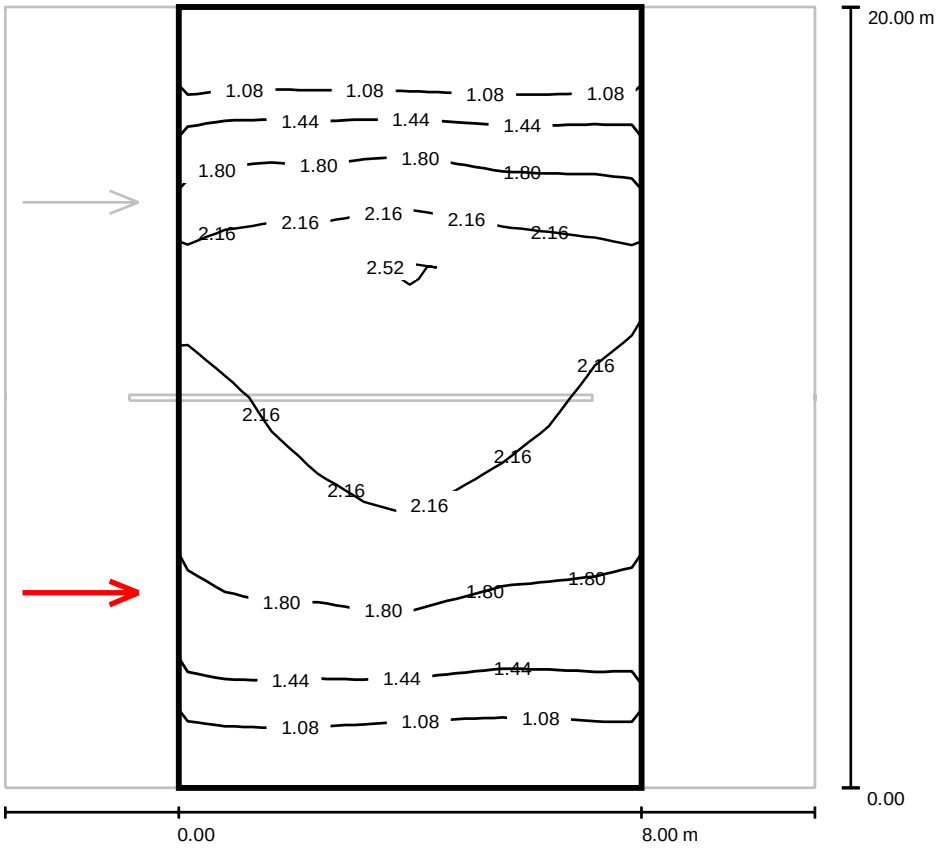

Figure 4.4: **Isoline diagram of MH luminaire in photopic region**

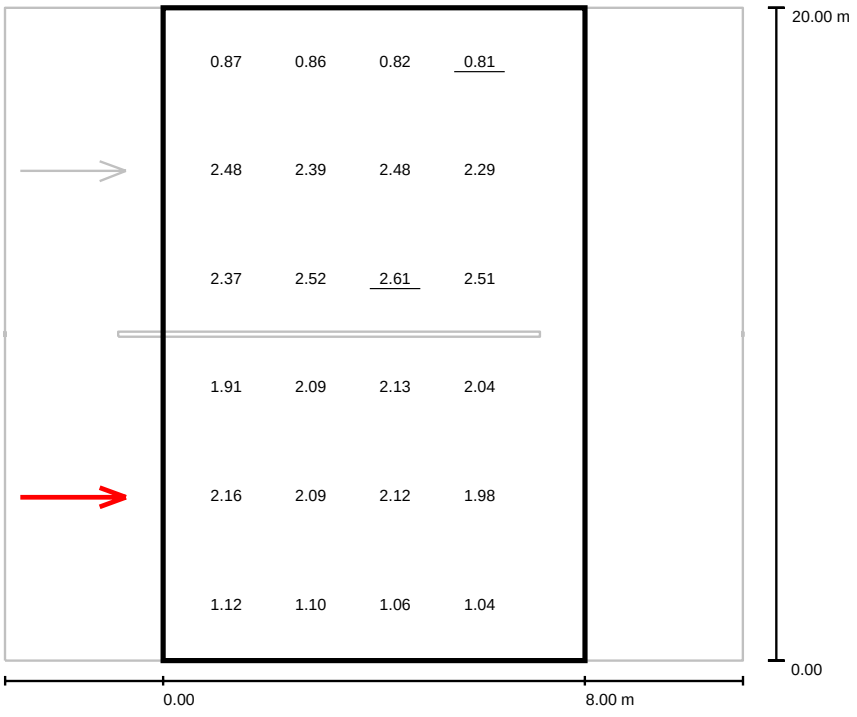

Figure 4.5: **Value chart of MH luminaire in photopic region**

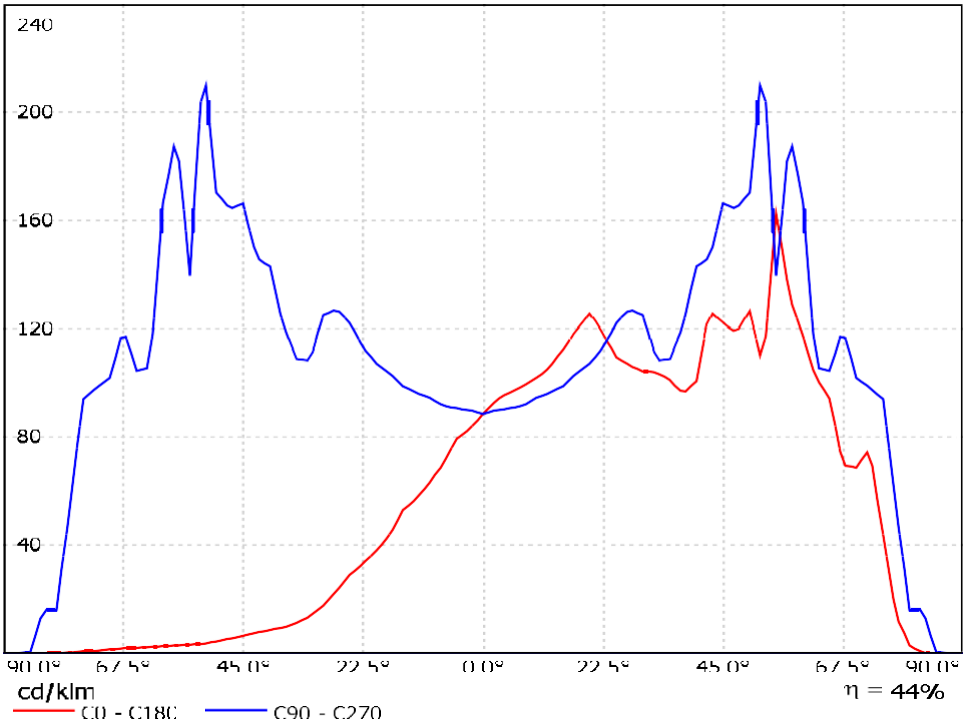

Figure 4.6: **LDC (linear) graph of MH luminaire in photopic region**

4.3.3 Lighting Design using LED luminaire

Design considerations:

- Luminaire used: SILVERSUN STHP150NWS Street Light 150W 4000K
- Area of the road width: 20m
- Number of lanes: 2
- Illuminance class: ME4a
- Luminaire arrangement: double row, opposing
- Luminaire mounting height: 9m
- Distance between two poles: 12m
- Boom length: 0.5m
- Boom angle: 25
- Overhang: 2m
- Distance pole to roadway: -1.5m
- Light loss factor: 0.67

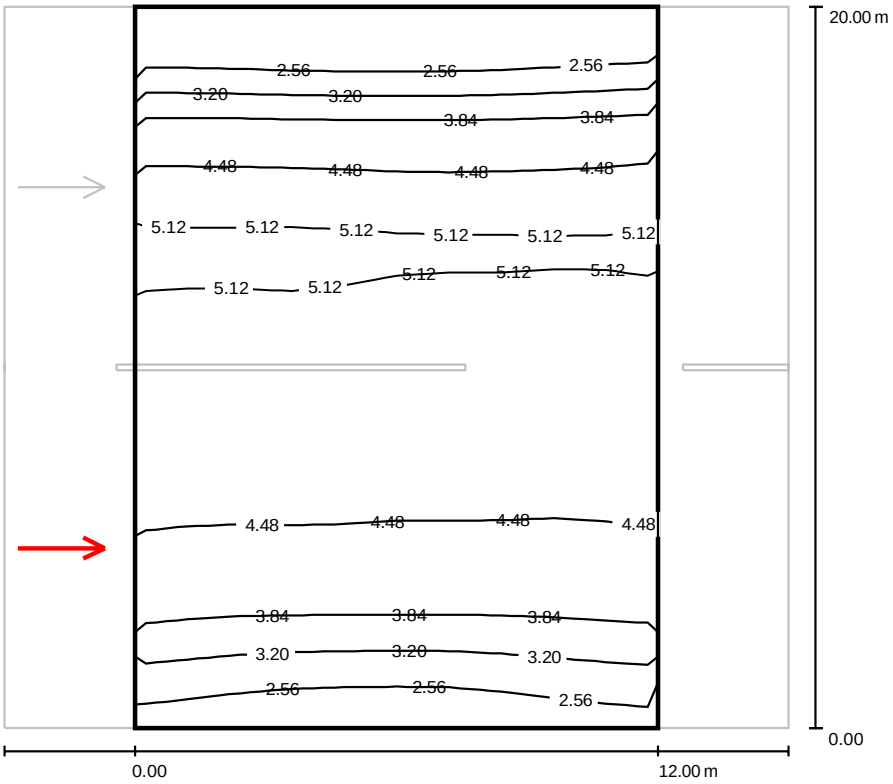

Figure 4.7: **Isolines Diagram of LED luminaire in photopic region**

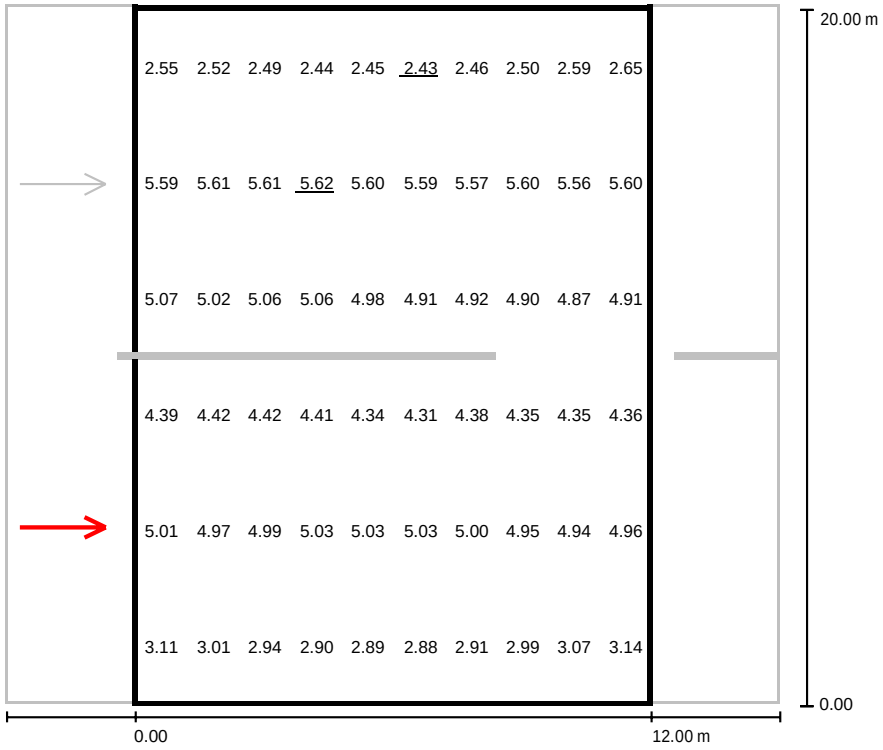

Figure 4.8: **Value Chart of LED luminaire in photopic region**

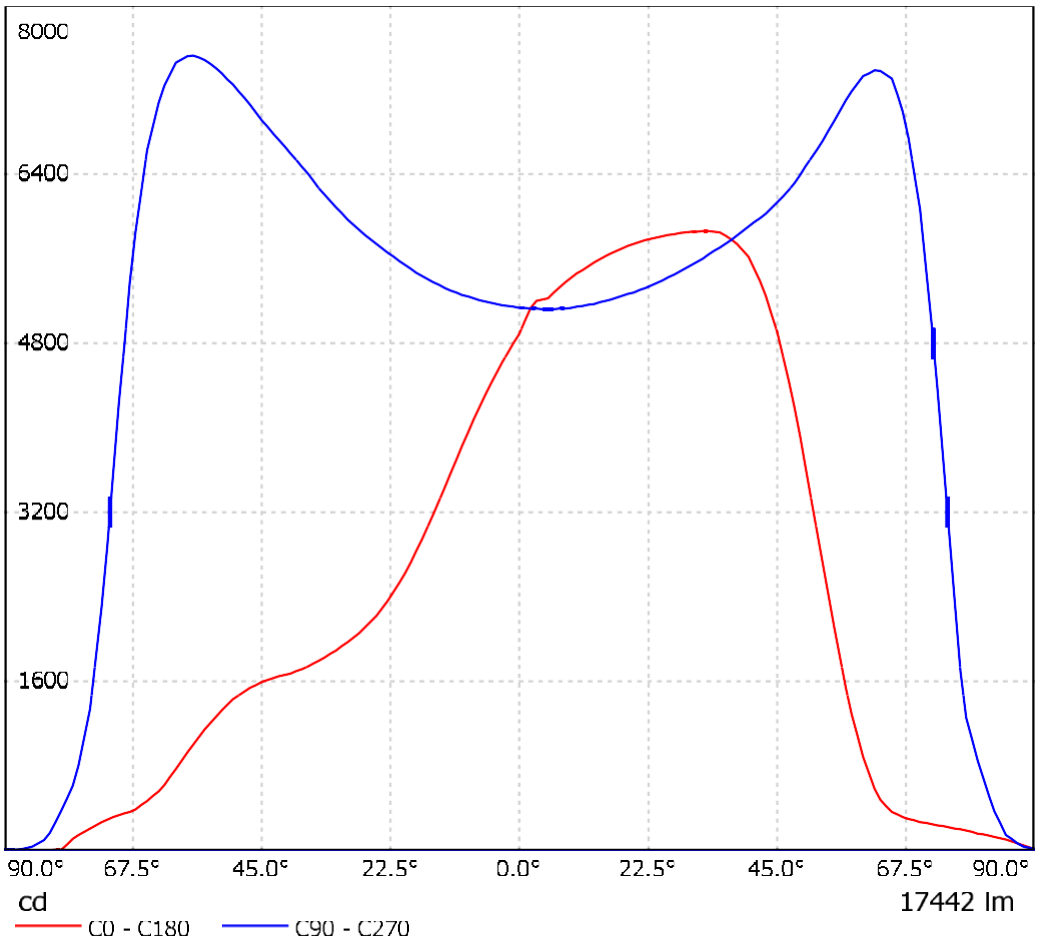

Figure 4.9: **LDC (linear) graph of MH luminaire in photopic region**

4.3.4 An overview of the designs in Photopic region

The summary calculations provided in the table 4.2 offer a comprehensive overview of the luminaires' designs in the photopic region. This table presents the average photopic luminance (**L_p**) and the overall uniformity (**U_o**) for High-Pressure Sodium Vapor (HPSV), Metal Halide (MH), and Light Emitting Diode (LED) luminaires when applied to road lighting conditions. The details the performance results for each light source, focusing exclusively on their behavior under photopic conditions.

Table 4.2: **Design Summary for All the luminaires in photopic region**

Main Light source	Average photopic luminance ($\mathbf{L_p}$)	Overall Uniformity ($\mathbf{U_o}$)
HPSV	2.44	0.70
MH	2.41	0.50
LED	4.24	0.57

4.2 Lighting Design in Mesopic Region

4.2.1 Conversion process for photopic data to corresponding mesopic data

In the context of optimizing road lighting systems, the conversion process from photopic data to corresponding mesopic data. This section outlines the detailed steps involved in this conversion process, adhering to the CIE 191:2010 standards.

Calculation of Mesopic Luminance (L_m)

The first step in the conversion process is the calculation of photopic luminance ($\mathbf{L_p}$) and its subsequent conversion to mesopic luminance ($\mathbf{L_m}$). This conversion is guided by the CIE 191:2010 standards and relies heavily on the Scotopic/Photopic (S/P) ratio, a key factor that influences the perceived brightness of light sources under mesopic conditions. The S/P ratio is measured using a Scotopic/Photopic meter and is essential for evaluating the performance of different light sources, such as Metal Halide (MH), Light Emitting Diodes (LED), and High-Pressure Sodium Vapor (HPSV), in mesopic lighting environments.

Calculation of the Mesopic vs. Photopic Ratio (M/P)

Once the mesopic luminance ($\mathbf{L_m}$) is determined, the next step is to calculate the Mesopic vs. Photopic ratio (M/P). This ratio, which is the quotient of photopic luminance ($\mathbf{L_p}$) to mesopic luminance ($\mathbf{L_m}$), serves as a comparative measure of the light source's effectiveness in mesopic versus photopic conditions. The M/P ratio is critical for adjusting photopic data so that it can be applied to mesopic conditions, ensuring that the lighting design is both visually effective and energy-efficient.

Adjustment of Photopic Luminance Values

Using the M/P ratio, photopic luminance values are adjusted to correspond with mesopic conditions. This adjustment is a necessary step to ensure that the lighting designs are optimized

for mesopic vision, which is particularly relevant for road lighting where human visual perception in low-light conditions must be considered. The adjustment is carried out using LDT Editor software, which modifies the original photopic luminance values in the photometric data to their mesopic equivalents.

Simulation in DIALux

The adjusted photometric data is then imported into DIALux software for simulation. The software enables precise simulation and evaluation of lighting designs under mesopic conditions while maintaining the same design parameters used in the photopic-based designs. This simulation step is crucial for validating the accuracy of the conversion process and ensuring that the lighting design meets all necessary criteria for energy efficiency, safety, and visual comfort.

Presentation of Conversion Data

The study includes a comprehensive table that presents the measured S/P ratios, the calculated mesopic luminance values according to the CIE 191:2010 standards, and the corresponding M/P ratios for road lighting luminaires. This data serves as a reference for verifying the consistency and accuracy of the converted photometric data, ensuring that the mesopic lighting design is appropriate for real-world applications.

This conversion process from photopic to mesopic data is essential for developing lighting strategies that are not only energy-efficient and visually effective but also aligned with the human visual system's response under mesopic conditions. By adhering to CIE 191:2010 standards and utilizing tools such as the Scotopic/Photopic meter and LDT Editor software, the study ensures that the lighting designs are optimized for a wide range of conditions, thereby enhancing both the functional and experiential aspects of road lighting.

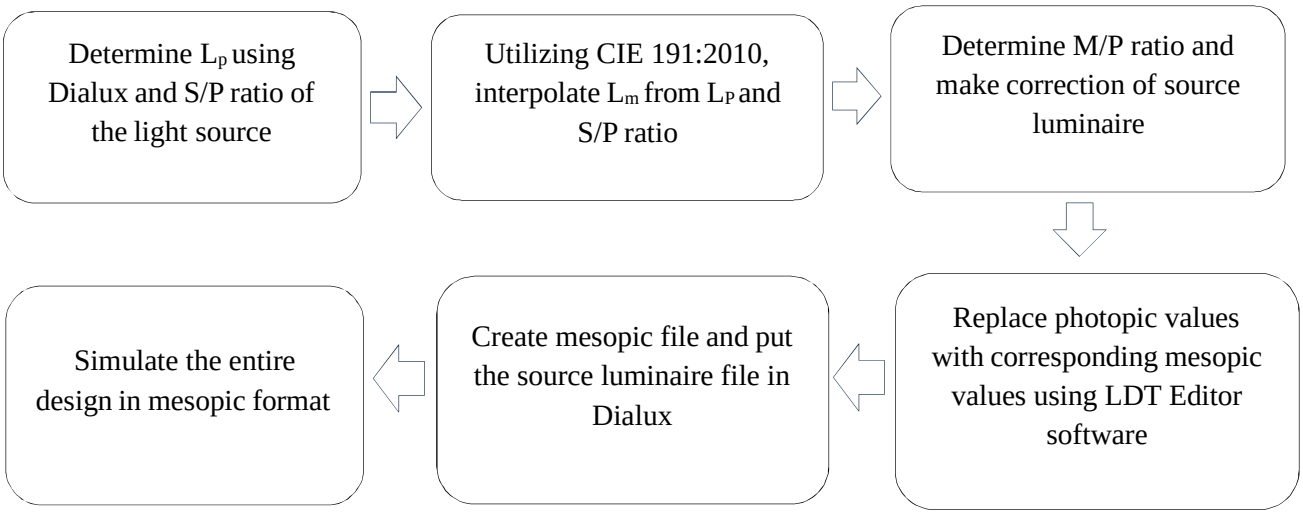

Figure 4.10: **Conceptual flow diagram of the proposed study methodology**

Table 4.3: **Values of L_m of the recommended mesopic system as a function of photopic luminance and s/p ratio**

	Photopic luminance / cd·m^{-2}						
S/P	0,01	0,03	0,1	0,3	1	3	4,5
LPS ~ 0,25	0,002 5	0,014 5	0,070 5	0,246 7	0,913 0	2,926 5	4,478 2
0,35	0,003 5	0,017 4	0,075 0	0,254 5	0,925 3	2,936 7	4,481 2
0,45	0,004 5	0,019 8	0,079 3	0,262 0	0,937 3	2,946 8	4,484 2
HPS ~ 0,55	0,005 7	0,022 0	0,083 4	0,269 3	0,949 2	2,956 8	4,487 2
0,65	0,006 9	0,023 9	0,087 3	0,276 4	0,960 8	2,966 6	4,490 1
0,75	0,007 9	0,025 8	0,091 1	0,283 3	0,972 2	2,976 3	4,492 9
0,85	0,008 8	0,027 5	0,094 7	0,290 1	0,983 5	2,985 9	4,495 8
0,95	0,009 6	0,029 2	0,098 3	0,296 7	0,994 5	2,995 3	4,498 6
1,05	0,010 4	0,030 8	0,101 7	0,303 2	1,005 4	3,004 6	4,501 4
MH warm white ~ 1,15	0,011 1	0,032 3	0,105 1	0,309 6	1,016 1	3,013 9	4,504 1
1,25	0,011 8	0,033 8	0,108 3	0,315 8	1,026 7	3,023 0	4,506 8
1,35	0,012 5	0,035 3	0,111 5	0,322 0	1,037 1	3,031 9	4,509 5
1,45	0,013 2	0,036 7	0,114 7	0,328 0	1,047 3	3,040 8	4,512 2
1,55	0,013 8	0,038 1	0,117 8	0,333 9	1,057 5	3,049 6	4,514 8
1,65	0,014 5	0,039 5	0,120 8	0,339 8	1,067 4	3,058 2	4,517 4
1,75	0,015 1	0,040 8	0,123 8	0,345 5	1,077 3	3,066 8	4,520 0
1,85	0,015 7	0,042 1	0,126 7	0,351 2	1,087 0	3,075 3	4,522 5
1,95	0,016 3	0,043 4	0,129 5	0,356 8	1,096 6	3,083 6	4,525 0
2,05	0,016 9	0,044 6	0,132 4	0,362 3	1,106 0	3,091 9	4,527 5
2,15	0,017 4	0,045 9	0,135 2	0,367 7	1,115 4	3,100 1	4,529 9
2,25	0,018 0	0,047 1	0,137 9	0,373 1	1,124 6	3,108 2	4,532 3
MH day-light ~ 2,35	0,018 5	0,048 3	0,140 6	0,378 4	1,133 8	3,116 2	4,534 7
2,45	0,019 1	0,049 5	0,143 3	0,383 6	1,142 8	3,124 1	4,537 1
2,55	0,019 6	0,050 6	0,145 9	0,388 8	1,151 7	3,131 9	4,539 5
2,65	0,020 1	0,051 8	0,148 5	0,393 9	1,160 5	3,139 6	4,541 8
2,75	0,020 7	0,052 9	0,151 1	0,398 9	1,169 3	3,147 3	4,544 1

All the measured s/p ratio, calculated mesopic luminance value using CIE 191:2010 and m/p ratio are shown table 4.4 and M/P ratio=Lm/Lp.

Table 4.4: **Measured and calculated value**

Main source	Average photopic luminance (L_p)	Measured S/P ratio	Calculated mesopic luminance (L_m) using CIE 191:2010	Calculated M/P ratio
HPSV	2.44	0.62	2.39	0.979
MH	2.41	1.2	2.46	1.021
LED	4.24	1.6	4.27	1.007

4.2.2 Modified Photometric file creation through LDT Editor software and implementation in DIALux design

In the context of road lighting design, the creation of modified photometric files through LDT Editor software and their subsequent implementation in DIALux is a crucial process for optimizing lighting systems under mesopic conditions. This section outlines the step-by-step procedure used to convert photopic data to mesopic data, specifically focusing on an example with an HPSV luminaire.

Step-by-Step Process for Modifying Photometric Files for Mesopic Conditions:

Uploading the IES File into LDT Editor: The process begins by uploading the IES file of the luminaire into the LDT Editor software. This file contains the photometric data, including the luminous intensity distribution based on photopic conditions. Upon upload, the software displays key luminaire details such as wattage, beam angle, and initial luminous flux. In figure 4.11, a sample of HPSV luminaire details in LDT Editor software is shown. For example:

- **Luminaire:** PHILIPS SRP501/SONT150W, P1, LT, TOEIN 10 CLOSED, 'N' POT
- **Power:** 170W
- **Initial Luminous Flux (Photopic):** 10,202 lumens

Adjusting Luminous Intensity Data: To modify the photometric data for mesopic conditions, navigate to the "Luminous Intensities" section within LDT Editor. This section presents a table of luminous intensity values organized by angles, representing the intensity of light emitted in various directions under photopic conditions. The next step involves replacing these photopic intensity values with the corresponding mesopic values. These mesopic values are calculated based on the Scotopic/Photopic (S/P) ratio and other relevant factors. The adjustment generally results in higher intensity values for specific directions under mesopic conditions. In figure 4.12 & 4.13, the difference between photopic and converted mesopic luminous intensity table has been shown.
For instance:

- **Photopic Luminous Intensity (at 90 degrees):** 188 cd
- **Converted Mesopic Luminous Intensity (at 90 degrees):** 180 cd

Saving Implementing the Modified File in DIALux Design: After modifying the luminous intensity values to adapt for mesopic conditions, it is crucial to save the file with a new name that reflects this adaptation, distinguishing it from the original photopic-based file. This modified IES file is then imported into DIALux software for road lighting design.

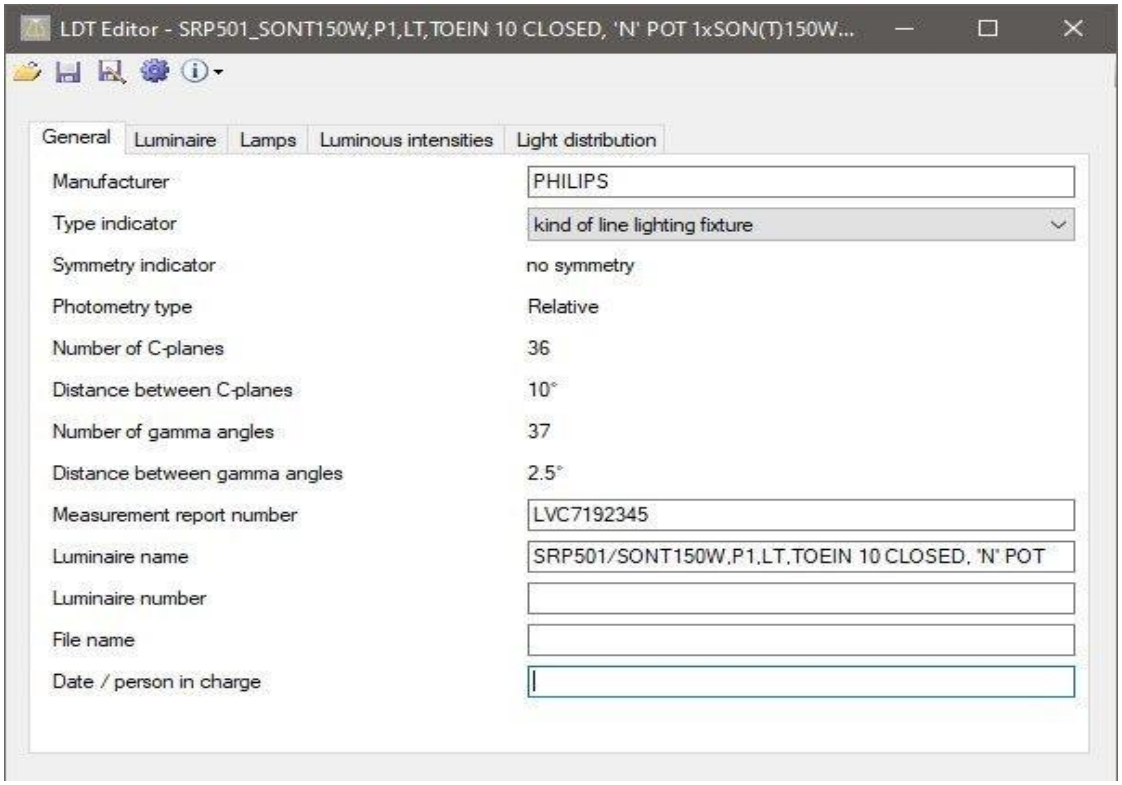

Figure 4.11: **A sample of HPSV luminaire details in LDT Editor software**

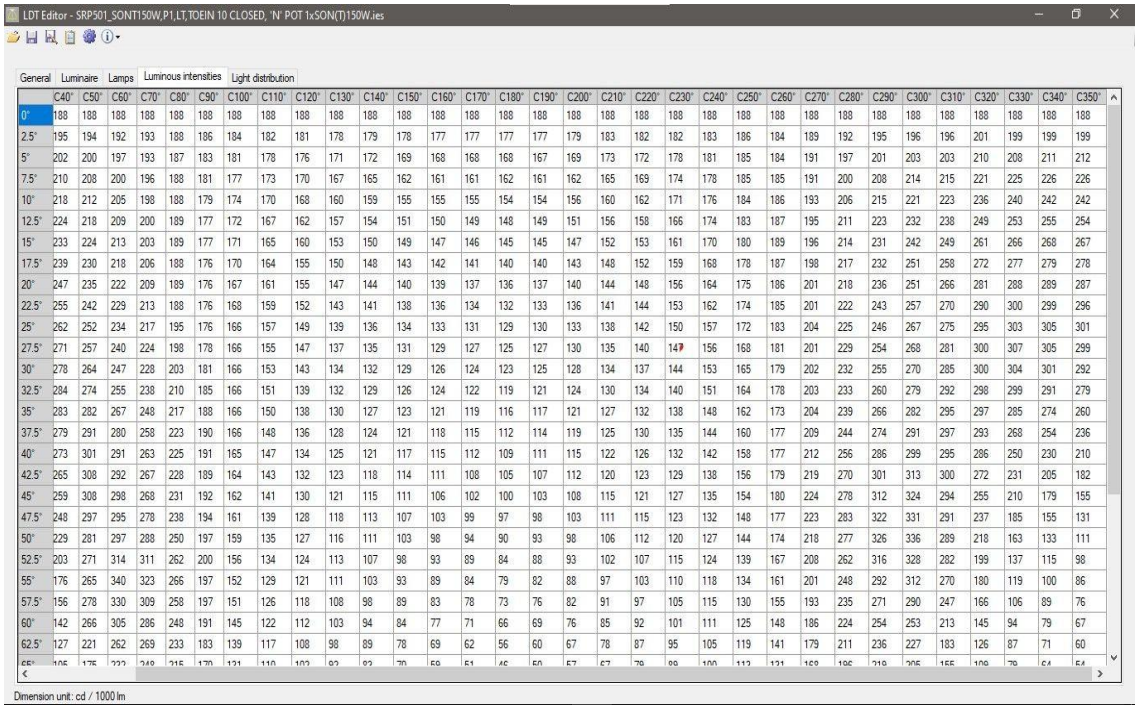

	C40°	C50°	C60°	C70°	C80°	C90°	C100°	C110°	C120°	C130°	C140°	C150°	C160°	C170°	C180°	C190°	C200°	C210°	C220°	C230°	C240°	C250°	C260°	C270°	C280°	C290°	C300°	C310°	C320°	C330°	C340°	C350°
0°	188	188	188	188	188	188	188	188	188	188	188	188	188	188	188	188	188	188	188	188	188	188	188	188	188	188	188	188	188	188	188	188
2.5°	195	194	192	193	188	186	184	182	181	178	179	178	177	177	177	177	179	183	182	182	183	186	184	189	192	195	196	196	201	199	199	199
5°	202	200	197	193	187	183	181	178	176	171	172	169	168	168	168	167	169	173	172	178	181	185	184	191	197	201	203	203	210	208	211	212
7.5°	210	208	200	196	188	181	177	173	170	167	165	162	161	161	162	161	162	165	169	174	178	185	185	191	200	208	214	215	221	225	226	226
10°	218	212	205	198	188	179	174	170	168	160	159	155	155	155	154	154	156	160	162	171	176	184	186	193	206	215	221	223	236	240	242	242
12.5°	224	218	209	200	189	177	172	167	162	157	154	151	150	149	148	149	151	156	158	166	174	183	187	195	211	223	232	238	249	253	255	254
15°	233	224	213	203	189	177	171	165	160	153	150	149	147	146	145	145	147	152	153	161	170	180	189	196	214	231	242	249	261	266	268	267
17.5°	239	230	218	206	188	176	170	164	155	150	148	143	142	141	140	140	143	148	152	159	168	178	187	198	217	232	251	258	272	277	279	278
20°	247	235	222	209	189	176	167	161	155	147	144	140	139	137	136	137	140	144	148	156	164	175	186	201	218	236	251	266	281	288	289	287
22.5°	255	242	229	213	188	176	168	159	152	143	141	138	136	134	132	133	136	141	144	153	162	174	185	201	222	243	257	270	290	300	299	296
25°	262	252	234	217	195	176	166	157	149	139	136	134	133	131	129	130	133	138	142	150	157	172	183	204	225	246	267	275	295	303	305	301
27.5°	271	257	240	224	198	178	166	155	147	137	135	131	129	127	125	127	130	135	140	147	156	168	181	201	229	254	268	281	300	307	305	299
30°	278	264	247	228	203	181	166	153	143	134	132	129	126	124	123	125	128	134	137	144	153	165	179	202	232	255	270	285	300	304	301	292
32.5°	284	274	255	238	210	185	166	151	139	132	129	126	124	122	119	121	124	130	134	140	151	164	178	203	233	260	279	292	298	299	291	279
35°	283	282	267	248	217	188	166	150	138	130	127	123	121	119	116	117	121	127	132	138	148	162	173	204	239	266	282	295	297	285	274	260
37.5°	279	291	280	258	223	190	166	148	136	128	124	121	118	115	112	114	119	125	130	135	144	160	177	209	244	274	291	297	293	268	254	236
40°	273	301	291	263	225	191	165	147	134	125	121	117	115	112	109	111	115	122	126	132	142	158	177	212	256	286	299	295	286	250	230	210
42.5°	265	308	292	267	228	189	164	143	132	123	118	114	111	108	105	107	112	120	123	129	138	156	179	219	270	301	313	300	272	231	205	182
45°	259	308	298	268	231	192	162	141	130	121	115	111	106	102	100	103	108	115	121	127	135	154	180	224	278	312	324	294	255	210	179	155
47.5°	248	297	295	278	238	194	161	139	128	118	113	107	103	99	97	98	103	111	115	123	132	148	177	223	283	322	331	291	237	185	155	131
50°	229	281	297	288	250	197	159	135	127	116	111	103	98	94	90	93	98	106	112	120	127	144	174	218	277	326	336	289	218	163	133	111
52.5°	203	271	314	311	262	200	156	134	124	113	107	98	93	89	84	88	93	102	107	115	124	139	167	208	262	316	328	282	199	137	115	98
55°	176	265	340	323	266	197	152	129	121	111	103	93	89	84	79	82	88	97	103	110	118	134	161	201	248	292	312	270	180	119	100	86
57.5°	156	278	330	309	258	197	151	126	118	108	98	89	83	78	73	76	82	91	97	105	115	130	155	193	235	271	290	247	166	106	89	76
60°	142	266	305	286	248	191	145	122	112	103	94	84	77	71	66	69	76	85	92	101	111	125	148	186	224	254	253	213	145	94	79	67
62.5°	127	221	262	269	233	183	139	117	108	98	89	78	69	62	56	60	67	78	87	95	105	119	141	179	211	236	227	183	126	87	71	60

Figure 4.12: **Original intensity data table of HPSV luminaire in photopic**

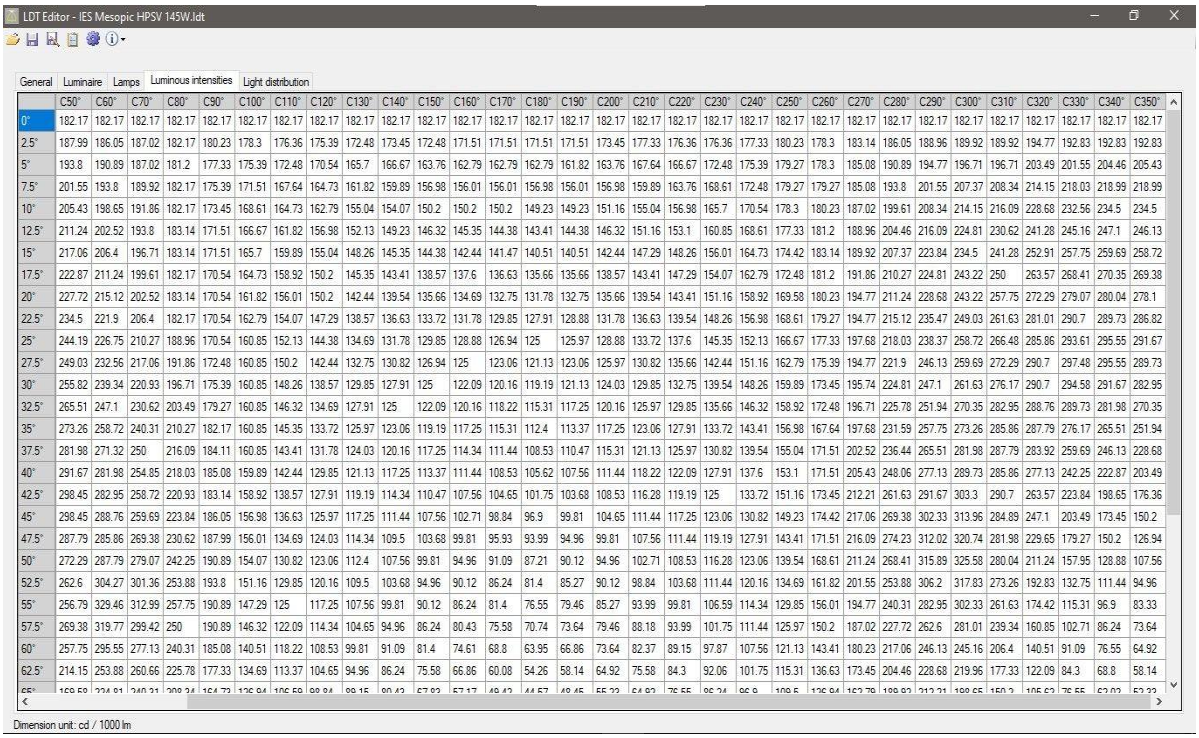

Figure 4.13: **Modified intensity data table of HPSV luminaire in mesopic region**

Table 4.5: **Modified Luminaires with Specification**

Name of Luminaire	Details of Fixture	Light Distribution Curve
PHILIPS SRP501/SONT150W, P1,LT,TOEIN 10 CLOSED, 'N' POT	Luminous flux (Luminaire): 9886 lm Luminous flux (Lamps): 14000 lm Luminaire Wattage: 170.0 W Luminaire classification according to CIE: 100 CIE flux code: 43 79 97 100 71 Fitting: 1 x SON(T)150W (Correction Factor 1.000).	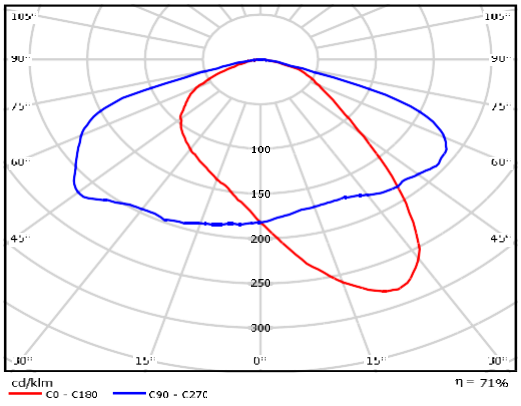

COOPER LIGHTING 175W STREETWORKS LUMINAIRE	Luminous flux (Luminaire): 9750 lm Luminous flux (Lamps): 14000 lm Luminaire Wattage: 175.0 W Luminaire classification according to CIE: 100 CIE flux code: 32 67 95 100 44 Fitting: 1 x 175 WATT MH CLEAR ED17 (Correction Factor 1.000).	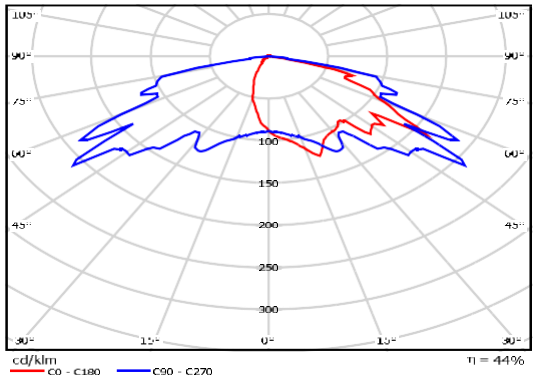
SILVERSUN STHP150NWS Street Light 150W 4000K	Luminous flux (Luminaire): 12650 lm Luminous flux (Lamps): 17442 lm Luminaire Wattage: 145.1 W Luminaire classification according to CIE: 100 CIE flux code: 42 81 98 100 100 Fitting: 0 x User defined (Correction Factor 1.000).	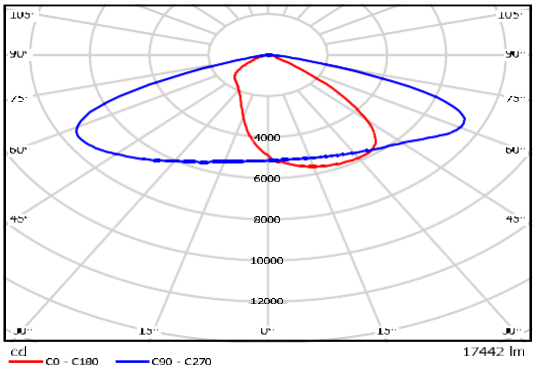

4.2.3 Lighting Design using modified HPSV luminaire

Design considerations:

- Luminaire used: PHILIPS SRP501/SONT150W,P1,LT,TOEIN 10 CLOSED, 'N' POT
- Area of the road width: 20m
- Number of lanes: 2
- Illuminance class: ME4a
- Luminaire arrangement: double row, opposing
- Luminaire mounting height: 9m
- Distance between two poles: 12m
- Boom length: 0.5m
- Boom angle: 25
- Overhang: 2m
- Distance pole to roadway: -1.5m
- Light loss factor: 0.67

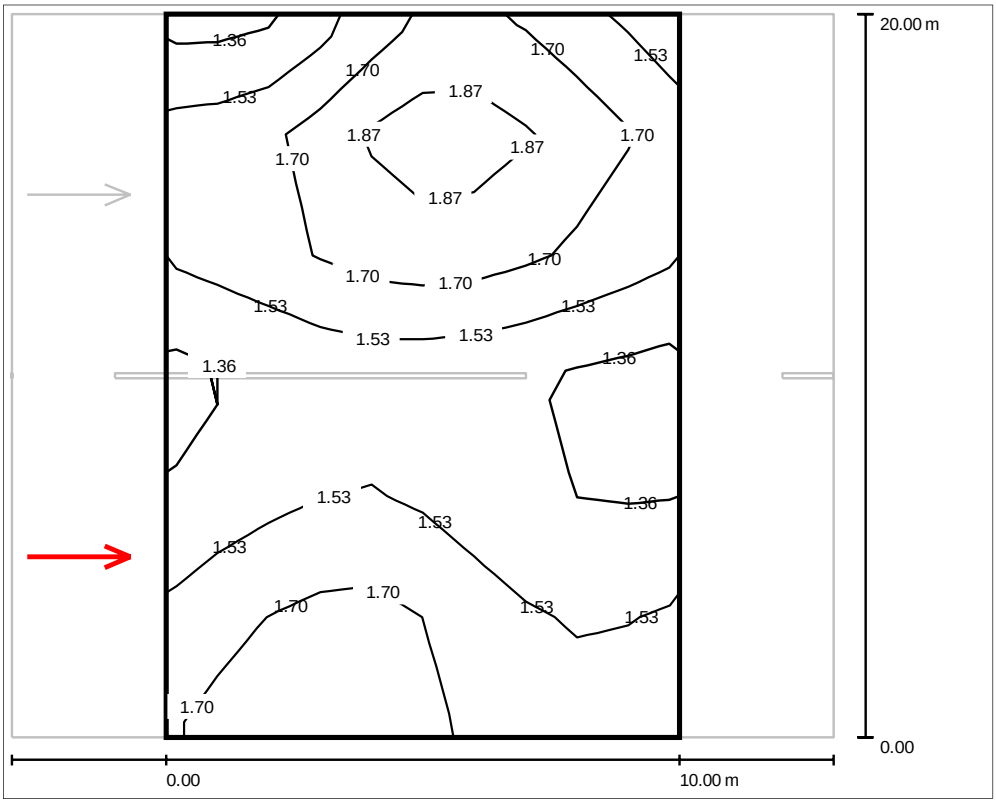

Figure 4.14: **Isoline diagram of modified HPSV for mesopic region**

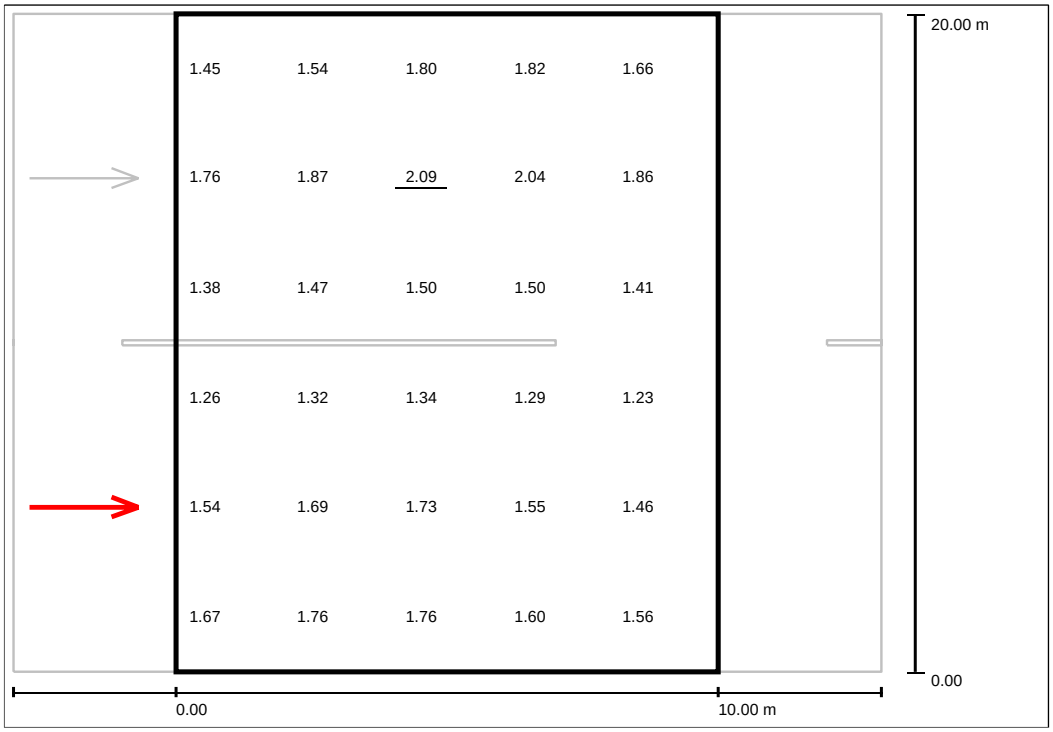

Figure 4.15: **Value chart of modified HPSV for mesopic region**

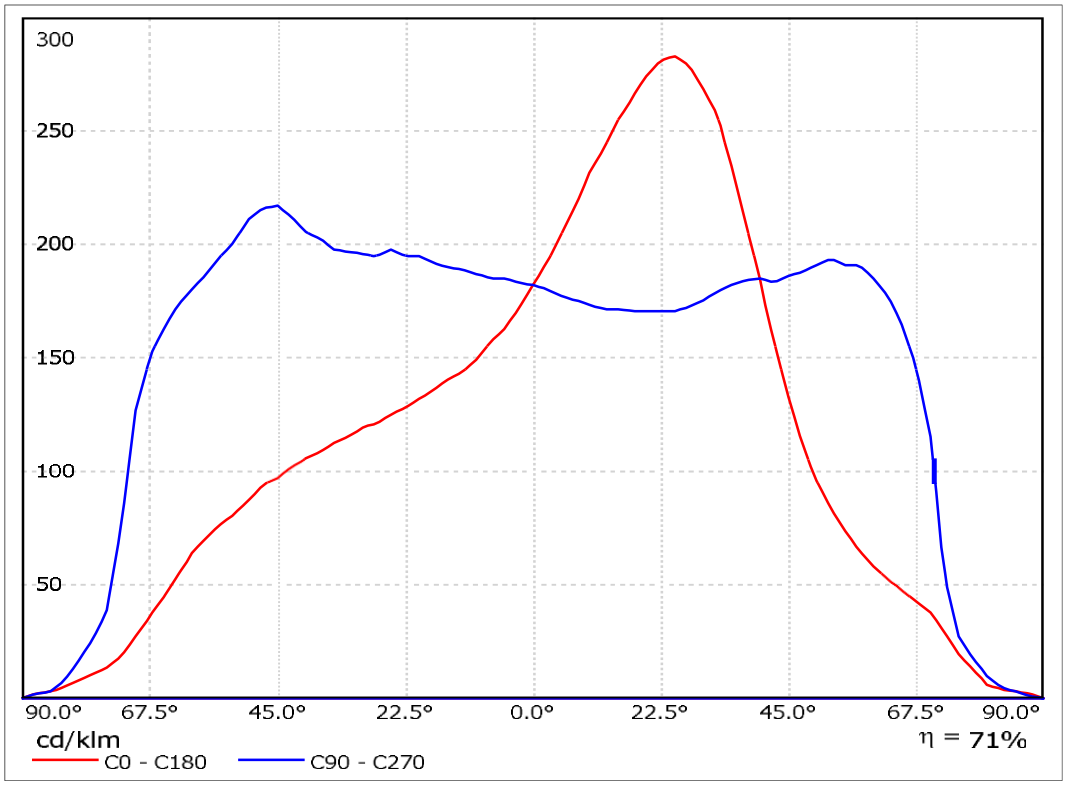

Figure 4.16: **LDC (linear) of modified HPSV for mesopic region**

4.2.4 Lighting Design using modified MH luminaire

Design Considerations:

- Luminaire used: COOPER LIGHTING 175W STREETWORKS LUMINAIRE
- Area of the road width: 20m
- Number of lanes: 2
- Illuminance class: ME4a
- Luminaire arrangement: double row, opposing
- Luminaire mounting height: 9m
- Distance between two poles: 12m
- Boom length: 0.5m
- Boom angle: 25
- Overhang: 2m
- Distance pole to roadway: -1.5m
- Light loss factor: 0.67

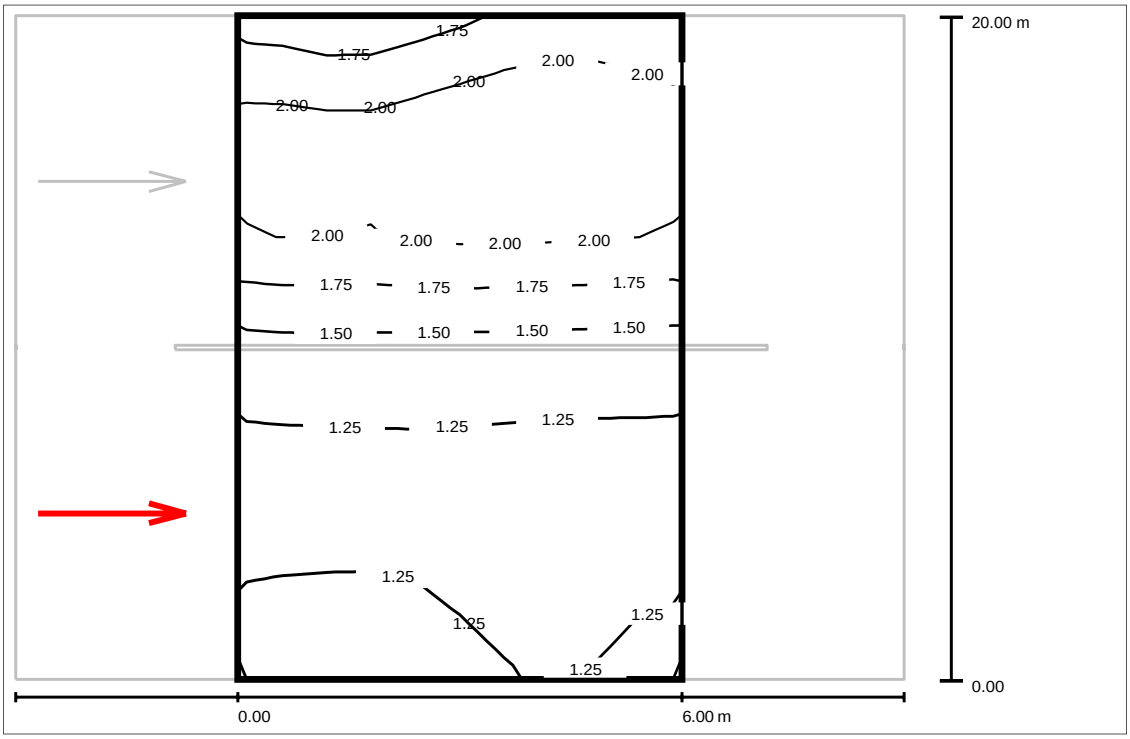

Figure 4.17: **Isoline diagram of modified MH luminaire in mesopic region**

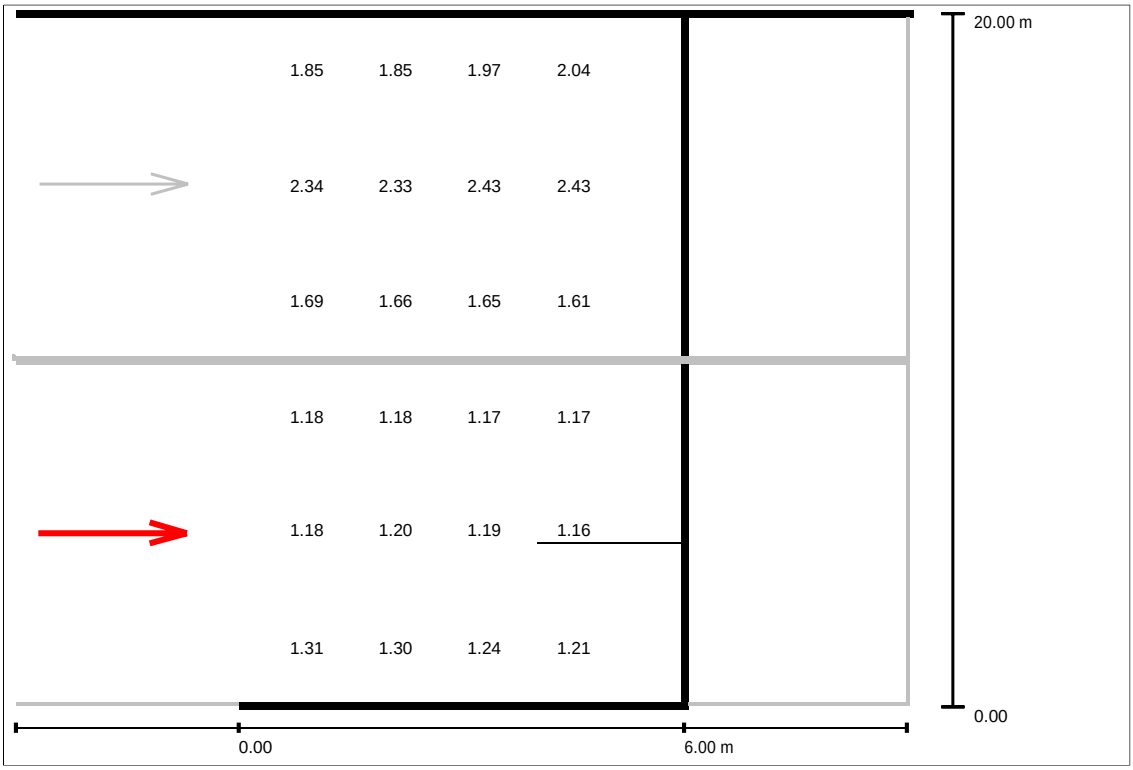

Figure 4.18: **Value chart of modified MH luminaire in mesopic region**

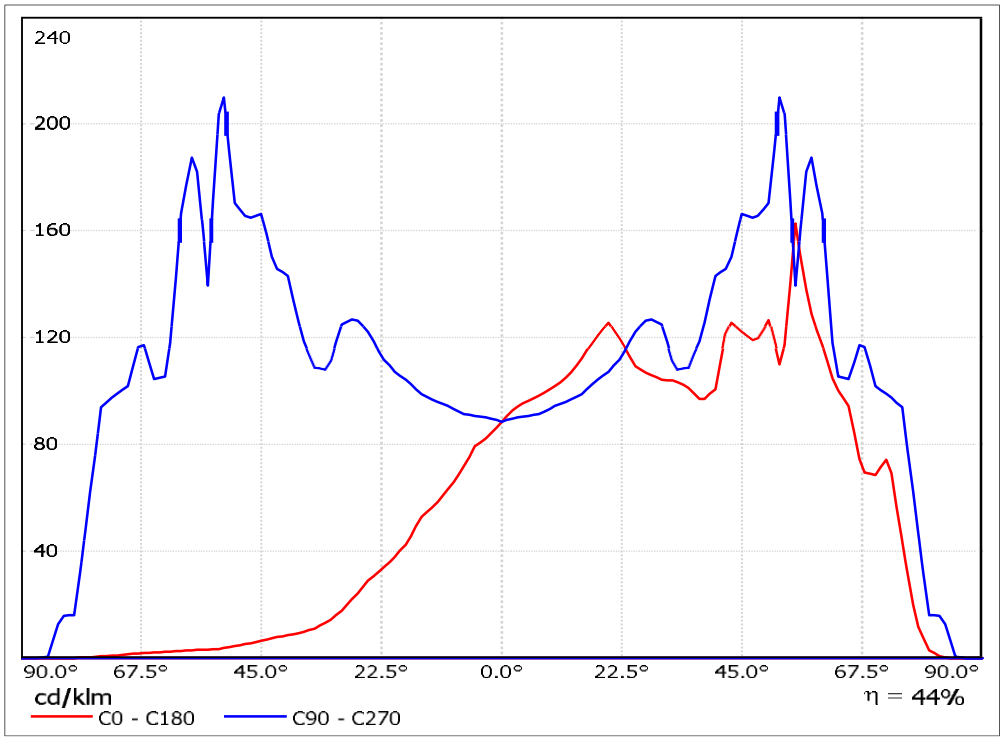

Figure 4.19: **LDC (linear) of modified MH luminaire in mesopic region**

4.2.5 Lighting Design using modified LED luminaire

Design Considerations:

- Luminaire used: SILVERSUN STHP150NWS Street Light 150W 4000K
- Area of the road width: 20m
- Number of lanes: 2
- Illuminance class: ME4a
- Luminaire arrangement: double row, opposing
- Luminaire mounting height: 9m
- Distance between two poles: 12m
- Boom length: 0.5m
- Boom angle: 25
- Overhang: 2m
- Distance pole to roadway: -1.5m
- Light loss factor: 0.67

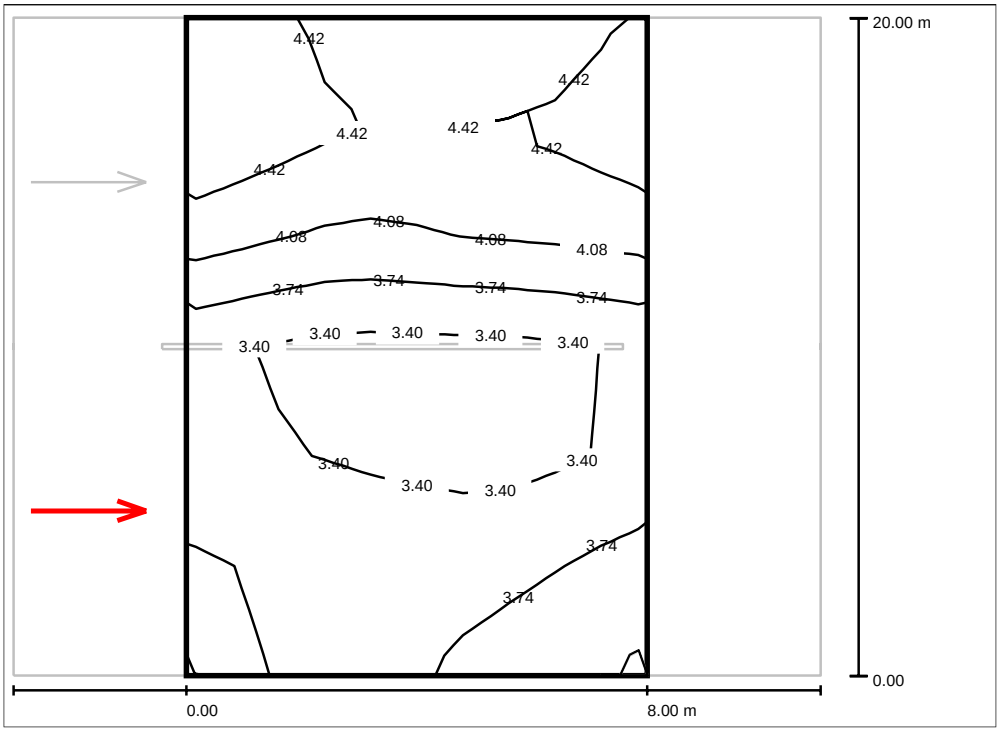

Figure 4.20: **Isoline diagram of modified LED luminaire in mesopic region**

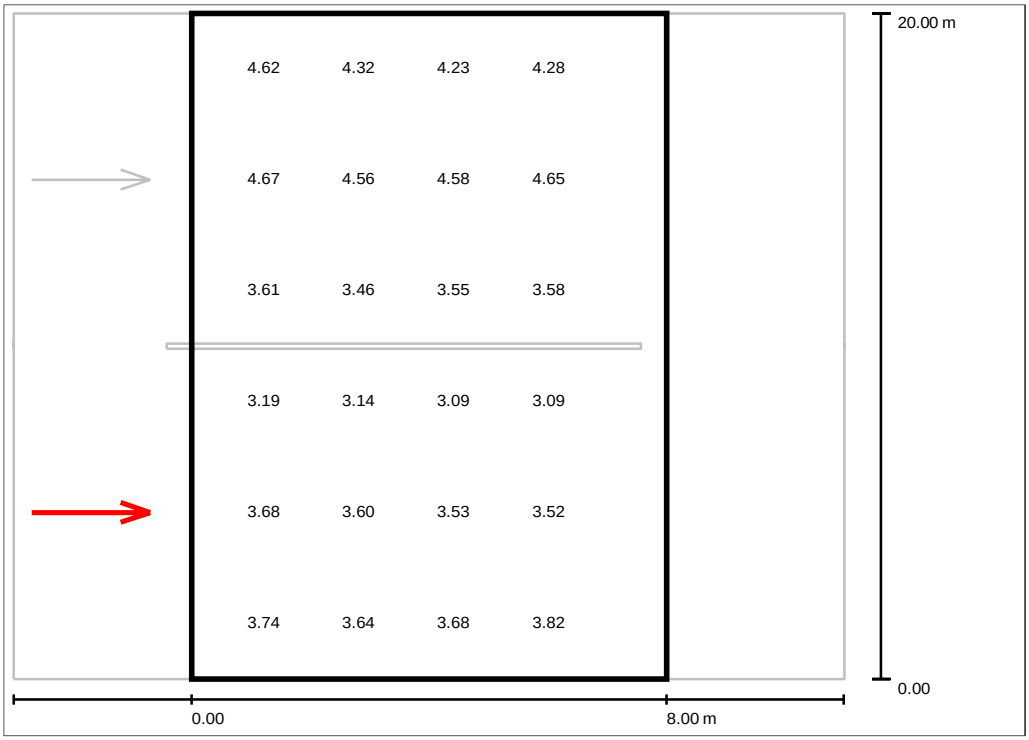

Figure 4.21: **Value chart of modified LED luminaire in mesopic region**

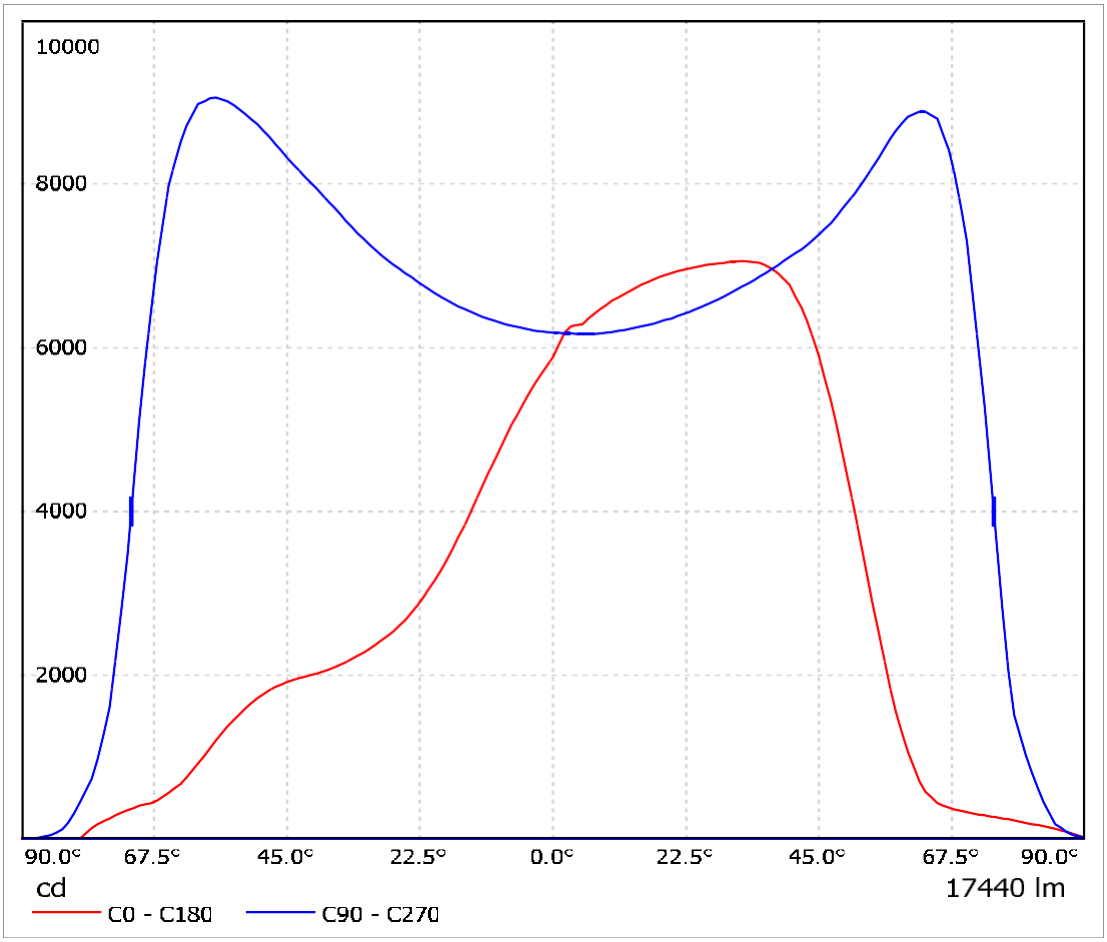

Figure 4.22: **LDC (linear) of modified LED luminaire in mesopic region**

4.2.6 An overview of the designs in Mesopic region

Table 4.6 provides a detailed summary of luminaires' performance in the mesopic region. It includes values for average mesopic luminance ($\mathbf{L_m}$) and overall uniformity ($\mathbf{U_o}$) for High-Pressure Sodium Vapor (HPSV), Metal Halide (MH), and Light Emitting Diode (LED) luminaires within road lighting applications. The table presents a comparative analysis of these luminaires, specifically evaluating their effectiveness and uniformity under mesopic conditions. Additionally, the table integrates data for both photopic and mesopic regions, offering a comprehensive overview of each light source's performance across different lighting conditions.

Table 4.6: **Design Summary for all the luminaires in photopic and mesopic region**

Luminaire	**Average photopic luminance L_{avg} (L_p)**	**Uniformity (U_o)**	**s/p ratio**	**Calculated mesopic luminance (L_m) using CIE 191:2010**	**Calculated m/p ratio (L_m/L_p)**	**Simulated mesopic luminance (L_{ms})**	**Uniformity (U_o)**
HPSV	2.44	0.70	0.62	2.39	0.979	2.40	0.70
MH	2.41	0.50	1.2	2.46	1.021	2.46	0.51
LED	4.24	0.57	1.8	4.27	1.007	4.27	0.58

4.3 Data analysis

In this study, the analysis of results involved a detailed comparison between photopic and mesopic luminance values for various types of luminaires. Initially, photopic luminance for a designated road area was simulated using different lamp types, including High-Pressure Sodium Vapor (HPSV), Metal Halide (MH), and Light Emitting Diodes (LED). The corresponding mesopic luminance values were then calculated based on the CIE 191:2010 standard, which provides a framework for adjusting photopic data to reflect mesopic conditions.

To further validate these calculations, mesopic luminance for the same road was simulated using methods previously outlined in this study. This dual approach facilitated a thorough comparison among three key metrics: simulated photopic luminance (**L_p**), calculated mesopic luminance (**L_m**), and simulated mesopic luminance (**L_{ms}**). The comparison of these metrics across different lamp types highlighted the performance variations of each lighting technology under both photopic and mesopic conditions.

The results revealed the differences in how each light source performs in real-world road lighting scenarios, particularly in settings where mesopic vision plays a significant role. This comprehensive analysis not only assessed the accuracy of simulation methods but also demonstrated the varying effectiveness of each lamp type in achieving optimal lighting conditions for road environments.

Comparison of Simulated photopic luminance (L_p), Calculated mesopic luminance (L_m) & Simulated mesopic luminance (L_{ms})

In context of High-Pressure Sodium Vapour (HPSV) luminaire

For designs employing High-Pressure Sodium Vapor (HPSV) luminaires, Table 4.7 presents the values for photopic luminance (**L_p**), calculated mesopic luminance (**L_m**), and simulated mesopic luminance (**L_{ms}**). Figure 4.23 illustrates that HPSV luminaires, characterized by a lower S/P ratio, exhibit a reduction in mesopic luminance (**L_m**) compared to photopic luminance (**L_p**) within the mesopic zone. This trend indicates a decrease in effective luminance in mesopic conditions relative to photopic conditions when using HPSV lamps.

Additionally, a minor discrepancy is observed between the calculated mesopic luminance (L_m) and the simulated mesopic luminance (**L_{ms}**). The uniformity of the photopic (**U_o,p**) and mesopic (**U_o,m**) regions is detailed in the same Table 4.7, while Figure 4.24 provides a visual comparison of uniformity between the simulated photopic and mesopic regions. This comparison highlights the variations in luminance performance and uniformity of HPSV luminaires under different lighting conditions.

Table 4.7: **Average luminance values & photopic, mesopic region uniformity of HPSV luminaire**

Main source	Simulated photopic luminance (**L_p**)	Calculated mesopic luminance (**L_m**)	Simulated mesopic luminance (**L_{ms}**)	Photopic region uniformity (**U_o,p**)	Mesopic region uniformity (**U_o,m**)
HPSV	2.44	2.39	2.40	0.70	0.70

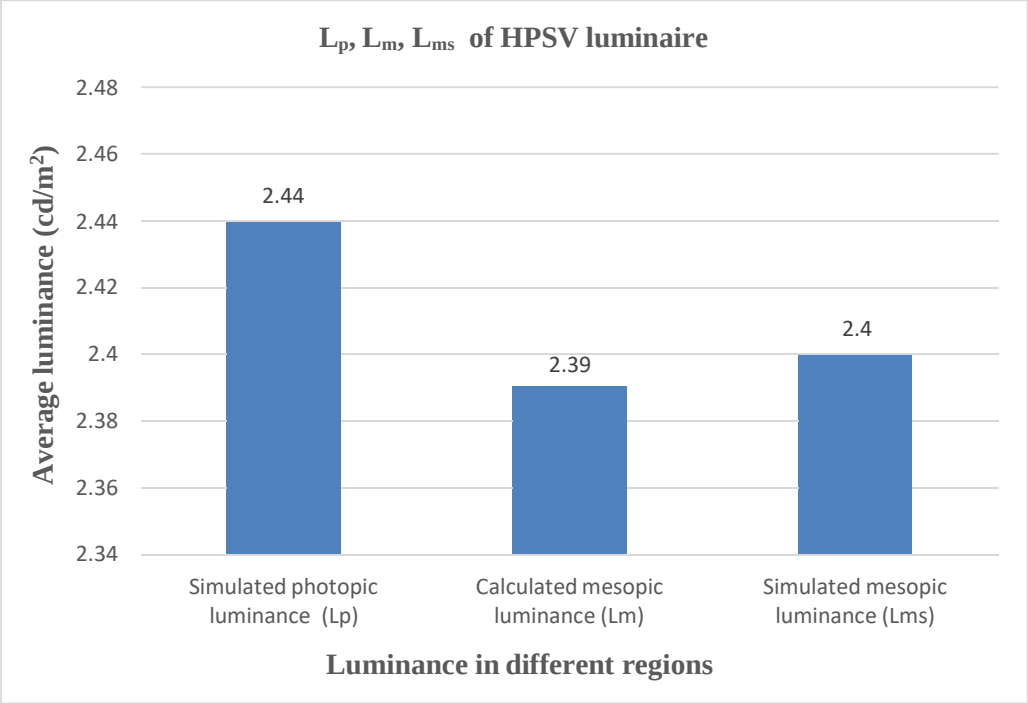

Figure 4.23: **Comparison of L_p, L_m, L_{ms} of HPSV luminaire**

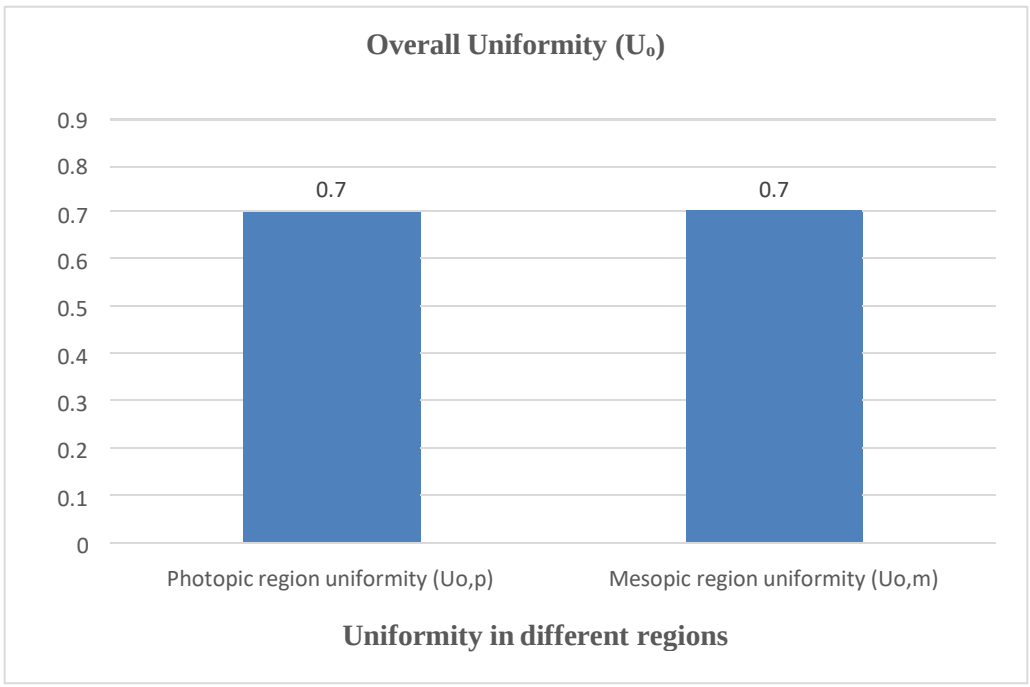

Figure 4.24: **Comparison of photopic and mesopic uniformity of HPSV luminaire**

In context of Metal Halide (MH) luminaire

For designs utilizing only Metal Halide (MH) luminaires, Table 4.8 presents the values for photopic luminance (**L_p**), calculated mesopic luminance (**L_m**), and simulated mesopic luminance (**L_{ms}**). As illustrated in Figure 4.25, MH lamps, which generally possess a higher S/P ratio compared to HPSV lamps, demonstrate **L_m** values that closely align with **L_p** values in the mesopic region. This alignment suggests that the effective luminance in mesopic vision is relatively well-preserved when using MH lamps, compared to their photopic luminance. Despite this, a slight discrepancy remains between the calculated mesopic luminance (**L_m**) and the simulated mesopic luminance (**L_{ms}**), indicating minor variations between theoretical calculations and simulation outcomes. The uniformity for both photopic (**U_o,p)** and mesopic (**U_o,m**) conditions is also detailed in Table 4.8, with Figure 4.26 illustrating the comparison of uniformity between the simulated photopic and mesopic regions. The findings suggest that MH luminaires provide more consistent lighting performance across both photopic and mesopic conditions, maintaining effective luminance and uniformity.

Table 4.8: **Average luminance values & photopic, mesopic region uniformity of MH luminaire**

Main source	Simulated photopic luminance (**L_p**)	Calculated mesopic luminance (**L_m**)	Simulated mesopic luminance (**L_{ms}**)	Photopic region uniformity (**U_o,p**)	Mesopic region uniformity (**U_o,m**)
MH	2.41	2.46	2.46	0.50	0.51

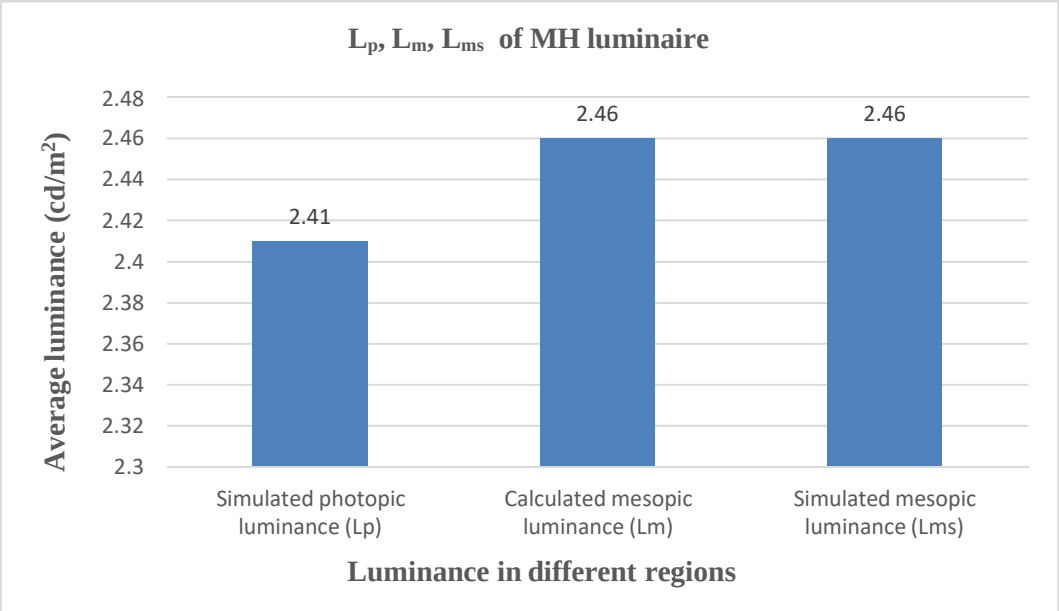

Figure 4.25: **Comparison of L_p, L_m, L_{ms} of MH luminaire**

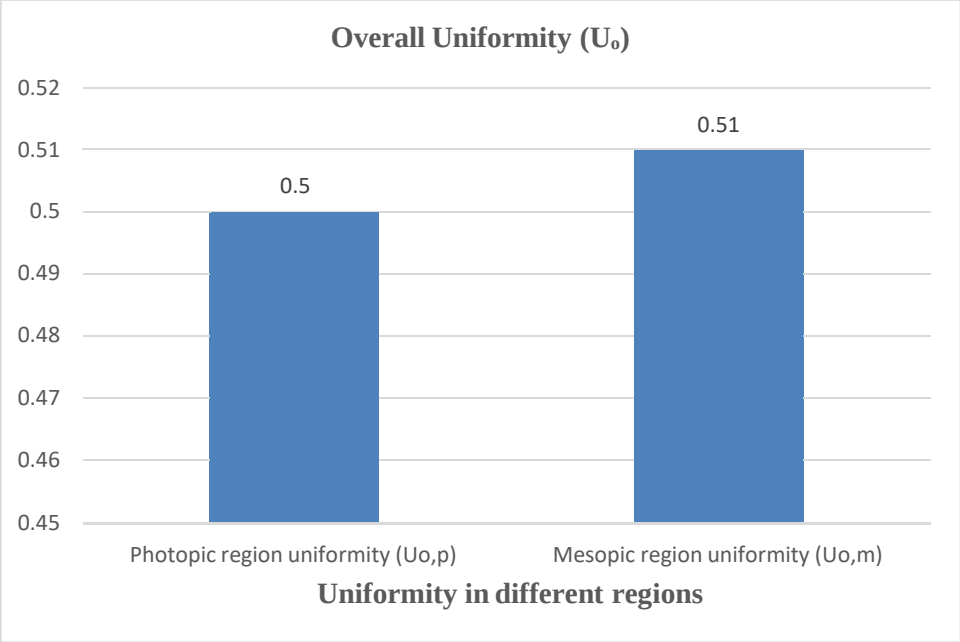

Figure 4.26: **Comparison of photopic and mesopic uniformity of MH luminaire**

In context of Light Emitting Diode (LED) luminaire

For designs utilizing only LED luminaires, the values for photopic luminance ($\mathbf{L_p}$), calculated mesopic luminance ($\mathbf{L_m}$), and simulated mesopic luminance ($\mathbf{L_{ms}}$) are detailed in Table 4.9. As shown in Figure 4.27, LED lamps, which are characterized by a high S/P ratio, exhibit $\mathbf{L_m}$ values that are nearly equivalent to $\mathbf{L_p}$ values in the mesopic region. This close alignment indicates that LED luminaires effectively maintain luminance in mesopic vision almost as well as in photopic conditions, making them particularly suitable for environments with varying lighting requirements. The slight discrepancy between the calculated mesopic luminance ($\mathbf{L_m}$) and the simulated mesopic luminance ($\mathbf{L_{ms}}$) is minimal, underscoring the accuracy and reliability of LED lighting in both simulation and real-world scenarios. The uniformity for both photopic ($\mathbf{U_o,p}$) and mesopic ($\mathbf{U_o,m}$) regions is also presented in Table 4.9, with Figure 4.28 illustrating the comparison between uniformity in simulated photopic and mesopic regions. The findings confirm that LED luminaires deliver consistent and uniform lighting performance across different visual conditions, which is advantageous for both energy efficiency and visual clarity in road lighting designs.

Table 4.9: **Average luminance values & photopic, mesopic region uniformity of LED luminaire**

Main source	Simulated photopic luminance (L_p)	Calculated mesopic luminance (L_m)	Simulated mesopic luminance (L_{ms})	Photopic region uniformity (U_o,p)	Mesopic region uniformity (U_o,m)
LED	4.24	4.27	4.28	0.56	0.58

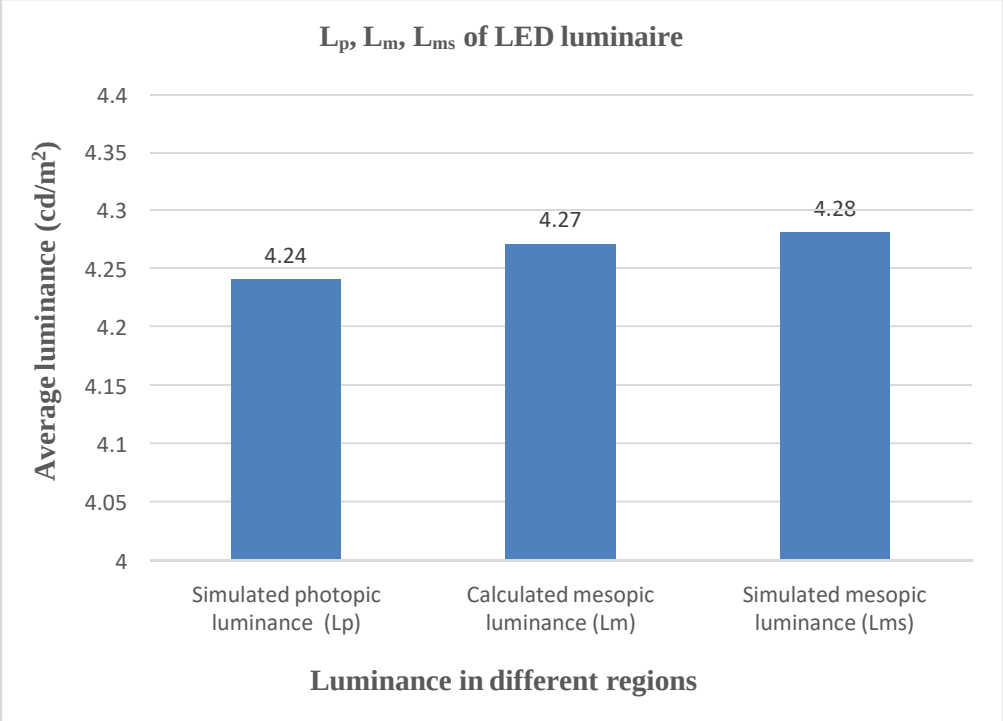

Figure 4.27: **Comparison of L_p, L_m, L_{ms} of MH luminaire**

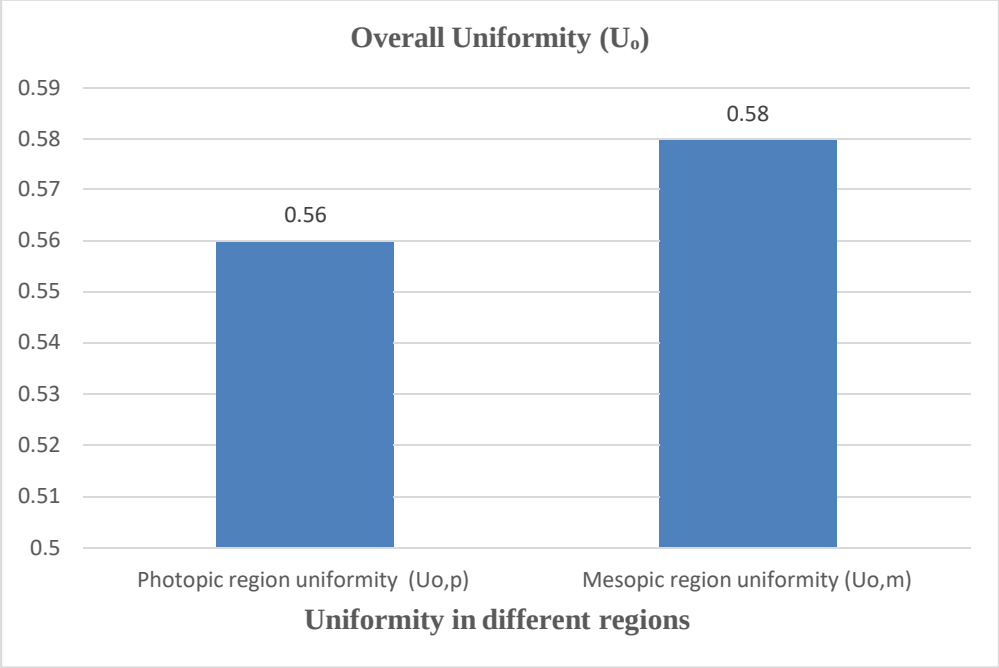

Figure 4.28: **Comparison of photopic and mesopic uniformity of LED luminaire**

Comparison of average luminance for all luminaires altogether

Table 4.10 presents a comprehensive comparison of simulated photopic luminance ($\mathbf{L_p}$), calculated mesopic luminance ($\mathbf{L_m}$), and simulated mesopic luminance ($\mathbf{L_{ms}}$) for HPSV, Metal Halide (MH), and LED lamps. As illustrated in Figure 4.29, High-Pressure Sodium Vapor (HPSV) lamps, which possess a lower S/P ratio, exhibit mesopic luminance values that are lower than their corresponding photopic luminance values. This reduction in luminance under mesopic conditions results in a dimmer environment, which may require higher wattage lamps to maintain adequate brightness for road lighting.

In contrast, Metal Halide (MH) and LED lamps, both of which have higher S/P ratios, display mesopic luminance values that exceed their photopic counterparts. This indicates that MH and LED lamps are more energy-efficient for outdoor lighting, as they provide greater perceived brightness in mesopic conditions while consuming less power. In figure 4.30 the overall uniformity of all luminaires is noted. Among the luminaires compared, LED lamps stand out as the most effective option, not only due to their higher mesopic luminance relative to photopic luminance but also because of their ability to enhance overall uniformity in road lighting. This makes LEDs the superior choice over HPSV and MH lamps, particularly in terms of efficiency and performance in mesopic lighting conditions.

Table 4.10: **Average luminance values of HPSV, MH, LED luminaires**

Main source	Simulated photopic luminance (L_p)	Calculated mesopic luminance (L_m)	Simulated mesopic luminance (L_{ms})
HPSV	2.44	2.39	2.40
MH	2.41	2.46	2.46
LED	4.24	4.27	4.28

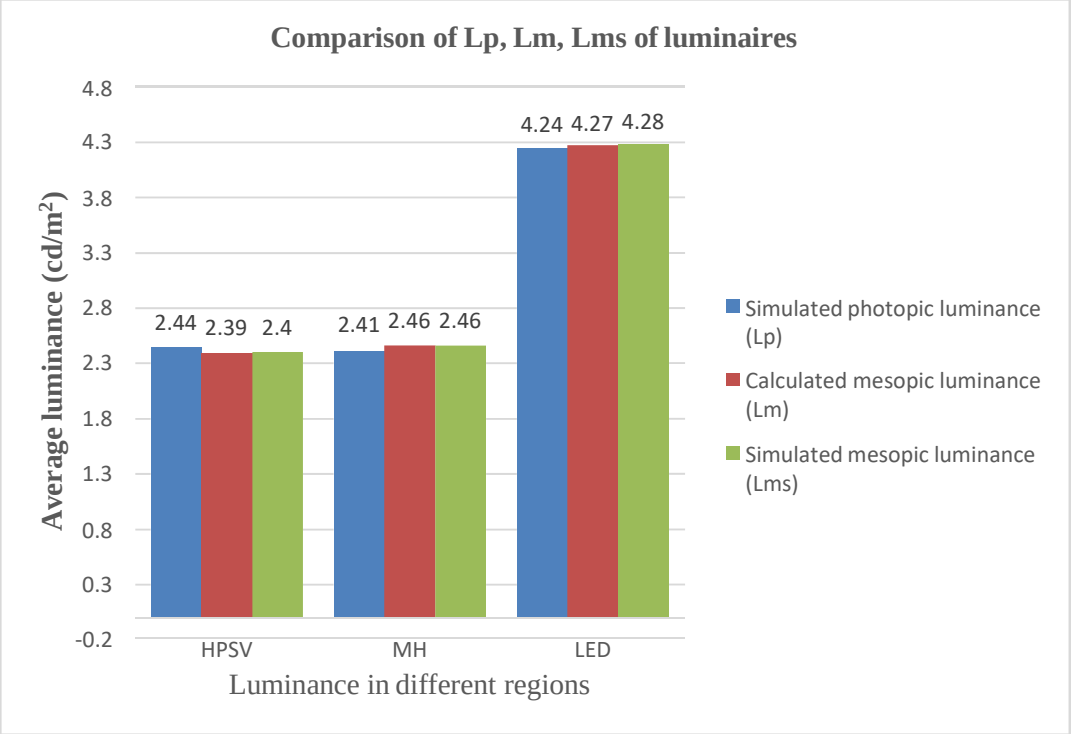

Figure 4.29: **Comparison of L_p, L_m, L_{ms} for HPSV, MH, LED luminaires**

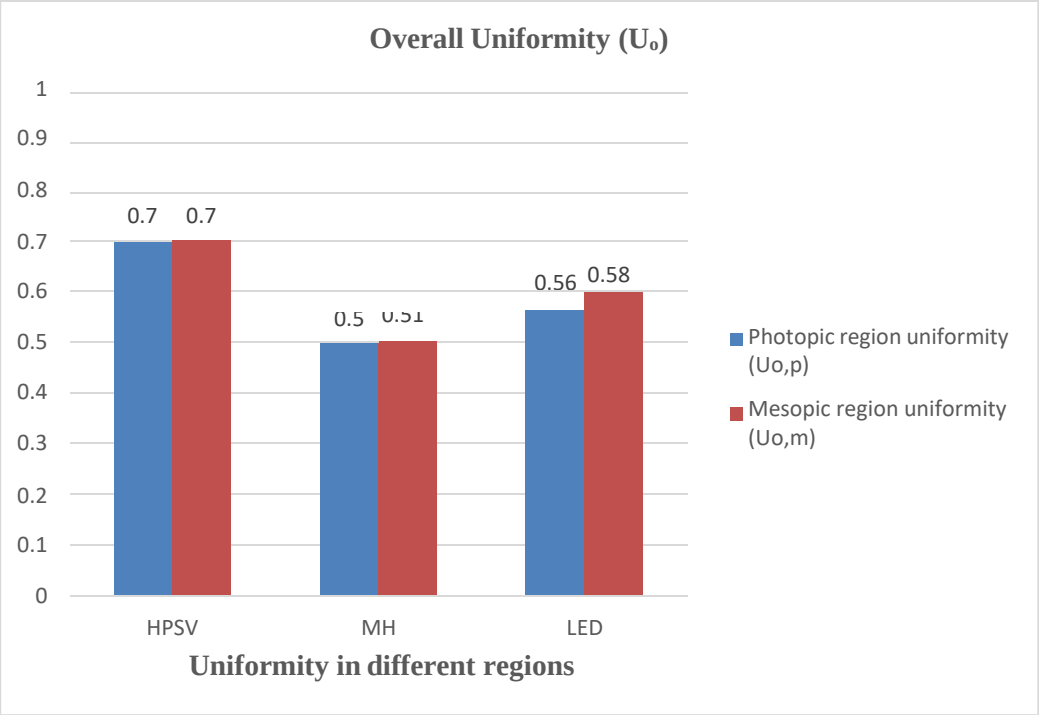

Figure 4.30: **Comparison of overall uniformity for HPSV, MH, LED luminaires**

Luminous flux comparison

In the context of road lighting scenarios, Table 4.11 presents the luminous flux (luminaire) data for HPSV, Metal Halide (MH), and LED luminaires, highlighting the differences between photopic and mesopic regions. The comparison reveals that designing lighting systems based on mesopic conditions can lead to reduced electrical consumption. Specifically, the findings show that mesopic design considerations are more energy-efficient, as the luminous flux required for sufficient illumination is lower in the mesopic region. Accurately determining luminous flux values under mesopic conditions necessitates calculating key parameters such as the maintenance factor (MF), utilization factor (UF), and total area. These factors ensure that the lighting design is optimized for both energy efficiency and effective illumination under mesopic vision.

Figures 4.31, 4.32, and 4.33 illustrate the differences in luminous flux between photopic and mesopic conditions for HPSV, MH, and LED luminaires, respectively. The analysis indicates that in mesopic conditions, HPSV luminaires require more power due to their higher luminous flux, as they are less efficient under photopic conditions. In contrast, MH and LED luminaires show a decrease in luminous flux in mesopic conditions, leading to lower power consumption while emitting more effective light compared to HPSV. This trend highlights the superior energy efficiency of MH and LED luminaires in mesopic settings. Figure 4.34 provides a comparative graph of the luminous flux for all three luminaires, demonstrating that lighting designs based on

mesopic conditions result in reduced power consumption, making them more energy-efficient, particularly when using MH and LED luminaires.

Table 4.11: **Comparison of luminous flux between photopic and mesopic conditions**

Light source	Luminous flux in Photopic region (lm)	Luminous flux in Mesopic region (lm)
HPSV	10202	9886
MH	9527	9750
LED	12000	12650

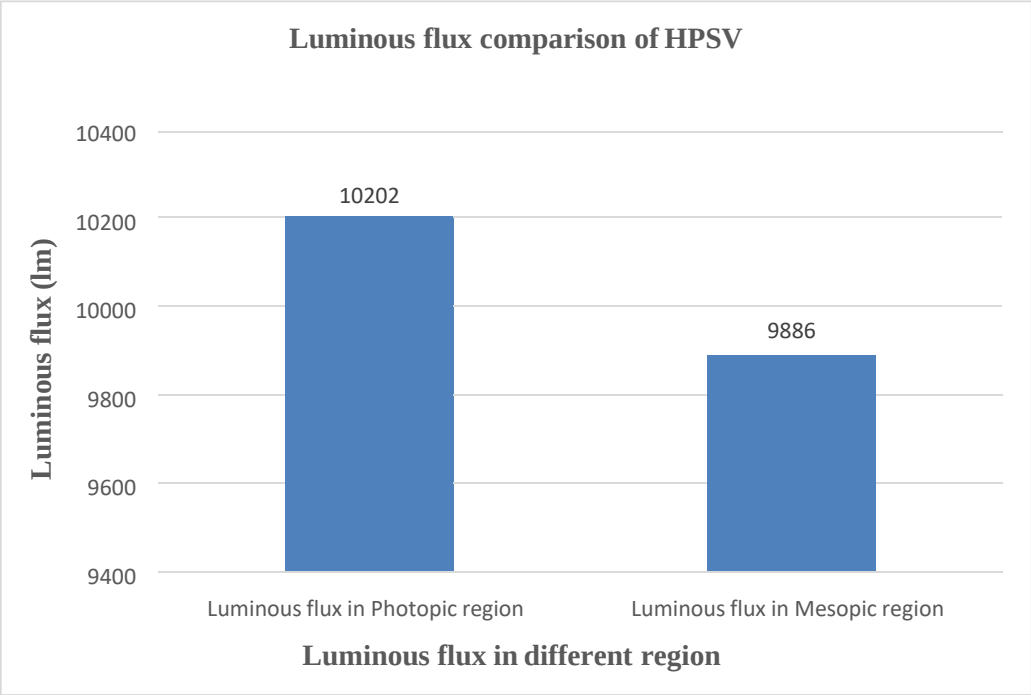

Figure 4.31: **Luminous flux comparison of HPSV luminaire**

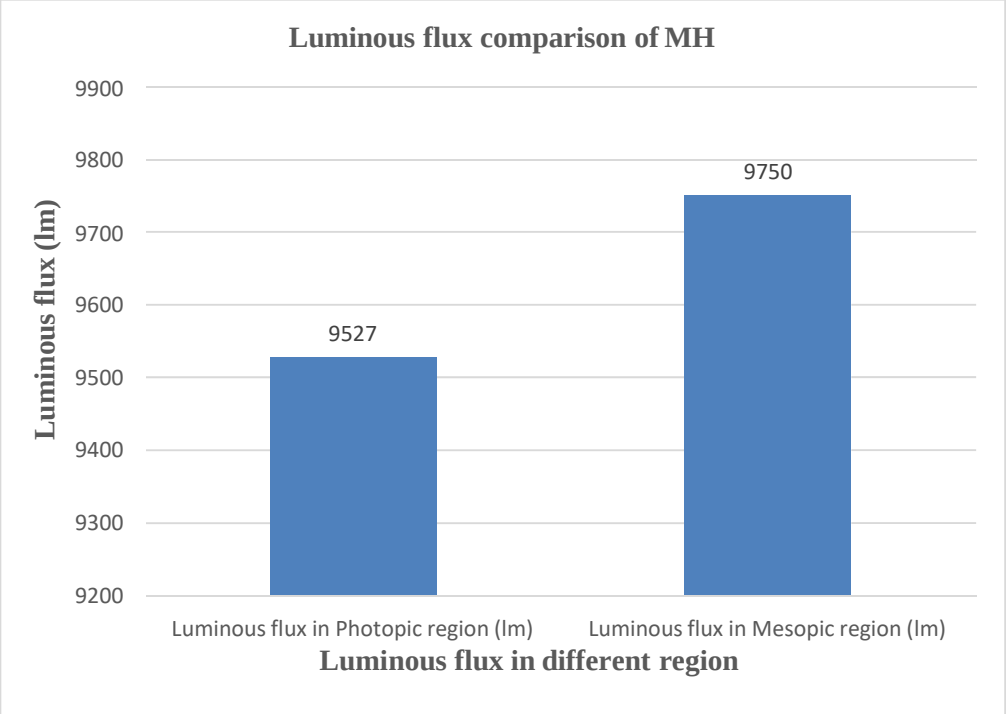

Figure 4.32: **Luminous flux comparison of MH luminaire**

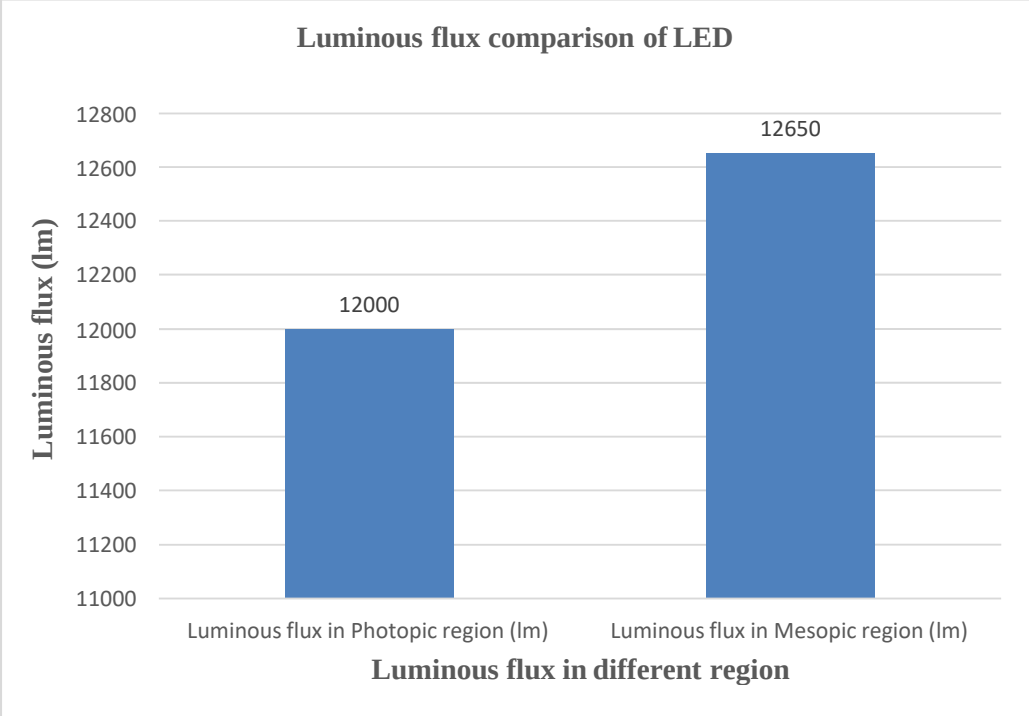

Figure 4.33: **Luminous flux comparison of LED luminaire**

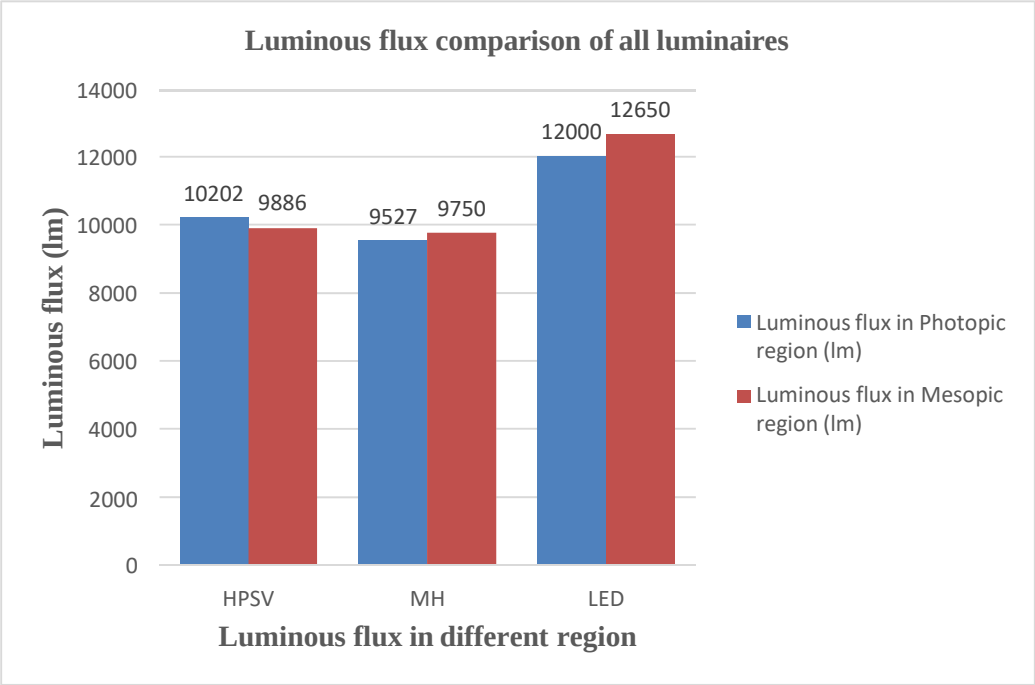

Figure 4.34: **Luminous flux comparison of HPSV, MH, LED luminaires**

Luminous efficacy

In the context of road lighting, Table 4.12 provides the luminous efficacy data for HPSV, Metal Halide (MH), and LED luminaires. Luminous efficacy, expressed in lumens per watt (lm/W), measures the efficiency with which a light source converts electrical power into visible light. A higher luminous efficacy indicates that a light source produces more light per unit of power consumed, signifying greater efficiency. The formula used to calculate luminous efficacy is: Luminous efficacy (lm/W) = Total Light Output (lm)/Total Power Consumption (W)

Luminous efficacy is a critical factor in energy efficiency for road lighting applications. Light sources with higher efficacy not only produce lighter while consuming less energy but also contribute to significant reductions in energy consumption and lower electricity costs. This is particularly important in large-scale road lighting projects where energy savings can be substantial. In lighting design, understanding and selecting luminaires with high luminous efficacy ensures optimal performance and energy efficiency. Among the luminaires studied, LED lamps typically exhibit the highest luminous efficacy, making them the most efficient choice for road lighting. This efficiency not only reduces energy consumption but also supports environmental sustainability by lowering overall energy demand and reducing carbon emissions, aligning with sustainability.

Table 4.12: **Luminous efficacy of different luminaires**

Light source	Rated power (W)	Efficacy in photopic region (lm/w)	Efficacy in mesopic region (lm/w)
HPSV	170	60.01	58.15
MH	175	54.44	55.71
LED	145	82.76	87.24

Comparative Analysis of Luminous Efficacy

High-Pressure Sodium Vapor (HPSV)

HPSV lamps, operating at 170 watts, have traditionally been used in street lighting due to their relatively high efficacy compared to older technologies. In the photopic region, HPSV lamps exhibit a luminous efficacy of 60.01 lm/W, which decreases slightly to 58.15 lm/W in the mesopic region. Despite their historical use and moderate efficiency, HPSV lamps are increasingly overshadowed by more advanced lighting technologies, particularly LEDs, due to their lower energy efficiency and limited color rendering capabilities. In figure 4.35 noted the comparison between luminous efficacy of HPSV luminaire.

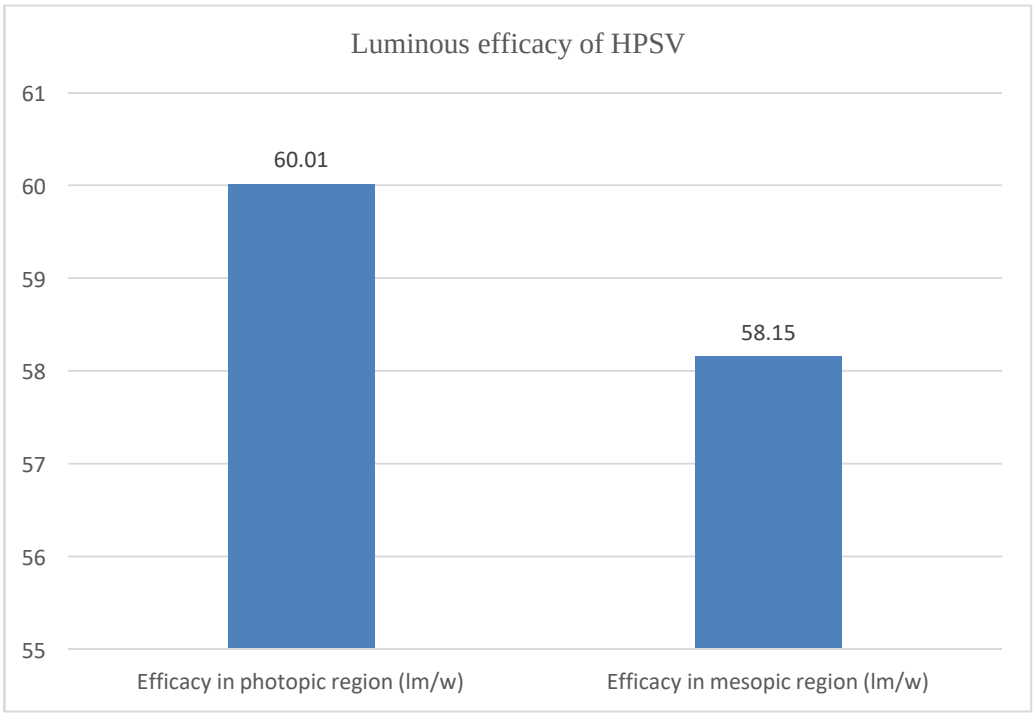

Figure 4.35: **Luminous efficacy of HPSV luminaire**

Metal Halide (MH)

MH lamps, rated at 175 watts, are commonly deployed in areas requiring intense lighting, such as roadways and large commercial spaces. The luminous efficacy of MH lamps is 54.44 lm/W in the photopic region and 55.71 lm/W in the mesopic region. While MH lamps are somewhat more efficient than HPSV lamps, their higher energy consumption for the same level of illumination, shorter lifespan, and higher maintenance costs reduce their desirability in energy-conscious road lighting designs. In figure 4.36 noted the comparison between luminous efficacy of MH luminaire.

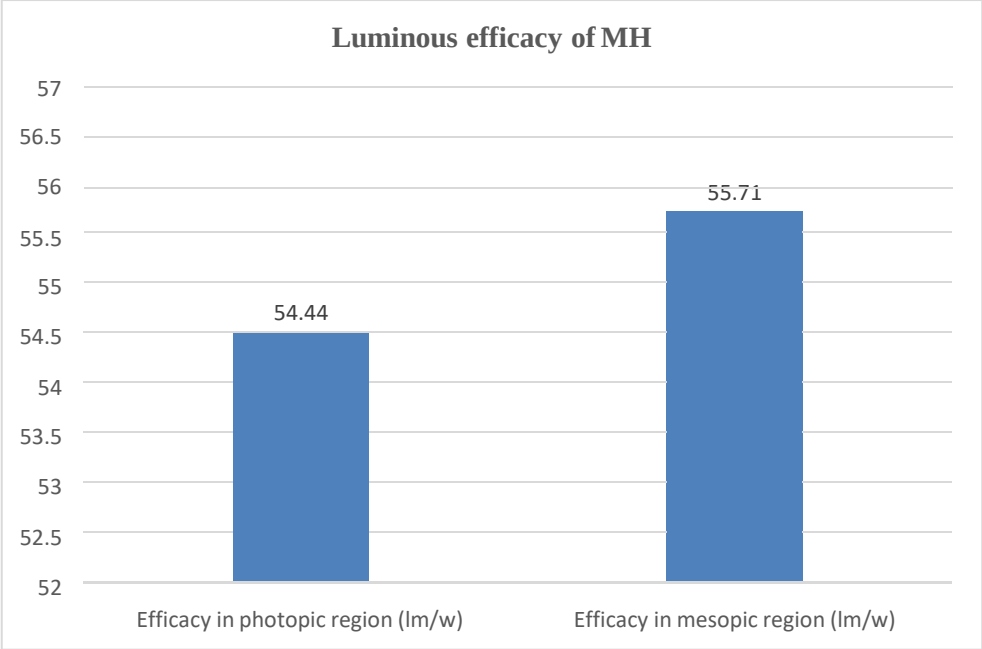

Figure 4.36: **Luminous efficacy of MH luminaire**

Light-Emitting Diode (LED)

LEDs, with a rated power of 145 watts, represent the most efficient lighting technology in this analysis. LEDs exhibit luminous efficacy values of 120.29 lm/W in the photopic region and 121.72 lm/W in the mesopic region, significantly outperforming both HPSV and MH lamps. This superior efficacy underscores the energy efficiency of LEDs, which produce more light per watt consumed, leading to substantial energy savings and reduced environmental impact. Additionally, LEDs offer advantages such as a longer lifespan, lower maintenance costs, and superior color rendering, making them the most suitable choice for modern road lighting applications. In figure 4.37 noted the comparison between luminous efficacy of LED luminaire.

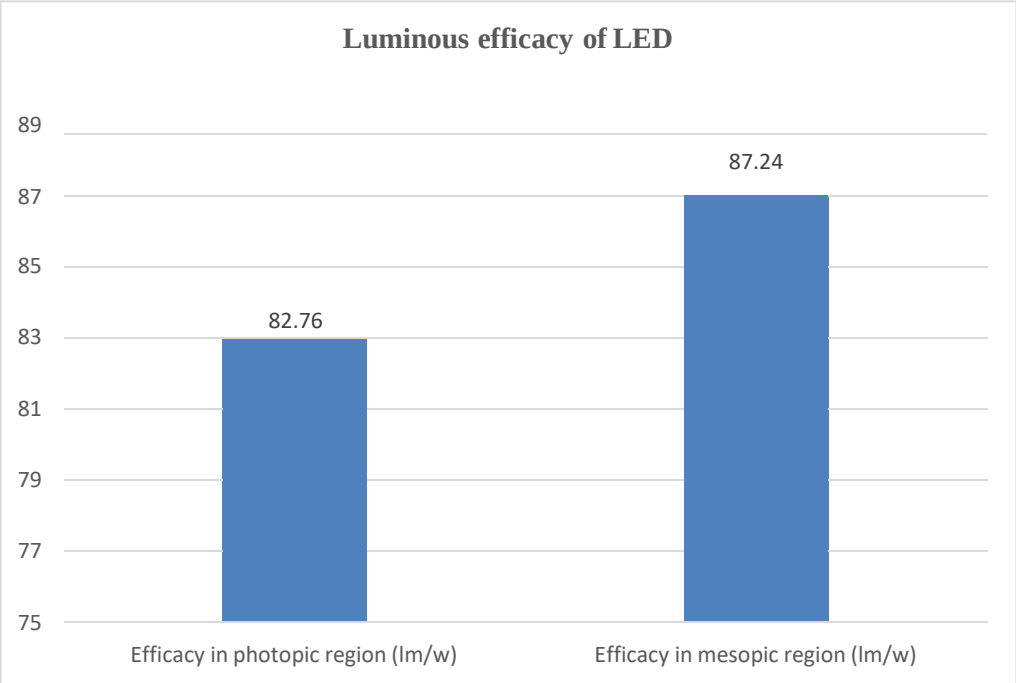

Figure 4.37: **Luminous efficacy of LED luminaire**

The comparative analysis clearly demonstrates that LEDs are the most efficient and environmentally friendly option among the three luminaire types. While HPSV and MH lamps provide moderate efficacy, their performance is eclipsed by the advanced technology and higher luminous efficacy of LEDs. This analysis highlights the importance of selecting luminaires with high luminous efficacy in road lighting design to maximize energy efficiency and support sustainability goals. As lighting technology evolves, the adoption of LEDs will play a crucial role in reducing energy consumption and enhancing the quality of road lighting.

Optical Efficiency comparison

Optical Efficiency quantifies how effectively a luminaire's optical system distributes the light it receives from the light source. It is calculated by dividing the effective luminous output by the total luminous output and expressing the result as a percentage. This metric helps assess how well a luminaire converts the light emitted by the lamp into usable illumination, highlighting the effectiveness of its optical design. Here in the table 4.13 narrates optical efficiency of all luminaires that are commonly used in street lighting scenarios.

Optical Efficiency (%) = (Luminous Flux (input) / Luminous Flux (output)) × 100

Here, Luminous Flux (output) is the amount of light emitted by the luminaire that reaches the desired area and the Luminous Flux (input) is the total amount of light generated by the light source inside the luminaire.

Table 4.13: **Optical efficiency of different luminaires**

Light source	Rated power (W)	Optical efficiency in photopic region (%)	Optical efficiency in mesopic region (%)
HPSV	170	72.87	70.61
MH	175	68.05	69.64
LED	145	68.79	72.53

High-Pressure Sodium Vapor (HPSV)

HPSV luminaires generally exhibit moderate optical efficiency due to their diffuse light output, which is challenging to control effectively. The design of the luminaire, including components like reflectors and diffusers, often results in light being absorbed or scattered, reducing the amount that reaches the intended area. In road lighting designs, the optical efficiency of HPSV lamps is 72.87% in the photopic region and decreases to 70.61% in the mesopic region, indicating a slight reduction in efficiency under mesopic conditions. This reduction in optical efficiency highlights the need for larger or more complex luminaire designs to optimize light distribution, though this can lead to additional light losses.

Metal Halide (MH)

Metal Halide lamps typically offer better optical efficiency compared to HPSV lamps, with a more focused and whiter light output that allows for more effective light direction to the target area. Despite this, some losses still occur due to the complexity of their optical systems. In road lighting designs, MH lamps show an optical efficiency of 68.05% in the photopic region, increasing to 69.64% in the mesopic region, indicating improved efficiency under mesopic conditions. This enhanced optical efficiency, combined with better color rendering and light control, makes MH lamps suitable for applications requiring precise lighting, such as sports arenas or large commercial spaces.

Light-Emitting Diode (LED)

LED luminaires are known for their high optical efficiency, as they emit light in a specific direction, reducing the need for reflectors and diffusers. This directional light output allows LED lamps to direct nearly all the produced light to the desired area with minimal losses. In road lighting designs, LEDs exhibit an optical efficiency of 68.79% in the photopic region, which increases to 72.53% in the mesopic region, demonstrating their superior performance in varying lighting conditions. This high optical efficiency of LEDs leads to significant energy savings, improved lighting performance, and reduced operational costs, making them the most effective choice for road lighting applications where precise light distribution is critical.

High optical efficiency is crucial in lighting systems, particularly in road lighting, as it ensures that a greater portion of the light produced by the lamp is directed to its intended purpose, minimizing energy waste and enhancing overall performance. Luminaires with high optical efficiency reduce energy consumption by requiring less power to achieve the desired illumination levels, thereby enhancing the uniformity and effectiveness of lighting, which is vital for safety and visibility. Additionally, high optical efficiency contributes to better overall system efficiency, leading to lower operational costs. Conversely, luminaires with low optical efficiency waste lighter within the luminaire, necessitating more power to achieve the same level of illumination. This results in less uniform and effective lighting, potentially compromising safety and visibility while increasing both energy consumption and operational costs.

CHAPTER 5: DESIGN AND DEVELOPMENT OF LOW WATTAGE TUNABLE LED LUMINAIRE

5.1 : Prototype LED luminaire

This chapter presents a prototype LED luminaire designed to operate with a dimming controller circuit, enabling precise brightness adjustments according to user needs. The luminaire features both cool and warm white LED arrays, providing the flexibility to select the desired color temperature based on personal preference and specific lighting requirements. Figure 5.1 illustrates the proposed LED luminaire, while Figures 5.2, 5.3 and 5.4 show the configurations of full bright LED when turned on, the cool and warm white LED arrays, respectively. The integration of both cool and warm white LEDs aims to create an energy-efficient lighting solution that offers users the ability to manually adjust the color temperature, accommodating a variety of lighting scenarios. The subsequent chapter will delve into the operation of the dimming controller circuit in conjunction with this prototype LED luminaire, detailing how it facilitates these brightness and color temperature adjustments. The details of the controllable LED dimming circuit, which plays a key role in achieving these outcomes, will be discussed in the following chapter.

The prototype LED luminaire described in this chapter incorporates both cool and warm white LED arrays. Specifically, it utilizes two arrays of cool white LEDs and two arrays of warm white LEDs, arranged sequentially. This configuration allows for controllable color tuning, enabling the selection of either cool or warm white light based on user preference. Designed to operate at a low wattage, the luminaire achieves an output of 4800 lumens. The LED arrays in this prototype are intentionally constructed with lower output, focusing on the ability to precisely control both the color temperature and brightness. The controllable circuit that facilitates these adjustments will be detailed in the next chapter.

A significant advantage of this tunable LED luminaire is its ability to transition between photopic and mesopic regions. By utilizing a rotating encoder, the luminaire's dimming can be precisely controlled to achieve the desired mesopic luminance level. This feature is particularly beneficial for outdoor lighting applications, such as road lighting, where accurate luminance is crucial for both visibility and energy efficiency. In road lighting scenarios, the prototype LED luminaire offers dual benefits: it allows users to select either cool or warm lighting conditions, and it contributes to energy savings by enabling dimming based on calculated mesopic luminance. This capability not only reduces electrical costs but also ensures that the lighting provided meets the specific luminance requirements for enhanced visibility under mesopic conditions.

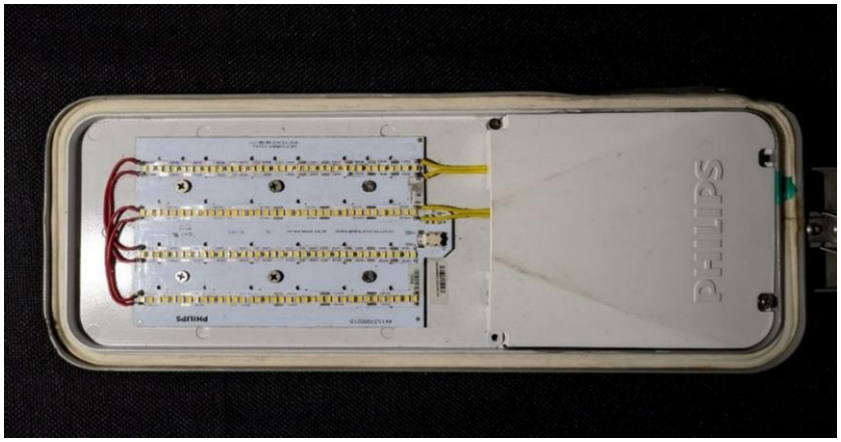

Figure 5.1: **Proposed prototype LED**

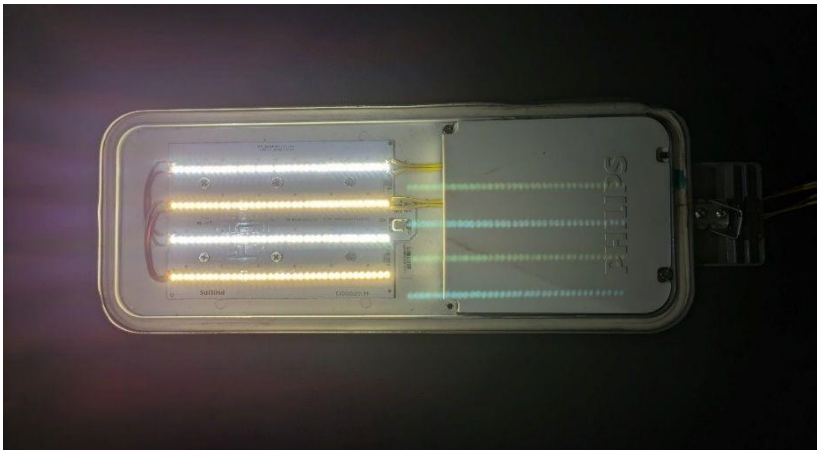

Figure 5.2: **Prototype LED luminaire when it is on**

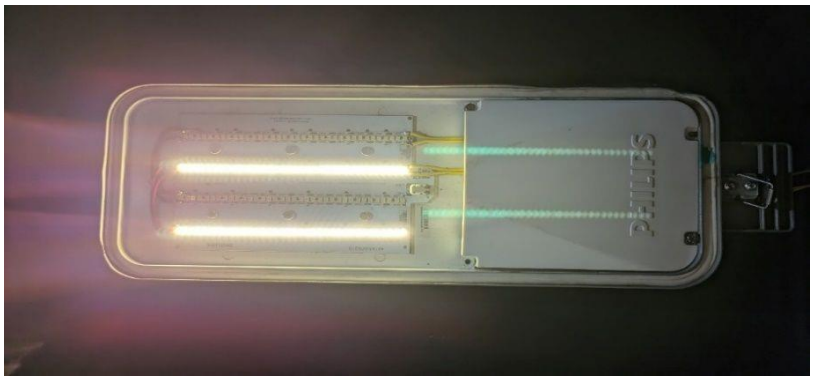

Figure 5.3: **Prototype LED luminaire when Cool white array is on**

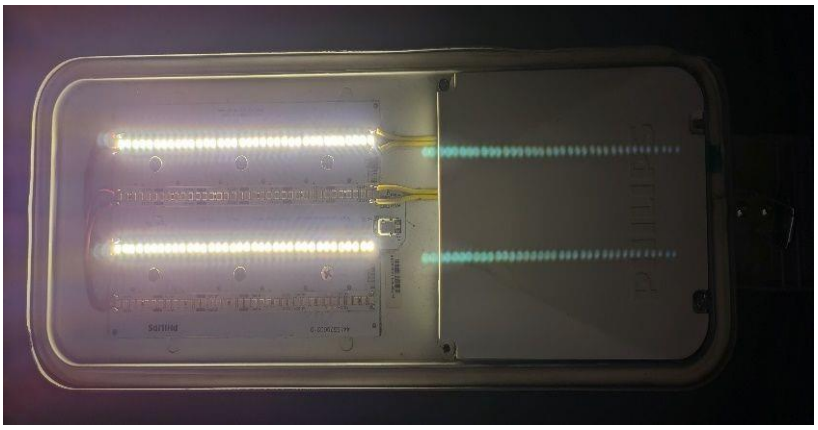

Figure 5.4: **Prototype LED luminaire when Warm white array is on**

5.2 Instrument used for measurement

This section details the instruments and procedures used to measure key parameters of the proposed luminaire, including the S/P ratio, correlated color temperature (CCT), color rendering index (CRI), wavelength, and color purity of both the cool and warm white LED arrays, individually and in combination. Additionally, the current-to-voltage ratio is measured in relation to the dimming levels to verify the performance of the proposed luminaire.

- **Scotopic/Photopic Meter:** Scotopic/Photopic Ratio for the particular source was measured (s/p = 1.7) using Scotopic/Photopic Meter of "SOLAR Light", Sl. No. 3101 as shown in figure 5.5. This meter has two sensors equipped with CIE V(λ) and V'(λ) sensitivity functions respectively. It evaluates and shows scotopic and photopic illuminance as seen by the sensor. The S/P ratio of a source can be obtained by dividing the measured scotopic illuminance with photopic illuminance.
  Range: Photopic Detector (PMA 2130):0 to 150000lux
  Scotopic Detector (PMA 2131): 0 to 150000lux

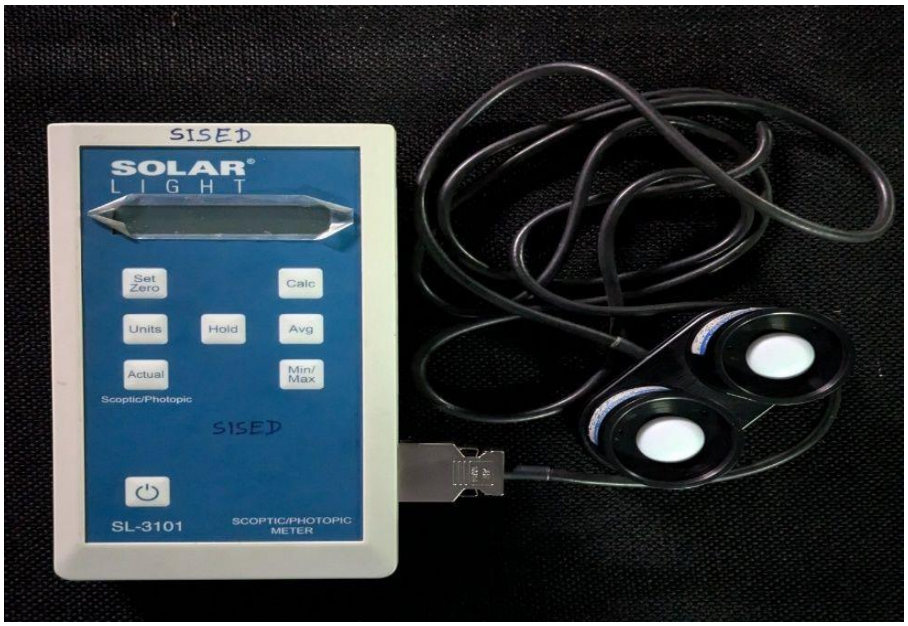

Figure 5.5: **Scotopic/photopic meter**

- **Chromameter**: For measurements of CCT of the lamps, a Chromameter of "Konica Minolta" Make, Model: CL70F was used as shown in figure
  Range: 0.1 to 99990lux,
  2000K to 10000K

Figure 5.6: **CL70F Chromameter**

- **Programmable AC/DC power source**: Variation in input voltage affects the luminous output of a lamp. To maintain a constant voltage throughout the experimental procedure, a programmable AC/DC power supply was used. The line voltage was first fed to this machine and from there was fed to the luminaire under the experiment.
  Range: AC I/P :750VA (100 to 180V), 1000VA (180 to 250V)
  DC I/P: 750VA (100 to 180V), 1000VA (180 to 250V)
  AC O/P Voltage: 0 to 155Vrms(100V), 0 to 310 V_{rms} (200V)
  DC O/P Voltage: - 220V to +220V(100V), - 440V to +440V(200V)
  AC O/P Current: 10A(100V), 5A(200V)
  DC O/P Current: 10A(100V), 5A(200V)
  Frequency: 1Hz to 550Hz

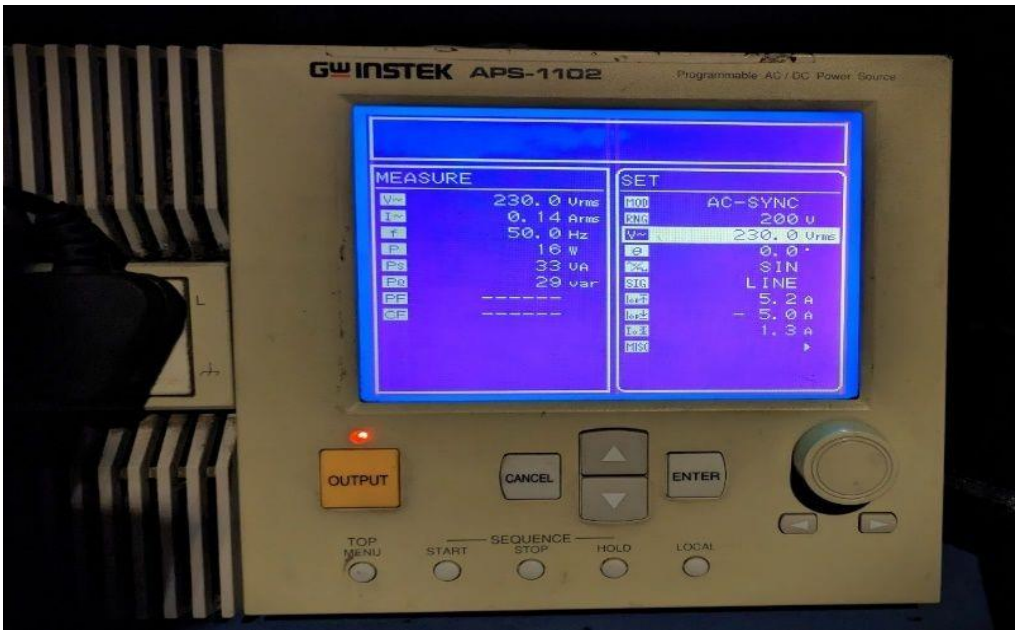

Figure 5.7: **Programmable AC/DC power source**

- **SMPS (Single Mode Power Supply):** A Switched-Mode Power Supply (SMPS) is an efficient power supply that uses a switching regulator to convert voltage levels with minimal energy loss. It operates at high frequencies, making it compact and versatile, and is commonly used in applications like computers, LED lighting, and industrial equipment. In this setup, an SMPS is used to supply power to the LED arrays. It operates with an input voltage range of 100-240V at 50/60Hz and provides an output of 12V at 5A.

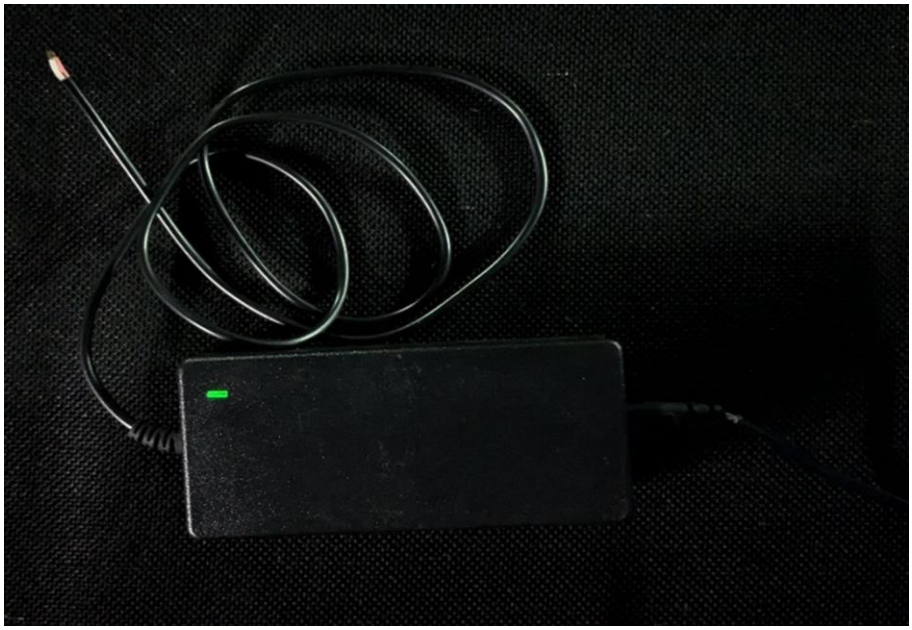

Figure 5.8: **Single Mode Power Supply**

5.3 Detailed of cool white LED array at 100% duty cycle

The data has been taken by chromameter CL70F, when the cool white LED array is in full glow. The detailed data is shown in table downwards.

Table 5.1: **Data obtained for cool white LED array**

Duty Cycle (%)	Illuminance (lx)	CCT (K)	Voltage (V)	Current (I)	Power (W)	Peak Wavelength [nm]	Dominant Wavelength [nm]	Purity [%]
100	218	4102	230	0.1	10.5	449	578	25.67

Table 5.2: **Tristimulus values of cool white LED array**

Tristimulus Value X	Tristimulus Value Y	Tristimulus Value Z	CIE1931 x	CIE1931 y	CIE1931 z	CIE1976 u'	CIE1976 v'
218.3571	217.8385	143.856	0.3764	0.3756	0.248	0.223	0.5005

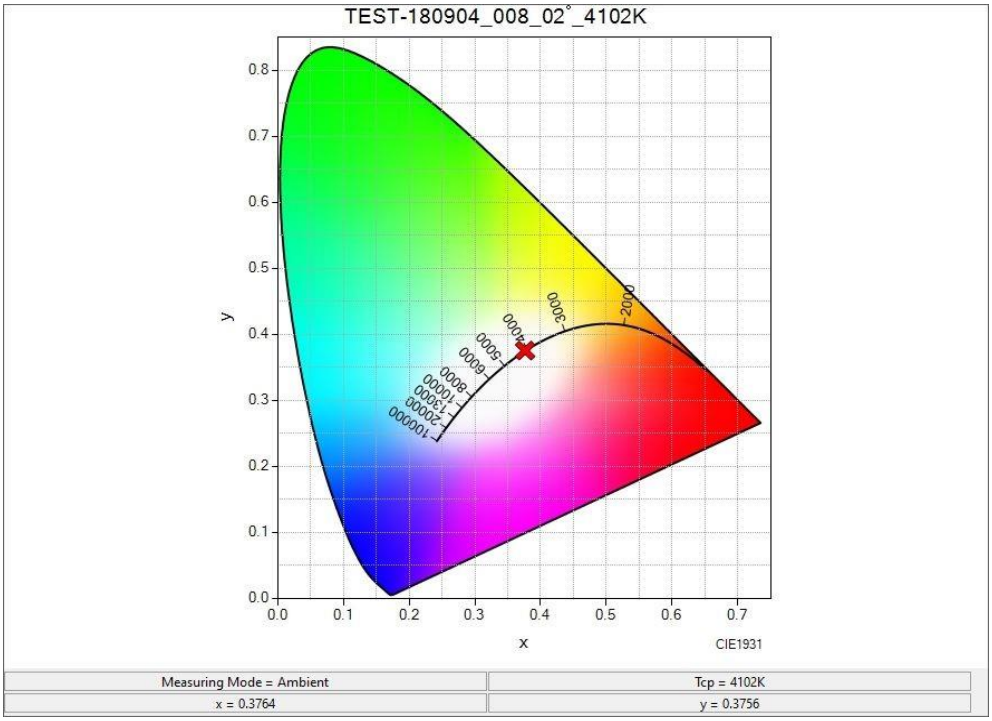

Figure 5.9: **CIE 1931 chromaticity coordinate**

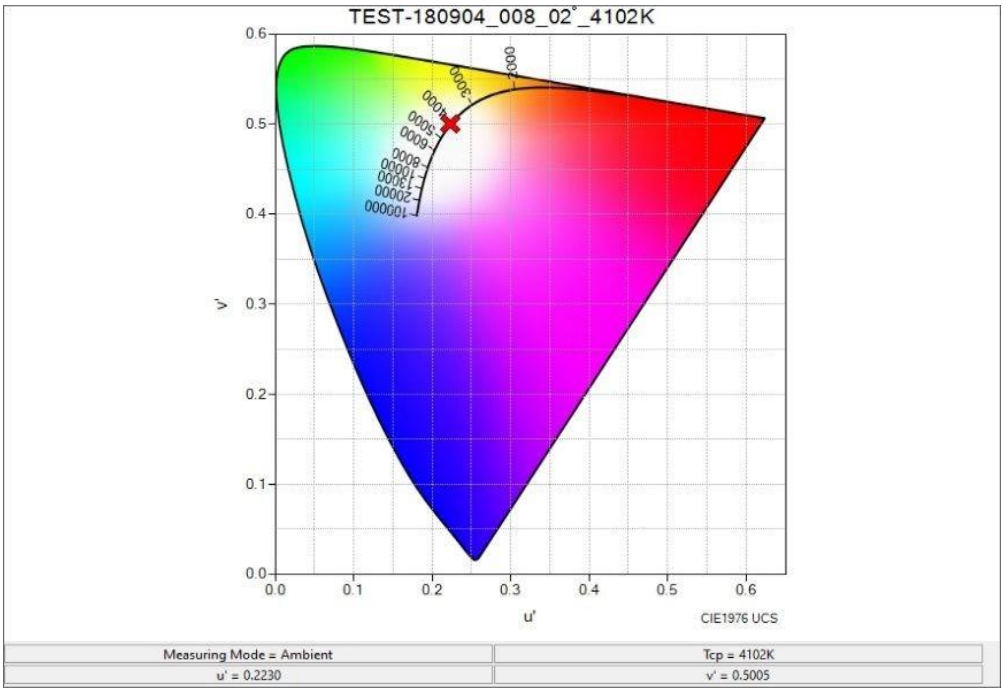

Figure 5.10: **CIE 1976 uniform chromaticity coordinate**

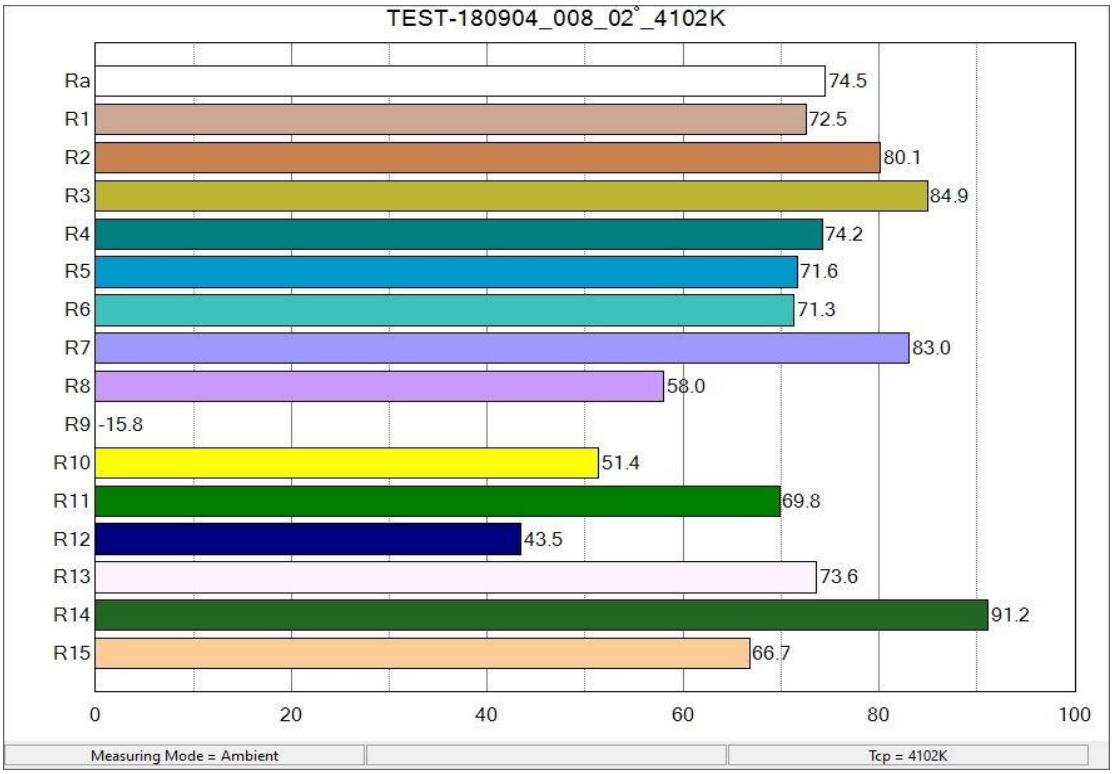

Figure 5.11: **Color Rending Index (CRI)**

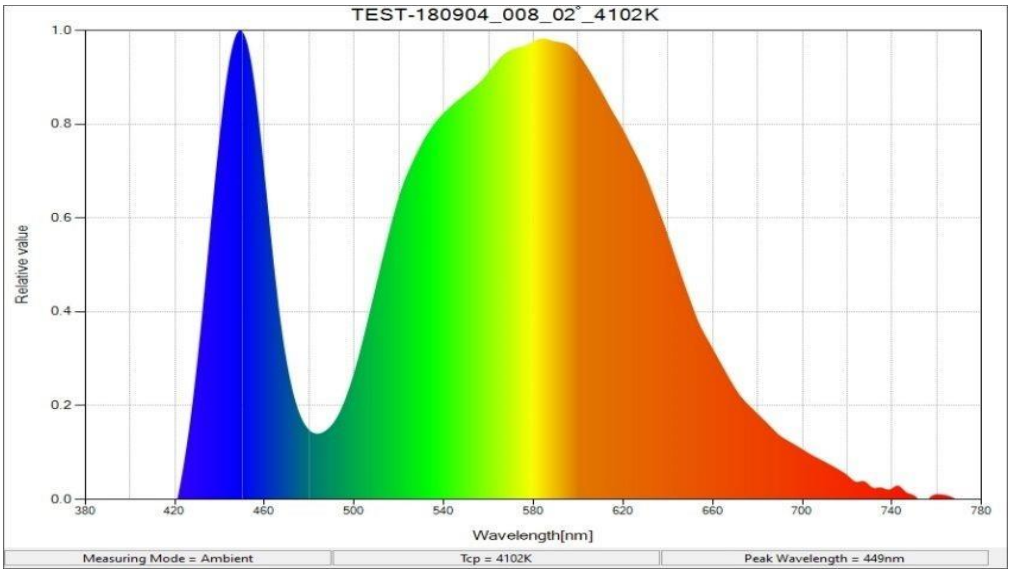

Figure 5.12: **Spectral power Distribution**

5.4 Detailed of warm white LED array at 100% duty cycle

The data has been taken by chromameter CL70F, when the warm white LED array is in full glow. The detailed data is shown in table downwards.

Table 5.3: **Data obtained for warm white LED array**

Duty Cycle (%)	Illuminance (lx)	CCT (K)	Voltage (V)	Current (I)	Power (W)	Peak Wavelength [nm]	Dominant Wavelength [nm]	Purity [%]
100	159	2700	230	0.09	9	598	582	75.39

Table 5.4: **Tristimulus values of warm white LED array**

Tristimulus Value X	Tristimulus Value Y	Tristimulus Value Z	CIE1931 x	CIE1931 y	CIE1931 z	CIE1976 u'	CIE1976 v'
171.9055	158.9471	29.8253	0.4766	0.4407	0.0827	0.2599	0.5407

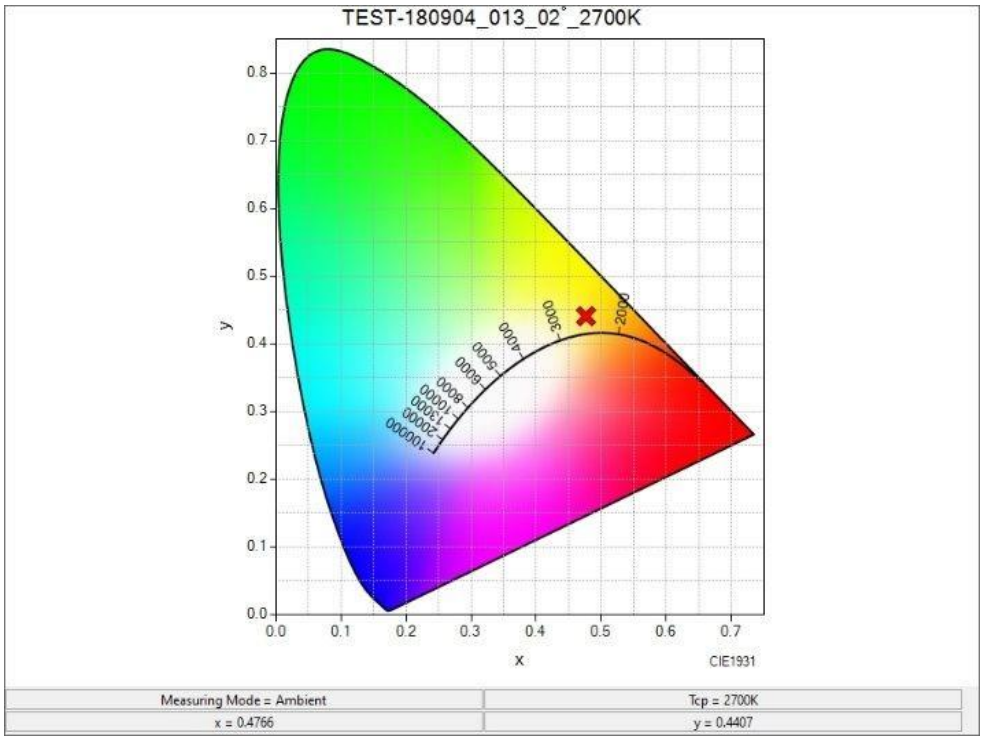

Figure 5.13: **CIE 1931 chromaticity coordinate**

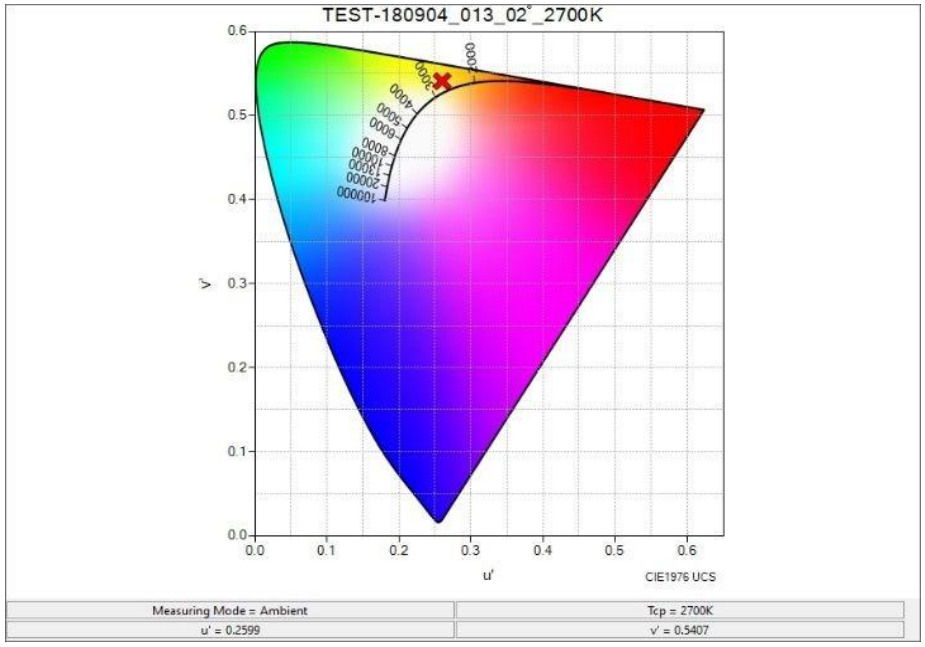

Figure 5.14**: CIE 1976 uniform chromaticity coordinate**

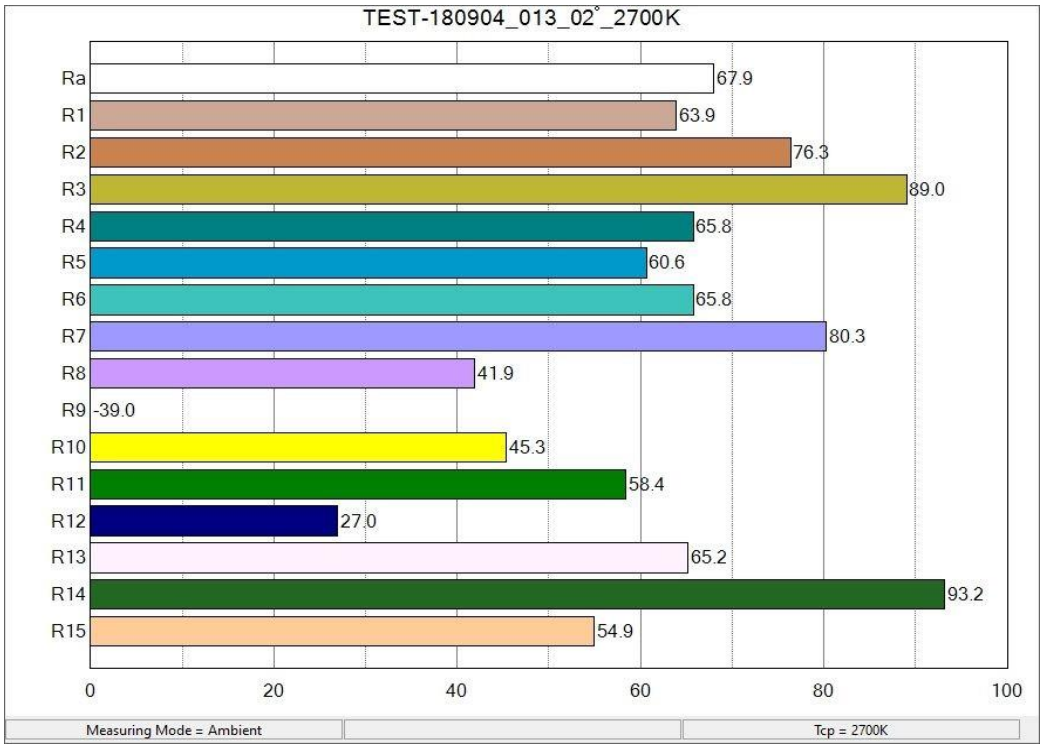

Figure 5.15: **Color Rending Index (CRI)**

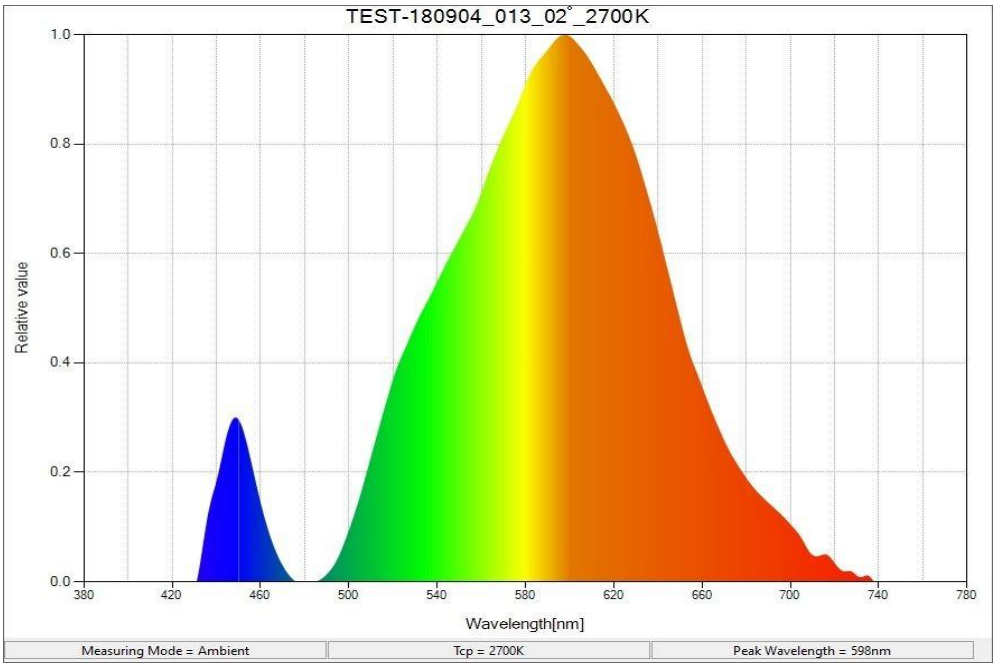

Figure 5.16: **Spectral power Distribution**

5.5 Detailed of combined cool & warm white LED array at 100% duty cycle

The data has been taken by chromameter CL70F, when the warm white LED array is in full glow. The detailed data is shown in table downwards.

Table 5.5: **Data obtained for warm white LED array**

Duty Cycle (%)	Illuminance (lx)	CCT (K)	Voltage (V)	Current (I)	Power (W)	Peak Wavelength [nm]	Dominant Wavelength [nm]	Purity [%]
100	324	3454	230	0.14	16	595	581	41.17

Table 5.6: **Tristimulus values of warm white LED array**

Tristimulus Value X	Tristimulus Value Y	Tristimulus Value Z	CIE1931 x	CIE1931 y	CIE1931 z	CIE1976 u'	CIE1976 v'
335.443	323.7273	161.1594	0.4089	0.3946	0.1965	0.2364	0.5134

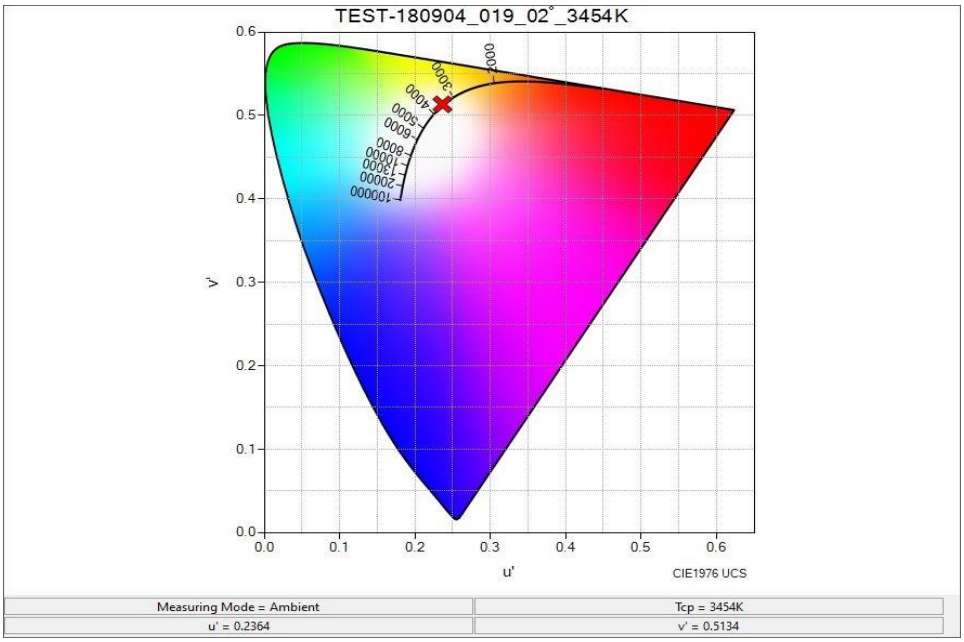

Figure 5.17: **CIE 1931 chromaticity coordinate**

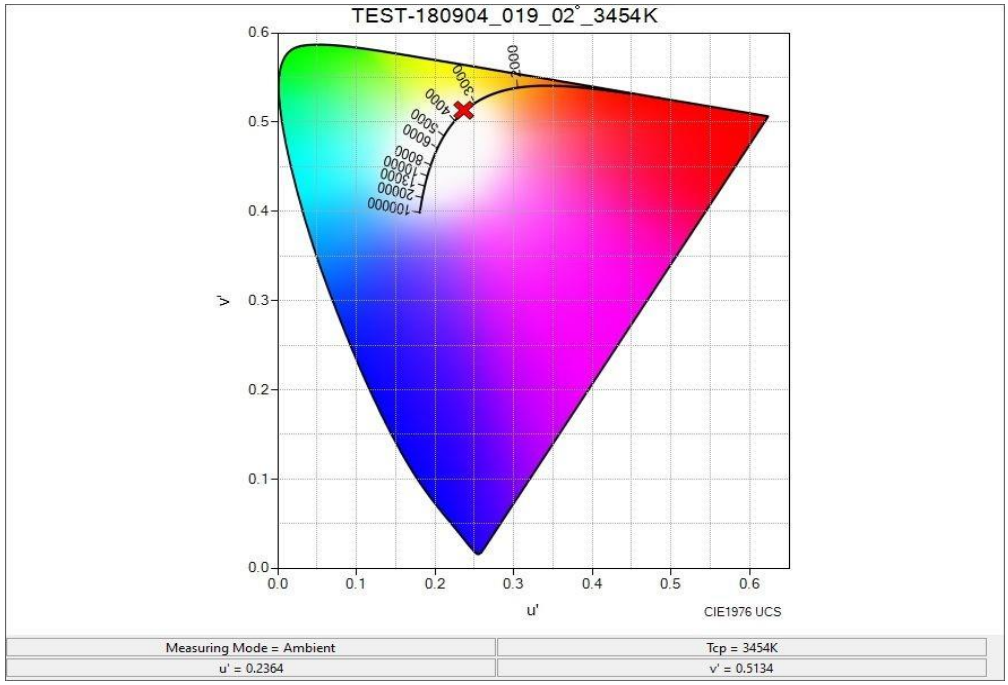

Figure 5.18: **CIE 1976 uniform chromaticity coordinate**

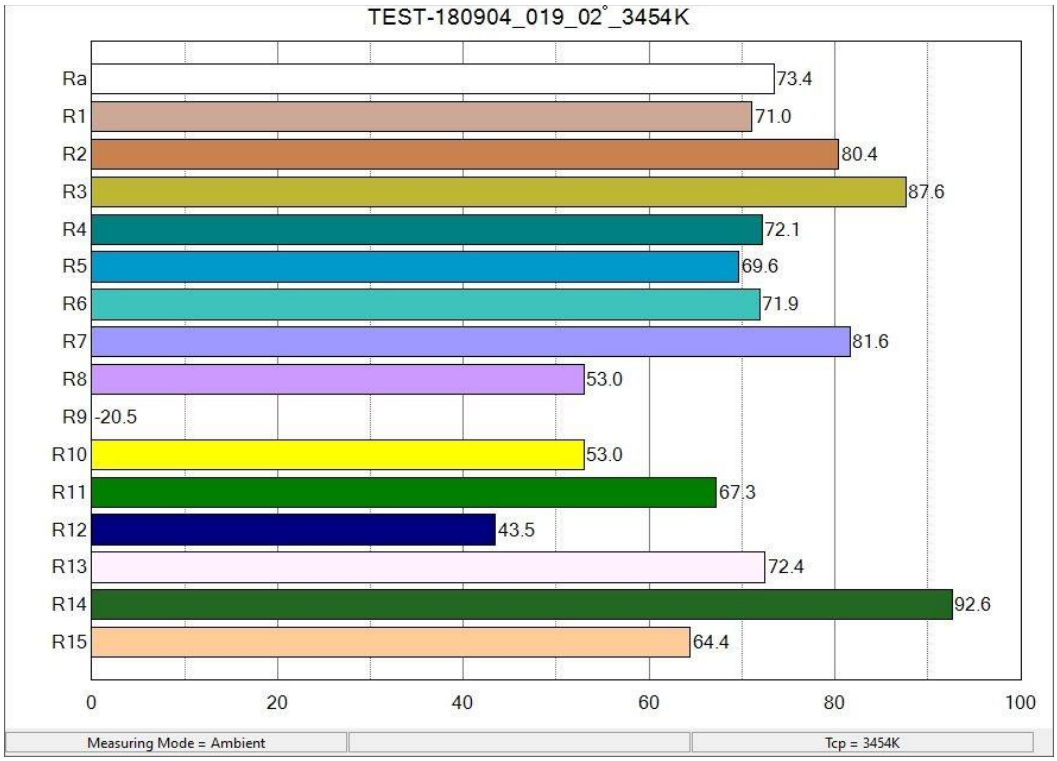

Figure 5.19: **Color Rending Index (CRI)**

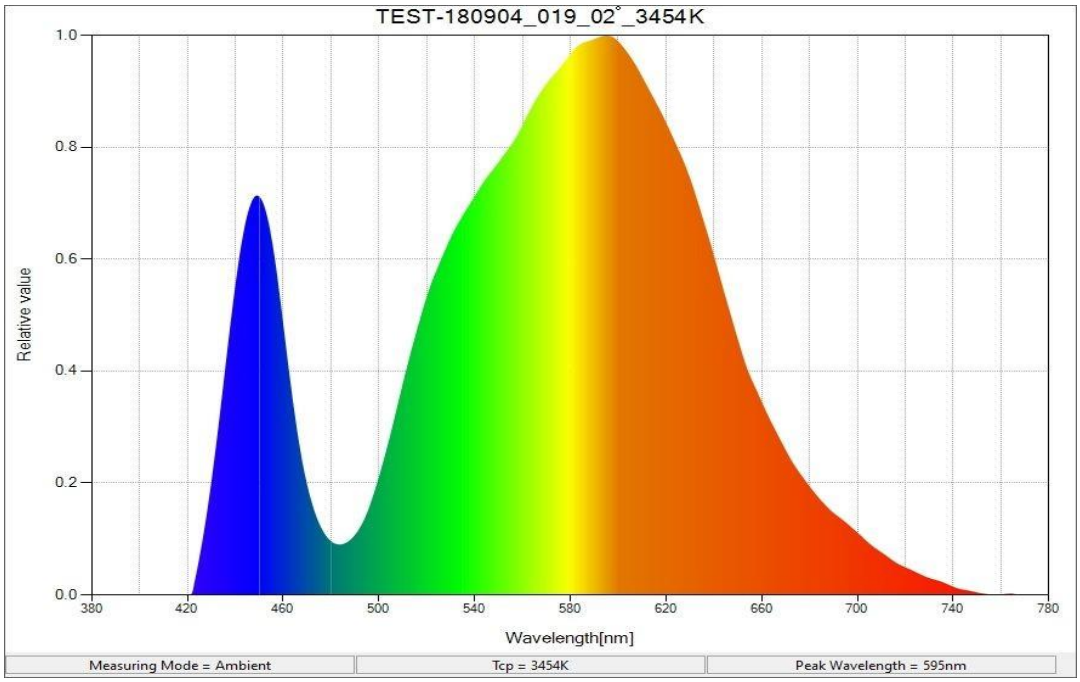

Figure 5.20: **Spectral Power Distribution**

CHAPTER 6: MANUALLY CONTROLLED LED CONTROLLER FOR A TUNABLE LED LUMINAIRE

6.1 Introduction

This chapter examines the role of Light Emitting Diodes (LEDs) in modern lighting systems, focusing on their widespread adoption due to their long lifespan, high light output, and exceptional energy efficiency. A key feature of the proposed LED system is its ability to dim from 0% to 100%, with detailed analysis of duty cycle variations for both cool and warm white arrays, individually and in combination. The system allows separate control of the cool and warm white arrays, providing flexibility to meet specific lighting needs by turning either array on or off as required. This precise dimming capability, from minimal to full brightness, not only offers customizable lighting but also enhances energy efficiency by reducing electrical consumption according to demand.

The core principle of LED technology is electroluminescence, where light is emitted when an electrical current is applied. However, increasing the driving current to enhance light output presents a significant challenge: around 80% of the input energy is converted into heat rather than visible light. This heat generation can limit the performance and lifespan of LEDs, making effective thermal management a critical aspect of LED design. A major advantage of LEDs is their ability to respond quickly to electrical variations, enabling precise control over light levels. Among the methods used to regulate LED output, Pulse Width Modulation (PWM) dimming is especially effective. PWM dimming controls light output by adjusting the duty cycle of a pulsed DC signal, allowing for brightness adjustments without significantly raising the LED's junction temperature, which helps extend its lifespan [15,16,33,59].

PWM dimming delivers a pulsed DC signal to LEDs, adjusting the duty cycle to control light output. This technique is beneficial as it prevents a significant rise in junction temperature, thereby extending the lifespan of LEDs. PWM dimming uses a square wave power source, allowing precise control over light flux, which enhances energy efficiency and provides flexibility in lighting design for adaptable environments [20, 21,29,60].

This chapter delves into the development and implementation of an LED dimmer circuit, with a focus on the benefits of PWM dimming and explore the design considerations, hardware components, and software algorithms integral to the manually directed LED controller. Additionally, it will address challenges related to manual tuning, such as maintaining color consistency and preventing flicker, and discuss how these challenges can be mitigated through thoughtful system design. The successful deployment of this controller represents a significant advancement in tunable LED systems, providing enhanced flexibility and user control across diverse lighting applications by analyzing advancements in LED dimming technology, the chapter highlights how these circuits enhance energy efficiency and promote sustainability in modern lighting design.

6.2 : Dimmer controller circuit

An apparatus that controls how physical devices function is called a controller. Whenever it concerns lighting, a dimmer regulates the brightness of a light by adjusting the switching mechanism through the use of power electrical components like triacs or thyristors. Using the use of microprocessors included in modern dimmers, lighting levels may be precisely controlled by converting digital impulses into control signals for these switches. Improved control and monitoring of the lighting system is made possible by their ability to give the lighting controller digital input.

Energy conservation and the adjustment of lighting levels to suit human requirements depend on dimming control. Pulse-width modulation (PWM) dimming and analogue dimming, commonly referred to as amplitude-modulation (AM) dimming, are the two main techniques for dimming LEDs.

- Analogue dimming, also known as AM dimming, modifies the current passing through the lamp to change the brightness of LEDs. It is frequently utilized in street lights, tunnel lights, and emergency lighting applications where a high luminous quality is not necessary. Nevertheless, at low currents, AM dimming can result in noticeable color spectrum alterations, is nonlinear, and has a narrow dimming range. [12]
- PWM notes as Pulse-Width Modulation dimming. Applying this technique, the brightness is controlled by varying the current pulse width. PWM dimming reduces the average current by varying the pulse width while maintaining a constant operating current amplitude. Because it offers more precise dimming control without changing the light's color spectrum, this method is frequently employed in the industry. [13]

To provide LED power sources a steady current output, constant current LED drivers are adopted. Even at a reduced proportion of their maximum brightness, dimming LED lights can result in significant energy savings. Dimming an LED light to 10% of its maximum brightness, for instance, may reduce energy usage by 90%, making it an effective strategy for saving energy. This thesis investigates the implementation of pulse width modulation (PWM) in controlled dimming technology. PWM dimming and analogue dimming based on triacs are the two main techniques for dimming. Triac-based dimming, which modifies light intensity by severing the line voltage signal's phase, has disadvantages that make it unsuitable for automated dimming applications. These disadvantages include flickering, colour temperature fluctuations, and decreased efficiency. By contrast, triac dimming's drawbacks may be avoided by use pure DC voltage in combination with extra components to provide controlled dimming. [14]

About 80% of the input power in high-power LED chips is converted to heat, with the remaining 20% being released as light. The chips produce a lot of heat when attempts are made to make LEDs brighter. In order to save expenses and satisfy lighting specifications, LEDs are frequently assembled into multichip modules. Dimming is a method of controlling the output of LED light.

Pulse width modulation (PWM) and changing the DC level are the two most used dimming techniques. These techniques control the LEDs' heat output while enabling light intensity modification. [15] The two methods used for dimming LEDs include pulse width modulation (PWM), which modifies the light flow by changing the duty cycle of a square wave power supply, and modulating the DC current amplitude, which regulates the luminous flux by regulating the DC level. [16]

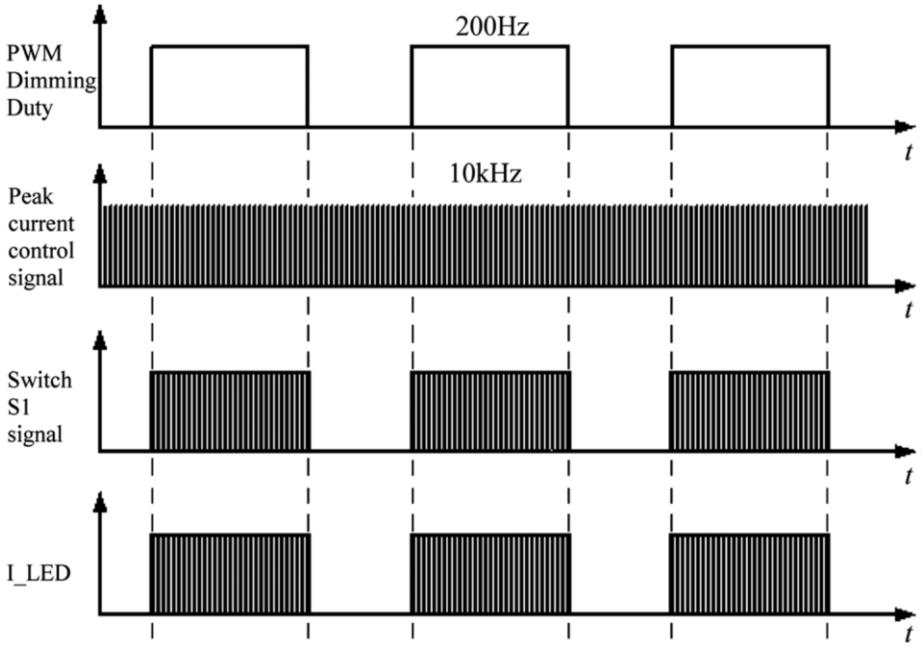

Figure 6.1: **Theoretical waveforms of the studied PWM dimming. [2]**

6.3 Components used for making LED dimmer circuit

- **Arduino Nano**: The Arduino Nano is a small and convenient microcontroller board for a breadboard. The dimension of this microcontroller is 7g in weight, 18mm in width & 45mm in length. The board has a Mini-B USB connection and pin headers for simple breadboard hookup. There are 13 built-in LED pins, 14 digital I/O pins, 8 analogue input pins, and 6 PWM pins on the Arduino Nano. It has two pins for communication, A4 (Serial Data Line, SDA) and A5 (Serial Clock Line, SCL), which facilitate I²C communication. There has a 16 MHz clock speed. Additionally, pins D11 (COPI), D12 (CIPO), and D13 (SCK) facilitate Serial Peripheral Interface (SPI) connection. The board has a nominal input voltage range of 7–12V, an I/O voltage of 5V, and a DC current of 20 mA per I/O pin. [17]

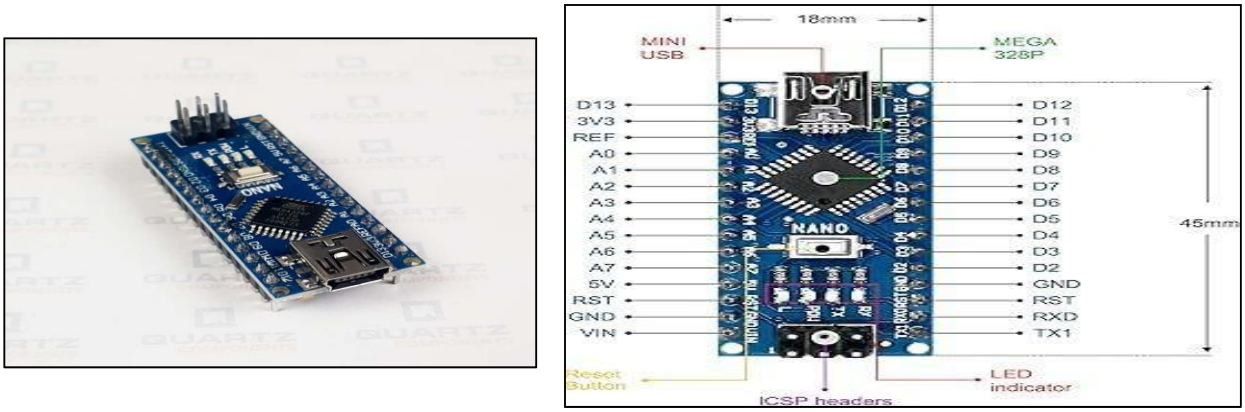

Figure 6.2: **Detailed specification of Arduino Nano microcontroller**

- **Rotary Encoder**: The rotary encoder has been utilized to independently adjust the dimming percentage for each of the two LED arrays, from 0% to 100%Magnetic rotary encoders are used in this circuit. A rotary encoder is an electromechanical device that produces an electrical output signal in accordance with the location of a rotating component, such as a motor shaft. A magnetized wheel attached to the shaft powers magnetic rotary encoders. A magnetic sensor fixed on the component's casing determines the magnetized wheel's location as the shaft rotates. [18]

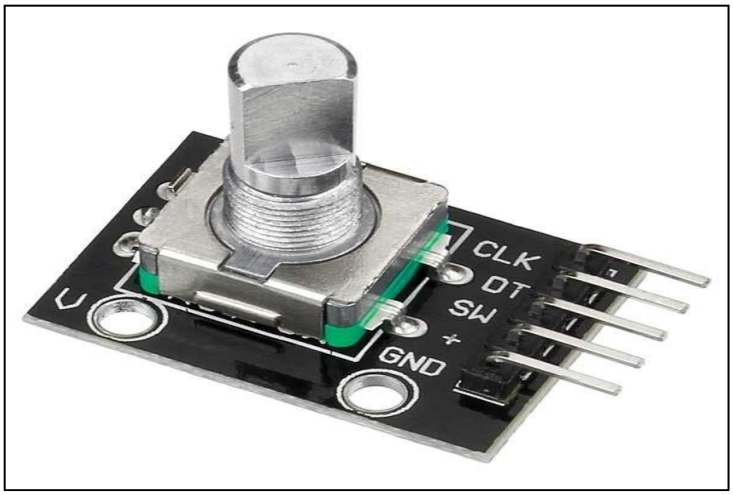

Figure 6.3: **Rotary Encoder**

- **OLED Display**: This circuit uses an OLED display to show the percentage of dimming while the rotary encoder is manually turned. The display is 0.91 inches and has a pixel resolution of 128 x 32. There are four pins on it: GND (power ground), VCC (power positive), SCL (clock line) and SDA (data line).

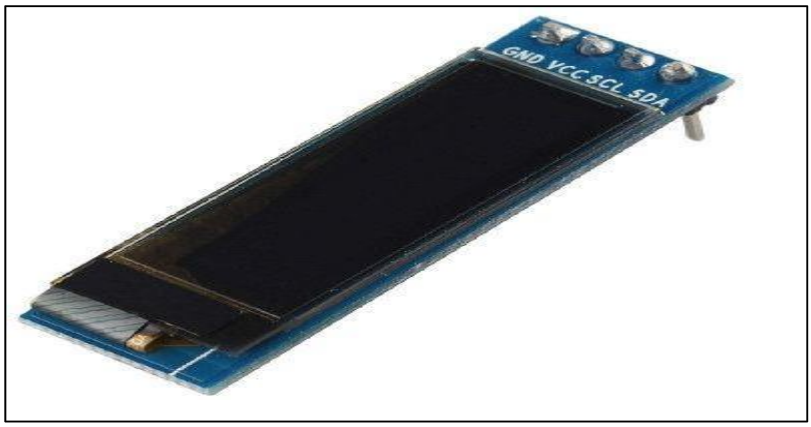

Figure 6.4: **OLED Display**

- **Optocoupler**: An optocoupler is used in this design to move electrical signals between two separate circuits that are placed in between a BJT and a microcontroller. The optocoupler's main job is to isolate the circuits electrically by preventing a direct connection between them. The removal of electrical noise from signals, the separation of low-voltage components from high-voltage circuits, and the avoidance of ground loops in machinery that manages a remote load are other advantages.

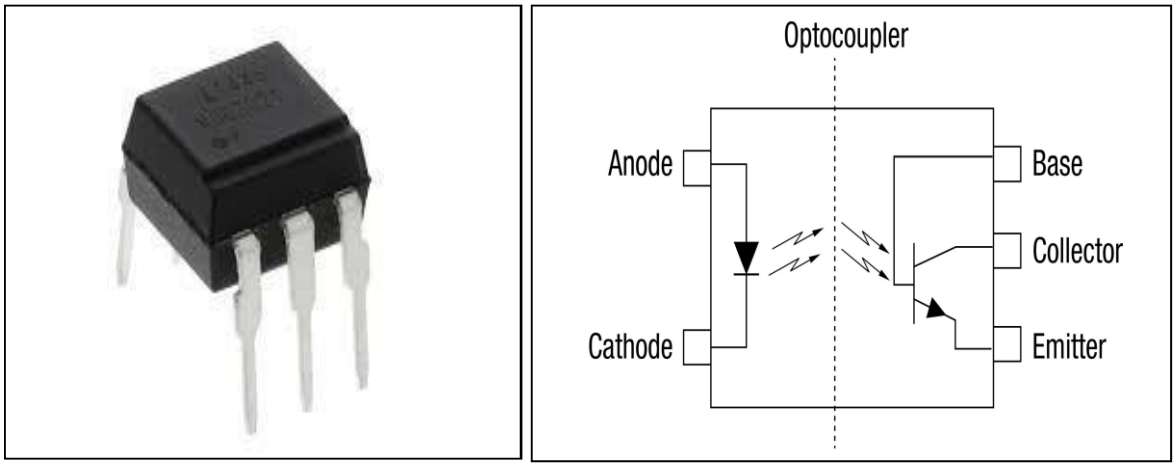

Figure 6.5: **Optocoupler**

- **Resistors**: Three resistors, measuring 1 ohm, 10 ohms, and 220 ohms, are utilized in this circuit to provide internal connections between the various parts. A resistor is a two-terminal passive electrical component used as a circuit element to create electrical resistance. Resistors are used in electronic circuits for a variety of purposes, including as lowering current flow, modifying signal levels, splitting voltages, biassing active components, and cutting transmission lines.

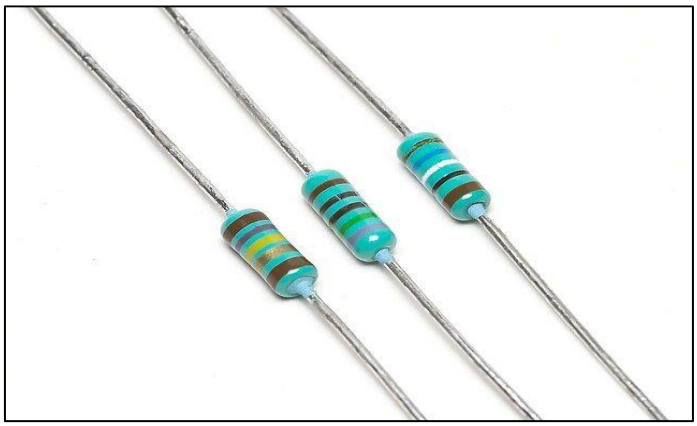

Figure 6.6: **Resistors**

- **Bipolar Junction Transistor (BJT)**: The intended full cycle output signal is made possible in this circuit by a full 360-degree phase shift made possible by two Bipolar Junction Transistors (BJTs). The circuit can rotate a shaft both clockwise and anticlockwise thanks to the BJTs, which make it easier to regulate the direction and speed of rotation. Usually, a certain design that includes the BJTs as a component of a larger setup that allows for bidirectional control is used to accomplish this. Because BJTs are amplifiers, they can handle higher currents required to operate the motor with fewer control signals. This is especially crucial in situations where the controller's power requirements cannot be directly met by the control circuit. Furthermore, the speed of the controller may be accurately regulated by varying the duty cycle of the signal delivered to the BJTs via Pulse Width Modulation (PWM).

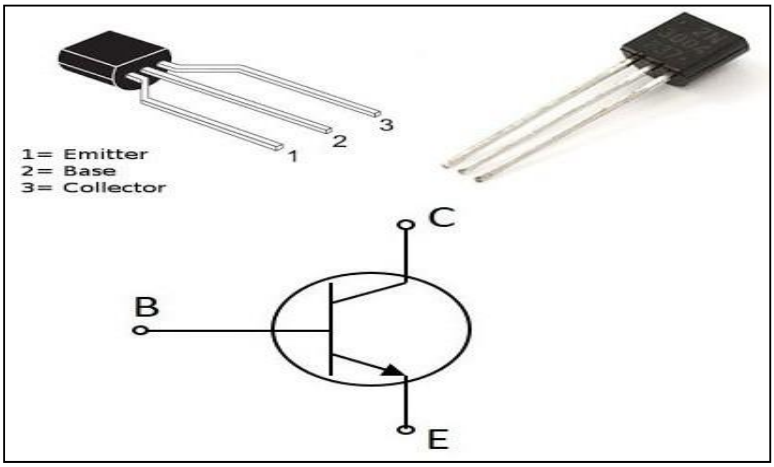

Figure 6.7: **Bipolar Junction Transistor**

- **MOSFET**: Two IRFZ44N MOSFETs are utilized in this circuit to independently control arrays of warm and cool white LEDs. Electronic components called Metal Oxide Silicon Field Effect Transistors (MOSFETs) are frequently used in circuits to switch or increase voltage. The Source, Gate, and Drain terminals are the three terminals on these voltage-controlled devices. In this application, the MOSFETs regulate the current flow through the LED arrays, giving the user exact control over how the arrays operate**.**

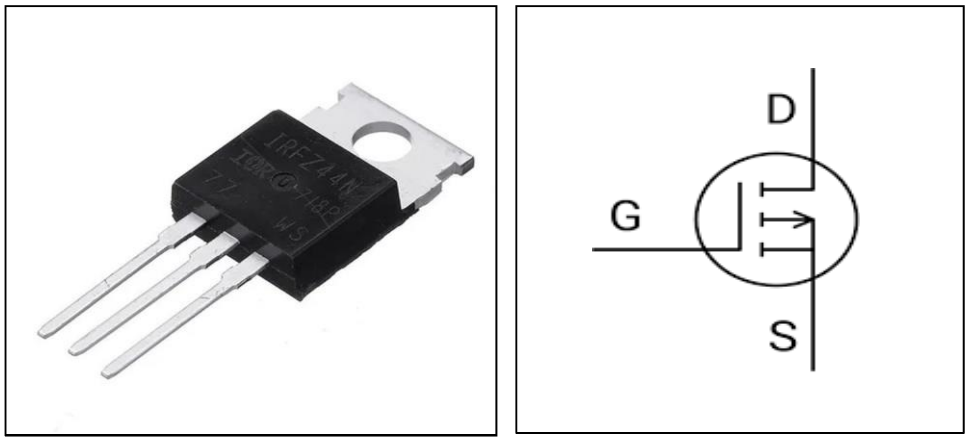

Figure 6.8: **MOSFET**

- **Voltage regulator**: There is only one voltage regulator employed in this circuit. An electrical or electronic device termed a voltage regulator is made to maintain a power source's voltage within acceptable limits. It is essential to protect electrical equipment from voltage fluctuations that might harm sensitive components by ensuring that the voltage remains within the specified range.

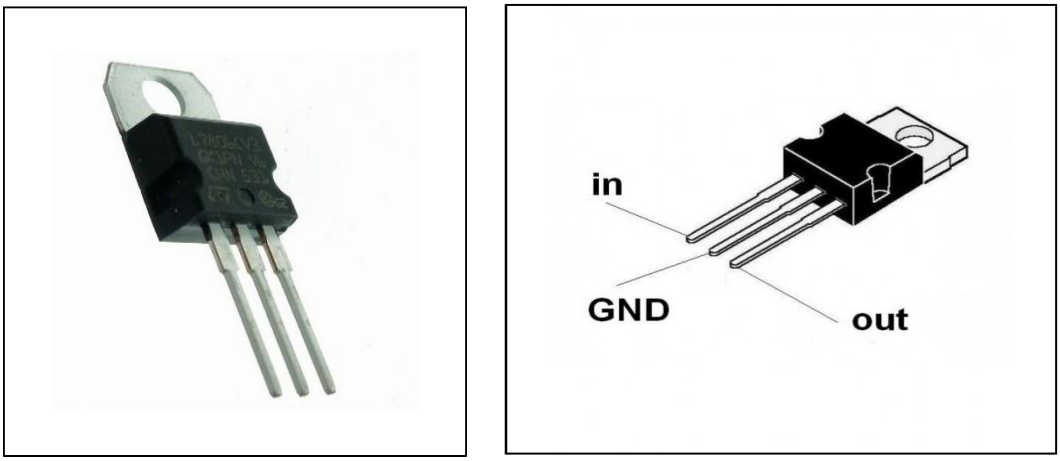

Figure 6.9: **Voltage regulator**

- **OP-AMP**: The LM358 operational amplifier, often known as an op-amp, is used in this circuit to protect against power surges and give the microcontroller a steady power supply. An operational amplifier is an integrated circuit (IC) that produces an amplified signal through its output pin after amplifying the voltage difference between its two input pins. due to its low output impedance and high input impedance, the LM358 op-amp is perfect for preserving signal integrity and protecting the microcontroller from fluctuations in voltage**.**

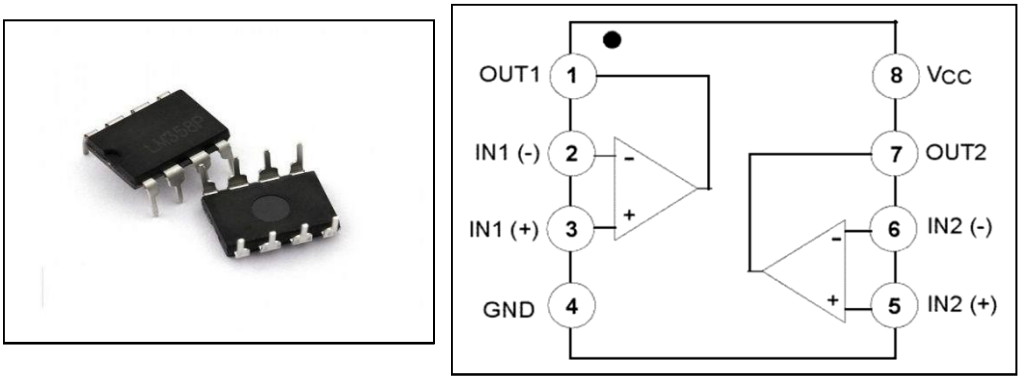

Figure 6.10: **OP-AMP**

- **PCB connector**: Three PCB connections are used in this circuit to enable the passage of power and signals. The third connector serves as the primary supply via a Switch Mode Power Supply (SMPS), with the other two connectors serving as the power supply for the warm white and cool white LED arrays. The efficient control and distribution of electrical power inside the circuit is ensured by these connections**.**

Figure 6.11: **PCB connector**

6.4 Design and development of proposed LED controller

Block diagram overview:

An advanced LED control system's fundamental structure is outlined in the block diagram in Figure 6.12. A tunable LED configuration, containing both warm white and cool white LED arrays, can have its brightness and corelated color temperature (CCT) controlled and adjusted by this system. The controller circuit and the power circuit compose the two logical components of the system. To get exact control over the LED properties, each segment has distinct components and functional blocks that collaborate with one another.

Controller Circuit:

The Microcontroller Unit (MCU) is the core component of the controller circuit. The MCU functions as the system's brain, processing inputs and executing preset algorithms to control the LED arrays. Two independent encoders, E1 for the cool white LED array and E2 for the warm white LED array, are connected to the MCU. These encoders are in charge of producing signals that represent the intended modifications to the duty cycle of the LEDs, which is a parameter that regulates how long the LEDs glow for in a certain amount of time in that particular phase.

The MCU receives signals from the rotating encoders and interprets them using a pre-programmed code. The MCU's response is controlled from this code, which converts the encoder signals into expected PWM (Pulse Width Modulation) signals. By altering the duty cycle, which in turn controls the amount of power supplied to the LEDs, PWM is a technique used to adjust the brightness of LEDs. The LED will shine brighter the higher the duty cycle. After processing this input, the MCU uses an OLED display to show the necessary output numerical data. This display displays continuous feedback on the current CCT and brightness levels and acts as an interface for monitoring and modifying the system's configuration.

A vital aspect of this technology is the ability to create an adjustable LED with shifting CCT. By adjusting the relative intensities of the cold white and warm white LEDs, the system can dim PWM control dimming to generate a wide range of color temperatures, from cool tones to warm ambient illumination. Applications such road lighting, tunnel illumination, and specialized industrial situations that demand precise lighting management require this adaptability.

Power Circuit

A vital part of the system, the power circuit controls the power supply and makes sure that every component operates safely and effectively. The Gate Driver Block, the Regulator Block, and the Optical Isolation Block are important components in this area.

- **Gate Driver Block**: The gate driver block interfaces (Metal-Oxide-Semiconductor Field-Effect Transistors) that interface the MCU to the power MOSFETs. The MCU's control signals get amplified by the gate driver to a level which enables the MOSFETs to be controlled. By operating as electronic switches, these MOSFETs control the current that is provided to the LED arrays. The gate driver provides the amplification required to satisfy the high-power needs of the LEDs while ensuring the effective operation of the MOSFETs.
- **Regulator Block**: The system needs to function consistently for the voltage supply to remain constant. The function of the regulator block is to maintain the output voltage constant regardless variations in the input power the source. This is particularly important for protecting vulnerable components like the MCU as well as making ensure the LEDs having a steady supply of power, both of which have an immediate effect on the quality and consistency of the light output.
- Optical Isolation Block: The system contains optical isolators, additionally referred to as optocouplers, to protect the MCU and other sensitive control components from electrical noise and high voltage interruptions. These small devices offer electrical isolation between multiple circuit components through the use of light to transfer electrical signals over an isolation barrier. This separation is essential to avoiding power surges or failures in the power circuit that might harm the control equipment.

An SMPS (Switched-Mode Power Supply), which effectively transforms electrical power from an external source into the DC voltage required by the system, controls the power supply for the system. All electronic components require a steady and controlled power output from the SMPS in order for them to operate as designed.

Circuit Diagram Details

The circuit diagram in Figure 6.13 investigates the complicated details of the hardware arrangement of the system, clarifying the functions and connections between different parts. It emphasizes the encoders (E1 and E2) as vital input devices. By physically rotating, these encoders translate changes in mechanical position into electrical impulses that alter according to the rotation level. By modifying the duty cycle of the PWM signals, this variation regulates the LEDs' brightness and color temperature.

Once the MCU processes the signals from the encoders, two separate optocouplers conduct out the transmission of control signals. The electrical isolation that occurs between the high-power LED driving circuit and the low-power control circuitry is maintained in a significant way by these optocouplers. Optocouplers protect the sensitive components of the control side from noise or excessive voltage from the power side by transmitting the signal through light.

Discharge resistors are an important component of the circuit that ensure the secure discharge of stored electrical energy and to maintain the voltage supply. To prevent charge accumulation, which could lead to in unwanted surges or component damage, these resistors are linked across multiple locations in the circuit such as among optocoupler, BJT, MOSFET.

The circuit additionally includes an operational amplifier (OPAMP), the LM358. The LM358 is employed as a buffer and amplifier owing to its high input impedance and low output impedance. It protects the system from surges in voltage that might otherwise result in unpredictable conduct or damage through providing the MCU an uninterrupted consistent output signal. For accurate signal processing and consistent LED operation, a clean, constant power signal is maintained with the assistance of the OPAMP.

In a nutshell the system is a representation of an advanced method for controlling LED lighting. It combines innovative components and techniques that precisely adjust light output. A robust and dependable system is enhanced by the separation of the circuits into controller and power sections, the use of encoders and optocouplers, and the addition of safety elements such discharge resistors and an OPAMP. This approach ensures the longevity and the preservation of the electronic components involved in addition to providing flexibility in modifying the LED's CCT and brightness. Considering the ability to regulate lighting automatically depending on pre-established criteria and provide human control, this type of system is perfect for applications requiring for accurate lighting solutions.

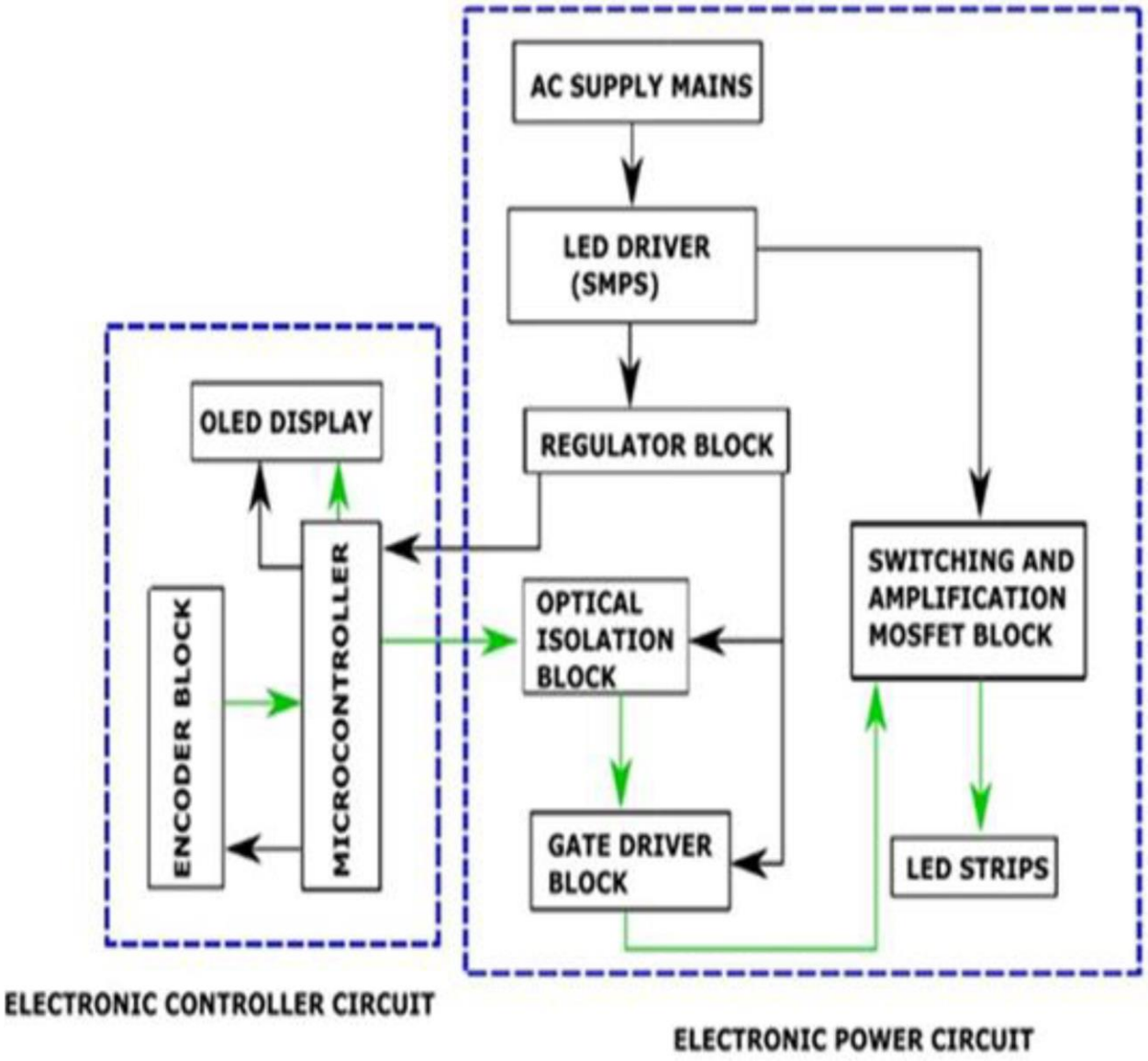

Figure 6.12: **Block Diagram of LED controller**

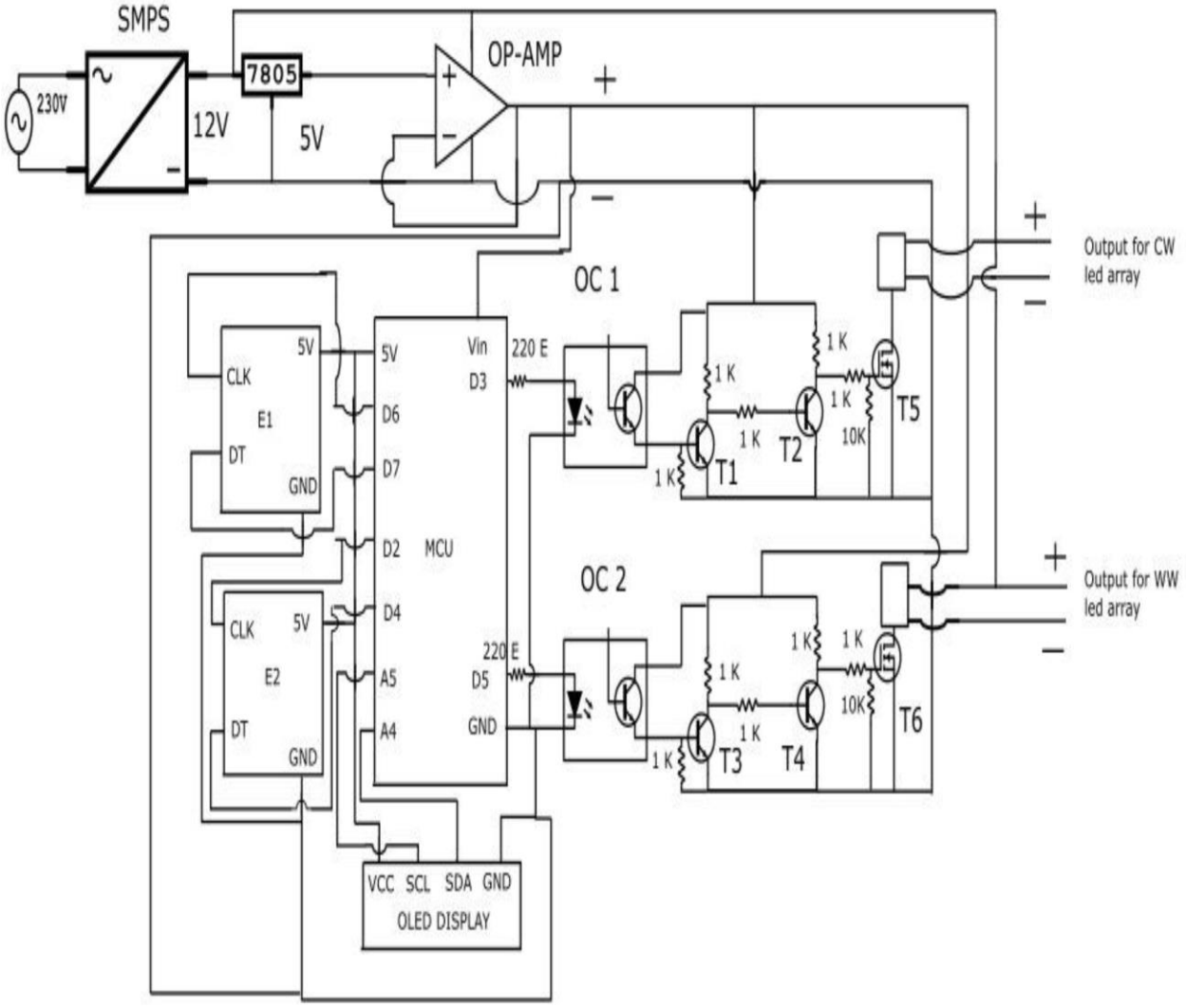

Figure 6.13: **Circuit Diagram of the proposed controller**

6.5 : Experimental set up for tuning LED with controller

Overview of the Prototype LED Luminaire

A specifically created prototype LED luminaire with two cold white (CW) and two warm white (WW) LED arrays makes up the experimental arrangement. For this experiment, these arrays have been reshaped and designed to provide optimal integration with a heat sink. In order to preserve thermal stability and extend the life of the LEDs, the heat sink is essential for draining excess heat produced by the LEDs. Under controlled conditions, this configuration enables a thorough analysis of the light output characteristics.

Power Supply and Control Circuit

A DC programmable power supply powers the LED arrays, providing a steady and adjustable power source required for precise testing. A PWM (Pulse Width Modulation) control circuit is used to regulate the LED arrays. PWM is an effective technique for controlling the amount of power supplied to LEDs as well as other electrical devices. It controls the apparent brightness of the LEDs by altering the duty cycle, or the proportion of time the signal is on vs off.

The control circuit contains an OLED display for monitoring in real time and is completely combined to the LED arrays. A visual representation of the control signals being supplied to the LEDs is provided by the OLED display, that additionally displays the duty cycle and analogue input levels. For precise control and modifications to be made throughout the experiment, this capability is important. The rotary encoders connected to each LED in the array are used to adjust the PWM duty cycle. Precise control over the light output of each array is made possible by the encoders for the warm white and cool white arrays.

Microcontroller and Coding

For executing the control circuit into execution, an Arduino NANO microcontroller is utilized. Since it is simple to integrate and program, the Arduino NANO is a microcontroller board that is both small and adaptable, making it an excellent choice for experimental setups. It adjusts the duty cycles of the PWM signals by processing inputs from the rotary encoders and executing the specified code. Depending on how the encoders rotate, the code establishes the link between the encoder locations and the PWM duty cycle, enabling a seamless transition from 0% to 100% duty cycle, or vice versa.

The Arduino NANO modifies the PWM signals in accordance with the rotation of the encoders. This modulation creates a tunable light source by adjusting the LED arrays' brightness and color temperature. For example, the brightness of the cold white LEDs may be changed independently of the warm white LEDs by spinning the encoder connected to them, and vice versa. For investigations that need the investigation of various color temperatures and brightness levels, this configuration is essential.

Measurement and Data Collection

A Metravi 1310 Light Meter is used to precisely measure the illuminance (light intensity) on the working plane under various circumstances. This instrument, sometimes referred to as an illuminance meter, provides information in lux (lx), or the quantity of light that reaches a surface. Measurements are made at different duty cycles in the experimental setup, with a 20% variation between each measurement point. This methodical procedure guarantees thorough data collecting in a variety of light intensities. Based on standards like IS 1944-1 and 2:1970, which imply that LEDs cannot deliver enough light at lower duty cycles to be important for practical applications, a 20% duty cycle increase was chosen.

A Konika Minolta colorimeter, more especially, the CL-70F model—is used for colorimetric analysis. This gadget measures the color attributes of the light that the LEDs output, such as the dominant wavelength, peak wavelength, Correlated Color Temperature (CCT), and Color Rendering Index (CRI). Understanding the quality and qualities of the light, which can change substantially with changes in the PWM duty cycle, depends on these parameters.

Experimental Procedure

The process involves evaluating the properties of the light output once the CW and WW arrays' duty cycles have been adjusted to certain levels. The duty cycle can be adjusted to, for example, 50% CW and 50% WW or any other combination, such as 75% CW and 75% WW. The study of varied illumination conditions and their effects on the workplace is made possible by this flexibility. The spectral characteristics, CCT, CRI, and illumination of each configuration are recorded, resulting in a full dataset for study.

The experiment takes place out in a controlled environment, a laboratory with dark illumination especially, in order to reduce the impact of outside light sources and reflections. For the duration of the experiment, the luminaire is fixed at a height of one meter on an adjustable street light pole. In order to guarantee uniformity over all data points and standardize the measuring settings, this height was selected. The absence of ambient light influences the accuracy of the light meter and colorimeter readings, which are ensured by the dark laboratory environment.

Data Analysis

Following the data collection process, a thorough analysis is carried out after an exact tabulation. The investigation encompasses an examination of the effects of duty cycle modifications on peak wavelength, dominant wavelength, CCT, CRI, and total illuminance. This information is essential for comprehending how well the LED luminaire performs in diverse environments and can offer suggestions for enhancing lighting schemes for a range of uses.

For instance, keeping the CW and WW arrays' duty cycles identical can produce a balanced color temperature that is appropriate for settings needing neutral illumination. On the other hand,

altering the duty cycle ratios might result in warmer or colder illumination, which may be preferable in some situations, such bright shop places or comfortable domestic areas.

The results of this experiment may guide the development and application of future LED luminaires by offering suggestions on how to accomplish particular lighting effects or energy-saving objectives. The entire picture of the experimental setup, as shown in Fig. 6, clearly demonstrates how all the components are arranged and connected, giving insight into how the system functions.

In conclusion, this experiment offers insightful information on how PWM control and circuits based on microcontrollers might be used to tune LED luminaires. It emphasizes how crucial it is to have exact control over LED characteristics and how lighting solutions may be tailored to fit particular requirements. The thorough recording and analysis of the experimental setup open up new avenues for improved lighting technology research and development.

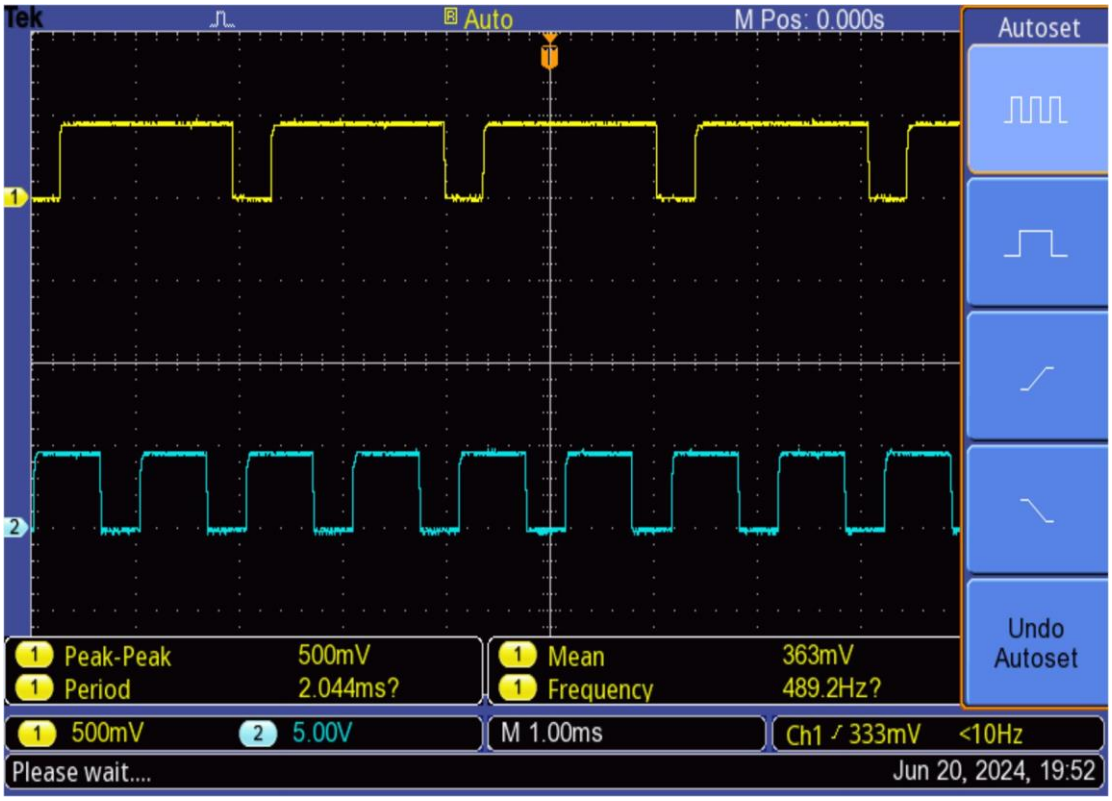

Figure 6.14: **Sample PWM signal**

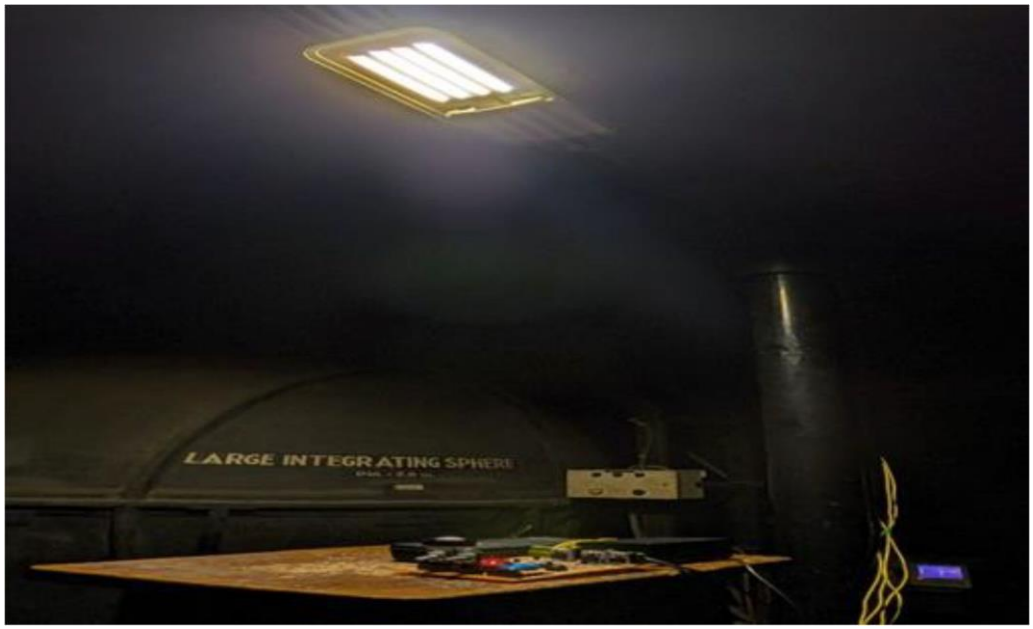

Figure 6.15: **Protype LED Luminaire**

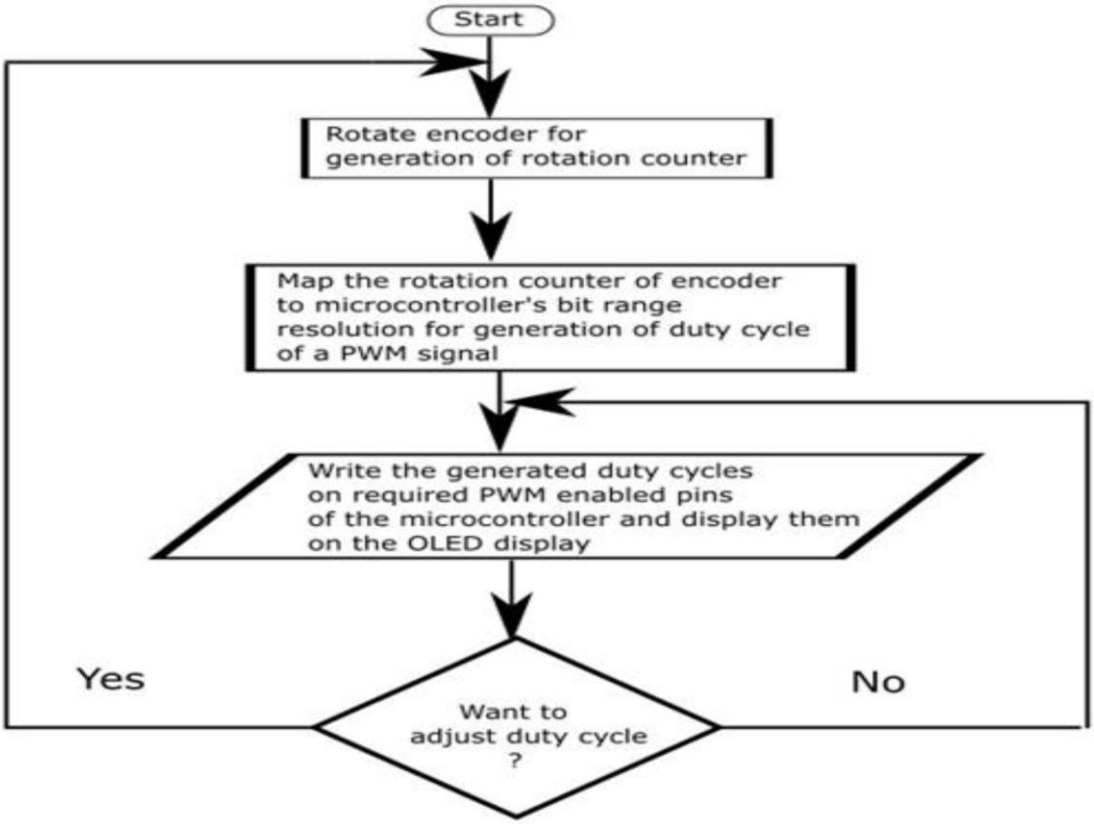

Figure 6.16: **Flow chart for PWM dimming signal**

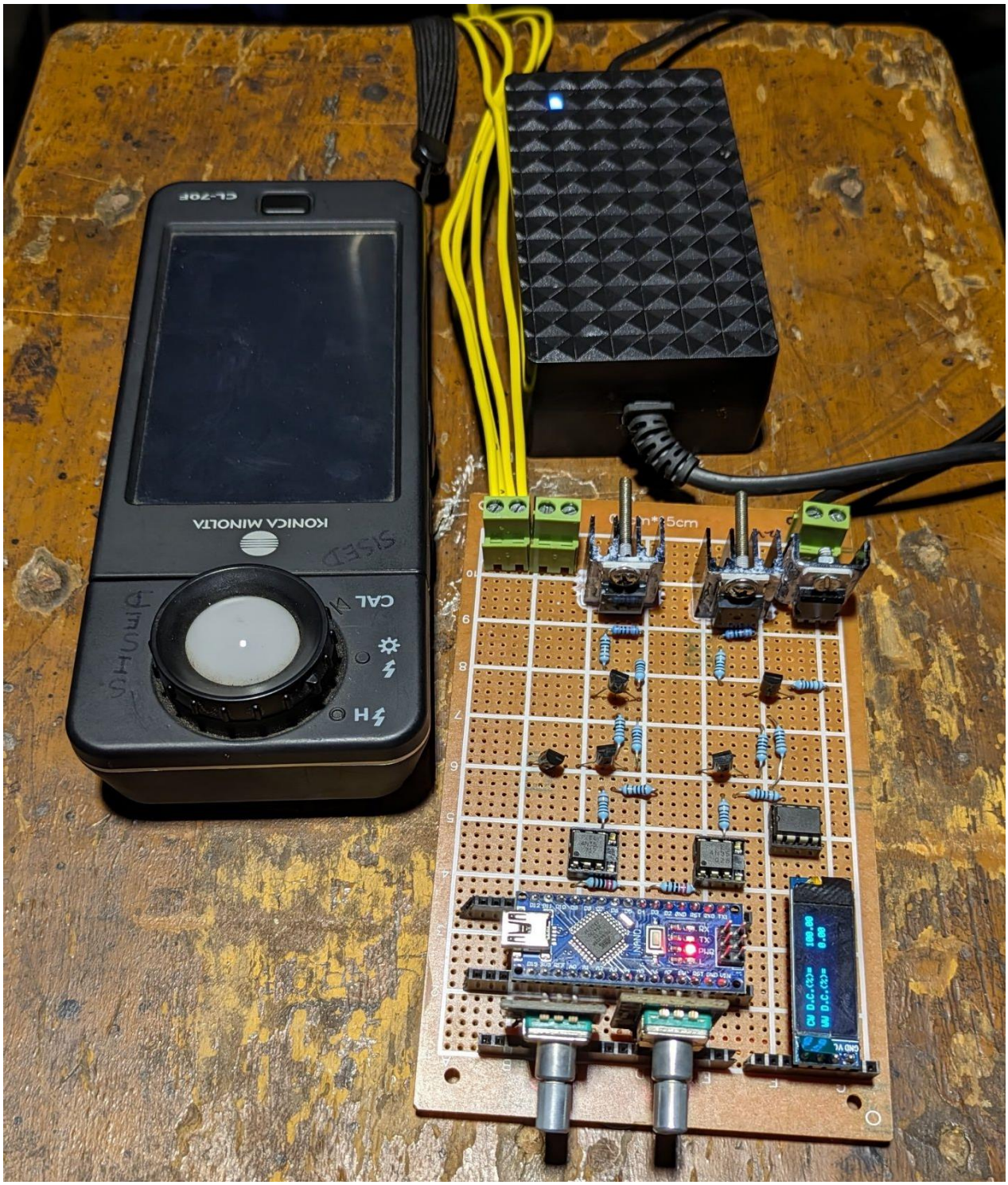

Figure 6.17: **Data recording by using LED controller**

In Figure 6.14, the flowchart for the Pulse Width Modulation (PWM) dimming signal is presented, with data collected separately for cool white, warm white, and their combined arrays. The dimming process was analyzed at five distinct intervals: 20%, 40%, 60%, 80%, and 100%, with data recorded as the encoder was rotated. The subsequent sections provide a detailed analysis of the dimming performance at each of these intervals, focusing specifically on the cool white array. This analysis is crucial for understanding the behavior and efficiency of the cool and warm white array under varying dimming conditions.

Table 6.1: Detailed data for cool white array

Duty Cycle (%)	Illuminance (lx)	CCT (K)	Voltage (V)	Current (I)	Power (W)	Dominant Wavelength [nm]	Purity [%]
20	63.7	3410	230	0.06	4	579	50.88
40	74.9	3454	230	0.07	5	579	48.44
60	120	3693	230	0.08	7	579	38.09
80	165	3844	230	0.09	9	578	33.53
100	218	4102	230	0.1	10.5	578	25.67

Table 6.2: Detailed data for warm white array

Duty Cycle (%)	Illuminance (lx)	CCT (K)	Voltage (V)	Current (I)	Power (W)	Dominant Wavelength [nm]	Purity [%]
20	30.6	2226	230	0.05	3.5	584	99.13
40	53.9	2352	230	0.06	5	582	98.8
60	89.1	2519	230	0.07	6	582	88.85
80	124	2617	230	0.08	7	582	82.36
100	159	2700	230	0.09	9	582	75.39

Table 6.3: Detailed data for cool and warm white array in combine form

Duty Cycle (%)	Illuminance (lx)	CCT (K)	Voltage (V)	Current (I)	Power (W)	Dominant Wavelength [nm]	Purity [%]
20	56.6	2736	230	0.06	5	581	80.67
40	140	3178	230	0.08	8	580	54.66
60	217	3319	230	0.1	10.5	580	47.54
80	294	3411	230	0.12	13	580	43.5
100	324	3454	230	0.14	16	581	41.17

6.6 : Details Circuit Diagram of the proposed controller

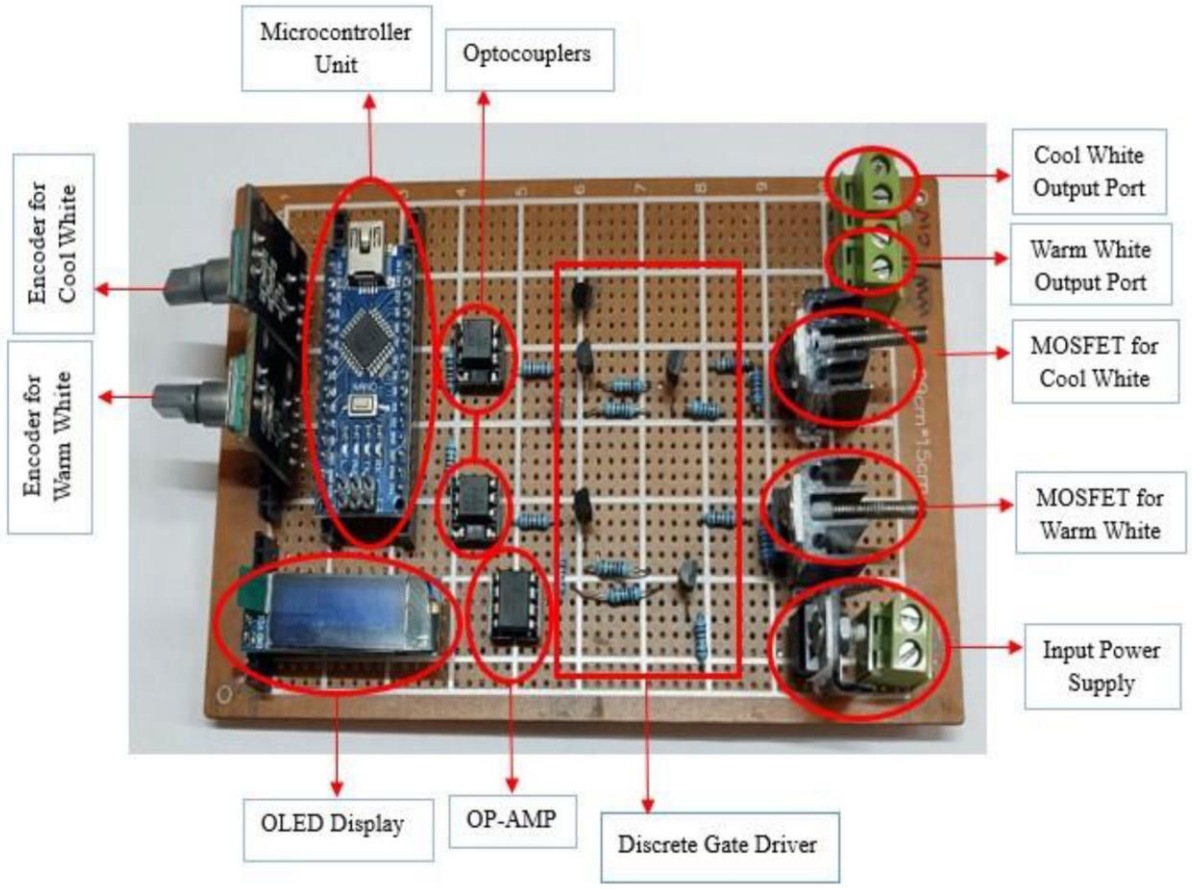

Figure 6.18: **Detailed labeled components of circuit diagram**

The circuit diagram presented in the above figure illustrates the connections between various components, specifically the encoders and OLED display, with the microcontroller. The connections are detailed as follows:

1. **Encoder E1 (Cool White LED Control):**

- **CLK (Clock):** Connected to pin D6 on the microcontroller.
- **DT (Data):** Connected to pin D7 on the microcontroller.
- **5V:** Connected to the 5V pin on the microcontroller, which also powers the 5V inputs of encoder E2 and the VCC of the OLED display.
- **GND:** Connected to the common ground (GND) shared by encoder E2, the microcontroller, and the OLED display.

2. **Encoder E2 (Warm White LED Control):**

- **CLK (Clock):** Connected to pin D2 on the microcontroller.
- **DT (Data):** Connected to pin D4 on the microcontroller.
- **5V:** Connected to the same 5V pin on the microcontroller as encoder E1 and the VCC of the OLED display.
- **GND:** Connected to the common ground (GND) shared by encoder E1, the microcontroller, and the OLED display.

3. **OLED Display:**

- **GND:** Connected to the GND on the microcontroller.
- **VCC:** Connected to the 5V pin on the microcontroller, along with the 5V inputs of encoders E1 and E2.
- **SCK (Serial Clock):** Connected to pin A5 on the microcontroller.
- **SDA (Serial Data):** Connected to pin A4 on the microcontroller.

This configuration ensures proper communication and power distribution among the components, enabling the control and monitoring functions required for the LED tuning system. The microcontroller, through the encoders, adjusts the duty cycle of the PWM signals to control the brightness of the cool and warm white LED arrays, while the OLED display provides real-time feedback on system parameters.

6.7 Data Analysis

A CL-70F colorimeter was implemented in the laboratory study to measure the different light exposure properties which the LED luminaire emitted. To ensure precise measurements, the colorimeter was carefully placed right away underneath the light source. Illuminance, supply

current, voltage, and correlated color temperature (CCT) were among the important factors studied. The experiments were conducted out separately for the warm white (WW) and cool white (CW) LED arrays over a variety of duty cycle values. In order to comprehend how the two light sources interact, the combined impacts of the CW and WW LEDs were evaluated as well.

The findings from the experiment demonstrated that the illuminance levels developed linearly increasing the duty cycle. This connection indicates that varying the duty cycle may reliably regulate the LEDs' brightness, making it a dependable technique for modifying light output. In addition to brightness, the CCT showed a linear pattern of variation. With variations in the duty cycle, the CCT adjusts proportionately, making it possible to precisely alter the light's color temperature. This feature is very helpful in situations when certain lighting conditions are needed, including in various street light applications.

Furthermore, the supply current and voltage measurements confirmed the CCT and illuminance patterns. Both current and voltage increased in direct proportion to the duty cycle. According to this finding, the relationship between power input and light output is predictable since the amount of electrical power used by the LEDs increases linearly with the duty cycle. The capacity to adjust electrical consumption based on necessary lighting conditions is made possible by this predictability, which is beneficial for developing energy-efficient lighting systems.

Additional information has been discovered from the combined examination of the CW and WW LEDs. The resultant light might be adjusted to obtain a desired balance between warm white and cool white by adjusting the duty cycles of both arrays. Since CW and WW LED output may be combined, an exciting range of color temperatures can be produced, providing adaptability in the development of different lighting environments. For instance, when the duty cycle of the CW LEDs is increased while the duty cycle of the WW LEDs is decreased, the resultant light may be cooler, but the reverse change may provide a warmer tone. This function is very helpful in situations that need changing illumination, such places where ambiance alterations are preferred.

The evaluation results, as shown in Fig. 7, validate the prototype LED luminaire's ability to deliver a dynamic and adaptable lighting solution. The adaptability of this system is demonstrated by the ability to adjust the CCT and the illuminance level using a variable duty cycle controller. Because users may alter the illumination according to their own needs or tastes, it's a very flexible option for a variety of situations. This LED luminaire can satisfy a variety of lighting specifications, whether the objective is to produce a daylight-like environment or an inviting, comfortable atmosphere.

The investigation concludes by demonstrating the effectiveness and viability of utilizing PWM-controlled LED arrays to generate lighting environments that are adjustable. The system's controllability and predictability are demonstrated by the linear relationships that come from adjusting the duty cycle, and these relationships also show changes in supply current, voltage,

CCT, and illumination. This makes it an appealing option for a range of applications, guaranteeing that illumination can be adjusted to enhance functionality, comfort, and aesthetics.

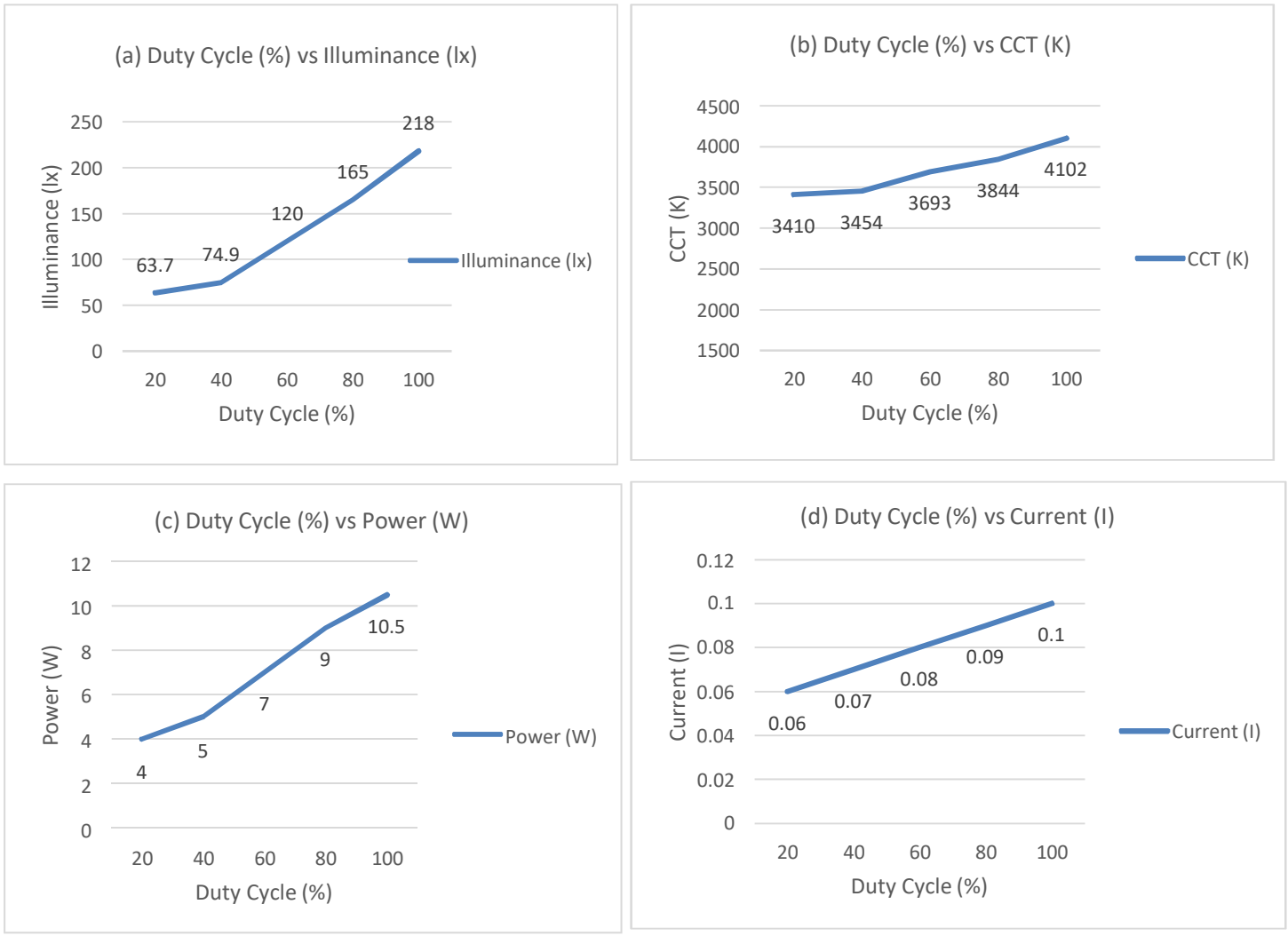

Figure 6.19: **Variation in (a)illuminance, (b) CCT, (c) current & (d) power with duty cycle for Cool White LED.**

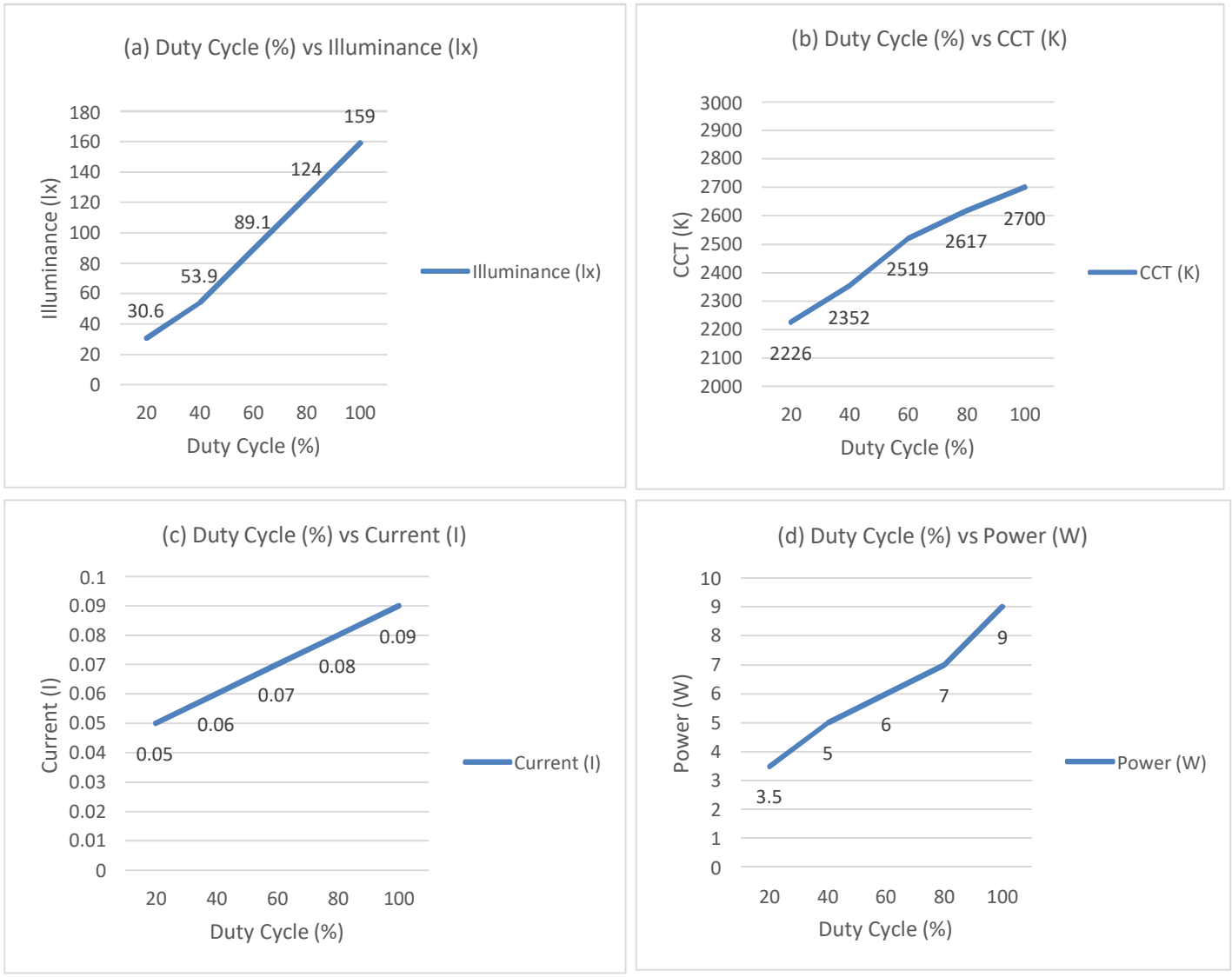

Figure 6.20: **Variation in (a)illuminance, (b)CCT, (c)current & (d)power with duty cycle for Warm White LED**

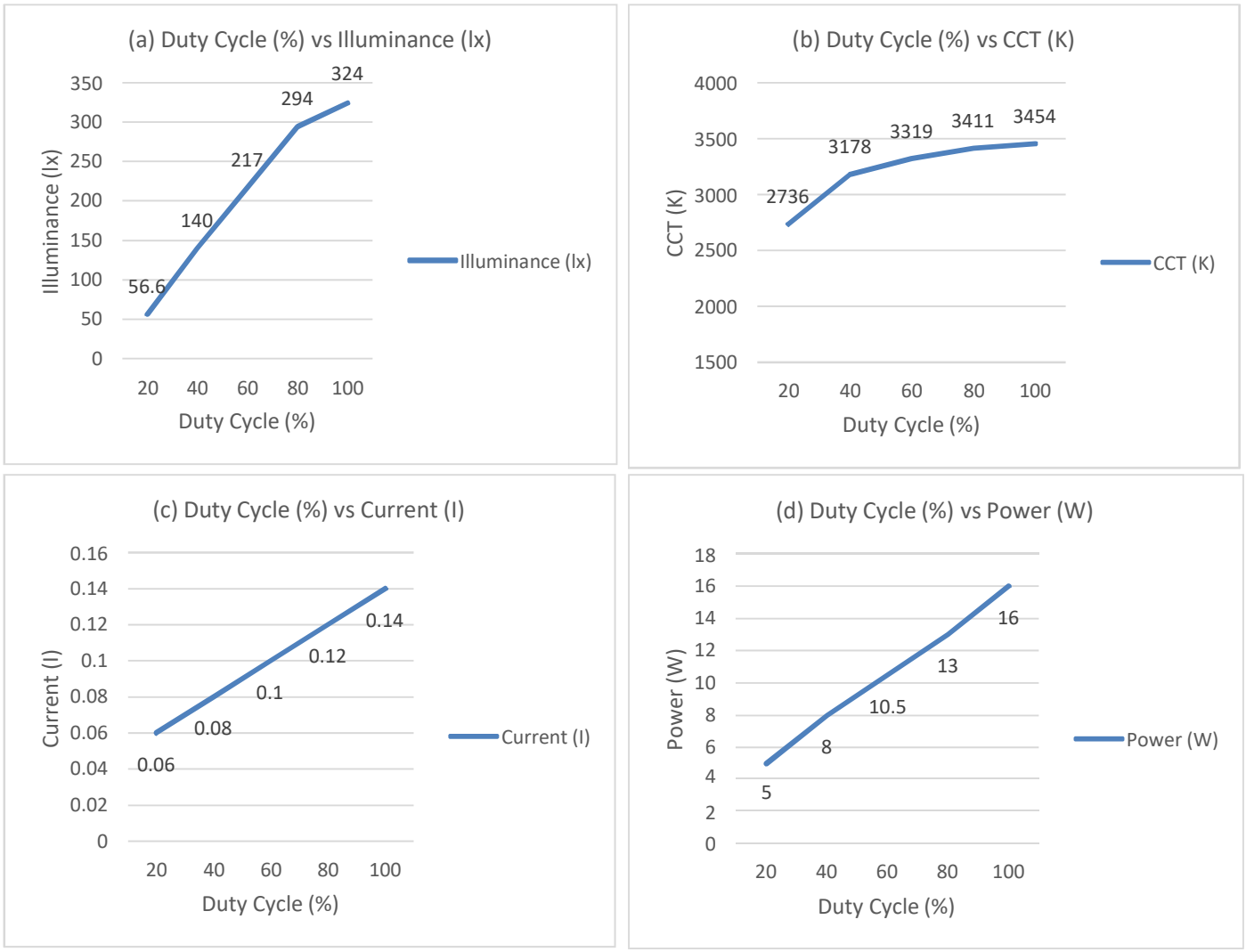

Figure 6.21: **Comparison among (a)illuminance, (b)CCT, (c)current & (d)power with duty cycle for the combined LED luminaire**

CHAPTER 7: RESULT ANALYSIS

In this chapter, the analysis focuses on the comparison between photopic and mesopic luminance for floodlight luminaires in outdoor lighting design. The study highlights the differences in luminance between these two regions, emphasizing the effectiveness of mesopic vision in enhancing visual task performance and its impact on human-centric lighting. The comparison extends to various internal characteristics, including luminous flux, luminous efficacy, and optical efficiency, providing a comprehensive evaluation of the luminaires used in both area and street lighting.

The results demonstrate a clear distinction between simulated photopic luminance (Lp), calculated mesopic luminance (Lm), and simulated mesopic luminance (Lms) for the luminaires studied. Additionally, the overall uniformity of lighting in both photopic and mesopic regions has been compared, revealing significant insights into the accuracy and effectiveness of outdoor lighting design based on mesopic luminance.

The analysis concludes that designing lighting systems based on mesopic luminance (Lm) provides a more accurate and efficient approach for outdoor lighting, particularly in floodlight applications. This conclusion is supported by detailed comparisons presented in earlier chapters, where it was shown that mesopic-based designs offer superior performance in terms of both visual perception and energy efficiency. The proposal for model validation, illustrated in the figures below, further reinforces the advantages of adopting mesopic luminance in lighting design.

7.1 Validation of the proposed Model for area lighting

The proposed model analysis compares the calculated mesopic luminance (Lm) using the CIE 191:2010 method with the simulated mesopic luminance (Lms) obtained through DIALux for various lamps, including HPSV, MH, and LED. As illustrated in Figure 7.1, the Lm values (represented in red) closely align with the Lms values (represented in green), demonstrating a strong correlation between the two methods.

A similar comparison, including additional CFL luminaires, is presented in Figure 7.2. These results confirm that the approach used in this thesis is consistent with the standards outlined in CIE 191:2010, both in scenarios with and without the inclusion of CFL lighting. This alignment validates the accuracy and reliability of the mesopic luminance calculations and supports the overall methodology presented in this research.

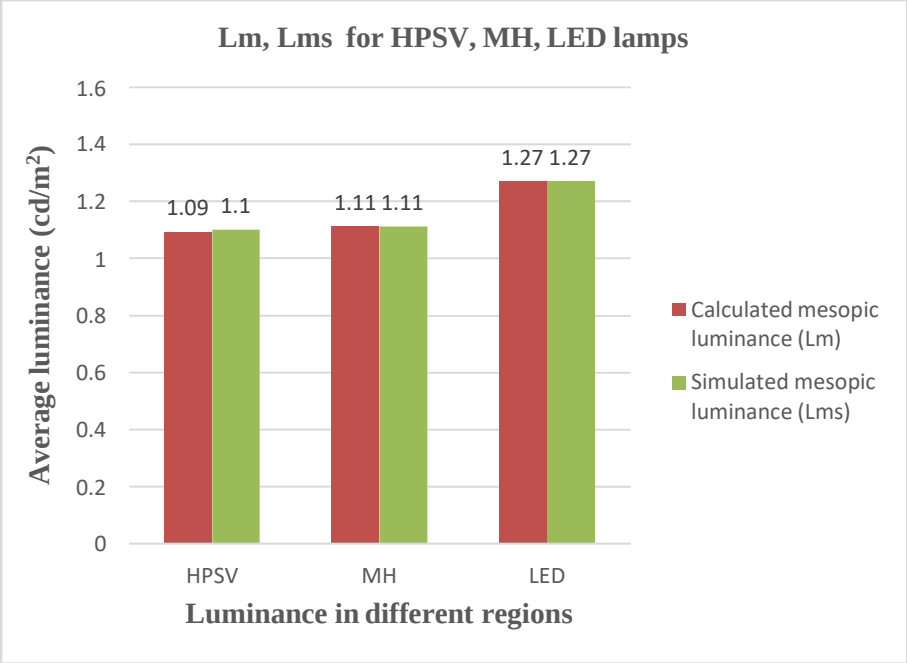

Figure 7.1: **Comparison of Lm, Lms for HPSV, MH, LED floodlight luminaire**

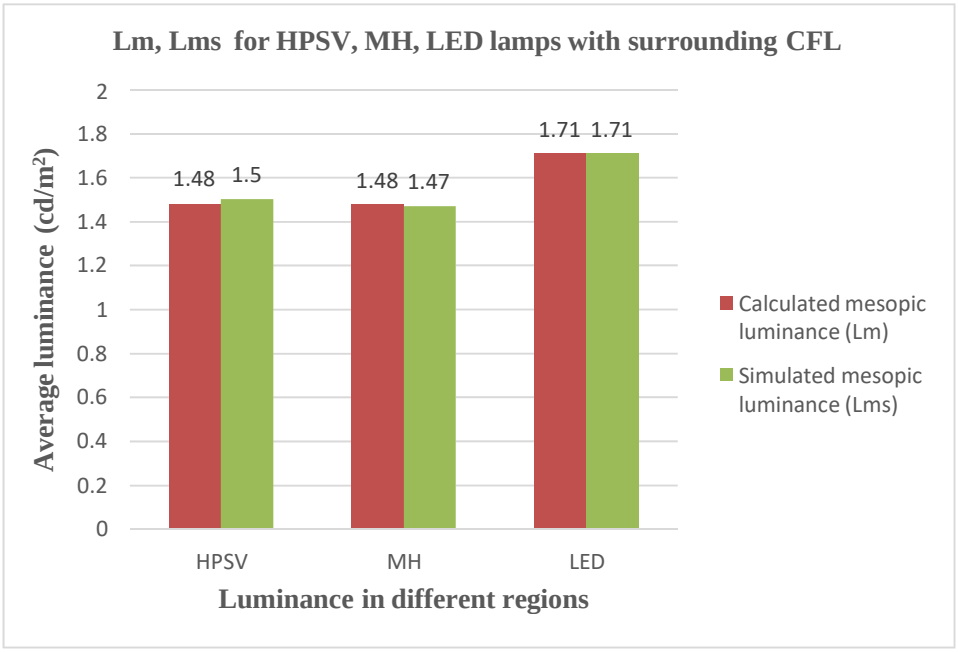

Figure 7.2: **Comparison of Lm, Lms for HPSV, MH, LED with additional surrounding luminaire**

7.2 Validation of the proposed Model for road lighting

In the context of road lighting, the calculated mesopic luminance values (Lm) determined using the CIE 191:2010 standard, represented in blue, closely align with the simulated mesopic luminance values (Lms) obtained through DIALux, represented in red. This comparison is illustrated in Figure 4.31 for various lamps, including HPSV, MH, and LED. The findings demonstrate that the proposed method in this chapter is consistent with the conditions outlined in CIE 191:2010, validating the accuracy and reliability of the approach for road lighting scenarios. Moreover, the results confirm that LED luminaires, due to their superior performance in mesopic conditions, are the most effective choice for road lighting. LEDs offer significant advantages over HPSV and MH lamps in terms of luminance and overall lighting efficiency, making them the preferred option for modern road lighting designs.

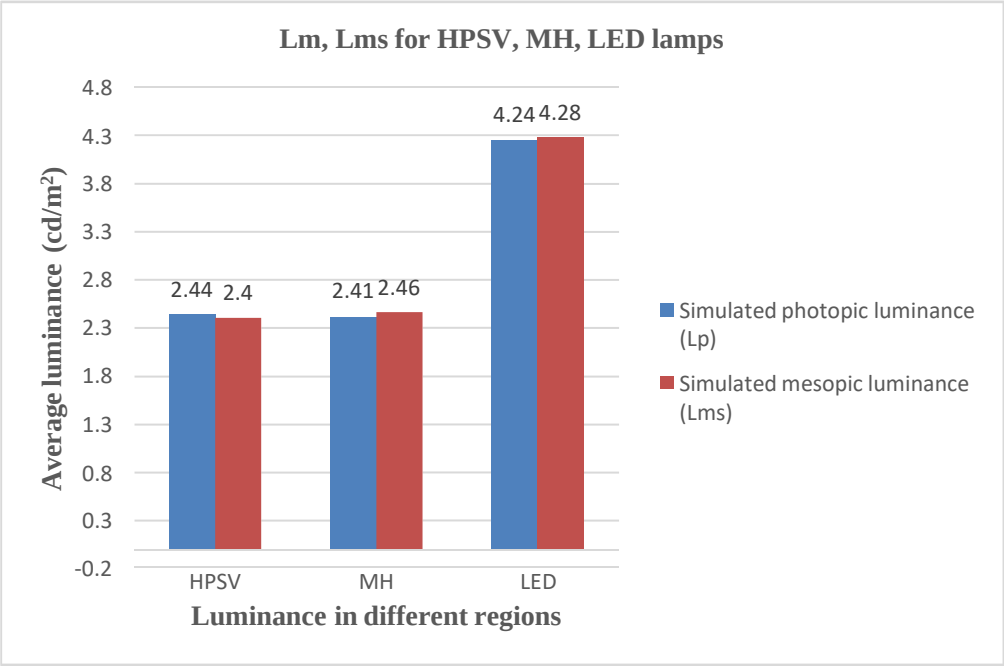

Figure 7.3: **Comparison of Lm, Lms for HPSV, MH, LED street luminaire**

7.3 Tunable Led and its advancement convenience

In the laboratory study, a CL-70F colorimeter was used to measure the LED luminaire's light exposure properties, including illuminance, supply current, voltage, and correlated color temperature (CCT). The measurements were taken for both warm white (WW) and cool white (CW) LED arrays across various duty cycle values, and the combined effects of the CW and WW LEDs were also evaluated.

The results showed that illuminance and CCT increased linearly with the duty cycle, indicating that the duty cycle can effectively control LED brightness and color temperature. This linear relationship was confirmed by the corresponding increases in supply current and voltage, demonstrating a predictable relationship between power input and light output. This predictability supports the development of energy-efficient lighting systems. The combined analysis of CW and WW LEDs revealed that adjusting the duty cycles of both arrays allows for a wide range of color temperatures. For example, increasing the CW duty cycle while decreasing the WW duty cycle results in cooler light, whereas the reverse produces warmer light. This feature provides flexibility for various lighting applications, including ambiance adjustments.

Overall, the results validate the prototype LED luminaire's capability to deliver a dynamic and adaptable lighting solution. The ability to precisely control CCT and illuminance through PWM dimming demonstrates the system's effectiveness and versatility, making it suitable for a range of applications where customizable lighting is required.

CHAPTER 8: CONCLUSION AND FUTURE SCOPES

This thesis has explored the advancements in lighting technology, focusing on enhancing the functionality of DIALux software for outdoor and street lighting applications, particularly in mesopic conditions, as well as the development and evaluation of a PWM dimmer circuit for LED lighting. Each study area contributes to a broader understanding of how modern lighting systems can be optimized for energy efficiency, human visual perception, and overall sustainability.

The enhancement of DIALux software, traditionally centered on photopic calculations, by integrating mesopic values has proven to be a significant step forward in the field of lighting design. This enhancement is particularly relevant for outdoor and street lighting, where human vision operates under mesopic conditions. The study compared mesopic luminance values generated by DIALux with those derived from photopic values and S/P ratios using the CIE 191:2010 method. The close agreement between these values across various lighting scenarios demonstrates the feasibility and reliability of incorporating mesopic calculations into DIALux. This integration allows lighting designers to create more accurate and efficient lighting systems that better align with human visual perception in low-light environments.

The study also highlighted the varying impacts of different light sources on perceived brightness under mesopic conditions. High-Pressure Sodium Vapor (HPSV) lamps, known for their durability, were found to have lower S/P ratios, resulting in reduced mesopic luminance compared to photopic luminance. This creates a dimmer perceived environment, necessitating the use of higher wattage lamps to achieve the desired brightness, which in turn increases energy consumption. Despite their longevity, the lower efficiency of HPSV lamps in mesopic conditions makes them less optimal for street lighting applications.

In contrast, LEDs, with their higher S/P ratios, exhibited superior performance under mesopic conditions. They provided higher mesopic luminance, making them more energy-efficient and better suited for mesopic environments. The study emphasizes that LEDs should be the preferred choice for modern road lighting designs, as they offer greater perceived brightness while consuming less energy. This characteristic positions LEDs as the most effective solution for enhancing visibility and energy efficiency in varying lighting conditions.

The need for a shift in street lighting design from a photopic-based approach to one that incorporates mesopic considerations was also underscored. Current street lighting designs and luminaire manufacturing predominantly focus on photopic conditions, which do not fully account for human visual perception in low-light environments. The analysis of luminous flux, luminous efficacy, and optical efficiency under both photopic and mesopic conditions supports the conclusion that street lighting designs should be based on mesopic photometry to enhance both visibility and energy efficiency.

The other focus of this research was the development and evaluation of a Pulse Width Modulation (PWM) dimmer circuit for LED lighting applications. PWM dimming is a highly

effective method for controlling LED light output by adjusting the duty cycle of a pulsed DC signal. This method offers precise control over light levels, which is essential for applications were adjusting brightness rather than turning off lights entirely is more efficient, such as in nighttime settings.

The experimental outputs and waveform analysis conducted on a prototype PWM dimmer circuit demonstrated several key advantages. One of the most significant benefits is the ability to accurately control the LED current, allowing for precise adjustments in brightness levels. This capability is crucial for maintaining comfort and safety while reducing energy consumption. By dimming the lights instead of turning them off, energy usage can be minimized without compromising on lighting quality.

Additionally, PWM dimming extends the lifespan of LEDs by reducing the thermal stress caused by frequent on/off cycles. This not only enhances the durability of LED systems but also contributes to their overall energy efficiency. The study showed that PWM dimming is a versatile and effective method for creating adaptable lighting configurations, suitable for both residential and commercial applications. The flexibility and cost-effectiveness of this technology make it a valuable tool for modern lighting systems.

The findings suggest that LEDs, with their superior performance in mesopic conditions and compatibility with advanced dimming techniques like PWM, are the optimal choice for contemporary lighting solutions. The integration of mesopic calculations into lighting design software and the adoption of PWM dimming in LED systems represent significant advancements that contribute to sustainability, energy efficiency, and improved lighting quality. As the demand for more efficient and adaptable lighting systems continues to grow, these technologies will play a crucial role in meeting the challenges of modern lighting design.

For future research in area lighting, there is a strong need to focus on the collection and standardization of mesopic lighting data across a broader spectrum of light sources and varying environmental conditions. This would enable the creation of more accurate and reliable mesopic lighting designs within DIALux, thereby improving the software's utility for real-world applications. As lighting conditions in outdoor environments are diverse and often complex, having a comprehensive database of mesopic lighting data would significantly enhance the precision of lighting simulations. This feature would enable lighting designers to create more context-appropriate lighting designs that better match human visual perception under different lighting conditions, ultimately leading to more efficient and effective lighting solutions.

Additionally, collaboration with lighting fixture manufacturers is recommended to develop products specifically optimized for mesopic conditions. By focusing on light sources to mesopic vision, manufacturers can create lighting systems that not only enhance energy efficiency but also improve overall lighting performance in outdoor and low-light environments.

Exploring the integration of adaptive lighting systems that utilize real-time sensors to adjust to mesopic conditions could provide substantial benefits. Such systems would dynamically respond to changes in lighting needs, improving energy efficiency while ensuring safety in environments with varying visibility conditions. The development of these technologies could significantly advance the field of lighting design, particularly for outdoor and low-light scenarios, by offering innovative solutions that enhance both functionality and sustainability.

Similar to area lighting, the future scope for street lighting involves the application of standardized mesopic lighting data to improve the accuracy of lighting designs within DIALux. Street lighting, which plays a critical role in public safety and urban planning, would benefit from the enhanced capability to design luminaires that are optimized for mesopic conditions. The internal characteristics of street lighting luminaires, as explored in this thesis, provide a foundation for developing ideal designs in the mesopic region.

Future research should also focus on improving the practical application of these designs by working closely with luminaire manufacturers to produce street lights specifically designed for mesopic environments. This approach would ensure that street lighting systems are not only energy-efficient but also tailored to the unique needs of mesopic vision, resulting in better visibility and safety for road users.

For the LED dimmer circuit, future work aims to expand the capabilities of the system by integrating multiple LED arrays into a single, unified configuration. This system would allow for the independent operation of each LED array, offering a higher degree of flexibility and adaptability. The ability to mix and match different types of LEDs within one system could provide customized lighting solutions for a wide range of applications, from residential to commercial and industrial settings. A particularly promising direction for future development is the integration of IoT-based control systems. These systems could significantly enhance the cost-effectiveness and energy efficiency of LED dimming circuits by enabling precise control over brightness adjustments and ON/OFF timings based on real-time sensor data. By incorporating advanced IoT technologies such as Bluetooth modules, ESP32, and ESP8266, the lighting system could automatically manage and monitor itself, responding dynamically to environmental conditions and user needs. Furthermore, the adoption of cloud-based systems for data processing and storage would revolutionize the management of lighting systems. Such systems would enable real-time monitoring and remote control of lighting, while data analytics could provide valuable insights into usage patterns and energy consumption. This would facilitate the creation of more efficient lighting schedules, potentially leading to reduced operating costs and increased sustainability. Overall, the incorporation of IoT and cloud-based technologies into LED dimmer circuits represents a significant advancement in the development of smart lighting systems.
These innovations promise to make lighting systems more versatile, efficient, and user-friendly, paving the way for the next generation of lighting solutions that are both environmentally conscious and technologically advanced.

REFERENCES

1. Eloholma, M., 2005. *Development of visual performance based mesopic photometry*. Helsinki University of Technology.
2. Smith, V.C. and Pokorny, J., 1975. Spectral sensitivity of the foveal cone photopigments between 400 and 500 nm. *Vision research*, *15*(2), pp.161-171.
3. Berman, S.M., 1992. Energy efficiency consequences of scotopic sensitivity. *Journal of the Illuminating Engineering Society*, *21*(1), pp.3-14.
4. George Wald and Donald R. Griffin, "The Change in Refractive Power of the Human Eye in Dim and Bright Light," J. Opt. Soc. Am. 37, 321-336 (1947)
5. Şener Yılmaz, F. (2018) 'Human factors in retail lighting design: an experimental subjective evaluation for sales areas', *Architectural Science Review*, 61(3), pp. 156–170. doi: 10.1080/00038628.2018.1450725.
6. Road Lighting: Fundamentals, Technology and Application" , Wout van bommel.Springer,2015.
7. Shpak, M., Kärhä, P. and Ikonen, E., 2017. Mathematical limitations of the CIE mesopic photometry system. *Lighting Research & Technology*, *49*(1), pp.111-121.
8. Rea, M.S., Bullough, J.D., Freyssinier-Nova, J.P. and Bierman, A., 2004. A proposed unified system of photometry. *Lighting Research & Technology*, *36*(2), pp.85-109.
9. Rea, M.S. and Bullough, J.D., 2007. Making the move to a unified system of photometry. *Lighting Research & Technology*, *39*(4), pp.393-408.
10. Petroski, J., 2002, November. Thermal challenges facing new-generation light-emitting diodes (LEDs) for lighting applications. In *Solid state lighting II* (Vol. 4776, pp. 215-222). SPIE.
11. Yam FK, Hassan Z. Innovative advances in LED technology. Microelectronics Journal. 2005 Feb 1;36(2):129-37.
12. Kudsieh, N., Bhutta, M.K. and Raja, M.Y.A., 2015. High power LED assemblies for solid state lighting–Thermal analysis. *Optik*, *126*(22), pp.3452-3456.
13. Tsao, J.Y., Crawford, M.H., Coltrin, M.E., Fischer, A.J., Koleske, D.D., Subramania, G.S., Wang, G.T., Wierer, J.J. and Karlicek Jr, R.F., 2014. Toward smart and ultra-efficient solid-state lighting. *Advanced Optical Materials*, *2*(9), pp.809-836.
14. Rodrigues, W.A., Morais, L.M.F., Donoso-Garcia, P.F., Cortizo, P.C. and Seleme, S.I., 2011, November. Comparative analysis of power LEDs dimming methods. In *IECON 2011-37th Annual Conference of the IEEE Industrial Electronics Society* (pp. 2907-2912). IEEE.
15. Kiyak, İ., Topuz, V. and Oral, B., 2009, November. Modeling of high power led illumination distribution using ann. In 2009 International Conference on Electrical and Electronics Engineering-ELECO 2009 (pp. II-137). IEEE.
16. Cheng, T., Luo, X., Huang, S. and Liu, S., 2010. Thermal analysis and optimization of multiple LED packaging based on a general analytical solution. International Journal of Thermal Sciences, 49(1), pp.196-201.

17. Attia, H., Omar, A., Takruri, M. and Ali, H.Y., 2017. Pulse width modulation based decentralized street LED light dimming system. *International Journal of Power Electronics and Drive Systems*, *8*(3), p.1220.
18. Kudryashov, A.V., Kalinina, A.S. and Yagovkin, G.N., 2017, May. Pulse width modulated LED light control and vision adaptation. In *2017 International Conference on Industrial Engineering, Applications and Manufacturing (ICIEAM)* (pp. 1-4). IEEE.
19. Cheng, H.L., Chang, Y.N., Cheng, C.A., Chang, C.H. and Lin, Y.H., 2016. High-power-factor dimmable LED driver with low-frequency pulse-width modulation. *IET Power Electronics*, *9*(10), pp.2139-2146.
20. Filatov, D.A., Terentyev, P.V., Sokolova, A.A. and Devyatkin, I.S., 2022, June. Comparative analysis of the energy efficiency of dimmable LED lamps with different types of luminous flux control. In IOP Conference Series: Earth and Environmental Science (Vol. 1045, No. 1, p. 012146). IOP Publishing.
21. Hamza, S.A.E. and Mustafa, A.B.A., 2014. The use of pulse width modulation "PWM" Technique in LED lighting systems. International Journal of Science and Research, 3(11), pp.2316-2320.
22. Navarrete-de Galvez, E., Gago-Calderon, A., Garcia-Ceballos, L., Contreras-Lopez, M.A. and Andres-Diaz, J.R., 2021. Adjustment of Lighting Parameters from Photopic to Mesopic Values in Outdoor Lighting Installations Strategy and Associated Evaluation of Variation in Energy Needs. Sustainability 2021, 13, 4089.
23. Uchida, T. and Ohno, Y., 2017. Simplified field measurement methods for the CIE mesopic photometry system. *Lighting Research & Technology*, *49*(6), pp.774-787.
24. Akashi, Y., Rea, M.S. and Bullough, J.D., 2007. Driver decision making in response to peripheral moving targets under mesopic light levels. *Lighting Research & Technology*, *39*(1), pp.53-67.
25. Uchida, T. and Ohno, Y., 2014. Defining the visual adaptation field for mesopic photometry: Does surrounding luminance affect peripheral adaptation?. *Lighting Research & Technology*, *46*(5), pp.520-533.
26. Kostic, M.B. and Djokic, L.S., 2012. A modified CIE mesopic table and the effectiveness of white light sources. *Lighting Research & Technology*, *44*(4), pp.416-426.
27. Berman, S.M., 1992. Energy efficiency consequences of scotopic sensitivity. *Journal of the Illuminating Engineering Society*, *21*(1), pp.3-14.
28. Kostic, A.M., Kremic, M.M., Djokic, L.S. and Kostic, M.B., 2013. Light-emitting diodes in street and roadway lighting–a case study involving mesopic effects. *Lighting Research & Technology*, *45*(2), pp.217-229.
29. Chiu, H.J., Lo, Y.K., Chen, J.T., Cheng, S.J., Lin, C.Y. and Mou, S.C., 2009. A high-efficiency dimmable LED driver for low-power lighting applications. *IEEE Transactions on Industrial Electronics*, *57*(2), pp.735-743.

30. Chiu, H.J., Lo, Y.K., Lin, Y.L. and Jane, G.C., 2015. A cost-effective PWM dimming method for LED lighting applications. *International Journal of Circuit Theory and Applications*, *43*(3), pp.307-317.
31. Rodrigues, W.A., Morais, L.M.F., Donoso-Garcia, P.F., Cortizo, P.C. and Seleme, S.I., 2011, November. Comparative analysis of power LEDs dimming methods. In *IECON 2011-37th Annual Conference of the IEEE Industrial Electronics Society* (pp. 2907-2912). IEEE.
32. Ho, K.C., Wang, S.C. and Liu, Y.H., 2021. Dimming Techniques focusing on the improvement in luminous efficiency for high-brightness LEDs. *Electronics*, *10*(17), p.2163.
33. Kıyak, I., 2012. A Study on the Working Performance of Dimming Methods for Single- and Multichip Power LEDs. *International Journal of Photoenergy*, *2012*(1), p.513768.
34. Lewin, I., 2001. Lumen effectiveness multipliers for outdoor lighting design. *Journal of the Illuminating Engineering Society*, *30*(2), pp.40-52.
35. van Bommel, W. and van Bommel, W., 2015. Mesopic vision. Road Lighting: Fundamentals, Technology and Application, pp.71-82.
36. TC, C., 1989. Mesopic photometry: History, special problems, and practical solutions. CIE Pub., 81.
37. Dubnička, R. and Gašparovský, D., 2016, September. Classification system for lighting design under condition of mesopic photometry. In 2016 IEEE Lighting Conference of the Visegrad Countries (Lumen V4) (pp. 1-6). IEEE.
38. Rushton, W.A.H., Powell, D.S. and White, K.D., 1973. The spectral sensitivity of "red" and "green" cones in the normal eye. Vision Research, 13(11), pp.2003-2015.
39. Rodrigues, C.R., Almeida, P.S., Soares, G.M., Jorge, J.M., Pinto, D.P. and Braga, H.A., 2011, June. An experimental comparison between different technologies arising for public lighting: LED luminaires replacing high pressure sodium lamps. In 2011 IEEE International Symposium on Industrial Electronics (pp. 141-146). IEEE.
40. Casagrande, C.G., Nogueira, F.J., Campos, M.F., Braga, H.A. and Rodrigues, C.R., 2013, November. Evaluation of lighting systems through adaptation of photometric quantities. In *IECON 2013-39th Annual Conference of the IEEE Industrial Electronics Society* (pp. 6069-6074). IEEE.
41. Pokorny, J. and Cao, D., 2010. Rod and cone contributions to mesopic vision. *Proceedings of CIE 2010 Lighting Quality & Energy Efficiency*, pp.9-20.
42. Commission Internationale de l'Eclairage. Recommended System for Visual Performance Based Mesopic Photometry. CIE Publication 191:2010. Vienna: CIE, 2010. 2 Puolakka M, Halonen L. Implementation of CIE 191 mesopic photometry –ongoing and future actions: Proceedings of the CIE, Hangzhou, China, September 19–21: 2012: 64–70.
43. Barbur, J.L. and Stockman, A., 2010. Photopic, mesopic and scotopic vision and changes in visual performance. *Encyclopedia of the Eye*, *3*, pp.323-331.
44. Grassmeyer, J.J. and Munakomi, S., 2019. Photopic Vision.

45. Walters, J.W., 1971. Scotopic vision at photopic levels?. *Vision Research*, *11*(8), pp.787-798.
46. Eloholma, M., Viikari, M., Halonen, L., Walkey, H., Goodman, T., Alferdinck, J.W.A.M., Freiding, A., Bodrogi, P. and Várady, G., 2005. Mesopic models—from brightness matching to visual performance in night-time driving: a review. *Lighting Research & Technology*, *37*(2), pp.155-173.
47. Boyce, P.R., Brandston, H.M. and Cuttle, C., 2022. Indoor lighting standards and their role in lighting practice. *Lighting Research & Technology*, *54*(7), pp.730-744.
48. Karlen, M., Spangler, C. and Benya, J.R., 2017. *Lighting design basics*. John Wiley & Sons.
49. de Oliveira Grando, F. and Ghisi, E., 2021. Assessment of public lighting systems considering mesopic vision. *Journal of Cleaner Production*, *279*, p.123369.
50. Palmer, D.A., 1976. Rod–cone mechanism underlying the Purkinje shift. *Nature*, *262*(5569), pp.601-603.
51. Lin, Y., Chen, D. and Chen, W., 2006. The significance of mesopic visual performance and its use in developing a mesopic photometry system. Building and environment, 41(2), pp.117-125.
52. Kostic, M.B. and Djokic, L.S., 2012. A modified CIE mesopic table and the effectiveness of white light sources. *Lighting Research & Technology*, *44*(4), pp.416-426.
53. Puolakka, M., Cengiz, C., Wei, L. and Halonen, L., 2012. Implementation of CIE 191 mesopic photometry-ongoing and future actions. In *CIE Lighting Quality & Energy Efficiency 2012, Hangzhou, China, September 19-21, 2012* (pp. 64-70). International Commission on Illumination (CIE).
54. Goodman, T.M., Bergen, T., Blattner, P., Ohno, Y., Schanda, J. and Uchida, T., 2016. The use of terms and units in photometry-implementation of the CIE system for mesopic photometry. *Int. Comm. Illum, vol. CIE TN004*.
55. Roufs, J.A.J., 1978. Light as a true visual quantity: principles of measurement.
56. He, Y., Rea, M., Bierman, A. and Bullough, J., 1997. Evaluating light source efficacy under mesopic conditions using reaction times. *Journal of the Illuminating Engineering Society*, *26*(1), pp.125-138.
57. He, Y., Bierman, A. and Rea, M.S., 1998. A system of mesopic photometry. *International journal of lighting research and technology*, *30*(4), pp.175-181.
58. Lewis, A.L., 1998. Equating light sources for visual performance at low luminances. *Journal of the Illuminating Engineering Society*, *27*(1), pp.80-84.
59. Li, J., Ma, B., Wang, R. and Han, L., 2011. Study on a cooling system based on thermoelectric cooler for thermal management of high-power LEDs. Microelectronics Reliability, 51(12), pp.2210-2215.
60. Mahadeokar, S. and Sardeshmukh, M., 2015, October. Energy efficient PWM Dimmable Smart Digital LED driver. In 2015 International Conference on Energy Systems and Applications (pp. 306-311). IEEE.